IN THE UNITED STATES PATENT AND TRADEMARK OFFICE

In re application of:	)	Examiner: Hayes, Robert Clinton
	)	
Kevin P. BAKER, et al.	)	Art Unit: 1649
	)	
Application Serial No. 10/015,499	)	Confirmation No. 6886
	)	
Filed: December 11, 2001	)	Attorney's Docket No. GNE-2830 P1C42
	)	
For: **PRO1788 POLYPEPTIDES**	)	**Customer No. 77845**

FILED VIA EXPRESS MAIL NO. EM 305 114 229 US -- DECEMBER 5 , 2008

ON APPEAL TO THE BOARD OF PATENT APPEALS AND INTERFERENCES
APPELLANTS' BRIEF

MAIL STOP APPEAL BRIEF - PATENTS
Commissioner for Patents
P.O. Box 1450
Alexandria, Virginia 22313-1450

Dear Sir:

This Appeal Brief, filed in connection with the above captioned patent application, is responsive to the Final Office Actions mailed on March 10, 2008. A Notice of Appeal was filed on August 8, 2008. Appellants hereby appeal to the Board of Patent Appeals and Interferences from the final rejection in this case. This brief is timely filed, with a request for a two-month extension of time and authorization to charge the requisite fees.

A supplemental amendment and response to final office action is concurrently filed with the present brief.

The following constitutes the Appellants' Brief on Appeal.

I. REAL PARTY IN INTEREST

The real party in interest is Genentech, Inc., South San Francisco, California, by an assignment of the patent application U.S. Serial No. 09/946,374 recorded January 8, 2002, at Reel 012288 and Frame 0504.

II. RELATED APPEALS AND INTERFERENCES

The claims pending in the current application are directed to a polypeptide referred to herein as "PRO1788". There exist two related patent applications, (1) U.S. Serial No. 10/017,390, filed December 13, 2001 (containing claims directed to polynucleotides encoding PRO1788 polypeptides), and (2) U.S. Serial No. 10/015,653, filed December 11, 2001 (containing claims directed to antibodies that bind PRO1788 polypeptides). The 10/017,390 application is still pending. The 10/015,653 application is also under final rejection from the same Examiner and based upon the same outstanding rejection, and appeal of this final rejection is being pursued independently and concurrently herewith.

III. STATUS OF CLAIMS

Claims 28-35 and 38-40 are in this application.

Claims 1-27 and 36-37 are canceled.

Claims 28-35 and 38-40 stand rejected and Appellants appeal the rejection of these claims.

A copy of the rejected claims involved in the present Appeal is provided in the Claims Appendix.

IV. STATUS OF AMENDMENTS

A summary of the prosecution history for this case is as follows:

On March 10, 2008, a final Office action mailed from the USPTO. A Notice of Appeal was filed on August 8, 2008.

Claims 28-35 have been amended in a supplemental amendment/response to the final Office Action of March 10, 2008 filed concurrently with the present appeal. A copy of the rejected claims in the present Appeal is provided in the Claims Appendix, incorporating the amendment (Section VIII).

V. SUMMARY OF CLAIMED SUBJECT MATTER

The invention claimed in the present application is related to an isolated polypeptide comprising the amino acid sequence of the polypeptide of SEQ ID NO:397 (Claims 33a and 34); the amino acid sequence of the polypeptide of SEQ ID NO:397, lacking its associated signal peptide (Claims 33b and 35); or the amino acid sequence of the polypeptide encoded by the full-length coding sequence of the cDNA deposited under ATCC accession number 203480 (Claims 33c and 38). The invention is further directed to polypeptides having at least 80% (Claim 28), 85% (Claim 29), 90% (Claim 30), 95% (Claim 31), or 99% (Claim 32) amino acid sequence identity to the amino acid sequence of the polypeptide of SEQ ID NO:397; the amino acid sequence of the polypeptide of SEQ ID NO:397, lacking its associated signal peptide; or the amino acid sequence of the polypeptide encoded by the full-length coding sequence of the cDNA deposited under ATCC accession number 203480, wherein the nucleic acid encoding said polypeptide is amplified in colon tumors. The invention is further directed to a chimeric polypeptide comprising one of the above polypeptides fused to a heterologous polypeptide (Claim 39), and to a chimeric polypeptide wherein the heterologous polypeptide is an epitope tag or an Fc region of an immunoglobulin (Claim 40).

The full-length PRO1788 polypeptide having the amino acid sequence of SEQ ID NO:397 is described in the specification at, for example, page 32, line 36 to page 33, line 37, page 264, line 32 to page 266, line 34, page 353, lines 17-23, Example 119, in Figure 232 and in SEQ ID NO:397. The cDNA nucleic acid encoding PRO1788 is described in the specification at, for example, Example 119, in Figure 231 and in SEQ ID NO:396. Page 299, lines 13-17 of the specification provides the description for Figures 231 and 232. PRO polypeptide variants having at least about 80% amino acid sequence identity with a full length PRO polypeptide sequence or a PRO polypeptide sequence lacking the signal peptide are described in the specification at, for example, page 302, lines 4-26. The preparation of chimeric PRO polypeptides, including those wherein the heterologous polypeptide is an epitope tag or an Fc region of an immunoglobulin, is set forth in the specification at page 358, lines 11-34. Examples 128-131 describe the expression of PRO polypeptides in various host cells, including *E. coli*, mammalian cells, yeast and Baculovirus-infected insect cells. PRO1788 is described as having amino acid sequence identity with Dayhoff sequence "GARP_HUMAN", a leucine-rich repeat-

containing protein encoded by a gene localized in the 11q14 chromosomal region and as being a newly identified member of the leucine-rich repeat-containing family (see, for example, page 353, lines 17-23). Finally, Example 143, in the specification at page 494, line 20, to page 508, line 28, sets forth a Gene Amplification assay which shows that the PRO1788 gene is amplified in the genome of certain human colon cancers (see page 506, lines 26-33, and Table 8).

VI. GROUNDS OF REJECTION TO BE REVIEWED ON APPEAL

1. Whether Claims 28-35 and 38-40 satisfy the utility requirement under 35 U.S.C. §§101/112, first paragraph.

2. Whether Claims 28-35 and 38-40 satisfy the written description requirement of 35 U.S.C. §112, first paragraph.

VII. ARGUMENTS

Summary of the Arguments

Issue 1: Utility/ Enablement

Appellants rely upon the gene amplification data of the PRO1788 gene for patentable utility of the PRO1788 polypeptide. This data is clearly disclosed in the instant specification in Example 143 which discloses that the gene encoding PRO1788 showed significant amplification, ranging from 2.12 to 6-fold, in eight colon tumors.

Appellants have submitted, in their Response filed January 18, 2005, a Declaration by Dr. Audrey Goddard, which explains that a gene identified as being amplified at least 2-fold by the disclosed gene amplification assay in a tumor sample relative to a normal sample is useful as a marker for the diagnosis of cancer, and for monitoring cancer development and/or for measuring the efficacy of cancer therapy. Therefore, such a gene is useful as a marker for the diagnosis of colon cancer, and for monitoring cancer development and/or for measuring the efficacy of cancer therapy.

Appellants have also submitted throughout prosecution history ample evidence to show that, in general, if a gene is amplified in cancer, it is more likely than not that the encoded protein will be expressed at an elevated level. First, the articles by Orntoft *et al.*, Hyman *et al.*, and Pollack *et al.* collectively teach that in general, gene amplification increases mRNA expression.

Second, Appellants have submitted over a hundred references, along with the Declarations of Dr. Paul Polakis and Dr. Randy Scott with their Responses filed on January 18, 2005 and August 11, 2006, which collectively teach that, in general, there is a correlation between mRNA levels and polypeptide levels.

Further, Appellants submit that one of ordinary skill in the art would know how to make and use the recited polypeptide for the diagnosis of colon cancer without any undue experimentation, based on the detailed teachings in the specification.

Accordingly, this enablement rejection under 35 U.S.C. §§101 and 112, first paragraph should be withdrawn.

Issue 2: Written Description

Claims 28-33 and 39-40 stand rejected under 35 U.S.C. §112, first paragraph as allegedly lacking adequate written description. In particular, the Examiner asserts that "a recitation related to DNA does not reasonably constitute a 'functional limitation' for the claimed polypeptides." The Examiner further asserts that Appellants have not described "a representative number of species that have 80-99% homology to SEQ ID NO:397, such that it is clear that they were in possession of a genus of polypeptides functionally similar to SEQ ID NO:397." (Pages 10-11 of the Office Action mailed May 10, 2005).

Appellants respectfully submit that the instant claims are similar to the exemplary claim in Example 10 of the revised Training Manual on Written Description Guidelines issued by the U.S. Patent Office. Appellants respectfully submit that the instant specification evidences the actual reduction to practice of the amino acid sequence of SEQ ID NO:397. Thus, the genus of polypeptides with at least 80% sequence identity to SEQ ID NO:397, would meet the requirement of 35 U.S.C. §112, first paragraph, as providing adequate written description.

Response to Rejections

Issue 1. Claims 28-35 and 38-40 are Supported by a Credible, Specific and Substantial Asserted Utility, and Thus, Meet the Utility Requirement of 35 U.S.C. §§101/112, First Paragraph

The sole basis for the Examiner's rejection of Claims 28-35 and 38-40 under this section is that the data presented in Example 143 of the present specification is allegedly insufficient

under the present legal standards to establish a patentable utility under 35 U.S.C. §101 for the presently claimed subject matter.

Claims 28-35 and 38-40 stand further rejected under 35 U.S.C. §112, first paragraph, allegedly "since the claimed invention is not supported by either a specific and substantial asserted utility or a well established utility for the reasons set forth above, one skilled in the art clearly would not know how to use the claimed invention."

Appellants strongly disagree and, therefore, respectfully traverse the rejection.

A. The Legal Standard For Utility Under 35 U.S.C. §101

According to 35 U.S.C. §101:

> Whoever invents or discovers any new and *useful* process, machine, manufacture, or composition of matter, or any new and *useful* improvement thereof, may obtain a patent therefor, subject to the conditions and requirements of this title. (Emphasis added).

In interpreting the utility requirement, in *Brenner v. Manson,*[1] the Supreme Court held that the *quid pro quo* contemplated by the U.S. Constitution between the public interest and the interest of the inventors required that a patent Applicant disclose a "substantial utility" for his or her invention, *i.e.*, a utility "where specific benefit exists in currently available form."[2] The Court concluded that "a patent is not a hunting license. It is not a reward for the search, but compensation for its successful conclusion. A patent system must be related to the world of commerce rather than the realm of philosophy."[3]

Later, in *Nelson v. Bowler,*[4] the C.C.P.A. acknowledged that tests evidencing pharmacological activity of a compound may establish practical utility, even though they may not establish a specific therapeutic use. The Court held that "since it is crucial to provide researchers with an incentive to disclose pharmaceutical activities in as many compounds as

---

[1] *Brenner v. Manson,* 383 U.S. 519, 148 U.S.P.Q. (BNA) 689 (1966).

[2] *Id.* at 534, 148 U.S.P.Q. (BNA) at 695.

[3] *Id.* at 536, 148 U.S.P.Q. (BNA) at 696.

[4] *Nelson v. Bowler*, 626 F.2d 853, 206 U.S.P.Q. (BNA) 881 (C.C.P.A. 1980).

possible, we conclude adequate proof of any such activity constitutes a showing of practical utility."[5]

In *Cross v. Iizuka,*[6] the C.A.F.C. reaffirmed *Nelson*, and added that *in vitro* results might be sufficient to support practical utility, explaining that "*in vitro* testing, in general, is relatively less complex, less time consuming, and less expensive than *in vivo* testing. Moreover, *in vitro* results with the particular pharmacological activity are generally predictive of *in vivo* test results, i.e. there is a reasonable correlation there between."[7] The Court perceived, "No insurmountable difficulty" in finding that, under appropriate circumstances, "*in vitro* testing, may establish a practical utility."[8]

The case law has also clearly established that Appellants' statements of utility are usually sufficient, unless such statement of utility is unbelievable on its face.[9] The PTO has the initial burden to prove that Appellants' claims of usefulness are not believable on their face.[10] In general, an Appellant's assertion of utility creates a presumption of utility that will be sufficient to satisfy the utility requirement of 35 U.S.C. §101, "unless there is a reason for one skilled in the art to question the objective truth of the statement of utility or its scope."[11,12]

---

[5] *Id.* at 856, 206 U.S.P.Q. (BNA) at 883.

[6] *Cross v. Iizuka*, 753 F.2d 1047, 224 U.S.P.Q. (BNA) 739 (Fed. Cir. 1985).

[7] *Id.* at 1050, 224 U.S.P.Q. (BNA) at 747.

[8] *Id.*

[9] *In re Gazave*, 379 F.2d 973, 154 U.S.P.Q. (BNA) 92 (C.C.P.A. 1967).

[10] *Ibid.*

[11] *In re Langer*, 503 F.2d 1380,1391, 183 U.S.P.Q. (BNA) 288, 297 (C.C.P.A. 1974).

[12] *See also In re Jolles*, 628 F.2d 1322, 206 U.S.P.Q. 885 (C.C.P.A. 1980); *In re Irons*, 340 F.2d 974, 144 U.S.P.Q. 351 (1965); *In re Sichert*, 566 F.2d 1154, 1159, 196 U.S.P.Q. 209, 212-13 (C.C.P.A. 1977).

Compliance with 35 U.S.C. §101 is a question of fact.[13] The evidentiary standard to be used throughout *ex parte* examination in setting forth a rejection is a preponderance of the totality of the evidence under consideration.[14] Thus, to overcome the presumption of truth that an assertion of utility by the Appellant enjoys, the Examiner must establish that it is more likely than not that one of ordinary skill in the art would doubt the truth of the statement of utility. Only after the Examiner made a proper *prima facie* showing of lack of utility, does the burden of rebuttal shift to the Appellant. The issue will then be decided on the totality of evidence.

The well established case law is clearly reflected in the Utility Examination Guidelines ("Utility Guidelines"),[15] which acknowledge that an invention complies with the utility requirement of 35 U.S.C. §101, if it has at least one asserted "specific, substantial, and credible utility" or a "well-established utility." Under the Utility Guidelines, a utility is "specific" when it is particular to the subject matter claimed. For example, it is generally not enough to state that a nucleic acid is useful as a diagnostic without also identifying the conditions that are to be diagnosed.

In explaining the "substantial utility" standard, M.P.E.P. §2107.01 cautions, however, that Office personnel must be careful not to interpret the phrase "immediate benefit to the public" or similar formulations used in certain court decisions to mean that products or services based on the claimed invention must be "currently available" to the public in order to satisfy the utility requirement. "Rather, any reasonable use that an applicant has identified for the invention that can be viewed as providing a public benefit should be accepted as sufficient, at least with regard to defining a 'substantial' utility."[16] Indeed, the Guidelines for Examination of

---

[13] *Raytheon v. Roper*, 724 F.2d 951, 956, 220 U.S.P.Q. (BNA) 592, 596 (Fed. Cir. 1983) *cert. denied,* 469 US 835 (1984).

[14] *In re Oetiker*, 977 F.2d 1443, 1445, 24 U.S.P.Q.2d (BNA) 1443, 1444 (Fed. Cir. 1992).

[15] 66 Fed. Reg. 1092 (2001).

[16] M.P.E.P. §2107.01.

Applications for Compliance With the Utility Requirement,[17] gives the following instruction to patent examiners: "If the Applicant has asserted that the claimed invention is useful for any particular practical purpose . . . and the assertion would be considered credible by a person of ordinary skill in the art, do not impose a rejection based on lack of utility."

B. Proper Application of the Legal Standard

Appellants submit that the evidentiary standard to be used throughout *ex parte* examination of a patent application is a preponderance of the totality of the evidence under consideration. Thus, to overcome the presumption of truth that an assertion of utility by the Appellant enjoys, the Examiner must establish that it is more likely than not that one of ordinary skill in the art would doubt the truth of the statement of utility. Only after the Examiner has made a proper *prima facie* showing of lack of utility, does the burden of rebuttal shift to the Appellant.

Appellants respectfully submit that the data presented in Example 143 starting on page 494 of the specification of the specification and the cumulative evidence of record, which underlies the current dispute, indeed support a "specific, substantial and credible" asserted utility for the presently claimed invention.

Patentable utility for the PRO1788 polypeptides and their antibodies is based upon the gene amplification data for the gene encoding the PRO1788 polypeptide. Example 143 describes the results obtained using a very well-known and routinely employed polymerase chain reaction (PCR)-based assay, the TaqMan™ PCR assay, also referred to herein as the gene amplification assay. This assay allows one to quantitatively measure the level of gene amplification in a given sample, say, a tumor extract, or a cell line. It was well known in the art at the time the invention was made that gene amplification is an essential mechanism for oncogene activation. Appellants isolated genomic DNA from a variety of primary cancers and cancer cell lines that are listed in Table 8, including primary lung cancers of the type and stage indicated in Table 7. The tumor samples were tested in triplicates with Taqman™ primers and with internal controls, beta-actin and GADPH in order to quantitatively compare DNA levels between samples. As a negative

[17] M.P.E.P. §2107 II(B)(1).

control, DNA was isolated from the cells of ten normal healthy individuals, which was pooled and used as a control. Gene amplification was monitored using real-time quantitative TaqMan™ PCR. Table 8 shows the resulting gene amplification data. Further, Example 143 explains that the results of TaqMan™ PCR are reported in ΔCt units, wherein one unit corresponds to one PCR cycle or approximately a 2-fold amplification relative to control, two units correspond to 4-fold amplification, 3 units to 8-fold amplification etc.

Appellants respectfully submit that a ΔCt value of at least 1.0 was observed for PRO1788 in at least eight of the tumors listed in Table 8. PRO1788 showed approximately 1.09-2.58 ΔCt units which corresponds to $2^{1.09}$-$2^{2.58}$ fold amplification or 2.12-fold to 6-fold amplification in primary colon tumors (CT1, CT3, CT4, CT8, CT9, CT10, CT12 and CT14). (See Table 8 and p page 506, lines 26-33 of the specification). Accordingly, the present specification clearly discloses overwhelming evidence that the gene encoding the PRO1788 polypeptide is significantly amplified in colon tumors.

In support of their showing that these gene amplification values are significant, Appellants submitted, in the Response filed January 18, 2005, a Declaration by Dr. Audrey Goddard. Appellants particularly draw the Board's attention to page 3 of the Goddard Declaration which clearly states that:

> It is further my considered scientific opinion that an at least **2-fold increase** in gene copy number in a tumor tissue sample relative to a normal (*i.e.*, non-tumor) sample is significant and useful in that the detected increase in gene copy number in the tumor sample relative to the normal sample serves as a basis for using relative gene copy number as quantitated by the TaqMan PCR technique as a diagnostic marker for the presence or absence of tumor in a tissue sample of unknown pathology. Accordingly, a gene identified as being amplified at least 2-fold by the quantitative TaqMan PCR assay in a tumor sample relative to a normal sample is **useful as a marker for the diagnosis of cancer**, for monitoring cancer development and/or for measuring the efficacy of cancer therapy.
> (Emphasis added).

Appellants point out that the Declaration by Dr. Audrey Goddard provides a statement by an expert in the relevant art that "fold amplification" values of at least 2-fold are considered significant in the TaqMan™ PCR gene amplification assay. Appellants particularly draw the Board's attention to page 3 of the Goddard Declaration which clearly states that:

> It is further my considered scientific opinion that an at least **2-fold increase** in gene copy number in a tumor tissue sample relative to a normal (*i.e.*, non-tumor) sample is significant and useful in that the detected increase in gene copy number in the tumor sample relative to the normal sample serves as a basis for using relative gene copy number as quantitated by the TaqMan PCR technique as a diagnostic marker for the presence or absence of tumor in a tissue sample of unknown pathology. Accordingly, a gene identified as being amplified at least 2-fold by the quantitative TaqMan PCR assay in a tumor sample relative to a normal sample is **useful as a marker for the diagnosis of cancer**, for monitoring cancer development and/or for measuring the efficacy of cancer therapy.
> (Emphasis added).

Thus, According to the Goddard Declaration, Appellants maintain that the 2.12 to 6-fold amplification disclosed for the PRO1788 gene is significant and forms the basis for the utility claimed herein. As any skilled artisan in the field of oncology would easily appreciate that this gene is a good candidate marker for diagnosing colon tumor and would clearly find utility for the PRO1788 gene as a diagnostic for colon cancer or for diagnosing individuals at risk for developing colon cancer.

The Examiner has asserted that in order for PRO1788 polypeptides to be overexpressed in tumors, amplified genomic DNA would have to correlate with increased mRNA levels and increased polypeptide levels. The Examiner has further asserted that the specification does not provide data regarding PRO1788 mRNA or PRO1788 polypeptide levels in colon tumors. (Page 6 of the Final Office Action mailed March 10, 2008).

The Examiner's reference to the lack of necessary correlation or accurate prediction in some of the rejections clearly shows that the Examiner applies an improper legal standard when making this rejection. The evidentiary standard to be used throughout *ex parte* examination in setting forth a rejection is a preponderance of the totality of the evidence under consideration. Thus, to overcome the presumption of truth that an assertion of utility by the Applicant enjoys, the Examiner must establish that it is more likely than not that one of ordinary skill in the art would doubt the truth of the statement of utility. Only after the Examiner has made a proper *prima facie* showing of lack of utility, does the burden of rebuttal shift to the Applicant. As discussed below, the references cited by the Examiner do not suffice to make a *prima facie* case that more

likely than not no generalized correlation exists between gene (DNA) amplification and increased polypeptide levels.

In contrast, Appellants have submitted ample evidence to show that, in general, if a gene is amplified in cancer, it is more likely than not that the encoded protein will be expressed at an elevated level. First, the articles by Orntoft *et al.*, Hyman *et al.*, and Pollack *et al.*, (made of record in Appellants' Response filed August 19, 2004) collectively teach that in general, gene amplification increases mRNA expression. Second, as the Examiner has acknowledged, the art teaches that, in general, there is a correlation between mRNA levels and polypeptide levels.

Accordingly, one of skill in the art would reasonably expect in this instance, based on the amplification data for the PRO1788 gene, that the PRO1788 polypeptide is concomitantly overexpressed. Thus, the claimed antibodies to the PRO1788 polypeptide have utility in the diagnosis of cancer.

The Examiner has asserted that further research would have been required of the skilled artisan to reasonably confirm that PRO1788 is overexpressed in any cancer to the extent that it could be used as a cancer diagnostic agent; thus the asserted utility is not substantial. (Page 8 of the Final Office Action mailed March 10, 2008).

As discussed in previous responses of record, M.P.E.P. §2107.01 cautions Office personnel not to interpret the phrase "immediate benefit to the public" or similar formulations used in certain court decisions to mean that products or services based on the claimed invention must be "currently available" to the public in order to satisfy the utility requirement. "Rather, any reasonable use that an Applicant has identified for the invention that can be viewed as providing a public benefit should be accepted as sufficient, at least with regard to defining a 'substantial' utility."[18] Indeed, the Guidelines for Examination of Applications for Compliance With the Utility Requirement,[19] gives the following instruction to patent examiners: "If the Applicant has asserted that the claimed invention is useful for any particular practical purpose . . . and the assertion would be considered credible by a person of ordinary skill in the art, do not impose a rejection based on lack of utility."

---

[18] M.P.E.P. §2107.01.

[19] M.P.E.P. §2107 II(B)(1).

Appellants' position is based on the overwhelming evidence from gene amplification data disclosed in the specification which clearly indicate that the gene encoding PRO1788 is significantly amplified in certain lung and colon tumors. Based on the working hypothesis among those skilled in the art that if a gene is amplified in cancer, the encoded protein is likely to be expressed at an elevated level, one skilled in the art would simply accept that since the PRO1788 gene is amplified, the PRO1788 polypeptide would be more likely than not over-expressed. Thus, data relating to PRO1788 polypeptide expression may be used for the same diagnostic and prognostic purposes as data relating to PRO1788 gene expression. Therefore, based on the disclosure in the specification, no further research would be necessary to determine how to use the claimed PRO1788 polypeptides, because the current invention is fully enabled by the disclosure of the present application.

Accordingly, Appellants submit that based on the general knowledge in the art at the time the invention was made and the teachings in the specification, the specification provides clear guidance as to how to interpret and use the data relating to PRO1788 polypeptide expression and that the claimed PRO1788 polypeptide have utility in the diagnosis of cancer.

C. A *prima facie* case of lack of utility has not been established

Appellants respectfully submit that the Examiner has not made a proper *prima facie* showing of lack of utility, because the Examiner has not shown that Appellants' asserted utility is more likely than not incorrect.

The Examiner has asserted that "[t]he claimed functional use of DNA for detecting colon tumors is not equivalent to identifying a use for the claimed polypeptide." (Page 4 of the Office Action mailed March 10, 2008). The Examiner has further asserted that the "'increase in gene copy number' (i.e., DNA data) is not equivalent to increased polypeptide levels." (Page 4 of the Office Action mailed March 10, 2008). In support of this assertion, the Examiner refers to the references of record by Haynes, Hu, Chen, Pennica and Konopka.

As a preliminary matter, Appellants respectfully submit that it is not a legal requirement to establish that gene amplification "necessarily" results in increased expression at the mRNA and polypeptide levels or that polypeptide levels can be "accurately predicted." As discussed above, the evidentiary standard to be used throughout *ex parte* examination of a patent application is a preponderance of the totality of the evidence under consideration. Accordingly,

Appellants submit that in order to overcome the presumption of truth that an assertion of utility by the applicant enjoys, the Examiner must establish that **it is more likely than not** that one of ordinary skill in the art would doubt the truth of the statement of utility. Therefore, it is not legally required that there be a "necessary" correlation between the data presented and the claimed subject matter. The law requires only that one skilled in the art should accept that such a correlation is **more likely than not to exist**. Appellants respectfully submit that when the proper evidentiary standard is applied, a correlation must be acknowledged.

Pennica *et al.*

Appellants submit that Pennica *et al.* does not show a lack of correlation between gene (DNA) amplification and mRNA levels. According to the quoted statement from Pennica *et al.*, "WISP-1 gene amplification in human lung tumors showed a correlation between DNA amplification and over-expression, whereas overexpression of WISP-3 RNA was seen in the absence of DNA amplification. In contrast, WISP-2 DNA was amplified in lung tumors, but its mRNA expression was significantly reduced in the majority of tumors compared with expression in normal lungic mucosa from the same patient." From this, the Examiner correctly concludes that increased copy number does not *necessarily* result in increased polypeptide expression. The standard, however, is not absolute certainty. The fact that in the case of a specific class of closely related molecules there seemed to be no correlation with gene amplification and the level of mRNA/protein expression, does not establish that it is more likely than not, in general, that such correlation does not exist. The Examiner has not shown whether the lack or correlation observed for the family of WISP polypeptides is typical, or is merely a discrepancy, an exception to the rule of correlation. Indeed, the working hypothesis among those skilled in the art is that, if a gene is amplified in cancer, the encoded protein is likely to be expressed at an elevated level. In fact, as noted even in Pennica *et al.*, "[a]n analysis of *WISP*-1 gene amplification and expression in human lung tumors *showed a correlation between DNA amplification and over-expression* . . . ." (Pennica *et al.*, page14722, left column, first full paragraph, emphasis added).

Accordingly, Appellants respectfully submit that Pennica *et al.* teaches nothing conclusive regarding the absence of correlation between amplification of a gene and over-expression of the encoded WISP polypeptide. More importantly, the teaching of Pennica *et al.* is

specific to *WISP* genes. Pennica *et al.* has no teaching whatsoever about the correlation of gene amplification and protein expression in general.

Konopka *et al.*

Regarding Konopka *et al.*, Appellants submit that the Examiner has completely misinterpreted the teachings in the cited reference. Contrary to the Examiner's assertions, Konopka *et al.* does not support the position that DNA amplification is not correlated with mRNA overexpression. Konopka *et al.* show only that, of the cell lines known to have increased abl protein expression, only one had amplification of the abl gene (page 4051, col. 1). This result proves only that increased mRNA and protein expression levels can result from causes other than gene amplification. Konopka *et al.* do not demonstrate that when gene amplification does occur, it does not result in increased mRNA and protein expression levels, particularly given that the cell line with amplification of the abl gene did show increased abl mRNA and protein expression levels. Furthermore, Konopka *et al.* supports Appellants' position that mRNA levels correlate with protein levels. Konopka *et al.* state that "the 8-kb mRNA that encodes $P210^{c\text{-}abl}$ was detected at a 10-fold higher level in SK-CML7bt-333 (Fig. 3A, +) than in SK-CML16Bt-1 (B, +), which **correlated** with the relative level of $P210^{c\text{-}abl}$ detected in each cell line. Analysis of additional cell lines demonstrated that the level of 8-kb mRNA **directly correlated** with the level of $P210^{c\text{-}abl}$ (Table 1)" (page 4050, col. 2, emphasis added).

Haynes *et al*

The Examiner has cited Haynes *et al.* as allegedly providing evidence that "polypeptide levels cannot be accurately predicted from mRNA levels, and that variances as much as 40-fold or even 50-fold were not uncommon." (Page 6 of the Office Action mailed May 10, 2005). The law does not require the existence of a strong or linear correlation between mRNA and protein levels. Nor does the law require that protein levels be "accurately" predicted. According to the authors themselves, the Haynes data confirm that there is a "general trend" between protein expression and transcript levels (page 1863, col. 1), which meets the "more likely than not standard" and shows that a positive correlation exists between mRNA and protein. For example, in Figure 1, there is a positive correlation between mRNA and protein levels amongst most of the 80 yeast proteins studied. In fact, very few data points deviated or scattered away from the expected normal and no data points showed a negative correlation between mRNA and protein

levels (*i.e.* an increase in mRNA resulted in a decrease in protein levels). The analysis by Haynes *et al.* is not relevant to the current application. Haynes *et al.* studied yeast cells and not human cells. Haynes *et al.* note that their analysis focused on the 80 most abundant proteins in the yeast lysate (page 1867). Haynes *et al.* state that "since many important regulatory protein are present only at low abundance, these would not be amenable to analysis" (page 1867). Further, Haynes *et al.* compared the protein expression levels of these naturally abundant proteins to mRNA expression levels from published SAGE frequency tables (page 1863). Accordingly, Haynes *et al.* did not compare mRNA expression levels and protein levels in the same yeast cells. Thus the analysis by Haynes *et al.* is not applicable to the present application.

Hu *et al.*

The Examiner has further cited Hu *et al.* to the effect that genes displaying a 5-fold change or less in mRNA expression in tumors compared to normal showed no evidence of a correlation between altered gene expression and a known role in the disease. However, among genes with a 10-fold or more change in expression level, there was a strong and significant correlation between expression level and a published role in the disease. (Page 5 of the Office Action mailed May 10, 2005).

Appellants submit that in order to overcome the presumption of truth that an assertion of utility by the applicant enjoys, the Examiner must establish that it is more likely than not that one of ordinary skill in the art would doubt the truth of the statement of utility. Accordingly, contrary to the Examiner's assertion, Appellants submit that Hu *et al.* does not conclusively show that it is more likely than not that gene amplification does not result in increased expression at the mRNA and polypeptide levels. First, the title of Hu *et al.* is "Analysis of Genomic and Proteomic Data Using Advanced Literature Mining." As the title clearly suggests, the conclusion suggested by Hu *et al.* is merely based on a statistical analysis of the information disclosed in the published literature. As Hu *et al.* states, "We have utilized a computational approach to literature mining to produce a comprehensive set of gene-disease relationships." In particular, Hu *et al.* relied on the MedGene Database and the Medical Subject Heading (MeSH) files to analyze the gene-disease relationship. More specifically, Hu *et al.* "compared the MedGene breast cancer gene list to a gene expression data set generated from a micro-array

analysis comparing breast cancer and normal breast tissue samples." (See page 408, right column).

Therefore, Appellants first submit that the reference by Hu *et al.* only studies the statistical analysis of micro-array data and not gene amplification data. Therefore, their findings would not be directly applicable to gene amplification data. In addition, Appellants respectfully submit that the Hu *et al.* reference does not show that a lack of correlation between microarray data and the biological significance of cancer genes is typical.

According to Hu *et al.*, "*different* statistical methods" were applied to "*estimate* the strength of gene-disease relationships and evaluated the results." (See page 406, left column, emphasis added). Using these different statistical methods, Hu *et al.* "[a]ssessed the relative strengths of gene-disease relationships based on the frequency of both co-citation and single citation." (See page 411, left column). It is well known in the art that various statistical methods allow different variables to be manipulated to affect the outcome. For example, the authors admit, "Initial attempts to search the literature using" the list of genes, gene names, gene symbols, and frequently used synonyms, generated by the authors "revealed several sources of false positives and false negatives." (See page 406, right column). The authors further admit that the false positives caused by "duplicative and unrelated meanings for the term" were "difficult to manage." Therefore, in order to minimize such false positives, Hu *et al.* disclose that these terms "had to be eliminated entirely, thereby reducing the false positive rate but unavoidably under-representing some genes." *Id.* Hence, Appellants respectfully submit that in order to minimize the false positives and negatives in their analysis, Hu *et al.* manipulated various aspects of the input data.

Appellants further submit that the statistical analysis by Hu *et al.* is not a reliable standard because the frequency of citation reflects only the current research interest of a molecule rather than the true biological function of the molecule. Indeed, the authors acknowledge that "[r]elationship established by frequency of co-citation do not necessarily represent a true biological link." (See page 411, right column). It often happens in scientific study that important molecules are overlooked by the scientific society for many years until the discovery of their true function. Therefore, Appellants submit that Hu *et al.* drew their conclusion based on

a very unreliable standard and that their research does not provide any meaningful information regarding the correlation between microarray data and the biological significance of a molecule.

Even assuming that Hu *et al.* provide evidence to support a true relationship, the conclusion in Hu *et al.* only applies to a specific type of breast tumor (estrogen receptor (ER)-positive breast tumor) and can not be generalized as a principle governing microarray study of breast cancer in general, let alone the various other types of cancer genes in general. In fact, even Hu *et al* admit that." [i]t is likely that this threshold will change depending on the disease as well as the experiment. Interestingly, the observed correlation was only found among ER-positive (breast) tumors not ER-negative tumors." (See page 412, left column). Therefore, based on these findings, the authors add, "This may reflect a bias in the literature to study the more prevalent type of tumor in the population. Furthermore, this emphasizes that caution must be taken when interpreting experiments that may contain subpopulations that behave very differently." *Id.* (Emphasis added).

In summary, Appellants respectfully submit that the Examiner has not shown that a lack of correlation between microarray data and the biological significance of cancer genes, as observed for ER-positive breast tumor, is typical. Since the standard is not absolute certainty, a *prima facie* showing of lack of utility has not been made in this instance.

Chen *et al.*

The Examiner has cited Chen et al. to show that an increase in mRNA level does not correlate with an increase in protein level (Page 5 of the Office Action mailed March 10, 2008)

First, Appellants note that proteins selected for study by Chen *et al.*, were those detectable by staining of 2D gels. As noted in, for example, Haynes *et al.* there are problems with selecting proteins detectable by 2D gels. "It is apparent that without prior enrichment only a relatively small and highly selected population of long-lived, highly expressed proteins is observed. There are many more proteins in a given cell which are not visualized by such methods. Frequently, it is the low abundance proteins that execute key regulatory functions" (Haynes, p. 1870, col. 1). Thus, Chen *et al.* by selecting proteins detectable by staining of 2D gels are likely to have excluded from their analysis many of the proteins most likely to be significant as cancer markers.

Secondly, Chen *et al.* looked at expression levels across a set of samples including a large number of tumor samples (76) along with a much smaller number of normal samples (9). The tumor samples were taken from stage 1 and stage III lung adenocarcinomas, which were classified as bronchoaveolar, bronchial derived or both bronchial and bronchoaveolar derived. Accordingly, the tissues examined were from different tissues in different stages of normal or cancerous growth. The authors determined the relationship between mRNA and protein expression by using the average expression values for all samples. The average value for each protein or mRNA was generated using all 85 lung tissue samples. This resulted in negative normalized protein values in some cases. Further, the authors chose an arbitrary threshold of 0.115 for the correlation to be considered significant. Accordingly, the Chen paper does not account for different expression in different tissues or different stages of cancer.

Thirdly, no attempt was made to compare expression levels in normal versus tumor samples, and in fact the authors concede that they had too few normal samples for meaningful analysis (Chen, p. 310, col. 2). As a result, the analysis in the Chen paper shows only that a number of randomly selected proteins have varying degrees of correlation between mRNA and protein expression levels within a set of different lung adenocarcinoma samples. The Chen paper does not address the issue of whether increased mRNA levels in the tumor samples taken together as one group, as compared to the normal samples as a group, correlated with increased protein levels in tumor tissue versus normal tissue. Accordingly, the results presented in the Chen paper are not applicable to the present application.

The correct test of utility is whether the utility is "more likely than not." In the case of the Chen reference, even if the analysis presented is correct (which is disputed), a review of the correlation coefficient data presented in the Chen *et al.* paper indicates that it is more likely than not that increased mRNA expression correlates with increased protein expression. A review of Table 1, which lists 66 genes [the paper incorrectly states there are 69 genes listed] for which only one protein isoform is expressed, shows that 40 genes out of 66 had a positive correlation between mRNA expression and protein expression. This clearly meets the test of "more likely than not." Similarly, in Table II, 30 genes with multiple isoforms [again the paper incorrectly states there are 29] were presented. In this case, at least 22 genes had one isoform showing a positive correlation between mRNA expression and protein expression. Furthermore, 12 genes

out of 29 showed a significant positive correlation [as determined by the authors] for at least one isoform. No genes showed a significant negative correlation. It is not surprising that not all isoforms for each gene positively correlate with mRNA expression. As the Examiner may be aware, some isoforms are likely non-functional proteins. Thus, Table II further supports Appellants' assertion that it is more likely than not that protein levels correlate with mRNA expression levels.

Lewin

The Examiner has referred to Lewin as teaching that "control of gene expression can occur at multiple stages, and that production of mRNA cannot inevitably be equated with production of protein." (Page 6 of the Office Action mailed March 10, 2008).

Appellants respectfully submit that the utility standard is not **absolute certainty**. Rather, to overcome the presumption of truth that an assertion of utility by an applicant enjoys, the PTO must establish that it is **more likely than not** that one of ordinary skill in the art would doubt the truth of the statement of utility. Therefore, Appellants **do not need** to establish that transcription initiation is **the only means** of regulating gene expression in order to meet the utility standard. Instead, as long as it is the most common point of regulation, as admitted by the Examiner, it would be more likely than not that a change in the transcription level of a gene gives rise to a change in translation level of a gene. Appellants note that Lewin makes clear that it is far more likely than not that protein levels for any given gene are regulated at the transcriptional level. In particular, Lewin states that "having acknowledged that control of gene expression can occur at multiple stages, and that production of RNA cannot inevitably be equated with production of protein, it is clear that the overwhelming majority of regulatory events occur at the initiation of transcription." *Genes VI* at 847-848 (Emphasis added). Thus, the utility standard is met.

Futcher *et al.*

The Examiner has referred to the reference of record by Futcher et al. as stating that "Gygi et al. feel that mRNA abundance is a poor predictor of protein abundance." (Page 7 of the Office Action mailed March 10, 2008).

Appellants respectfully point out that Futcher *et al.* refer to Gygi *et al.* in the process of explaining in detail why their results did show a correlation between mRNA and protein levels even for low abundance proteins, while the previous study by Gygi *et al.* did not. In fact,

Futcher *et al.* concluded that "**several statistical methods show a strong and significant correlation between mRNA abundance and protein abundance.**" (Page 7360, col. 2; Emphasis added).

The authors note that Gygi *et al.* completed a similar study that generated broadly similar data, but reached different conclusions. Futcher *et al.* point out that "the different conclusions are also partly due to different methods of statistical analysis, and to real differences in data." Futcher *et al.* note that Gygi *et al.* used the Pearson product-moment correlation coefficient (r_p) and point out that "a calculation of r_p is inappropriate" because the mRNA and protein abundances are not normally distributed. (Page 7367, col. 1). In contrast, Futcher *et al.* used two different statistical approaches to determining the correlation between mRNA and protein abundances. First, they used the Spearman rank correlation coefficient (r_s), an nonparametric statistic that does not require the data to be normally distributed. Using the r_s, the authors found that mRNA abundance was well correlated with protein abundance ($r_s = 0.74$). Applying this statistical approach to the data of Gygi *et al.* **also** resulted in a good correlation ($r_s = 0.59$), although the correlation was not quite as strong as for the Futcher *et al.* data. In a second approach, Futcher *et al.* transformed the mRNA and protein data to forms where they were normally distributed, in order to allow calculation of an r_p. Two types of transformation (Box-Cox and logarithmic) were used, and **both** resulted in good correlations between mRNA and protein abundance for Futcher *et al.*'s data.

Futcher *et al.* also note that the two studies used different methods of measuring protein abundance. Gygi *et al.* cut spots out of each gel and measured the radiation in each spot by scintillation counting, whereas Futcher *et al.* used phosphorimaging of intact gels coupled to image analysis. Futcher *et al.* point out that Gygi *et al.* may have systematically overestimated the amount of the lowest-abundance proteins, because of the difficulty in accurately cutting out very small spots from the gel, and because of difficulties in background subtraction for small, weak spots.

In addition, Futcher *et al.* note that they used both SAGE data and RNA hybridization data to determine mRNA abundances, which is most helpful to accurately measure the least abundant mRNAs. As a result, while the Futcher data set "maintains a good correlation between mRNA and protein abundance even at low protein abundance" (page 7367, col. 2), the Gygi data

shows a strong correlation for the most abundant proteins, but a poor correlation for the least abundant proteins in their data set. Futcher *et al.* conclude that "**the poor correlation of protein to mRNA for the nonabundant proteins of Gygi *et al.* may reflect difficulty in accurately measuring these nonabundant proteins and mRNAs, rather than indicating a truly poor correlation *in vivo.***" (Page 7367, col. 2; Emphasis added). Thus, while these lowest abundant proteins do show a poor correlation, this is almost certainly due to the less accurate methods used to measure the abundance of these proteins, and **not** to any actual lack of correlation.

Appellants further note that, as Futcher *et al.* was published later than Gygi *et al.*, Futcher's conclusions should be considered as the updated view in the art, which supports the existence of a correlation between mRNA and protein levels.

In summary, the Patent Office has failed to meet its initial burden of proof that Appellants' claims of utility are not substantial or credible. The arguments presented by the Examiner in combination with the cited articles do not provide sufficient reasons to doubt the statements by Appellants that PRO1788 has utility. As discussed above, the law does not require that DNA amplification is "always" associated with overexpression of the gene product. Therefore, Appellants submit that the Examiner's reasoning is based on a misrepresentation of the scientific data presented in the above cited reference and application of an improper, heightened legal standard. In fact, contrary to what the Examiner contends, the art indicates that, if a gene is amplified in cancer, it is more likely than not that the encoded protein will be expressed at an elevated level.

It is "more likely than not" for amplified genes to have increased mRNA

On the contrary, Appellants submit that Example 143 of the specification further discloses that, "(a)mplification is associated with overexpression of the gene product, indicating that the polypeptides are useful targets for therapeutic intervention in certain cancers such as lung, colon, breast and other cancers and diagnostic determination of the presence of those cancers" (Emphasis added). Besides, Appellants have submitted ample evidence to show that, in general, if a gene is amplified in cancer, it is "more likely than not" that the corresponding mRNA will also be expressed at an elevated level.

For instance, Appellants presented the articles by Orntoft *et al.*, Hyman *et al.*, and Pollack *et al.* (made of record in Appellants' Response filed January 18, 2005), who collectively

teach that in general, for most genes, DNA amplification increases mRNA expression. The results presented by Orntoft *et al.*, Hyman *et al.*, and Pollack *et al.* are based upon wide ranging analyses of a large number of tumor associated genes. Orntoft *et al.* studied transcript levels of 5600 genes in malignant bladder cancers, many of which were linked to the gain or loss of chromosomal material, and found that in general (18 of 23 cases) chromosomal areas with more than 2-fold gain of DNA showed a corresponding increase in mRNA transcripts. Hyman *et al.* compared DNA copy numbers and mRNA expression of over 12,000 genes in breast cancer tumors and cell lines, and found that there was evidence of a prominent global influence of copy number changes on gene expression levels. In Pollack *et al.*, the authors profiled DNA copy number alteration across 6,691 mapped human genes in 44 predominantly advanced primary breast tumors and 10 breast cancer cell lines, and found that on average, a 2-fold change in DNA copy number was associated with a corresponding 1.5-fold change in mRNA levels. In summary, the evidence supports the Appellants' position that gene amplification is more likely than not predictive of increased mRNA and polypeptide levels.

Second, Appellants have submitted over a hundred references, along with the Declarations of Dr. Paul Polakis and Dr. Randy Scott with their Responses filed on January 18, 2005 and August 11, 2006, which collectively teach that, in general, there is a correlation between mRNA levels and polypeptide levels.

In their Response filed January 18, 2005, Appellants submitted a Declaration by Dr. Polakis, principal investigator of the Tumor Antigen Project of Genentech, Inc., the assignee of the present application, to show that mRNA expression correlates well with protein levels, in general. As Dr. Polakis explains, the primary focus of the microarray project was to identify tumor cell markers useful as targets for both the diagnosis and treatment of cancer in humans. The scientists working on the project extensively rely on results of microarray experiments in their effort to identify such markers. As Dr. Polakis explains, using microarray analysis, Genentech scientists have identified approximately 200 gene transcripts (mRNAs) that are present in human tumor cells at significantly higher levels than in corresponding normal human cells. To the date of the Declaration, they have generated antibodies that bind to about 30 of the tumor antigen proteins expressed from these differentially expressed gene transcripts and have used these antibodies to quantitatively determine the level of production of these tumor antigen

proteins in both human cancer cells and corresponding normal cells. Having compared the levels of mRNA and protein in both the tumor and normal cells analyzed, they found a very good correlation between mRNA and corresponding protein levels. Specifically, in approximately 80% of their observations they have found that increases in the level of a particular mRNA correlates with changes in the level of protein expressed from that mRNA. While the proper legal standard is to show that the existence of correlation between mRNA and polypeptide levels is more likely than not, the showing of approximately 80% correlation for the molecules tested according to the Polakis Declaration greatly exceeds this legal standard. Based on these experimental data and his vast scientific experience of more than 20 years, Dr. Polakis states that, for human genes, increased mRNA levels typically correlate with an increase in abundance of the encoded protein. He further confirms that "it remains a central dogma in molecular biology that increased mRNA levels are predictive of corresponding increased levels of the encoded protein." Appellants respectfully point out that the Declaration by Dr. Polakis (Polakis II) presents evidentiary data in Exhibit B. Exhibit B of the Declaration identifies 28 gene transcripts out of 31 gene transcripts (*i.e.*, greater than 90%) that showed good correlation between tumor mRNA and tumor protein levels. As Dr. Polakis' Declaration (Polakis II) says "[a]s such, in the cases where we have been able to quantitatively measure both (i) mRNA and (ii) protein levels in both (i) tumor tissue and (ii) normal tissue, we have observed that in the vast majority of cases, there is a very strong correlation between increases in mRNA expression and increases in the level of protein encoded by that mRNA."

Appellants have also submitted, with their Response filed on August 11, 2006, a Declaration by Dr. Randy Scott ("the Scott Declaration"). Dr. Scott was a co-founder of Incyte Pharmaceuticals, Inc., the world's first genomic information business, and is currently the Chairman and Chief Executive Officer of Genomic Health, Inc., a life sciences company located in Redwood City, California, which provides individualized information on the likelihood of disease recurrence and response to certain types of therapy using gene expression profiling. Based on his more than 15 years of personal experience with the DNA microarray technique and its various uses in the diagnostic and therapeutic fields, and his familiarity with the relevant art, Dr. Scott unequivocally confirms that, as a general rule, there is a good correlation between mRNA and protein levels in a particular tissue.

As stated in paragraph 8 of the Scott Declaration:

> DNA microarray analysis has been extensively used in drug development and in diagnosis of various diseases. ..... Due to its importance in drug discovery and in the field of diagnostics, microarray technology has not only become a laboratory mainstay but also created a world-wide market of over $600 million in the year of 2005. A long line of companies, including Incyte, Affymetrix, Agilent, Applied Biosystems, and Amersham Biosciences, made microarray technology a core of their business.

In paragraph 10 of his Declaration, Dr. Scott explains the reasons for the wide-spread use and impressive commercial success of this technique, stating:

> One reason for the success and wide-spread use of the DNA microarray technique, which has led to the emergence of a new industry, is that generally there is a good correlation between mRNA levels determined by microarray analysis and expression levels of the translated protein. Although there are some exceptions on an individual gene basis, **it has been a consensus in the scientific community that elevated mRNA levels are good predictors of increased abundance of the corresponding translated proteins in a particular tissue**. Therefore, diagnostic markers and drug candidates can be readily and efficiently screened and identified using this technique, without the need to directly measure individual protein expression levels. (Emphasis added).

The Declaration, which is based on Dr. Scott's unparalleled experience with both the microarray technique and its industrial and clinical applications, supports Appellants' position that the microarray technology is not only mature, reliable and well-accepted in the art, but also has been extensively used in drug development and in diagnosis of various diseases and produced enormous commercial success. Therefore, if a gene, such as the gene encoding the PRO1788 polypeptide, has been identified to be over-expressed in a certain disease, such as colon cancer, it is more likely than not that the protein product is also overexpressed in the disease.

Thus, taken together, all of the submitted evidence supports Appellants' position that gene amplification is more likely than not predictive of increased mRNA and polypeptide levels.

Thus, the Examiner appears to disregard the ample evidence provided in the above referenced articles based on misinterpretations of their teachings. Appellants submit that in fact, these articles lend significant support that for an amplified gene, it is more likely than not that the protein will also be overexpressed and would be viewed as reasonable and credible by one of ordinary skill in the art. The "more likely than not" standard is a much lower standard than a

"necessary" correlation or "accurate" prediction, and is clearly met in the claimed invention. Moreover, the Examiner has not cited any evidence or advanced any arguments as to why Appellants' statement of overexpression of protein would not be credible. Accordingly, this point is believed to be moot.

The Examiner has further asserted that the Hyman reference teaches "[l]ess than half (44%) of highly amplified genes showed mRNA overexpression (abstract)." (Page 6 of the Final Office Action mailed March 10, 2008).

Appellants submit the Examiner's assertion is not consistent with the interpretation Hyman *et al.* themselves place on their data, stating that, "The results illustrate **a considerable influence of copy number on gene expression patterns**." (page 6242. col. 1; emphasis added). In the more detailed discussion of their results, Hyman *et al.* teach that "[u]p to 44% of the highly amplified transcripts (CGH ratio, >2.5) were overexpressed (***i.e.*, belonged to the global upper 7% of expression ratios**) compared with only 6% for genes with normal copy number." (See page 6242, col. 1; emphasis added). These details make it clear that Hyman *et al.* set a highly restrictive standard for considering a gene to be overexpressed; yet almost half of all highly amplified transcripts met even this highly restrictive standard. Therefore, the analysis performed by Hyman *et al.* clearly shows that "it is more likely than not" that a gene which is amplified in tumor cells will have increased gene expression.

As stated above, the Orntoft *et al.,* Hyman *et al.,* and Pollack *et al.* articles were submitted to support the correlation between gene amplification and mRNA levels, which according to the Examiner is the sole basis of the maintained rejections. With regard to the correlation between mRNA expression and protein levels, Appellants previously submitted a Declaration by Dr. Polakis, principal investigator of the Tumor Antigen Project of Genentech, Inc., the assignee of the present application, along with over 100 supporting references (made of record in the Preliminary Amendment of March 9, 2007), to show that mRNA expression correlates well with protein levels, in general.

Even if a *prima facie* case of lack of utility has been established, it should be withdrawn on consideration of the totality of evidence

Even if one assumes *arguendo* that it is more likely than not that there is no correlation between gene amplification and increased mRNA/protein expression, which Appellants submit is

not true, a polypeptide encoded by a gene that is amplified in cancer would **still** have a specific, substantial, and credible utility. In support, Appellants respectfully draw the Board's attention to page 2 of the Declaration of Dr. Avi Ashkenazi (submitted with the Response filed January 18, 2005) which explains that,

> even when amplification of a cancer marker gene does not result in significant over-expression of the corresponding gene product, this very absence of gene product over-expression still provides significant information for cancer diagnosis and treatment. Thus, if over-expression of the gene product does not parallel gene amplification in certain tumor types but does so in others, then parallel monitoring of gene amplification and gene product over-expression enables more accurate tumor classification and hence better determination of suitable therapy. In addition, absence of over-expression is crucial information for the practicing clinician. If a gene is amplified but the corresponding gene product is not over-expressed, the clinician accordingly will decide not to treat a patient with agents that target that gene product.

Appellants thus submit that simultaneous testing of gene amplification and gene product over-expression enables more accurate tumor classification, even if the gene-product, the protein, is not over-expressed. This leads to better determination of a suitable therapy. Further, as explained in Dr. Ashkenazi's Declaration, absence of over-expression of the protein itself is crucial information for the practicing clinician. If a gene is amplified in a tumor, but the corresponding gene product is not over-expressed, the clinician will decide not to treat a patient with agents that target that gene product. This not only saves money, but also has the benefit that the patient can avoid exposure to the side effects associated with such agents.

This utility is further supported by the teachings of the article by Hanna and Mornin. (Pathology Associates Medical Laboratories, August (1999); submitted with the Response filed January 18, 2005). The article teaches that the HER-2/neu gene has been shown to be amplified and/or over-expressed in 10%-30% of invasive breast cancers and in 40%-60% of intraductal breast carcinomas. Further, the article teaches that diagnosis of breast cancer includes testing both the amplification of the HER-2/neu gene (by FISH) as well as the over-expression of the HER-2/neu gene product (by IHC). Even when the protein is not over-expressed, the assay relying on both tests leads to a more accurate classification of the cancer and a more effective treatment of it.

Hanna *et al.* clearly state that gene amplification (as measured by FISH) and polypeptide expression (as measured by immunohistochemistry, IHC) are well correlated ("in general, FISH and IHC results correlate well" (Hanna *et al.* p. 1, col. 2)). It is only a subset of tumors which show discordant results. Thus Hanna *et al.* support Appellants' position that it is more likely than not that gene amplification correlates with increased polypeptide expression.

Appellants have clearly shown that the gene encoding the PRO1788 polypeptide is amplified in at least eight colon tumors. Therefore, the PRO1788 gene, similar to the HER-2/neu gene disclosed in Hanna *et al.*, is a tumor associated gene. Furthermore, as discussed above, in the majority of amplified genes, the teachings in the art overwhelmingly show that gene amplification influences gene expression at the mRNA and protein levels. Therefore, one of skill in the art would reasonably expect in this instance, based on the amplification data for the PRO1788 gene, that the PRO1788 polypeptide is concomitantly overexpressed.

However, even if gene amplification does not result in overexpression of the gene product (*i.e.*, the protein) an analysis of the expression of the protein is useful in determining the course of treatment, as supported by the Ashkenazi Declaration and the Hanna paper. The Examiner asserts that "there is no evidence as to whether the gene products (such as the polypeptide) are over-expressed or not." (Page 4 of the instant Office Action). The Examiner appears to view the testing described in the Ashkenazi Declaration and the Hanna paper as experiments involving further characterization of the PRO1788 polypeptide itself. In fact, such testing is for the purpose of characterizing not the PRO1788 polypeptide, but the tumors in which the gene encoding PRO1788 is amplified. The PRO1788 polypeptides are therefore useful in tumor categorization, the results of which become an important tool in the hands of a physician enabling the selection of a treatment modality that holds the most promise for the successful treatment of a patient

For the reasons given above, Appellants respectfully submit that the present specification clearly describes, details and provides a patentable utility for the claimed invention. Accordingly, Appellants respectfully request reconsideration and reversal of the rejections of Claims 28-35 and 38-40 under 35 U.S.C. §101.

Thus, based on the asserted utility for PRO1788 in the diagnosis of selected lung and colon tumors, the reduction to practice of the instantly claimed protein sequence of SEQ ID

NO:77 in the present application, the disclosure of the step-by-step protocols for making chimeric PRO polypeptides, including those wherein the heterologous polypeptide is an epitope tag or an Fc region of an immunoglobulin in the specification, the disclosure of a step-by-step protocol for making and expressing PRO1788 in appropriate host cells, the step-by-step protocol for the preparation, isolation and detection of monoclonal, polyclonal and other types of antibodies against the PRO1788 protein in the specification (pages 372-380 and Examples 132-133) and the disclosure of the gene amplification assay in Example 143, the skilled artisan would know exactly how to make and use the claimed polypeptide and its antibodies for the diagnosis of lung and colon cancers. Appellants submit that based on the detailed information presented in the specification and the advanced state of the art in oncology, the skilled artisan would have found such testing routine and not 'undue'.

Therefore, Appellants respectfully request reconsideration and reversal of this outstanding rejections under 35 U.S.C. §101 and §112, First Paragraph to Claims 28-35 and 38-40.

ISSUE III: Claims 28-33 and 39-40 satisfy the written description requirement of 35 U.S.C. §112, First Paragraph

Claims 28-33 and 39-40 stand rejected under 35 U.S.C. §112, first paragraph as allegedly lacking adequate written description. In particular, the Examiner asserts that "a recitation related to DNA does not reasonably constitute a 'functional limitation' for the claimed polypeptides." The Examiner further asserts that Appellants have not described "a representative number of species that have 80-99% homology to SEQ ID NO:397, such that it is clear that they were in possession of a genus of polypeptides functionally similar to SEQ ID NO:397." (Pages 10-11 of the Office Action mailed May 10, 2005).

Claim 33

Appellants respectfully submit that Claim 33, directed to the full-length polypeptide of SEQ ID NO:397, with or without its signal peptide, meets the written description requirement under 35 U.S.C. §112, first paragraph. The Examiner has acknowledged that isolated polypeptides comprising the sequence set forth in SEQ ID NO:397 meet the written description provision of 35 U.S.C. §112, first paragraph. (Page 7 of the Office Action mailed September 16, 2004). Figure 232 of the specification discloses that the signal peptide of SEQ ID NO:397

comprises amino acid residues 1-16. Thus the specification has also described the amino acid sequence of the polypeptide of SEQ ID NO:397 lacking its associated signal peptide. Accordingly, the written description rejection does not apply to Claim 33 which does not recite any variants of SEQ ID NO:397.

Claims 28-32 and 39-40

Coupled with the general knowledge available in the art at the time of the invention, Appellants submit that the specification provides ample written support for the claimed polypeptides. Thus, based on the high percentage of sequence identity, one skilled in the art would have known at the time of the invention that the Appellants had possession of the claimed polypeptides.

A. The Legal Test for Written Description

The well-established test for sufficiency of support under the written description requirement of 35 U.S.C. §112, first paragraph is "whether the disclosure of the application as originally filed reasonably conveys to the artisan that the inventor had possession at that time of the later claimed subject matter, rather than the presence or absence of literal support in the specification for the claim language."[20,21] The adequacy of written description support is a factual issue and is to be determined on a case-by-case basis.[22] The factual determination in a written description analysis depends on the nature of the invention and the amount of knowledge imparted to those skilled in the art by the disclosure. [23,24]

In *Environmental Designs, Ltd. v. Union Oil Co.*,[25] , the Federal Circuit held, "Factors that may be considered in determining level of ordinary skill in the art include (1) the educational

---

[20] *In re Kaslow*, 707 F.2d 1366, 1374, 212 U.S.P.Q. 1089, 1096 (Fed. Cir. 1983).

[21] *See also Vas-Cath, Inc. v. Mahurkar*, 935 F.2d at 1563, 19 U.S.P.Q.2d at 1116 (Fed. Cir. 1991).

[22] *See e.g., Vas-Cath*, 935 F.2d at 1563; 19 U.S.P.Q.2d at 1116.

[23] *Union Oil v. Atlantic Richfield Co.*, 208 F.2d 989, 996 (Fed. Cir. 2000).

[24] *See also* M.P.E.P. §2163 II(A).

[25] 713 F.2d 693, 696, 218 U.S.P.Q. 865, 868 (Fed. Cir. 1983), *cert. denied*, 464 U.S. 1043 (1984).

level of the inventor; (2) type of problems encountered in the art; (3) prior art solutions to those problems; (4) rapidity with which innovations are made; (5) sophistication of the technology; and (6) educational level of active workers in the field." (Emphasis added).[26] Further, The "hypothetical 'person having ordinary skill in the art' to which the claimed subject matter pertains would, of necessity have the capability of understanding the scientific and engineering principles applicable to the pertinent art.[27, 28]

B. The Disclosure Provides Sufficient Written Description for the Claimed Invention

Appellants respectfully submit that the instant specification evidences the actual reduction to practice of the amino acid sequence of SEQ ID NO:397. Thus, the genus of polypeptides with at least 80% sequence identity to SEQ ID NO:397, would meet the requirement of 35 U.S.C. §112, first paragraph, as providing adequate written description.

Appellants respectfully submit that the instant claims are similar to the exemplary claim in Example 10 of the revised Training Manual on Written Description Guidelines issued by the U.S. Patent Office.

Example 10 of the Training Manual clearly states that the protein variants meet the requirements of 35 U.S.C. §112, first paragraph, as providing adequate written description for the claimed invention even if the specification contemplates but does not exemplify variants of the protein if: (1) the procedures for making such variant proteins is routine in the art, (2) the specification does not describe the complete structure or physical properties of the variants, although those skilled in the art would expect members of the genus to have properties similar to those of the reference sequence because of high degree of structural similarity, and (3) the variant proteins of the genus possess a significant degree of partial structure (see Claim 2 of Example 10).

---

[26] *See also* M.P.E.P. §2141.03.

[27] *Ex parte Hiyamizu*, 10 U.S.P.Q.2d 1393, 1394 (Bd. Pat. App. & Inter. 1988) (emphasis added).

[28] *See also* M.P.E.P. §2141.03.

Appellants submit that all the requirements in Example 10 are met for the variant polypeptides of Claims . In particular, Claims 28-32 and 39-40 require that the variant polypeptide of PRO1788 share a high sequence identity to SEQ ID NO:397. In addition, the procedures of making variant polypeptide of SEQ ID NO:397 are well-known in the art and described in detail in the specification. The instant specification includes extensive step-by-step guidance in the specification on how to make and prepare nucleic acids where the polypeptides have 80% to 99% identity to the polypeptide of SEQ ID NO: 397. For instance, the specification describes methods for the determination of percent identity between two amino acid sequences. In fact, the specification teaches specific parameters to be associated with the term "percent identity" as applied to the present invention. The specification further provides detailed guidance as to changes that may be made to a PRO polypeptide without adversely affecting its activity. This guidance includes a listing of exemplary and preferred substitutions for each of the twenty naturally occurring amino acids (Table 6). Accordingly, one of skill in the art could identify whether a variant PRO1788 sequence falls within the parameters of the claimed invention. Once such an amino acid sequence is identified, the specification sets forth methods for making the amino acid sequences and methods of preparing the PRO polypeptides. Appellants claim only those polypeptides which meet the stated guidelines.

Therefore, Appellants submit that the specification provides ample guidance such that one of skilled in the art would know that Appellants possessed the invention as claimed in the instant claims, at the time of filing of the application. Accordingly, Appellants respectfully request reconsideration and reversal of this outstanding rejection under 35 U.S.C. §112, first paragraph. Accordingly, Appellants respectfully request reconsideration and reversal of the written description rejection of Claims 28-32 and 39-40 under 35 U.S.C. §112, first paragraph.

CONCLUSION

For the reasons given above, Appellants submit that present specification clearly describes, details and provides a patentable utility for the claimed invention. Moreover, it is respectfully submitted that based upon this disclosed patentable utility, the present specification clearly teaches "how to use" the presently claimed polypeptide. As such, Appellants respectfully request reconsideration and reversal of the outstanding rejection of Claims 28-35 and 38-40.

The Commissioner is authorized to charge any fees which may be required, including extension fees, or credit any overpayment to Deposit Account No. **50-4634** (referencing Attorney's Docket No. **123851-181898 (GNE-2830-P1C42).**

Respectfully submitted,

Date: December 5,2008

By: _____
Christopher De Vry, Ph.D. (Reg. No. 61,425)

Goodwin Procter LLP
135 Commonwealth Drive
Menlo Park, CA 94025
T: 650.752.3100
F: 650.853.1038

VIII. CLAIMS APPENDIX

Claims on Appeal

28. An isolated polypeptide having at least 80% amino acid sequence identity to:

(a) the amino acid sequence of the polypeptide of SEQ ID NO:397;

(b) the amino acid sequence of the polypeptide of SEQ ID NO:397, lacking its associated signal peptide;

(c) the amino acid sequence of the polypeptide encoded by the full-length coding sequence of the cDNA deposited under ATCC accession number 203480;

29. The isolated polypeptide of Claim 28 having at least 85% amino acid sequence identity to:

(a) the amino acid sequence of the polypeptide of SEQ ID NO:397;

(b) the amino acid sequence of the polypeptide of SEQ ID NO:397, lacking its associated signal peptide;

(c) the amino acid sequence of the polypeptide encoded by the full-length coding sequence of the cDNA deposited under ATCC accession number 203480;

30. The isolated polypeptide of Claim 28 having at least 90% amino acid sequence identity to:

(a) the amino acid sequence of the polypeptide of SEQ ID NO:397;

(b) the amino acid sequence of the polypeptide of SEQ ID NO:397, lacking its associated signal peptide;

(c) the amino acid sequence of the polypeptide encoded by the full-length coding sequence of the cDNA deposited under ATCC accession number 203480;

31. The isolated polypeptide of Claim 28 having at least 95% amino acid sequence identity to:

(a) the amino acid sequence of the polypeptide of SEQ ID NO:397;

(b) the amino acid sequence of the polypeptide of SEQ ID NO:397, lacking its associated signal peptide;

(c) the amino acid sequence of the polypeptide encoded by the full-length coding sequence of the cDNA deposited under ATCC accession number 203480;

32. The isolated polypeptide of Claim 28 having at least 99% amino acid sequence identity to:

(a) the amino acid sequence of the polypeptide of SEQ ID NO:397;

(b) the amino acid sequence of the polypeptide of SEQ ID NO:397, lacking its associated signal peptide;

(c) the amino acid sequence of the polypeptide encoded by the full-length coding sequence of the cDNA deposited under ATCC accession number 203480;

33. An isolated polypeptide comprising:

(a) the amino acid sequence of the polypeptide of SEQ ID NO:397;

(b) the amino acid sequence of the polypeptide of SEQ ID NO:397, lacking its associated signal peptide;

(c) the amino acid sequence of the polypeptide encoded by the full-length coding sequence of the cDNA deposited under ATCC accession number 203480.

34. The isolated polypeptide of Claim 33 comprising the amino acid sequence of the polypeptide of SEQ ID NO:397.

35. The isolated polypeptide of Claim 33 comprising the amino acid sequence of the polypeptide of SEQ ID NO:397, lacking its associated signal peptide.

36. The isolated polypeptide of Claim 33 comprising the amino acid sequence of the extracellular domain of the polypeptide of SEQ ID NO:397.

38. The isolated polypeptide of Claim 33 comprising the amino acid sequence of the polypeptide encoded by the full-length coding sequence of the cDNA deposited under ATCC accession number 203480.

39. A chimeric polypeptide comprising a polypeptide according to Claim 28 fused to a heterologous polypeptide.

40. The chimeric polypeptide of Claim 39, wherein said heterologous polypeptide is an epitope tag or an Fc region of an immunoglobulin.

IX. EVIDENCE APPENDIX

1. Declaration of Audrey Goddard, Ph.D. under 35 C.F.R. §1.132, with attached Exhibits A-G:

   A. Curriculum Vitae of Audrey D. Goddard, Ph.D.
   B. Higuchi, R. *et al.*, "Simultaneous amplification and detection of specific DNA sequences," *Biotechnology* 10:413-417 (1992).
   C. Livak, K.J., *et al.*, "Oligonucleotides with fluorescent dyes at opposite ends provide a quenched probe system useful for detecting PCR product and nucleic acid hybridization," *PCR Methods Appl.* 4:357-362 (1995).
   D. Heid, C.A. *et al.*, "Real time quantitative PCR," *Genome Res.* 6:986-994 (1996).
   E. Pennica, D. *et al.*, "WISP genes are members of the connective tissue growth factor family that are up-regulated in Wnt-1-transformed cells and aberrantly expressed in human lung tumors," *Proc. Natl. Acad. Sci. USA* 95:14717-14722 (1998).
   F. Pitti, R.M. *et al.*, "Genomic amplification of a decoy receptor for Fas ligand in lung and lung cancer," *Nature* 396:699-703 (1998).
   G. Bieche, I. *et al.*, "Novel approach to quantitative polymerase chain reaction using real-time detection: Application to the detection of gene amplification in breast cancer," *Int. J. Cancer* 78:661-666 (1998).

2. Declaration of Avi Ashkenazi, Ph.D. under 35 C.F.R. §1.132, with attached Exhibit A (Curriculum Vitae).

3. Declaration of Paul Polakis, Ph.D. under 37 C.F.R. §1.132.

4. Hyman, E., *et al.*, "Impact of DNA Amplification on Gene Expression Patterns in Breast Cancer," *Cancer Research* 62:6240-6245 (2002).

5. Pollack, J.R., *et al.*, "Microarray Analysis Reveals a Major Direct Role of DNA Copy Number Alteration in the Transcriptional Program of Human Breast Tumors," *Proc. Natl. Acad. Sci. USA* 99:12963-12968 (2002).

6. Hanna *et al.*, "HER-2/neu Breast Cancer Predictive Testing," Pathology Associates Medical Laboratories (1999).

7. Orntoft, T.F., *et al.* Molecular & Cellular Proteomics – 1:37-45 (2002).

8. Hu, Y. et al., "Analysis of genomic and proteomic data using advanced literature mining," *Journal of Proteome Research* **2**:405-412 (2003).

9. Pennica, D. *et al.*, "WISP genes are members of the connective tissue growth factor family that are up-regulated in Wnt-1-transformed cells and aberrantly expressed in human colon tumors," Proc. Natl. Acad. Sci. USA 83: 4049-52 (1986)

10. Konopka *et al.*, "Variable Expression of the Translocated c-abl oncogene in Philadelphia-chromosome-positive B-lymphoid cell lines from chronic myelogenous leukemia patients" *Proc. Natl. Acad. Sci. USA* 83: 4049-52, (1986).

11. Chen *et al.*, "Discordant Proein and mRNA Expression in Lung Adenocarcinomas", 304 Molecular & Cellular Proteomics 1.4, The American Society for Biochemistry and Molecular Biology, Inc., (2002).

12. Lewin *et al.*, "VI Genes", Oxford University Press, (1997).

13. Futcher et al., "A Sampling of the Yeast Proteome", (1999).

Items 1-7 were submitted with Appellants' Response filed January 18, 2005, and were considered by the Examiner as indicated in the Final Office Action mailed April 28, 2005.

Item 8 was made of record by the Examiner in the Office Action mailed May 10, 2005.

Items 9-10 were made of record by the Examiner in the Office Action mailed March 10, 2008.

Items 11-13 were made of record by the Examiner in the Office Action mailed March 10, 2008.

X. RELATED PROCEEDINGS APPENDIX

None.

LIBC/3463872.1

OIPE IAP3
DEC 05 2008
PATENT & TRADEMARK OFFICE

PATENT

IN THE UNITED STATES PATENT AND TRADEMARK OFFICE

In re Application of: Ashkenazi et al. Serial No.: 09/903,925 Filed: July 11, 2001 For: SECRETED AND TRANSMEMBRANE POLYPEPTIDES AND NUCLEIC ACIDS	Group Art Unit: 1647 Examiner: Fozia Hamid CERTIFICATE OF MAILING I hereby certify that this correspondence is being deposited with the United States Postal Service with sufficient postage as first class mail in an envelope addressed to: Assistant Commissioner of Patents, Washington, D.C. 20231 on Date

DECLARATION OF AUDREY D. GODDARD, Ph.D UNDER 37 C.F.R. § 1.132

Assistant Commissioner of Patents
Washington, D.C. 20231

Sir:

I, Audrey D. Goddard, Ph.D. do hereby declare and say as follows:

1. I am a Senior Clinical Scientist at the Experimental Medicine/BioOncology, Medical Affairs Department of Genentech, Inc., South San Francisco, California 94080.

2. Between 1993 and 2001, I headed the DNA Sequencing Laboratory at the Molecular Biology Department of Genentech, Inc. During this time, my responsibilities included the identification and characterization of genes contributing to the oncogenic process, and determination of the chromosomal localization of novel genes.

3. My scientific Curriculum Vitae, including my list of publications, is attached to and forms part of this Declaration (Exhibit A).

4. I am familiar with a variety of techniques known in the art for detecting and quantifying the amplification of oncogenes in cancer, including the quantitative TaqMan PCR (i.e., "gene amplification") assay described in the above captioned patent application.

5. The TaqMan PCR assay is described, for example, in the following scientific publications: Higuchi *et al.*, Biotechnology 10:413-417 (1992) (Exhibit B); Livak *et al.*, PCR Methods Appl., 4:357-362 (1995) (Exhibit C) and Heid *et al.*, Genome Res. 6:986-994 (1996) (Exhibit D). Briefly, the assay is based on the principle that successful PCR yields a fluorescent signal due to Taq DNA polymerase-mediated exonuclease digestion of a fluorescently labeled oligonucleotide that is homologous to a sequence between two PCR primers. The extent of digestion depends directly on the amount of PCR, and can be quantified accurately by measuring the increment in fluorescence that results from decreased energy transfer. This is an extremely sensitive technique, which allows detection in the exponential phase of the PCR reaction and, as a result, leads to accurate determination of gene copy number.

6. The quantitative fluorescent TaqMan PCR assay has been extensively and successfully used to characterize genes involved in cancer development and progression. Amplification of protooncogenes has been studied in a variety of human tumors, and is widely considered as having etiological, diagnostic and prognostic significance. This use of the quantitative TaqMan PCR assay is exemplified by the following scientific publications: Pennica *et al.*, Proc. Natl. Acad. Sci. USA 95(25):14717-14722 (1998) (Exhibit E); Pitti *et al.*, Nature 396(6712):699-703 (1998) (Exhibit F) and Bieche *et al.*, Int. J. Cancer 78:661-666 (1998) (Exhibit G), the first two of which I am co-author. In particular, Pennica *et al.* have used the quantitative TaqMan PCR assay to study relative gene amplification of WISP and c-myc in various cell lines, colorectal tumors and normal mucosa. Pitti *et al.* studied the genomic amplification of a decoy receptor for Fas ligand in lung and colon cancer, using the quantitative TaqMan PCR assay. Bieche *et al.* used the assay to study gene amplification in breast cancer.

7. It is my personal experience that the quantitative TaqMan PCR technique is technically sensitive enough to detect at least a 2-fold increase in gene copy number relative to control. It is further my considered scientific opinion that an at least 2-fold increase in gene copy number in a tumor tissue sample relative to a normal (i.e., non-tumor) sample is significant and useful in that the detected increase in gene copy number in the tumor sample relative to the normal sample serves as a basis for using relative gene copy number as quantitated by the TaqMan PCR technique as a diagnostic marker for the presence or absence of tumor in a tissue sample of unknown pathology. Accordingly, a gene identified as being amplified at least 2-fold by the quantitative TaqMan PCR assay in a tumor sample relative to a normal sample is useful as a marker for the diagnosis of cancer, for monitoring cancer development and/or for measuring the efficacy of cancer therapy.

8. I declare further that all statements made herein of my own knowledge are true and that all statements made on information and belief are believed to be true. I declare that these statements were made with the knowledge that willful false statements and the like so made are punishable by fine or imprisonment, or both, under Section 1001 of Title 18 of the United States Code, and that such willful false statements may jeopardize the validity of the application or any patent issuing thereon.

Jan. 16, 2003
Date

Audrey Goddard
Audrey D. Goddard, Ph.D.

AUDREY D. GODDARD, Ph.D.

Genentech, Inc.
1 DNA Way
South San Francisco, CA, 94080
650.225.6429
goddarda@gene.com

110 Congo St.
San Francisco, CA, 94131
415.841.9154
415.819.2247 (mobile)
agoddard@pacbell.net

PROFESSIONAL EXPERIENCE

Genentech, Inc. **1993-present**
South San Francisco, CA

2001 - present **Senior Clinical Scientist**
Experimental Medicine / BioOncology, Medical Affairs

Responsibilities:
- *Companion diagnostic oncology products*
- *Acquisition of clinical samples from Genentech's clinical trials for translational research*
- *Translational research using clinical specimen and data for drug development and diagnostics*
- *Member of Development Science Review Committee, Diagnostic Oversight Team, 21 CFR Part 11 Subteam*

Interests:
- *Ethical and legal implications of experiments with clinical specimens and data*
- *Application of pharmacogenomics in clinical trials*

1998 - 2001 **Senior Scientist**
Head of the DNA Sequencing Laboratory, Molecular Biology Department, Research

Responsibilities:
- *Management of a laboratory of up to nineteen –including postdoctoral fellow, associate scientist, senior research associate and research assistants/associate levels*
- *Management of a $750K budget*
- *DNA sequencing core facility supporting a 350+ person research facility.*
- *DNA sequencing for high throughput gene discovery, - ESTs, cDNAs, and constructs*
- *Genomic sequence analysis and gene identification*
- *DNA sequence and primary protein analysis*

Research:
- *Chromosomal localization of novel genes*
- *Identification and characterization of genes contributing to the oncogenic process*
- *Identification and characterization of genes contributing to inflammatory diseases*
- *Design and development of schemes for high throughput genomic DNA sequence analysis*
- *Candidate gene prediction and evaluation*

1993 - 1998 Scientist
Head of the DNA Sequencing Laboratory, Molecular Biology Department, Research

Responsibilities
- *DNA sequencing core facility supporting a 350+ person research facility*
- *Assumed responsibility for a pre-existing team of five technicians and expanded the group into fifteen, introducing a level of middle management and additional areas of research*
- *Participated in the development of the basic plan for high throughput secreted protein discovery program – sequencing strategies, data analysis and tracking, database design*
- *High throughput EST and cDNA sequencing for new gene identification.*
- *Design and implementation of analysis tools required for high throughput gene identification.*
- *Chromosomal localization of genes encoding novel secreted proteins.*

Research:
- *Genomic sequence scanning for new gene discovery.*
- *Development of signal peptide selection methods.*
- *Evaluation of candidate disease genes.*
- *Growth hormone receptor gene SNPs in children with Idiopathic short stature*

Imperial Cancer Research Fund **1989-1992**
London, UK with Dr. Ellen Solomon

6/89 –12/92 Postdoctoral Fellow
- Cloning and characterization of the genes fused at the acute promyelocytic leukemia translocation breakpoints on chromosomes 17 and 15.
- Prepared a successfully funded European Union multi-center grant application

McMaster University **1983**
Hamilton, Ontario, Canada with Dr. G. D. Sweeney

5/83 – 8/83: NSERC Summer Student
- *In vitro* metabolism of β-naphthoflavone in C57Bl/6J and DBA mice

EDUCATION

Ph.D. "Phenotypic and genotypic effects of mutations in the human retinoblastoma gene." **Supervisor:** Dr. R. A. Phillips	University of Toronto Toronto, Ontario, Canada. Department of Medical Biophysics.	1989
Honours B.Sc "The *in vitro* metabolism of the cytochrome P-448 inducer β-naphthoflavone in C57BL/6J mice." **Supervisor:** Dr. G. D. Sweeney	McMaster University, Hamilton, Ontario, Canada. Department of Biochemistry	1983

ACADEMIC AWARDS

Imperial Cancer Research Fund Postdoctoral Fellowship	1989-1992
Medical Research Council Studentship	1983-1988
NSERC Undergraduate Summer Research Award	1983
Society of Chemical Industry Merit Award (Hons. Biochem.)	1983
Dr. Harry Lyman Hooker Scholarship	1981-1983
J.L.W. Gill Scholarship	1981-1982
Business and Professional Women's Club Scholarship	1980-1981
Wyerhauser Foundation Scholarship	1979-1980

INVITED PRESENTATIONS

Genentech's gene discovery pipeline: High throughput identification, cloning and characterization of novel genes. Functional Genomics: From Genome to Function, Litchfield Park, AZ, USA. October 2000

High throughput identification, cloning and characterization of novel genes. G2K:Back to Science, Advances in Genome Biology and Technology I. Marco Island, FL, USA. February 2000

Quality control in DNA Sequencing: The use of Phred and Phrap. Bay Area Sequencing Users Meeting, Berkeley, CA, USA. April 1999

High throughput secreted protein identification and cloning. Tenth International Genome Sequencing and Analysis Conference, Miami, FL, USA. September 1998

The evolution of DNA sequencing: The Genentech perspective. Bay Area Sequencing Users Meeting, Berkeley, CA, USA. May 1998

Partial Growth Hormone Insensitivity: The role of GH-receptor mutations in Idiopathic Short Stature. Tenth Annual National Cooperative Growth Study Investigators Meeting, San Francisco, CA, USA. October, 1996

Growth hormone (GH) receptor defects are present in selected children with non-GH-deficient short stature: A molecular basis for partial GH-insensitivity. 76th Annual Meeting of The Endocrine Society, Anaheim, CA, USA. June 1994

A previously uncharacterized gene, myl, is fused to the retinoic acid receptor alpha gene in acute promyelocytic leukemia. XV International Association for Comparative Research on Leukemia and Related Disease, Padua, Italy. October 1991

PATENTS

Goddard A, Godowski PJ, Gurney AL. NL2 Tie ligand homologue polypeptide. Patent Number: 6,455,496. Date of Patent: Sept. 24, 2002.

Goddard A, Godowski PJ and Gurney AL. NL3 Tie ligand homologue nucleic acids. Patent Number: 6,426,218. Date of Patent: July 30, 2002.

Godowski P, Gurney A, Hillan KJ, Botstein D, **Goddard A**, Roy M, Ferrara N, Tumas D, Schwall R. NL4 Tie ligand homologue nucleic acid. Patent Number: 6,4137,770. Date of Patent: July 2, 2002.

Ashkenazi A, Fong S, **Goddard A**, Gurney AL, Napier MA, Tumas D, Wood WI. Nucleic acid encoding A-33 related antigen poly peptides. Patent Number: 6,410,708. Date of Patent:: Jun. 25, 2002.

Botstein DA, Cohen RL, **Goddard AD**, Gurney AL, Hillan KJ, Lawrence DA, Levine AJ, Pennica D, Roy MA and Wood WI. WISP polypeptides and nucleic acids encoding same. Patent Number: 6,387,657. Date of Patent: May 14, 2002.

Goddard A, Godowski PJ and Gurney AL. Tie ligands. Patent Number: 6,372,491. Date of Patent: April 16, 2002.

Godowski PJ, Gurney AL, **Goddard A** and Hillan K. TIE ligand homologue antibody. Patent Number: 6,350,450. Date of Patent: Feb. 26, 2002.

Fong S, Ferrara N, **Goddard** A, Godowski PJ, Gurney AL, Hillan K and Williams PM. Tie receptor tyrosine kinase ligand homologues. Patent Number: 6,348,351. Date of Patent: Feb. 19, 2002.

Goddard A, Godowski PJ and Gurney AL. Ligand homologues. Patent Number: 6,348,350. Date of Patent: Feb. 19, 2002.

Attie KM, Carlsson LMS, Gesundheit N and **Goddard A**. Treatment of partial growth hormone insensitivity syndrome. Patent Number: 6,207,640. Date of Patent: March 27, 2001.

Fong S, Ferrara N, **Goddard A**, Godowski PJ, Gurney AL, Hillan K and Williams PM. Nucleic acids encoding NL-3. Patent Number: 6,074,873. Date of Patent: June 13, 2000

Attie K, Carlsson LMS, Gesunheit N and **Goddard A**. Treatment of partial growth hormone insensitivity syndrome. Patent Number: 5,824,642. Date of Patent: October 20, 1998

Attie K, Carlsson LMS, Gesunheit N and **Goddard A**. Treatment of partial growth hormone insensitivity syndrome. Patent Number: 5,646,113. Date of Patent: July 8, 1997

Multiple additional provisional applications filed

PUBLICATIONS

Seshasayee D, Dowd P, Gu Q, Erickson S, **Goddard AD** Comparative sequence analysis of the *HER2* locus in mouse and man. Manuscript in preparation.

Abuzzahab MJ, **Goddard A**, Grigorescu F, Lautier C, Smith RJ and Chernausek SD. Human IGF-1 receptor mutations resulting in pre- and post-natal growth retardation. Manuscript in preparation.

Aggarwal S, Xie, M-H, Foster J, Frantz G, Stinson J, Corpuz RT, Simmons L, Hillan K, Yansura DG, Vandlen RL, **Goddard AD** and Gurney AL. FHFR, a novel receptor for the fibroblast growth factors. Manuscript submitted.

Adams SH, Chui C, Schilbach SL, Yu XX, **Goddard AD**, Grimaldi JC, Lee J, Dowd P, Colman S., Lewin DA. (2001) BFIT, a unique acyl-CoA thioesterase induced in thermogenic brown adipose tissue: Cloning, organization of the human gene, and assessment of a potential link to obesity. *Biochemical Journal* **360**: 135-142.

Lee J. Ho WH. Maruoka M. Corpuz RT. Baldwin DT. Foster JS. **Goddard AD**. Yansura DG. Vandlen RL. Wood WI. Gurney AL. (2001) IL-17E, a novel proinflammatory ligand for the IL-17 receptor homolog IL-17Rh1. *Journal of Biological Chemistry* **276**(2): 1660-1664.

Xie M-H, Aggarwal S, Ho W-H, Foster J, Zhang Z, Stinson J, Wood WI, **Goddard AD** and Gurney AL. (2000) Interleukin (IL)-22, a novel human cytokine that signals through the interferon-receptor related proteins CRF2-4 and IL-22R. *Journal of Biological Chemistry* **275**: 31335-31339.

Weiss GA, Watanabe CK, Zhong A, **Goddard A** and Sidhu SS. (2000) Rapid mapping of protein functional epitopes by combinatorial alanine scanning. *Proc. Natl. Acad. Sci. USA* **97**: 8950-8954.

Guo S, Yamaguchi Y, Schilbach S, Wada T.;Lee J, **Goddard A**, French D , Handa H, Rosenthal A. (2000) A regulator of transcriptional elongation controls vertebrate neuronal development. *Nature* **408**: 366-369.

Yan M, Wang L-C, Hymowitz SG, Schilbach S, Lee J, **Goddard A**, de Vos AM, Gao WQ, Dixit VM. (2000) Two-amino acid molecular switch in an epithelial morphogen that regulates binding to two distinct receptors. *Science* **290**: 523-527.

Sehl PD, Tai JTN, Hillan KJ, Brown LA, **Goddard A**, Yang R, Jin H and Lowe DG. (2000) Application of cDNA microarrays in determining molecular phenotype in cardiac growth, development, and response to injury. *Circulation* **101**: 1990-1999.

Guo S, Brush J, Teraoka H, **Goddard A**, Wilson SW, Mullins MC and Rosenthal A. (1999) Development of noradrenergic neurons in the zebrafish hindbrain requires BMP, FGF8, and the homeodomain protein soulless/Phox2A. *Neuron* **24**: 555-566.

Stone D, Murone, M, Luoh, S, Ye W, Armanini P, Gurney A, Phillips HS, Brush, J, **Goddard A**, de Sauvage FJ and Rosenthal A. (1999) Characterization of the human suppressor of fused; a negative regulator of the zinc-finger transcription factor Gli. *J. Cell Sci.* **112**: 4437-4448.

Xie M-H, Holcomb I, Deuel B, Dowd P, Huang A, Vagts A, Foster J, Liang J, Brush J, Gu Q, Hillan K, **Goddard A** and Gurney, A.L. (1999) FGF-19, a novel fibroblast growth factor with unique specificity for FGFR4. *Cytokine* **11**: 729-735.

Yan M, Lee J, Schilbach S, **Goddard A** and Dixit V. (1999) mE10, a novel caspase recruitment domain-containing proapoptotic molecule. *J. Biol. Chem.* **274**(15): 10287-10292.

Gurney AL, Marsters SA, Huang RM, Pitti RM, Mark DT, Baldwin DT, Gray AM, Dowd P, Brush J, Heldens S, Schow P, **Goddard AD**, Wood WI, Baker KP, Godowski PJ and Ashkenazi A. (1999) Identification of a new member of the tumor necrosis factor family and its receptor, a human ortholog of mouse GITR. *Current Biology* **9**(4): 215-218.

Ridgway JBB, Ng E, Kern JA ,Lee J, Brush J, **Goddard A** and Carter P. (1999) Identification of a human anti-CD55 single-chain Fv by subtractive panning of a phage library using tumor and nontumor cell lines. *Cancer Research* 59: 2718-2723.

Pitti RM, Marsters SA, Lawrence DA, Roy M, Kischkel FC, Dowd P, Huang A, Donahue CJ, Sherwood SW, Baldwin DT, Godowski PJ, Wood WI, Gurney AL, Hillan KJ, Cohen RL, **Goddard AD**, Botstein D and Ashkenazi A. (1998) Genomic amplification of a decoy receptor for Fas ligand in lung and colon cancer. *Nature* **396**(6712): 699-703.

Pennica D, Swanson TA, Welsh JW, Roy MA, Lawrence DA, Lee J, Brush J, Taneyhill LA, Deuel B, Lew M, Watanabe C, Cohen RL, Melhem MF, Finley GG, Quirke P, **Goddard AD**, Hillan KJ, Gurney AL, Botstein D and Levine AJ. (1998) WISP genes are members of the connective tissue growth factor family that are up-regulated in wnt-1-transformed cells and aberrantly expressed in human colon tumors. *Proc. Natl. Acad. Sci. USA.* **95**(25): 14717-14722.

Yang RB, Mark MR, Gray A, Huang A, Xie MH, Zhang M, **Goddard A**, Wood WI, Gurney AL and Godowski PJ. (1998) Toll-like receptor-2 mediates lipopolysaccharide-induced cellular signalling. *Nature* **395**(6699): 284-288.

Merchant AM, Zhu Z, Yuan JQ, **Goddard A**, Adams CW, Presta LG and Carter P. (1998) An efficient route to human bispecific IgG. *Nature Biotechnology* **16**(7): 677-681.

Marsters SA, Sheridan JP, Pitti RM, Brush J, **Goddard A** and Ashkenazi A. (1998) Identification of a ligand for the death-domain-containing receptor Apo3. *Current Biology* **8**(9): 525-528.

Xie J, Murone M, Luoh SM, Ryan A, Gu Q, Zhang C, Bonifas JM, Lam CW, Hynes M, **Goddard A,** Rosenthal A, Epstein EH Jr. and de Sauvage FJ. (1998) Activating Smoothened mutations in sporadic basal-cell carcinoma. *Nature*. **391**(6662): 90-92.

Marsters SA, Sheridan JP, Pitti RM, Huang A, Skubatch M, Baldwin D, Yuan J, Gurney A, **Goddard AD**, Godowski P and Ashkenazi A. (1997) A novel receptor for Apo2L/TRAIL contains a truncated death domain. *Current Biology*. **7**(12): 1003-1006.

Hynes M, Stone DM, Dowd M, Pitts-Meek S, **Goddard A**, Gurney A and Rosenthal A. (1997) Control of cell pattern in the neural tube by the zinc finger transcription factor *Gli-1. Neuron* **19**: 15–26.

Sheridan JP, Marsters SA, Pitti RM, Gurney A., Skubatch M, Baldwin D, Ramakrishnan L, Gray CL, Baker K, Wood WI, **Goddard AD**, Godowski P, and Ashkenazi A. (1997) Control of TRAIL-Induced Apoptosis by a Family of Signaling and Decoy Receptors. *Science* **277** (5327): 818-821.

Goddard AD, Dowd P, Chernausek S, Geffner M, Gertner J, Hintz R, Hopwood N, Kaplan S, Plotnick L, Rogol A, Rosenfield R, Saenger P, Mauras N, Hershkopf R, Angulo M and Attie, K. (1997) Partial growth hormone insensitivity: The role of growth hormone receptor mutations in idiopathic short stature. *J. Pediatr.* **131**: S51-55.

Klein RD, Sherman D, Ho WH, Stone D, Bennett GL, Moffat B, Vandlen R, Simmons L, Gu Q, Hongo JA, Devaux B, Poulsen K, Armanini M, Nozaki C, Asai N, **Goddard A**, Phillips H, Henderson CE, Takahashi M and Rosenthal A. (1997) A GPI-linked protein that interacts with Ret to form a candidate neurturin receptor. *Nature*. **387**(6634): 717-21.

Stone DM, Hynes M, Armanini M, Swanson TA, Gu Q, Johnson RL, Scott MP, Pennica D, **Goddard A**, Phillips H, Noll M, Hooper JE, de Sauvage F and Rosenthal A. (1996) The tumour-suppressor gene patched encodes a candidate receptor for Sonic hedgehog. *Nature* **384**(6605): 129-34.

Marsters SA, Sheridan JP, Donahue CJ, Pitti RM, Gray CL, **Goddard AD**, Bauer KD and Ashkenazi A. (1996) Apo-3, a new member of the tumor necrosis factor receptor family, contains a death domain and activates apoptosis and NF-kappa β. *Current Biology* **6**(12): 1669-76.

Rothe M, Xiong J, Shu HB, Williamson K, **Goddard A** and Goeddel DV. (1996) I-TRAF is a novel TRAF-interacting protein that regulates TRAF-mediated signal transduction. *Proc. Natl. Acad. Sci. USA* **93**: 8241-8246.

Yang M, Luoh SM, **Goddard A**, Reilly D, Henzel W and Bass S. (1996) The bglX gene located at 47.8 min on the Escherichia coli chromosome encodes a periplasmic beta-glucosidase. *Microbiology* **142**: 1659-65.

Goddard AD and Black DM. (1996) Familial Cancer in Molecular Endocrinology of Cancer. Waxman, J. Ed. Cambridge University Press, Cambridge UK, pp.187-215.

Treanor JJS, Goodman L, de Sauvage F, Stone DM, Poulson KT, Beck CD, Gray C, Armanini MP, Pollocks RA, Hefti F, Phillips HS, **Goddard A**, Moore MW, Buj-Bello A, Davis AM, Asai N, Takahashi M, Vandlen R, Henderson CE and Rosenthal A. (1996) Characterization of a receptor for GDNF. *Nature* **382**: 80-83.

Klein RD, Gu Q, **Goddard A** and Rosenthal A. (1996) Selection for genes encoding secreted proteins and receptors. *Proc. Natl. Acad. Sci. USA* **93**: 7108-7113.

Winslow JW, Moran P, Valverde J, Shih A, Yuan JQ, Wong SC, Tsai SP, **Goddard A**, Henzel WJ, Hefti F and Caras I. (1995) Cloning of AL-1, a ligand for an Eph-related tyrosine kinase receptor involved in axon bundle formation. *Neuron* **14**: 973-981.

Bennett BD, Zeigler FC, Gu Q, Fendly B, **Goddard AD**, Gillett N and Matthews W. (1995) Molecular cloning of a ligand for the EPH-related receptor protein-tyrosine kinase Htk. *Proc. Natl. Acad. Sci. USA* **92**: 1866-1870.

Huang X, Yuang J, **Goddard A**, Foulis A, James RF, Lernmark A, Pujol-Borrell R, Rabinovitch A, Somoza N and Stewart TA. (1995) Interferon expression in the pancreases of patients with type I diabetes. *Diabetes* **44**: 658-664.

Goddard AD, Yuan JQ, Fairbairn L, Dexter M, Borrow J, Kozak C and Solomon E. (1995) Cloning of the murine homolog of the leukemia-associated PML gene. *Mammalian Genome* **6**: 732-737.

Goddard AD, Covello R, Luoh SM, Clackson T, Attie KM, Gesundheit N, Rundle AC, Wells JA, Carlsson LMTI and The Growth Hormone Insensitivity Study Group. (1995) Mutations of the growth hormone receptor in children with idiopathic short stature. *N. Engl. J. Med.* **333**: 1093-1098.

Kuo SS, Moran P, Gripp J, Armanini M, Phillips HS, **Goddard A** and Caras IW. (1994) Identification and characterization of Batk, a predominantly brain-specific non-receptor protein tyrosine kinase related to Csk. *J. Neurosci. Res.* **38**: 705-715.

Mark MR, Scadden DT, Wang Z, Gu Q, **Goddard A** and Godowski PJ. (1994) Rse, a novel receptor-type tyrosine kinase with homology to Axl/Ufo, is expressed at high levels in the brain. *Journal of Biological Chemistry* **269**: 10720-10728.

Borrow J, Shipley J, Howe K, Kiely F, **Goddard A**, Sheer D, Srivastava A, Antony AC, Fioretos T, Mitelman F and Solomon E. (1994) Molecular analysis of simple variant translocations in acute promyelocytic leukemia. *Genes Chromosomes Cancer* **9**: 234-243.

Goddard AD and Solomon E. (1993) Genetics of Cancer. *Adv. Hum. Genet.* **21**: 321-376.

Borrow J, **Goddard AD**, Gibbons B, Katz F, Swirsky D, Fioretos T, Dube I, Winfield DA, Kingston J, Hagemeijer A, Rees JKH, Lister AT and Solomon E. (1992) Diagnosis of acute promyelocytic leukemia by RT-PCR: Detection of *PML-RARA* and *RARA-PML* fusion transcripts. *Br. J. Haematol.* **82**: 529-540.

Goddard AD, Borrow J and Solomon E. (1992) A previously uncharacterized gene, PML, is fused to the retinoic acid receptor alpha gene in acute promyelocytic leukemia. *Leukemia* **6 Suppl 3**: 117S–119S.

Zhu X, Dunn JM, **Goddard AD**, Squire JA, Becker A, Phillips RA and Gallie BL. (1992) Mechanisms of loss of heterozygosity in retinoblastoma. *Cytogenet. Cell. Genet.* **59**: 248-252.

Foulkes W, **Goddard A.** and Patel K. (1991) Retinoblastoma linked with Seascale [letter]. *British Med. J.* **302**: 409.

Goddard AD, Borrow J, Freemont PS and Solomon E. (1991) Characterization of a novel zinc finger gene disrupted by the t(15;17) in acute promyelocytic leukemia. *Science* **254**: 1371-1374.

Solomon E, Borrow J and **Goddard AD.** (1991) Chromosomal aberrations in cancer. *Science* **254**: 1153-1160.

Pajunen L, Jones TA, **Goddard A**, Sheer D, Solomon E, Pihlajaniemi T and Kivirikko KI. (1991) Regional assignment of the human gene coding for a multifunctional peptide (P4HB) acting as the β–subunit of prolyl-4-hydroxylase and the enzyme protein disulfide isomerase to 17q25. *Cytogenet. Cell. Genet.* **56**: 165-168.

Borrow J, Black DM, **Goddard AD**, Yagle MK, Frischauf A.-M and Solomon E. (1991) Construction and regional localization of a *Not*I linking library from human chromosome 17q. *Genomics* **10**: 477–480.

Borrow J, **Goddard AD**, Sheer D and Solomon E. (1990) Molecular analysis of acute promyelocytic leukemia breakpoint cluster region on chromosome 17. *Science* **249**: 1577-1580.

Myers JC, Jones TA, Pohjolainen E-R, Kadri AS, **Goddard AD**, Sheer D, Solomon E and Pihlajaniemi T. (1990) Molecular cloning of 5(IV) collagen and assignment of the gene to the region of the region of the X-chromosome containing the Alport Syndrome locus. *Am. J. Hum. Genet.* **46**: 1024-1033.

Gallie BL, Squire JA, **Goddard A**, Dunn JM, Canton M, Hinton D, Zhu X and Phillips RA. (1990) Mechanisms of oncogenesis in retinoblastoma. *Lab. Invest.* **62**: 394-408.

Goddard AD, Phillips RA, Greger V, Passarge E, Hopping W, Gallie BL and Horsthemke B. (1990) Use of the RB1 cDNA as a diagnostic probe in retinoblastoma families. *Clinical Genetics* **37**: 117-126.

Zhu XP, Dunn JM, Phillips RA, **Goddard AD**, Paton KE, Becker A and Gallie BL. (1989) Germline, but not somatic, mutations of the RB1 gene preferentially involve the paternal allele. *Nature* **340**: 312-314.

Gallie BL, Dunn JM, **Goddard A**, Becker A and Phillips RA. (1988) Identification of mutations in the putative retinoblastoma gene. In Molecular Biology of The Eye: Genes, Vision and Ocular Disease. UCLA Symposia on Molecular and Cellular Biology, New Series, Volume 88. J. Piatigorsky, T. Shinohara and P.S. Zelenka, Eds. Alan R. Liss, Inc., New York, 1988, pp. 427-436.

Goddard AD, Balakier H, Canton M, Dunn J, Squire J, Reyes E, Becker A, Phillips RA and Gallie BL. (1988) Infrequent genomic rearrangement and normal expression of the putative RB1 gene in retinoblastoma tumors. *Mol. Cell. Biol.* **8**: 2082-2088.

Squire J, Dunn J, **Goddard A**, Hoffman T, Musarella M, Willard HF, Becker AJ, Gallie BL and Phillips RA. (1986) Cloning of the esterase D gene: A polymorphic gene probe closely linked to the retinoblastoma locus on chromosome 13. *Proc. Natl. Acad. Sci.* USA **83**: 6573-6577.

Squire J, **Goddard AD**, Canton M, Becker A, Phillips RA and Gallie BL (1986) Tumour induction by the retinoblastoma mutation is independent of N-*myc* expression. *Nature* **322**: 555-557.

Goddard AD, Heddle JA, Gallie BL and Phillips RA. (1985) Radiation sensitivity of fibroblasts of bilateral retinoblastoma patients as determined by micronucleus induction *in vitro*. *Mutation Research* **152**: 31-38.

RESEARCH

SIMULTANEOUS AMPLIFICATION AND DETECTION OF SPECIFIC DNA SEQUENCES

Russell Higuchi*, Gavin Dollinger[1], P. Sean Walsh and Robert Griffith

Roche Molecular Systems, Inc., 1400 53rd St., Emeryville, CA 94608. [1]Chiron Corporation, 1400 53rd St., Emeryville, CA 94608. *Corresponding author.

We have enhanced the polymerase chain reaction (PCR) such that specific DNA sequences can be detected without opening the reaction tube. This enhancement requires the addition of ethidium bromide (EtBr) to a PCR. Since the fluorescence of EtBr increases in the presence of double-stranded (ds) DNA an increase in fluorescence in such a PCR indicates a positive amplification, which can be easily monitored externally. In fact, amplification can be continuously monitored in order to follow its progress. The ability to simultaneously amplify specific DNA sequences and detect the product of the amplification both simplifies and improves PCR and may facilitate its automation and more widespread use in the clinic or in other situations requiring high sample throughput.

Although the potential benefits of PCR[1] to clinical diagnostics are well known[2,3], it is still not widely used in this setting, even though it is four years since thermostable DNA polymerases[4] made PCR practical. Some of the reasons for its slow acceptance are high cost, lack of automation of pre- and post-PCR processing steps, and false positive results from carryover-contamination. The first two points are related in that labor is the largest contributor to cost at the present stage of PCR development. Most current assays require some form of "downstream" processing once thermocycling is done in order to determine whether the target DNA sequence was present and has amplified. These include DNA hybridization[5,6], gel electrophoresis with or without use of restriction digestion[7,8], HPLC[9], or capillary electrophoresis[10]. These methods are labor-intense, have low throughput, and are difficult to automate. The third point is also closely related to downstream processing. The handling of the PCR product in these downstream processes increases the chances that amplified DNA will spread through the typing lab, resulting in a risk of "carryover" false positives in subsequent testing[11].

These downstream processing steps would be eliminated if specific amplification and detection of amplified DNA took place simultaneously within an unopened reaction vessel. Assays in which such different processes take place without the need to separate reaction components have been termed "homogeneous". No truly homogeneous PCR assay has been demonstrated to date, although progress towards this end has been reported. Chehab, et al.[12], developed a PCR product detection scheme using fluorescent primers that resulted in a fluorescent PCR product. Allele-specific primers, each with different fluorescent tags, were used to indicate the genotype of the DNA. However, the unincorporated primers must still be removed in a downstream process in order to visualize the result. Recently, Holland, et al.[13], developed an assay in which the endogenous 5′ exonuclease assay of *Taq* DNA polymerase was exploited to cleave a labeled oligonucleotide probe. The probe would only cleave if PCR amplification had produced its complementary sequence. In order to detect the cleavage products, however, a subsequent process is again needed.

We have developed a truly homogeneous assay for PCR and PCR product detection based upon the greatly increased fluorescence that ethidium bromide and other DNA binding dyes exhibit when they are bound to ds-DNA[14–16]. As outlined in Figure 1, a prototypic PCR

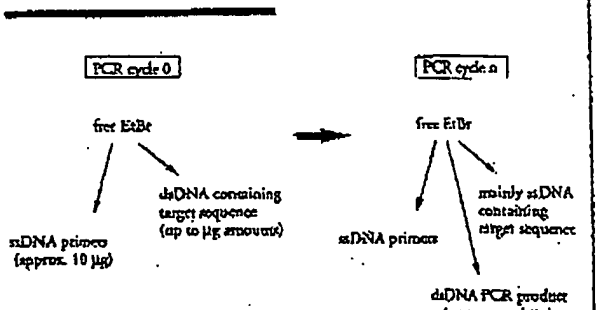

FIGURE 1 Principle of simultaneous amplification and detection of PCR product. The components of a PCR containing EtBr that are fluorescent are listed—EtBr itself, EtBr bound to either ssDNA or dsDNA. There is a large fluorescence enhancement when EtBr is bound to DNA and binding is greatly enhanced when DNA is double-stranded. After sufficient (n) cycles of PCR, the net increase in dsDNA results in additional EtBr binding, and a net increase in total fluorescence.

PAGE 2/6 * RCVD AT 7/19/2004 3:10:03 PM [Pacific Daylight Time] * SVR:SVCS01/0 * DNIS:6638 * CSID:650 952 9881 * DURATION (mm-ss):04-46

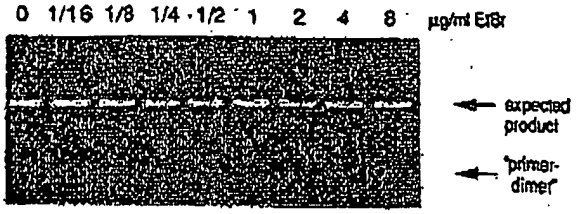

FIGURE 2 Gel electrophoresis of PCR amplification products of the human, nuclear gene, HLA DQα, made in the presence of increasing amounts of EtBr (up to 8 µg/ml). The presence of EtBr has no obvious effect on the yield or specificity of amplification.

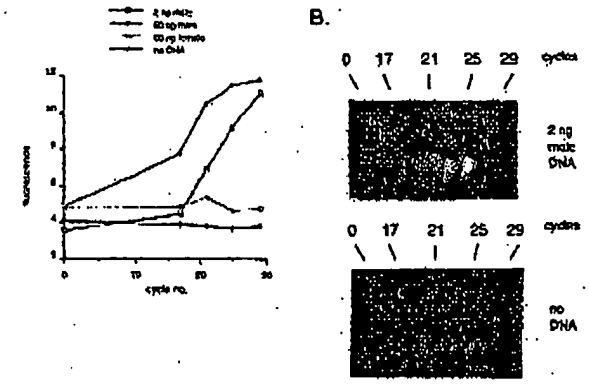

FIGURE 3 (A) Fluorescence measurements from PCRs that contain 0.5 µg/ml EtBr and that are specific for Y-chromosome repeat sequences. Five replicate PCRs were begun containing each of the DNAs specified. At each indicated cycle, one of the five replicate PCRs for each DNA was removed from thermocycling and its fluorescence measured. Units of fluorescence are arbitrary. (B) UV photography of PCR tubes (0.5 ml Eppendorf-style, polypropylene micro-centrifuge tubes) containing reactions, those starting from 2 ng male DNA and control reactions without any DNA, from (A).

begins with primers that are single-stranded DNA (ssDNA), dNTPs, and DNA polymerase. An amount of dsDNA containing the target sequence (target DNA) is also typically present. This amount can vary, depending on the application, from single-cell amounts of DNA[17] to micrograms per PCR[18]. If EtBr is present, the reagents that will fluoresce, in order of increasing fluorescence, are free EtBr itself, and EtBr bound to the single-stranded DNA primers and to the double-stranded target DNA (by its intercalation between the stacked bases of the DNA double-helix). After the first denaturation cycle, target DNA will be largely single-stranded. After a PCR is completed, the most significant change is the increase in the amount of dsDNA (the PCR product itself) of up to several micrograms. Formerly free EtBr is bound to the additional dsDNA, resulting in an increase in fluorescence. There is also some decrease in the amount of ssDNA primer, but because the binding of EtBr to ssDNA is much less than to dsDNA, the effect of this change on the total fluorescence of the sample is small. The fluorescence increase can be measured by directing excitation illumination through the walls of the amplification vessel before and after, or even continuously during, thermocycling.

RESULTS

PCR in the presence of EtBr. In order to assess the affect of EtBr in PCR, amplifications of the human HLA DQα gene[19] were performed with the dye present at concentrations from 0.06 to 8.0 µg/ml (a typical concentration of EtBr used in staining of nucleic acids following gel electrophoresis is 0.5 µg/ml). As shown in Figure 2, gel electrophoresis revealed little or no difference in the yield or quality of the amplification product whether EtBr was absent or present at any of these concentrations, indicating that EtBr does not inhibit PCR.

Detection of human Y-chromosome specific sequences. Sequence-specific, fluorescence enhancement of EtBr as a result of PCR was demonstrated in a series of amplifications containing 0.5 µg/ml EtBr and primers specific to repeat DNA sequences found on the human Y-chromosome[20]. These PCRs initially contained either 60 ng male, 60 ng female, 2 ng male human or no DNA. Five replicate PCRs were begun for each DNA. After 0, 17, 21, 24 and 29 cycles of thermocycling, a PCR for each DNA was removed from the thermocycler, and its fluorescence measured in a spectrofluorometer and plotted vs. amplification cycle number (Fig. 3A). The shape of this curve reflects the fact that by the time an increase in fluorescence can be detected, the increase in DNA is becoming linear and not exponential with cycle number. As shown, the fluorescence increased about three-fold over the background fluorescence for the PCRs containing human male DNA, but did not significantly increase for negative control PCRs, which contained either no DNA or human female DNA. The more male DNA present to begin with—60 ng versus 2 ng—the fewer cycles were needed to give a detectable increase in fluorescence. Gel electrophoresis on the products of these amplifications showed that DNA fragments of the expected size were made in the male DNA containing reactions and that little DNA synthesis took place in the control samples.

In addition, the increase in fluorescence was visualized by simply laying the completed, unopened PCRs on a UV transilluminator and photographing them through a red filter. This is shown in figure 3B for the reactions that began with 2 ng male DNA and those with no DNA.

Detection of specific alleles of the human β-globin gene. In order to demonstrate that this approach has adequate specificity to allow genetic screening, a detection of the sickle-cell anemia mutation was performed. Figure 4 shows the fluorescence from completed amplifications containing EtBr (0.5 µg/ml) as detected by photography of the reaction tubes on a UV transilluminator. These reactions were performed using primers specific for either the wild-type or sickle-cell mutation of the human β-globin gene[21]. The specificity for each allele is imparted by placing the sickle-mutation site at the terminal 3′ nucleotide of one primer. By using an appropriate primer annealing temperature, primer extension—and thus amplification—can take place only if the 3′ nucleotide of the primer is complementary to the β-globin allele present[23,22].

Each pair of amplifications shown in Figure 4 consists of a reaction with either the wild-type allele specific (left tube) or sickle-allele specific (right tube) primers. Three different DNAs were typed: DNA from a homozygous, wild-type β-globin individual (AA); from a heterozygous sickle β-globin individual (AS); and from a homozygous sickle β-globin individual (SS). Each DNA (50 ng genomic DNA to start each PCR) was analyzed in triplicate (3 pairs

of reactions each). The DNA type was reflected in the relative fluorescence intensities in each pair of completed amplifications. There was a significant increase in fluorescence only where a β-globin allele DNA matched the primer set. When measured on a spectrofluorometer (data not shown), this fluorescence was about three times that present in a PCR where both β-globin alleles were mismatched to the primer set. Gel electrophoresis (not shown) established that this increase in fluorescence was due to the synthesis of nearly a microgram of a DNA fragment of the expected size for β-globin. There was little synthesis of dsDNA in reactions in which the allele-specific primer was mismatched to both alleles.

Continuous monitoring of a PCR. Using a fiber optic device, it is possible to direct excitation illumination from a spectrofluorometer to a PCR undergoing thermocycling and to return its fluorescence to the spectrofluorometer. The fluorescence readout of such an arrangement, directed at an EtBr-containing amplification of Y-chromosome specific sequences from 25 ng of human male DNA, is shown in Figure 5. The readout from a control PCR with no target DNA is also shown. Thirty cycles of PCR were monitored for each.

The fluorescence trace as a function of time clearly shows the effect of the thermocycling. Fluorescence intensity rises and falls inversely with temperature. The fluorescence intensity is minimum at the denaturation temperature (94°C) and maximum at the annealing/extension temperature (50°C). In the negative-control PCR, these fluorescence maxima and minima do not change significantly over the thirty thermocycles, indicating that there is little dsDNA synthesis without the appropriate target DNA, and there is little if any bleaching of EtBr during the continuous illumination of the sample.

In the PCR containing male DNA, the fluorescence maxima at the annealing/extension temperature begin to increase at about 4000 seconds of thermocycling, and continue to increase with time, indicating that dsDNA is being produced at a detectable level. Note that the fluorescence minima at the denaturation temperature do not significantly increase, presumably because at this temperature there is no dsDNA for EtBr to bind. Thus the course of the amplification is followed by tracking the fluorescence increase at the annealing temperature. Analysis of the products of these two amplifications by gel electrophoresis showed a DNA fragment of the expected size for the male DNA containing sample and no detectable DNA synthesis for the control sample.

DISCUSSION

Downstream processes such as hybridization to a sequence-specific probe can enhance the specificity of DNA detection by PCR. The elimination of these processes means that the specificity of this homogeneous assay depends solely on that of PCR. In the case of sickle-cell disease, we have shown that PCR alone has sufficient DNA sequence specificity to permit genetic screening. Using appropriate amplification conditions, there is little non-specific production of dsDNA in the absence of the appropriate target allele.

The specificity required to detect pathogens can be more or less than that required to do genetic screening, depending on the number of pathogens in the sample and the amount of other DNA that must be taken with the sample. A difficult target is HIV, which requires detection of a viral genome that can be at the level of a few copies per thousands of host cells[6]. Compared with genetic screening, which is performed on cells containing at least one copy of the target sequence, HIV detection requires both more specificity and the input of more total

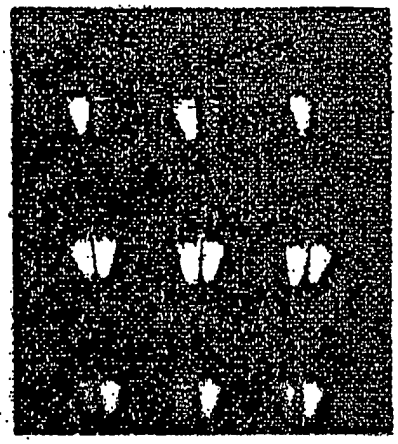

FIGURE 4 UV photography of PCR tubes containing amplifications using EtBr that are specific to wild-type (A) or sickle (S) alleles of the human β-globin gene. The left of each pair of tubes contains allele-specific primers to the wild-type alleles, the right tube primers to the sickle allele. The photograph was taken after 30 cycles of PCR, and the input DNAs and the alleles they contain are indicated. Fifty ng of DNA was used to begin PCR. Typing was done in triplicate (3 pairs of PCRs) for each input DNA.

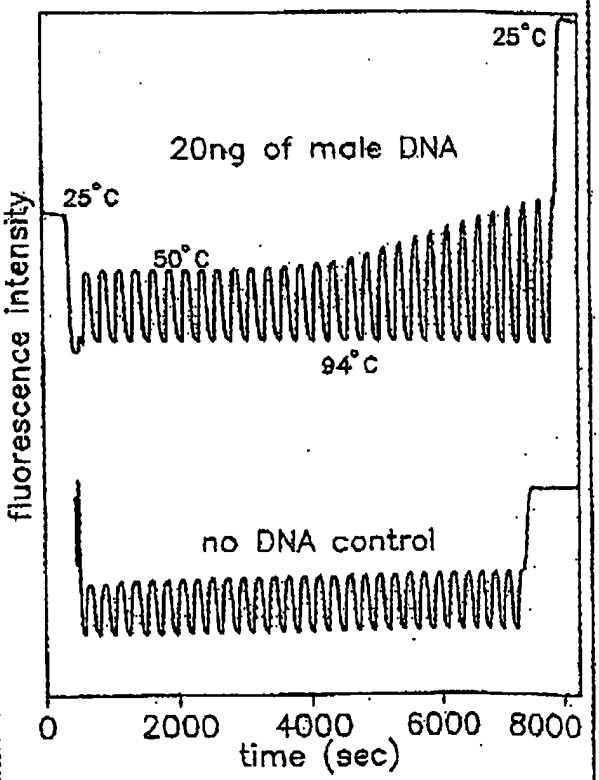

FIGURE 5 Continuous, real-time monitoring of a PCR. A fiber optic was used to carry excitation light to a PCR in progress and also emitted light back to a fluorometer (see Experimental Protocol). Amplification using human male-DNA specific primers in a PCR starting with 20 ng of human male DNA (top), or in a control PCR without DNA (bottom), were monitored. Thirty cycles of PCR were followed for each. The temperature cycled between 94°C (denaturation) and 50°C (annealing and extension). Note in the male DNA PCR, the cycle (time) dependent increase in fluorescence at the annealing/extension temperature.

DNA—up to microgram amounts—in order to have sufficient numbers of target sequences. This large amount of starting DNA in an amplification significantly increases the background fluorescence over which any additional fluorescence produced by PCR must be detected. An additional complication that occurs with targets in low copy-number is the formation of the "primer-dimer" artifact. This is the result of the extension of one primer using the other primer as a template. Although this occurs infrequently, once it occurs the extension product is a substrate for PCR amplification, and can compete with true PCR targets if those targets are rare. The primer-dimer product is of course dsDNA and thus is a potential source of false signal in this homogeneous assay.

To increase PCR specificity and reduce the effect of primer-dimer amplification, we are investigating a number of approaches, including the use of nested-primer amplifications that take place in a single tube[3], and the "hot-start", in which nonspecific amplification is reduced by raising the temperature of the reaction before DNA synthesis begins[23]. Preliminary results using these approaches suggest that primer-dimer is effectively reduced and it is possible to detect the increase in EtBr fluorescence in a PCR instigated by a single HIV genome in a background of 10^5 cells. With larger numbers of cells, the background fluorescence contributed by genomic DNA becomes problematic. To reduce this background, it may be possible to use sequence-specific DNA-binding dyes that can be made to preferentially bind PCR product over genomic DNA by incorporating the dye-binding DNA sequence into the PCR product through a 5′ "add-on" to the oligonucleotide primer[24].

We have shown that the detection of fluorescence generated by an EtBr-containing PCR is straightforward, both once PCR is completed and continuously during thermocycling. The ease with which automation of specific DNA detection can be accomplished is the most promising aspect of this assay. The fluorescence analysis of completed PCRs is already possible with existing instrumentation in 96-well format[25]. In this format, the fluorescence in each PCR can be quantitated before, after, and even at selected points during thermocycling by moving the rack of PCRs to a 96-microwell plate fluorescence reader[26].

The instrumentation necessary to continuously monitor multiple PCRs simultaneously is also simple in principle. A direct extension of the apparatus used here is to have multiple fiberoptics transmit the excitation light and fluorescent emissions to and from multiple PCRs. The ability to monitor multiple PCRs continuously may allow quantitation of target DNA copy number. Figure 3 shows that the larger the amount of starting target DNA, the sooner during PCR a fluorescence increase is detected. Preliminary experiments (Higuchi and Dollinger, manuscript in preparation) with continuous monitoring have shown a sensitivity to two-fold differences in initial target DNA concentration.

Conversely, if the number of target molecules is known—as it can be in genetic screening—continuous monitoring may provide a means of detecting false positive and false negative results. With a known number of target molecules, a true positive would exhibit detectable fluorescence by a predictable number of cycles of PCR. Increases in fluorescence detected before or after that cycle would indicate potential artifacts. False negative results due to, for example, inhibition of DNA polymerase, may be detected by including within each PCR an inefficiently amplifying marker. This marker results in a fluorescence increase only after a large number of cycles—many more than are necessary to detect a true positive. If a sample fails to have a fluorescence increase after this many cycles, inhibition may be suspected. Since, in this assay, conclusions are drawn based on the presence or absence of fluorescence signal alone, such controls may be important. In any event, before any test based on this principle is ready for the clinic, an assessment of its false positive/false negative rates will need to be obtained using a large number of known samples.

In summary, the inclusion in PCR of dyes whose fluorescence is enhanced upon binding dsDNA makes it possible to detect specific DNA amplification from outside the PCR tube. In the future, instruments based upon this principle may facilitate the more widespread use of PCR in applications that demand the high throughput of samples.

EXPERIMENTAL PROTOCOL

Human HLA-DQα gene amplifications containing EtBr. PCRs were set up in 100 µl volumes containing 10 mM Tris-HCl, pH 8.3; 50 mM KCl; 4 mM $MgCl_2$; 2.5 units of *Taq* DNA polymerase (Perkin-Elmer Cetus, Norwalk, CT); 20 pmole each of human HLA-DQα gene specific oligonucleotide primers GH26 and GH27[19] and approximately 10^3 copies of DQα PCR product diluted from a previous reaction. Ethidium bromide (EtBr; Sigma) was used at the concentrations indicated in Figure 2. Thermocycling proceeded for 20 cycles in a model 480 thermocycler (Perkin-Elmer Cetus, Norwalk, CT) using a "step-cycle" program of 94°C for 1 min. denaturation and 60°C for 30 sec. annealing and 72°C for 30 sec. extension.

Y-chromosome specific PCR. PCRs (100 µl total reaction volume) containing 0.5 µg/ml EtBr were prepared as described for HLA-DQα, except with different primers and target DNAs. These PCRs contained 15 pmole each male DNA-specific primers Y1.1 and Y1.2[20], and either 60 ng male, 60 ng female, 2 ng male, or no human DNA. Thermocycling was 94°C for 1 min. and 60°C for 1 min using a "step-cycle" program. The number of cycles for a sample were as indicated in Figure 3. Fluorescence measurement is described below.

Allele-specific, human β-globin gene PCR. Amplifications of 100 µl volume using 0.5 µg/ml of EtBr were prepared as described for HLA-DQα above except with different primers and target DNAs. These PCRs contained either primer pair HGP2/Hβ14A (wild-type globin specific primers) or HGP2/Hβ14S (sickle-globin specific primers) at 10 pmole each primer per PCR. These primers were developed by Wu et al.[21]. Three different target DNAs were used in separate amplifications—50 ng each of human DNA that was homozygous for the sickle trait (SS), DNA that was heterozygous for the sickle trait (AS), or DNA that was homozygous for the w.t. globin (AA). Thermocycling was for 30 cycles at 94°C for 1 min. and 55°C for 1 min. using a "step-cycle" program. An annealing temperature of 55°C had been shown by Wu et al.[21] to provide allele-specific amplification. Completed PCRs were photographed through a red filter (Wratten 23A) after placing the reaction tubes atop a model TM-36 transilluminator (UV-products San Gabriel, CA).

Fluorescence measurement. Fluorescence measurements were made on PCRs containing EtBr in a Fluorolog-2 fluorometer (SPEX, Edison, NJ). Excitation was at the 500 nm band with about 2 nm bandwidth with a GG 435 nm cut-off filter (Melles Grist, Inc., Irvine, CA) to exclude second-order light. Emitted light was detected at 570 nm with a bandwidth of about 7 nm. An OG 530 nm cut-off filter was used to remove the excitation light.

Continuous fluorescence monitoring of PCR. Continuous monitoring of a PCR in progress was accomplished using the spectrofluorometer and settings described above as well as a fiberoptic accessory (SPEX cat. no. 1950) to both send excitation light to, and receive emitted light from, a PCR placed in a well of a model 480 thermocycler (Perkin-Elmer Cetus). The probe end of the fiberoptic cable was attached with "5 minute-epoxy" to the open top of a PCR tube (a 0.5 ml polypropylene centrifuge tube with its cap removed) effectively sealing it. The exposed top of the PCR tube and the end of the fiberoptic cable were shielded from room light and the room lights were kept dimmed during each run. The monitored PCR was an amplification of Y-chromosome-specific repeat sequences as described above, except using an annealing/extension temperature of 50°C. The reaction was covered with mineral oil (2 drops) to prevent evaporation. Thermocycling and fluorescence measurement were started simultaneously. A time-base scan with a 10 second integration time

PAGE 5/6 * RCVD AT 7/19/2004 3:10:03 PM [Pacific Daylight Time] * SVR:SVCS01/0 * DNIS:6638 * CSID:650 952 9881 * DURATION (mm-ss):04-46

was used and the emission signal was ratioed to the excitation signal to control for changes in light-source intensity. Data were collected using the dm3000f, version 2.5 (SPEX) data system.

Acknowledgments

We thank Bob Jones for help with the spectrofluormetric measurements and Heatherbell Fong for editing this manuscript.

References

1. Mullis, K., Faloona, F., Scharf, S., Saiki, R., Horn, G. and Erlich, H. 1986. Specific enzymatic amplification of DNA *in vitro*: The polymerase chain reaction. CSHSQB 51:263–273.
2. White, T. J., Arnheim, N. and Erlich, H. A. 1989. The polymerase chain reaction. Trends Genet. 5:185–189.
3. Erlich, H. A., Gelfand, D. and Sninsky, J. J. 1991. Recent advances in the polymerase chain reaction. Science 252:1643–1651.
4. Saiki, R. K., Gelfand, D. H., Stoffel, S., Scharf, S. J., Higuchi, R., Horn, G. T., Mullis, K. B. and Erlich, H. A. 1988. Primer-directed enzymatic amplification of DNA with a thermostable DNA polymerase. Science 239:487–491.
5. Saiki, R. K., Walsh, P. S., Levenson, C. H. and Erlich, H. A. 1989. Genetic analysis of amplified DNA with immobilized sequence-specific oligonucleotide probes. Proc. Natl. Acad. Sci. USA 86:6230–6234.
6. Kwok, S. Y., Mack, D. H., Mullis, K. B., Poiesz, B. J., Ehrlich, G. D., Blair, D. and Friedman-Kien, A. S. 1987. Identification of human immunodeficiency virus sequences by using *in vitro* enzymatic amplification and oligomer cleavage detection. J. Virol. 61:1690–1694.
7. Chehab, F. F., Doherty, M., Cai, S. P., Kan, Y. W., Cooper, S. and Rubin, E. M. 1987. Detection of sickle cell anemia and thalassemias. Nature 329:293–294.
8. Horn, G. T., Richards, B. and Klinger, K. W. 1989. Amplification of a highly polymorphic VNTR segment by the polymerase chain reaction. Nuc. Acids Res. 16:2140.
9. Katz, E. D. and Dong, M. W. 1990. Rapid analysis and purification of polymerase chain reaction products by high-performance liquid chromatography. Biotechniques 8:546–555.
10. Heiger, D. N., Cohen, A. S. and Karger, B. L. 1990. Separation of DNA restriction fragments by high performance capillary electrophoresis with low and zero crosslinked polyacrylamide using continuous and pulsed electric fields. J. Chromatogr. 516:33–48.
11. Kwok, S. Y. and Higuchi, R. G. 1989. Avoiding false positives with PCR. Nature 339:237–238.
12. Chehab, F. F. and Kan, Y. W. 1989. Detection of specific DNA sequences by fluorescence amplification: a color complementation assay. Proc. Natl. Acad. Sci. USA 86:9178–9182.
13. Holland, P. M., Abramson, R. D., Watson, R. and Gelfand, D. H. 1991. Detection of specific polymerase chain reaction product by utilizing the 5' to 3' exonuclease activity of *Thermus aquaticus* DNA polymerase. Proc. Natl. Acad. Sci. USA 88:7276–7280.
14. Markovits, J., Roques, B. P. and Le Pecq, J. B. 1979. Ethidium dimer: a new reagent for the fluorimetric determination of nucleic acids. Anal. Biochem. 94:259–264.
15. Kapuscinski, J. and Szer, W. 1979. Interactions of 4',6-diamidine-2-phenylindole with synthetic polynucleotides. Nuc. Acids Res. 6:3519–3534.
16. Searle, M. S. and Embrey, K. J. 1990. Sequence-specific interaction of Hoechst 33258 with the minor groove of an adenine-tract DNA duplex studied in solution by ^{1}H NMR spectroscopy. Nuc. Acids Res. 18:3753–3762.
17. Li, H. H., Gyllensten, U. B., Cui, X. F., Saiki, R. K., Erlich, H. A. and Arnheim, N. 1988. Amplification and analysis of DNA sequences in single human sperm and diploid cells. Nature 335:414–417.
18. Abbott, M. A., Poiesz, B. J., Byrne, B. C., Kwok, S. Y., Sninsky, J. J. and Erlich, H. A. 1988. Enzymatic gene amplification: qualitative and quantitative methods for detecting proviral DNA amplified *in vitro*. J. Infect. Dis. 158:1158.
19. Saiki, R. K., Bugawan, T. L., Horn, G. T., Mullis, K. B. and Erlich, H. A. 1986. Analysis of enzymatically amplified β-globin and HLA-DQα DNA with allele-specific oligonucleotide probes. Nature 324:163–166.
20. Kogan, S. C., Doherty, M. and Gitschier, J. 1987. An improved method for prenatal diagnosis of genetic diseases by analysis of amplified DNA sequences. N. Engl. J. Med. 317:985–990.
21. Wu, D. Y., Ugozzoli, L., Pal, B. K. and Wallace, R. B. 1989. Allele-specific enzymatic amplification of β-globin genomic DNA for diagnosis of sickle cell anemia. Proc. Natl. Acad. Sci. USA 86:2757–2760.
22. Kwok, S., Kellogg, D. E., McKinney, N., Spasic, D., Goda, L., Levenson, C. and Sninsky, J. J. 1990. Effects of primer-template mismatches on the polymerase chain reaction: Human immunodeficiency virus type 1 model studies. Nuc. Acids Res. 18:999–1005.
23. Chou, Q., Russell, M., Birch, D., Raymond, J. and Bloch, W. 1992. Prevention of pre-PCR mis-priming and primer dimerization improves low-copy-number amplifications. Submitted.
24. Higuchi, R. 1989. Using PCR to engineer DNA. p. 61–70. *In*: PCR Technology. H. A. Erlich (Ed.). Stockton Press, New York, N.Y.
25. Hafft, L., Atwood, J. G., DiCesare, J., Katz, E., Pienaza, E., Williams, J. F. and Wondenberg, T. 1991. A high-performance system for automation of the polymerase chain reaction. Biotechniques 10:102–109, 106–112.
26. Tumosa, N. and Kahan, L. 1989. Fluorescent EIA screening of monoclonal antibodies to cell surface antigens. J. Immun. Meth. 116:59–63.

IBL

IMMUNO BIOLOGICAL LABORATORIES

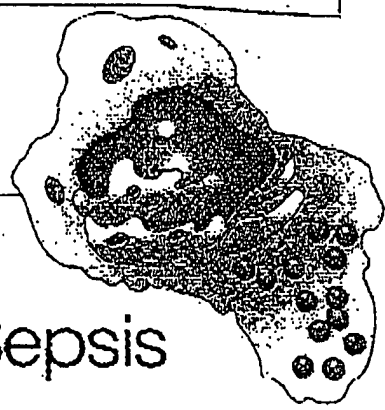

sCD-14 ELISA

Trauma, Shock and Sepsis

The CD-14 molecule is expressed on the surface of monocytes and some macrophages. Membrane-bound CD-14 is a receptor for lipopolysaccharide (LPS) complexed to LPS-Binding-Protein (LBP). The concentration of its soluble form is altered under certain pathological conditions. There is evidence for an important role of sCD-14 with polytrauma, sepsis, burnings and inflammations.

During septic conditions and acute infections it seems to be a prognostic marker and is therefore of value in monitoring these patients.

IBL offers an ELISA for quantitative determination of soluble CD-14 in human serum, -plasma, cell-culture supernatants and other biological fluids.

Assay features: 12 x 8 determinations (microtiter strips), precoated with a specific monoclonal antibody, 2x1 hour incubation, standard range: 3 - 96 ng/ml, detection limit: 1 ng/ml, CV: intra- and interassay < 8%

For more information call or fax

GESELLSCHAFT FÜR IMMUNCHEMIE UND -BIOLOGIE MBH

OSTERSTRASSE 86 · D-2000 HAMBURG 20 · GERMANY · TEL. +40/491 00 61-64 · FAX +40/40 11 98

GENENTECH, INC.
1 DNA Way
South San Francisco, CA 94080 USA
Phone: (650) 225-1000

FAX: (650) 952-9881

FACSIMILE TRANSMITTAL

Date: 19 July 2004

To: **Anna Barry**
Heller Ehrman

Re: Higuchi reference

Fax No: 324-6638

From: Patty Tobin, Assistant to Elizabeth M. Barnes, Ph.D.
Genentech, Inc. Legal Department

Number of Pages including this cover sheet: 6

RESEARCH

SIMULTANEOUS AMPLIFICATION AND DETECTION OF SPECIFIC DNA SEQUENCES

Russell Higuchi*, Gavin Dollinger[1], P. Sean Walsh and Robert Griffith

Roche Molecular Systems, Inc., 1400 53rd St., Emeryville, CA 94608. [1]Chiron Corporation, 1400 53rd St., Emeryville, CA 94608. *Corresponding author.

We have enhanced the polymerase chain reaction (PCR) such that specific DNA sequences can be detected without opening the reaction tube. This enhancement requires the addition of ethidium bromide (EtBr) to a PCR. Since the fluorescence of EtBr increases in the presence of double-stranded (ds) DNA an increase in fluorescence in such a PCR indicates a positive amplification, which can be easily monitored externally. In fact, amplification can be continuously monitored in order to follow its progress. The ability to simultaneously amplify specific DNA sequences and detect the product of the amplification both simplifies and improves PCR and may facilitate its automation and more widespread use in the clinic or in other situations requiring high sample throughput.

Although the potential benefits of PCR[1] to clinical diagnostics are well known[2,3], it is still not widely used in this setting, even though it is four years since thermostable DNA polymerases[4] made PCR practical. Some of the reasons for its slow acceptance are high cost, lack of automation of pre- and post-PCR processing steps, and false positive results from carryover-contamination. The first two points are related in that labor is the largest contributor to cost at the present stage of PCR development. Most current assays require some form of "downstream" processing once thermocycling is done in order to determine whether the target DNA sequence was present and has amplified. These include DNA hybridization[5,6], gel electrophoresis with or without use of restriction digestion[7,8], HPLC[9], or capillary electrophoresis[10]. These methods are labor-intense, have low throughput, and are difficult to automate. The third point is also closely related to downstream processing. The handling of the PCR product in these downstream processes increases the chances that amplified DNA will spread through the typing lab, resulting in a risk of "carryover" false positives in subsequent testing[11].

These downstream processing steps would be eliminated if specific amplification and detection of amplified DNA took place simultaneously within an unopened reaction vessel. Assays in which such different processes take place without the need to separate reaction components have been termed "homogeneous". No truly homogeneous PCR assay has been demonstrated to date, although progress towards this end has been reported. Chehab, et al.[12], developed a PCR product detection scheme using fluorescent primers that resulted in a fluorescent PCR product. Allele-specific primers, each with different fluorescent tags, were used to indicate the genotype of the DNA. However, the unincorporated primers must still be removed in a downstream process in order to visualize the result. Recently, Holland, et al.[13], developed an assay in which the endogenous 5′ exonuclease assay of *Taq* DNA polymerase was exploited to cleave a labeled oligonucleotide probe. The probe would only cleave if PCR amplification had produced its complementary sequence. In order to detect the cleavage products, however, a subsequent process is again needed.

We have developed a truly homogeneous assay for PCR and PCR product detection based upon the greatly increased fluorescence that ethidium bromide and other DNA binding dyes exhibit when they are bound to ds-DNA[14–16]. As outlined in Figure 1, a prototypic PCR

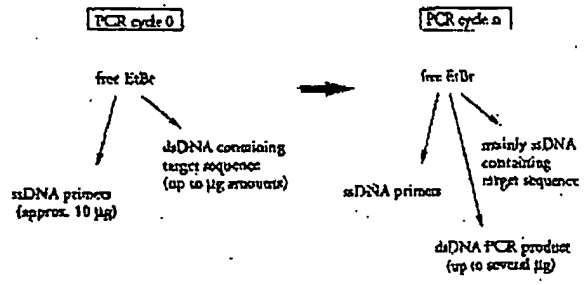

FIGURE 1 Principle of simultaneous amplification and detection of PCR product. The components of a PCR containing EtBr that are fluorescent are listed—EtBr itself, EtBr bound to either ssDNA or dsDNA. There is a large fluorescence enhancement when EtBr is bound to DNA and binding is greatly enhanced when DNA is double-stranded. After sufficient (n) cycles of PCR, the net increase in dsDNA results in additional EtBr binding, and a net increase in total fluorescence.

PAGE 2/6 * RCVD AT 7/19/2004 3:10:03 PM [Pacific Daylight Time] * SVR:SVCS01/0 * DNIS:6638 * CSID:650 952 9881 * DURATION (mm-ss):04-46

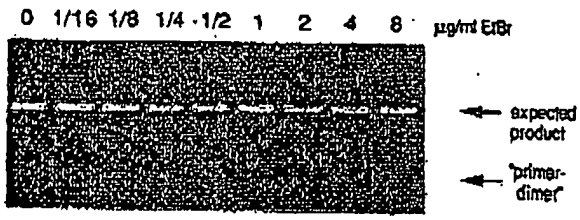

FIGURE 2 Gel electrophoresis of PCR amplification products of the human, nuclear gene, HLA DQα, made in the presence of increasing amounts of EtBr (up to 8 µg/ml). The presence of EtBr has no obvious effect on the yield or specificity of amplification.

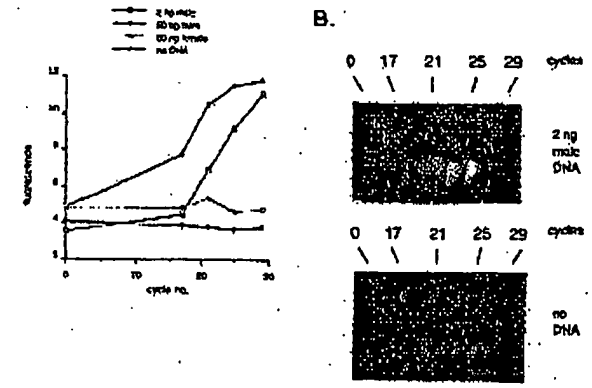

FIGURE 3 (A) Fluorescence measurements from PCRs that contain 0.5 µg/ml EtBr and that are specific for Y-chromosome repeat sequences. Five replicate PCRs were begun containing each of the DNAs specified. At each indicated cycle, one of the five replicate PCRs for each DNA was removed from thermocycling and its fluorescence measured. Units of fluorescence are arbitrary. (B) UV photography of PCR tubes (0.5 ml Eppendorf-style, polypropylene micro-centrifuge tubes) containing reactions, those starting from 2 ng male DNA and control reactions without any DNA, from (A).

begins with primers that are single-stranded DNA (ssDNA), dNTPs, and DNA polymerase. An amount of dsDNA containing the target sequence (target DNA) is also typically present. This amount can vary, depending on the application, from single-cell amounts of DNA[17] to micrograms per PCR[18]. If EtBr is present, the reagents that will fluoresce, in order of increasing fluorescence, are free EtBr itself, and EtBr bound to the single-stranded DNA primers and to the double-stranded target DNA (by its intercalation between the stacked bases of the DNA double-helix). After the first denaturation cycle, target DNA will be largely single-stranded. After a PCR is completed, the most significant change is the increase in the amount of dsDNA (the PCR product itself) of up to several micrograms. Formerly free EtBr is bound to the additional dsDNA, resulting in an increase in fluorescence. There is also some decrease in the amount of ssDNA primer, but because the binding of EtBr to ssDNA is much less than to dsDNA, the effect of this change on the total fluorescence of the sample is small. The fluorescence increase can be measured by directing excitation illumination through the walls of the amplification vessel before and after, or even continuously during, thermocycling.

RESULTS

PCR in the presence of EtBr. In order to assess the affect of EtBr in PCR, amplifications of the human HLA DQα gene[19] were performed with the dye present at concentrations from 0.06 to 8.0 µg/ml (a typical concentration of EtBr used in staining of nucleic acids following gel electrophoresis is 0.5 µg/ml). As shown in Figure 2, gel electrophoresis revealed little or no difference in the yield or quality of the amplification product whether EtBr was absent or present at any of these concentrations, indicating that EtBr does not inhibit PCR.

Detection of human Y-chromosome specific sequences. Sequence-specific, fluorescence enhancement of EtBr as a result of PCR was demonstrated in a series of amplifications containing 0.5 µg/ml EtBr and primers specific to repeat DNA sequences found on the human Y-chromosome[20]. These PCRs initially contained either 60 ng male, 60 ng female, 2 ng male human or no DNA. Five replicate PCRs were begun for each DNA. After 0, 17, 21, 24 and 29 cycles of thermocycling, a PCR for each DNA was removed from the thermocycler, and its fluorescence measured in a spectrofluorometer and plotted vs. amplification cycle number (Fig. 3A). The shape of this curve reflects the fact that by the time an increase in fluorescence can be detected, the increase in DNA is becoming linear and not exponential with cycle number. As shown, the fluorescence increased about three-fold over the background fluorescence for the PCRs containing human male DNA, but did not significantly increase for negative control PCRs, which contained either no DNA or human female DNA. The more male DNA present to begin with—60 ng versus 2 ng—the fewer cycles were needed to give a detectable increase in fluorescence. Gel electrophoresis on the products of these amplifications showed that DNA fragments of the expected size were made in the male DNA containing reactions and that little DNA synthesis took place in the control samples.

In addition, the increase in fluorescence was visualized by simply laying the completed, unopened PCRs on a UV transilluminator and photographing them through a red filter. This is shown in figure 3B for the reactions that began with 2 ng male DNA and those with no DNA.

Detection of specific alleles of the human β-globin gene. In order to demonstrate that this approach has adequate specificity to allow genetic screening, a detection of the sickle-cell anemia mutation was performed. Figure 4 shows the fluorescence from completed amplifications containing EtBr (0.5 µg/ml) as detected by photography of the reaction tubes on a UV transilluminator. These reactions were performed using primers specific for either the wild-type or sickle-cell mutation of the human β-globin gene[21]. The specificity for each allele is imparted by placing the sickle-mutation site at the terminal 3′ nucleotide of one primer. By using an appropriate primer annealing temperature, primer extension—and thus amplification—can take place only if the 3′ nucleotide of the primer is complementary to the β-globin allele present[21,22].

Each pair of amplifications shown in Figure 4 consists of a reaction with either the wild-type allele specific (left tube) or sickle-allele specific (right tube) primers. Three different DNAs were typed: DNA from a homozygous, wild-type β-globin individual (AA); from a heterozygous sickle β-globin individual (AS); and from a homozygous sickle β-globin individual (SS). Each DNA (50 ng genomic DNA to start each PCR) was analyzed in triplicate (3 pairs

of reactions each). The DNA type was reflected in the relative fluorescence intensities in each pair of completed amplifications. There was a significant increase in fluorescence only where a β-globin allele DNA matched the primer set. When measured on a spectrofluorometer (data not shown), this fluorescence was about three times that present in a PCR where both β-globin alleles were mismatched to the primer set. Gel electrophoresis (not shown) established that this increase in fluorescence was due to the synthesis of nearly a microgram of a DNA fragment of the expected size for β-globin. There was little synthesis of dsDNA in reactions in which the allele-specific primer was mismatched to both alleles.

Continuous monitoring of a PCR. Using a fiber optic device, it is possible to direct excitation illumination from a spectrofluorometer to a PCR undergoing thermocycling and to return its fluorescence to the spectrofluorometer. The fluorescence readout of such an arrangement, directed at an EtBr-containing amplification of Y-chromosome specific sequences from 25 ng of human male DNA, is shown in Figure 5. The readout from a control PCR with no target DNA is also shown. Thirty cycles of PCR were monitored for each.

The fluorescence trace as a function of time clearly shows the effect of the thermocycling. Fluorescence intensity rises and falls inversely with temperature. The fluorescence intensity is minimum at the denaturation temperature (94°C) and maximum at the annealing/extension temperature (50°C). In the negative-control PCR, these fluorescence maxima and minima do not change significantly over the thirty thermocycles, indicating that there is little dsDNA synthesis without the appropriate target DNA, and there is little if any bleaching of EtBr during the continuous illumination of the sample.

In the PCR containing male DNA, the fluorescence maxima at the annealing/extension temperature begin to increase at about 4000 seconds of thermocycling, and continue to increase with time, indicating that dsDNA is being produced at a detectable level. Note that the fluorescence minima at the denaturation temperature do not significantly increase, presumably because at this temperature there is no dsDNA for EtBr to bind. Thus the course of the amplification is followed by tracking the fluorescence increase at the annealing temperature. Analysis of the products of these two amplifications by gel electrophoresis showed a DNA fragment of the expected size for the male DNA containing sample and no detectable DNA synthesis for the control sample.

DISCUSSION

Downstream processes such as hybridization to a sequence-specific probe can enhance the specificity of DNA detection by PCR. The elimination of these processes means that the specificity of this homogeneous assay depends solely on that of PCR. In the case of sickle-cell disease, we have shown that PCR alone has sufficient DNA sequence specificity to permit genetic screening. Using appropriate amplification conditions, there is little non-specific production of dsDNA in the absence of the appropriate target allele.

The specificity required to detect pathogens can be more or less than that required to do genetic screening, depending on the number of pathogens in the sample and the amount of other DNA that must be taken with the sample. A difficult target is HIV, which requires detection of a viral genome that can be at the level of a few copies per thousands of host cells[6]. Compared with genetic screening, which is performed on cells containing at least one copy of the target sequence, HIV detection requires both more specificity and the input of more total

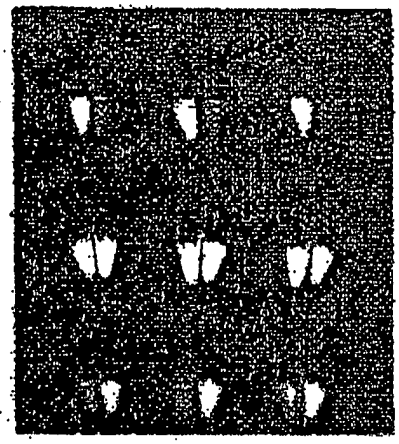

FIGURE 4 UV photography of PCR tubes containing amplifications using EtBr that are specific to wild-type (A) or sickle (S) alleles of the human β-globin gene. The left of each pair of tubes contains allele-specific primers to the wild-type alleles, the right tube primers to the sickle allele. The photograph was taken after 30 cycles of PCR, and the input DNAs and the alleles they contain are indicated. Fifty ng of DNA was used to begin PCR. Typing was done in triplicate (3 pairs of PCRs) for each input DNA.

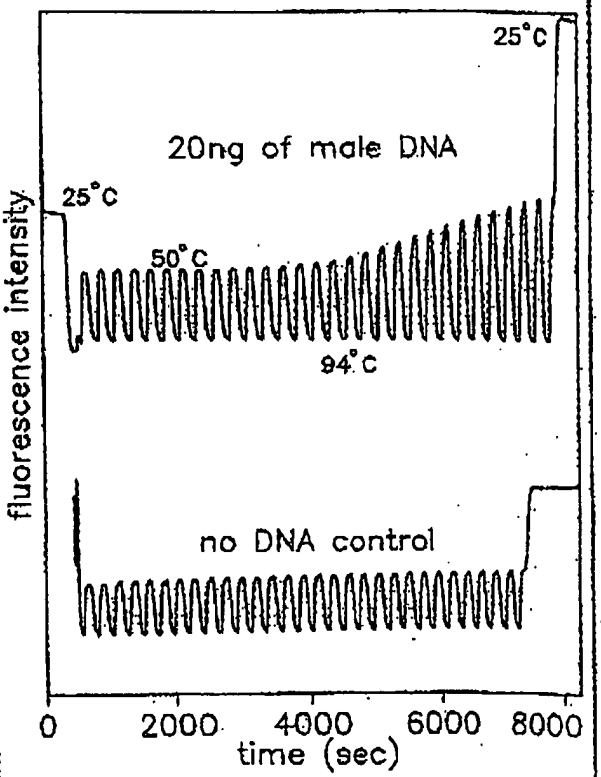

FIGURE 5 Continuous, real-time monitoring of a PCR. A fiber optic was used to carry excitation light to a PCR in progress and also emitted light back to a fluorometer (see Experimental Protocol). Amplification using human male-DNA specific primers in a PCR starting with 20 ng of human male DNA (top), or in a control PCR without DNA (bottom), were monitored. Thirty cycles of PCR were followed for each. The temperature cycled between 94°C (denaturation) and 50°C (annealing and extension). Note in the male DNA PCR, the cycle (time) dependent increase in fluorescence at the annealing/extension temperature.

DNA—up to microgram amounts—in order to have sufficient numbers of target sequences. This large amount of starting DNA in an amplification significantly increases the background fluorescence over which any additional fluorescence produced by PCR must be detected. An additional complication that occurs with targets in low copy-number is the formation of the "primer-dimer" artifact. This is the result of the extension of one primer using the other primer as a template. Although this occurs infrequently, once it occurs the extension product is a substrate for PCR amplification, and can compete with true PCR targets if those targets are rare. The primer-dimer product is of course dsDNA and thus is a potential source of false signal in this homogeneous assay.

To increase PCR specificity and reduce the effect of primer-dimer amplification, we are investigating a number of approaches, including the use of nested-primer amplifications that take place in a single tube[3], and the "hot-start", in which nonspecific amplification is reduced by raising the temperature of the reaction before DNA synthesis begins[23]. Preliminary results using these approaches suggest that primer-dimer is effectively reduced and it is possible to detect the increase in EtBr fluorescence in a PCR instigated by a single HIV genome in a background of 10^5 cells. With larger numbers of cells, the background fluorescence contributed by genomic DNA becomes problematic. To reduce this background, it may be possible to use sequence-specific DNA-binding dyes that can be made to preferentially bind PCR product over genomic DNA by incorporating the dye-binding DNA sequence into the PCR product through a 5' "add-on" to the oligonucleotide primer[24].

We have shown that the detection of fluorescence generated by an EtBr-containing PCR is straightforward, both once PCR is completed and continuously during thermocycling. The ease with which automation of specific DNA detection can be accomplished is the most promising aspect of this assay. The fluorescence analysis of completed PCRs is already possible with existing instrumentation in 96-well format[25]. In this format, the fluorescence in each PCR can be quantitated before, after, and even at selected points during thermocycling by moving the rack of PCRs to a 96-microwell plate fluorescence reader[26].

The instrumentation necessary to continuously monitor multiple PCRs simultaneously is also simple in principle. A direct extension of the apparatus used here is to have multiple fiberoptics transmit the excitation light and fluorescent emissions to and from multiple PCRs. The ability to monitor multiple PCRs continuously may allow quantitation of target DNA copy number. Figure 3 shows that the larger the amount of starting target DNA, the sooner during PCR a fluorescence increase is detected. Preliminary experiments (Higuchi and Dollinger, manuscript in preparation) with continuous monitoring have shown a sensitivity to two-fold differences in initial target DNA concentration.

Conversely, if the number of target molecules is known—as it can be in genetic screening—continuous monitoring may provide a means of detecting false positive and false negative results. With a known number of target molecules, a true positive would exhibit detectable fluorescence by a predictable number of cycles of PCR. Increases in fluorescence detected before or after that cycle would indicate potential artifacts. False negative results due to, for example, inhibition of DNA polymerase, may be detected by including within each PCR an inefficiently amplifying marker. This marker results in a fluorescence increase only after a large number of cycles—many more than are necessary to detect a true positive. If a sample fails to have a fluorescence increase after this many cycles, inhibition may be suspected. Since, in this assay, conclusions are drawn based on the presence or absence of fluorescence signal alone, such controls may be important. In any event, before any test based on this principle is ready for the clinic, an assessment of its false positive/false negative rates will need to be obtained using a large number of known samples.

In summary, the inclusion in PCR of dyes whose fluorescence is enhanced upon binding dsDNA makes it possible to detect specific DNA amplification from outside the PCR tube. In the future, instruments based upon this principle may facilitate the more widespread use of PCR in applications that demand the high throughput of samples.

EXPERIMENTAL PROTOCOL

Human HLA-DQα gene amplifications containing EtBr. PCRs were set up in 100 µl volumes containing 10 mM Tris-HCl, pH 8.3; 50 mM KCl; 4 mM $MgCl_2$; 2.5 units of *Taq* DNA polymerase (Perkin-Elmer Cetus, Norwalk, CT); 20 pmole each of human HLA-DQα gene specific oligonucleotide primers GH26 and GH27[19] and approximately 10^7 copies of DQα PCR product diluted from a previous reaction. Ethidium bromide (EtBr; Sigma) was used at the concentrations indicated in Figure 2. Thermocycling proceeded for 20 cycles in a model 480 thermocycler (Perkin-Elmer Cetus, Norwalk, CT) using a "step-cycle" program of 94°C for 1 min. denaturation and 60°C for 30 sec. annealing and 72°C for 30 sec. extension.

Y-chromosome specific PCR. PCRs (100 µl total reaction volume) containing 0.5 µg/ml EtBr were prepared as described for HLA-DQα, except with different primers and target DNAs. These PCRs contained 15 pmole each male DNA-specific primers Y1.1 and Y1.2[20], and either 60 ng male, 60 ng female, 2 ng male, or no human DNA. Thermocycling was 94°C for 1 min. and 60°C for 1 min using a "step-cycle" program. The number of cycles for a sample were as indicated in Figure 3. Fluorescence measurement is described below.

Allele-specific, human β-globin gene PCR. Amplifications of 100 µl volume using 0.5 µg/ml of EtBr were prepared as described for HLA-DQα above except with different primers and target DNAs. These PCRs contained either primer pair HGP1/Hβ14A (wild-type globin specific primers) or HGP2/Hβ14S (sickle-globin specific primers) at 10 pmole each primer per PCR. These primers were developed by Wu et al.[21]. Three different target DNAs were used in separate amplifications—50 ng each of human DNA that was homozygous for the sickle trait (SS), DNA that was heterozygous for the sickle trait (AS), or DNA that was homozygous for the w.t. globin (AA). Thermocycling was for 30 cycles at 94°C for 1 min. and 55°C for 1 min. using a "step-cycle" program. An annealing temperature of 55°C had been shown by Wu et al.[21] to provide allele-specific amplification. Completed PCRs were photographed through a red filter (Wratten 23A) after placing the reaction tubes atop a model TM-36 (transilluminator (UV-products San Gabriel, CA).

Fluorescence measurement. Fluorescence measurements were made on PCRs containing EtBr in a Fluorolog-2 fluorometer (SPEX, Edison, NJ). Excitation was at the 500 nm band with about 2 nm bandwidth with a GG 435 nm cut-off filter (Melles Grist, Inc., Irvine, CA) to exclude second-order light. Emitted light was detected at 570 nm with a bandwidth of about 7 nm. An OG 530 nm cut-off filter was used to remove the excitation light.

Continuous fluorescence monitoring of PCR. Continuous monitoring of a PCR in progress was accomplished using the spectrofluorometer and settings described above as well as a fiberoptic accessory (SPEX cat. no. 1950) to both send excitation light to, and receive emitted light from, a PCR placed in a well of a model 480 thermocycler (Perkin-Elmer Cetus). The probe end of the fiberoptic cable was attached with "5 minute-epoxy" to the open top of a PCR tube (a 0.5 ml polypropylene centrifuge tube with its cap removed) effectively sealing it. The exposed top of the PCR tube and the end of the fiberoptic cable were shielded from room light and the room lights were kept dimmed during each run. The monitored PCR was an amplification of Y-chromosome-specific repeat sequences as described above, except using an annealing/extension temperature of 50°C. The reaction was covered with mineral oil (2 drops) to prevent evaporation. Thermocycling and fluorescence measurement were started simultaneously. A time-base scan with a 10 second integration time

PAGE 5/6 * RCVD AT 7/19/2004 3:10:03 PM [Pacific Daylight Time] * SVR:SVCS01/0 * DNIS:6638 * CSID:650 952 9881 * DURATION (mm-ss):04-46

was used and the emission signal was ratioed to the excitation signal to control for changes in light-source intensity. Data were collected using the dm3000f, version 2.5 (SPEX) data system.

Acknowledgments

We thank Bob Jones for help with the spectrofluormetric measurements and Heatherbell Fong for editing this manuscript.

References

1. Mullis, K., Faloona, F., Scharf, S., Saiki, R., Horn, G. and Erlich, H. 1986. Specific enzymatic amplification of DNA *in vitro*: The polymerase chain reaction. CSHSQB 51:263–273.
2. White, T. J., Arnheim, N. and Erlich, H. A. 1989. The polymerase chain reaction. Trends Genet. 5:185–189.
3. Erlich, H. A., Gelfand, D. and Sninsky, J. J. 1991. Recent advances in the polymerase chain reaction. Science 252:1643–1651.
4. Saiki, R. K., Gelfand, D. H., Stoffel, S., Scharf, S. J., Higuchi, R., Horn, G. T., Mullis, K. B. and Erlich, H. A. 1988. Primer-directed enzymatic amplification of DNA with a thermostable DNA polymerase. Science 239:487–491.
5. Saiki, R. K., Walsh, P. S., Levenson, C. H. and Erlich, H. A. 1989. Genetic analysis of amplified DNA with immobilized sequence-specific oligonucleotide probes. Proc. Natl. Acad. Sci. USA 86:6230–6234.
6. Kwok, S. Y., Mack, D. H., Mullis, K. B., Poiesz, B. J., Ehrlich, G. D., Blair, D. and Friedman-Kien, A. S. 1987. Identification of human immunodeficiency virus sequences by using *in vitro* enzymatic amplification and oligomer cleavage detection. J. Virol. 61:1690–1694.
7. Chehab, F. F., Doherty, M., Cai, S. P., Kan, Y. W., Cooper, S. and Rubin, E. M. 1987. Detection of sickle cell anemia and thalassemias. Nature 329:293–294.
8. Horn, G. T., Richards, B. and Klinger, K. W. 1989. Amplification of a highly polymorphic VNTR segment by the polymerase chain reaction. Nuc. Acids Res. 16:2140.
9. Katz, E. D. and Dong, M. W. 1990. Rapid analysis and purification of polymerase chain reaction products by high-performance liquid chromatography. Biotechniques 8:546–555.
10. Heiger, D. N., Cohen, A. S. and Karger, B. L. 1990. Separation of DNA restriction fragments by high performance capillary electrophoresis with low and zero crosslinked polyacrylamide using continuous and pulsed electric fields. J. Chromatogr. 516:33–48.
11. Kwok, S. Y. and Higuchi, R. G. 1989. Avoiding false positives with PCR. Nature 339:237–238.
12. Chehab, F. F. and Kan, Y. W. 1989. Detection of specific DNA sequences by fluorescence amplification: a color complementation assay. Proc. Natl. Acad. Sci. USA 86:9178–9182.
13. Holland, P. M., Abramson, R. D., Watson, R. and Gelfand, D. H. 1991. Detection of specific polymerase chain reaction product by utilizing the 5′ to 3′ exonuclease activity of *Thermus aquaticus* DNA polymerase. Proc. Natl. Acad. Sci. USA 88:7276–7280.
14. Markovits, J., Roques, B. P. and Le Pecq, J. B. 1979. Ethidium dimer: a new reagent for the fluorimetric determination of nucleic acids. Anal. Biochem. 94:259–264.
15. Kapuscinski, J. and Szer, W. 1979. Interactions of 4′,6-diamidino-2-phenylindole with synthetic polynucleotides. Nuc. Acids Res. 6:3519–3534.
16. Searle, M. S. and Embrey, K. J. 1990. Sequence-specific interaction of Hoescht 33258 with the minor groove of an adenine-tract DNA duplex studied in solution by ^{1}H NMR spectroscopy. Nuc. Acids Res. 18:3753–3762.
17. Li, H. H., Gyllensten, U. B., Cui, X. F., Saiki, R. K., Erlich, H. A. and Arnheim, N. 1988. Amplification and analysis of DNA sequences in single human sperm and diploid cells. Nature 335:414–417.
18. Abbott, M. A., Poiesz, B. J., Byrne, B. C., Kwok, S. Y., Sninsky, J. J. and Erlich, H. A. 1988. Enzymatic gene amplification: qualitative and quantitative methods for detecting proviral DNA amplified *in vitro*. J. Infect. Dis. 158:1158.
19. Saiki, R. K., Bugawan, T. L., Horn, G. T., Mullis, K. B. and Erlich, H. A. 1986. Analysis of enzymatically amplified β-globin and HLA-DQα DNA with allele-specific oligonucleotide probes. Nature 324:163–166.
20. Kogan, S. C., Doherty, M. and Gitschier, J. 1987. An improved method for prenatal diagnosis of genetic diseases by analysis of amplified DNA sequences. N. Engl. J. Med. 317:985–990.
21. Wu, D. Y., Ugozzoli, L., Pal, B. K. and Wallace, R. B. 1989. Allele-specific enzymatic amplification of β-globin genomic DNA for diagnosis of sickle cell anemia. Proc. Natl. Acad. Sci. USA 86:2757–2760.
22. Kwok, S., Kellogg, D. E., McKinney, N., Spasic, D., Goda, L., Levenson, C. and Sninsky, J. J. 1990. Effects of primer-template mismatches on the polymerase chain reaction: Human immunodeficiency virus type 1 model studies. Nuc. Acids Res. 18:999–1005.
23. Chou, Q., Russell, M., Birch, D., Raymond, J. and Bloch, W. 1992. Prevention of pre-PCR mis-priming and primer dimerization improves low-copy-number amplifications. Submitted.
24. Higuchi, R. 1989. Using PCR to engineer DNA. p. 61–70. *In:* PCR Technology. H. A. Erlich (Ed.). Stockton Press, New York, N.Y.
25. Haff, L., Atwood, J. G., DiCesare, J., Katz, E., Pionzza, E., Williams, J. F. and Woudenberg, T. 1991. A high-performance system for automation of the polymerase chain reaction. Biotechniques 10:102–109, 106–112.
26. Tumosa, N. and Kahan, L. 1989. Fluorescent EIA screening of monoclonal antibodies to cell surface antigens. J. Immun. Meth. 116:59–63.

IBL

IMMUNO BIOLOGICAL LABORATORIES

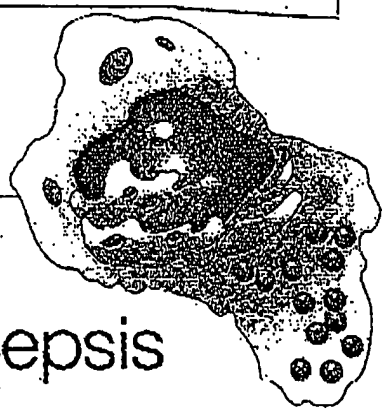

sCD-14 ELISA

Trauma, Shock and Sepsis

The CD-14 molecule is expressed on the surface of monocytes and some macrophages. Membrane-bound CD-14 is a receptor for lipopolysaccharide (LPS) complexed to LPS-Binding-Protein (LBP). The concentration of its soluble form is altered under certain pathological conditions. There is evidence for an important role of sCD-14 with polytrauma, sepsis, burnings and inflammations.

During septic conditions and acute infections it seems to be a prognostic marker and is therefore of value in monitoring these patients.

IBL offers an ELISA for quantitative determination of soluble CD-14 in human serum, -plasma, cell-culture supernatants and other biological fluids.

Assay features: 12 x 8 determinations (microtiter strips), precoated with a specific monoclonal antibody, 2x1 hour incubation, standard range: 3 - 96 ng/ml, detection limit: 1 ng/ml, CV: intra- and interassay < 8%

For more information call or fax

GESELLSCHAFT FÜR IMMUNCHEMIE UND -BIOLOGIE MBH

OSTERSTRASSE 86 · D-2000 HAMBURG 20 · GERMANY · TEL. +40/491 00 61-64 · FAX +40/40 11 98

Oligonucleotides with Fluorescent Dyes at Opposite Ends Provide a Quenched Probe System Useful for Detecting PCR Product and Nucleic Acid Hybridization

Kenneth J. Livak, Susan J.A. Flood, Jeffrey Marmaro, William Giusti, and Karin Deetz

Perkin-Elmer, Applied Biosystems Division, Foster City, California 94404

The 5′ nuclease PCR assay detects the accumulation of specific PCR product by hybridization and cleavage of a double-labeled fluorogenic probe during the amplification reaction. The probe is an oligonucleotide with both a reporter fluorescent dye and a quencher dye attached. An increase in reporter fluorescence intensity indicates that the probe has hybridized to the target PCR product and has been cleaved by the 5′→3′ nucleolytic activity of *Taq* DNA polymerase. In this study, probes with the quencher dye attached to an internal nucleotide were compared with probes with the quencher dye attached to the 3′-end nucleotide. In all cases, the reporter dye was attached to the 5′ end. All intact probes showed quenching of the reporter fluorescence. In general, probes with the quencher dye attached to the 3′-end nucleotide exhibited a larger signal in the 5′ nuclease PCR assay than the internally labeled probes. It is proposed that the larger signal is caused by increased likelihood of cleavage by *Taq* DNA polymerase when the probe is hybridized to a template strand during PCR. Probes with the quencher dye attached to the 3′-end nucleotide also exhibited an increase in reporter fluorescence intensity when hybridized to a complementary strand. Thus, oligonucleotides with reporter and quencher dyes attached at opposite ends can be used as homogeneous hybridization probes.

A homogeneous assay for detecting the accumulation of specific PCR product that uses a double-labeled fluorogenic probe was described by Lee et al.[1] The assay exploits the 5′→3′ nucleolytic activity of *Taq* DNA polymerase[2,3] and is diagramed in Figure 1. The fluorogenic probe consists of an oligonucleotide with a reporter fluorescent dye, such as a fluorescein, attached to the 5′ end; and a quencher dye, such as a rhodamine, attached internally. When the fluorescein is excited by irradiation, its fluorescent emission will be quenched if the rhodamine is close enough to be excited through the process of fluorescence energy transfer (FET).[4,5] During PCR, if the probe is hybridized to a template strand, *Taq* DNA polymerase will cleave the probe because of its inherent 5′→3′ nucleolytic activity. If the cleavage occurs between the fluorescein and rhodamine dyes, it causes an increase in fluorescein fluorescence intensity because the fluorescein is no longer quenched. The increase in fluorescein fluorescence intensity indicates that the probe-specific PCR product has been generated. Thus, FET between a reporter dye and a quencher dye is critical to the performance of the probe in the 5′ nuclease PCR assay.

Quenching is completely dependent on the physical proximity of the two dyes.[6] Because of this, it has been assumed that the quencher dye must be attached near the 5′ end. Surprisingly, we have found that attaching a rhodamine dye at the 3′ end of a probe still provides adequate quenching for the probe to perform in the 5′ nuclease PCR assay. Furthermore, cleavage of this type of probe is not required to achieve some reduction in quenching. Oligonucleotides with a reporter dye on the 5′ end and a quencher dye on the 3′ end exhibit a much higher reporter fluorescence when double-stranded as compared with single-stranded. This should make it possible to use this type of double-labeled probe for homogeneous detection of nucleic acid hybridization.

MATERIALS AND METHODS

Oligonucleotides

Table 1 shows the nucleotide sequence of the oligonucleotides used in this study. Linker arm nucleotide (LAN) phosphoramidite was obtained from Glen Research. The standard DNA phosphoramidites, 6-carboxyfluorescein (6-FAM) phosphoramidite, 6-carboxytetramethylrhodamine succinimidyl ester (TAMRA NHS ester), and Phosphalink for attaching a 3′-blocking phosphate, were obtained from Perkin-Elmer, Applied Biosystems Division. Oligonucleotide synthesis was performed using an ABI model 394 DNA synthesizer (Applied Biosystems). Primer and complement oligonucleotides were purified using Oligo Purification Cartridges (Applied Biosystems). Double-labeled probes were synthesized with 6-FAM-labeled phosphoramidite at the 5′ end, LAN replacing one of the T's in the sequence, and Phosphalink at the 3′ end. Following deprotection and ethanol precipitation, TAMRA NHS ester was coupled to the LAN-containing oligonucleotide in 250

4:357–362©1995 by Cold Spring Harbor Laboratory Press ISSN 1054-9803/95 $5.00

PAGE 2/7 * RCVD AT 10/24/2005 5:55:20 PM [Pacific Daylight Time] * SVR:SVCS01/0 * DNIS:6034 * CSID:(613) 991-5695 * DURATION (mm-ss):05-46

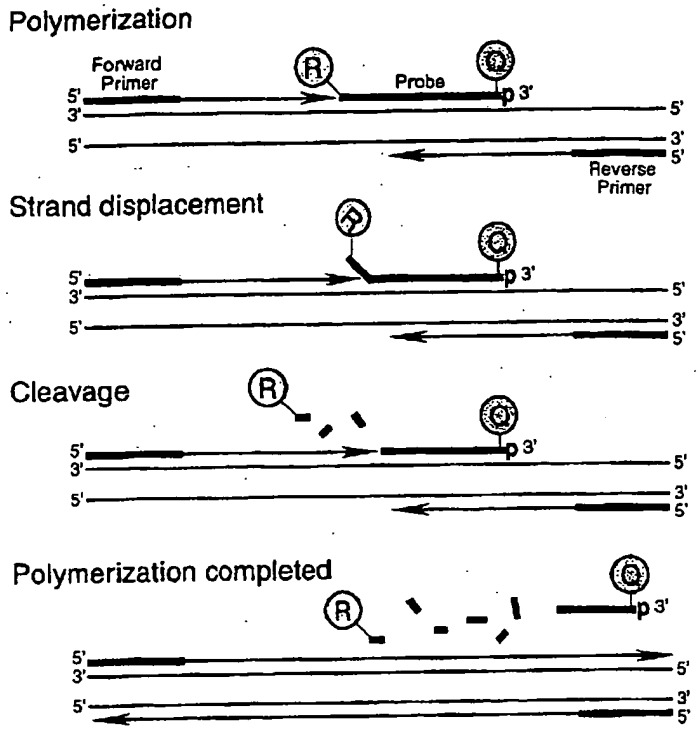

FIGURE 1 Diagram of 5′ nuclease assay. Stepwise representation of the 5′ → 3′ nucleolytic activity of *Taq* DNA polymerase acting on a fluorogenic probe during one extension phase of PCR.

mM Na-bicarbonate buffer (pH 9.0) at room temperature. Unreacted dye was removed by passage over a PD-10 Sephadex column. Finally, the double-labeled probe was purified by preparative high-performance liquid chromatography (HPLC) using an Aquapore C_8 220×4.6-mm column with 7-μm particle size. The column was developed with a 24-min linear gradient of 8–20% acetonitrile in 0.1 M TEAA (triethylamine acetate). Probes are named by designating the sequence from Table 1 and the position of the LAN–TAMRA moiety. For example, probe A1-7 has sequence A1 with LAN–TAMRA at nucleotide position 7 from the 5′ end.

PCR Systems

All PCR amplifications were performed in the Perkin-Elmer GeneAmp PCR System 9600 using 50-μl reactions that contained 10 mM Tris-HCl (pH 8.3), 50 mM KCl, 200 μM dATP, 200 μM dCTP, 200 μM dGTP, 400 μM dUTP, 0.5 unit of AmpErase uracil *N*-glycosylase (Perkin-Elmer), and 1.25 unit of AmpliTaq DNA polymerase (Perkin-Elmer). A 295-bp segment from exon 3 of the human β-actin gene (nucleotides 2141–2435 in the sequence of Nakajima-Iijima et al.)[7] was amplified using primers AFP and ARP (Table 1), which are modified slightly from those of du Breuil et al.[8] Actin amplification reactions contained 4 mM $MgCl_2$, 20 ng of human genomic DNA, 50 nM A1 or A3 probe, and 300 nM each primer. The thermal regimen was 50°C (2 min), 95°C (10 min), 40 cycles of 95°C (20 sec), 60°C (1 min), and hold at 72°C. A 515-bp segment was amplified from a plasmid that consists of a segment of λ DNA (nucleotides 32,220–32,747) inserted in the *SmaI* site of vector pUC119. These reactions contained 3.5 mM $MgCl_2$, 1 ng of plasmid DNA, 50 nM P2 or P5 probe, 200 nM primer F119, and 200 nM primer R119. The thermal regimen was 50°C (2 min), 95°C (10 min), 25 cycles of 95°C (20 sec), 57°C (1 min), and hold at 72°C.

Fluorescence Detection

For each amplification reaction, a 40-μl aliquot of a sample was transferred to an individual well of a white, 96-well microtiter plate (Perkin-Elmer). Fluorescence was measured on the Perkin-Elmer TaqMan LS-50B System, which consists of a luminescence spectrometer with plate reader assembly, a 485-nm excitation filter, and a 515-nm emission filter. Excitation was at 488 nm using a 5-nm slit width. Emission was measured at 518 nm for 6-FAM (the reporter or R value) and 582 nm for TAMRA (the quencher or Q value) using a 10-nm slit width. To determine the increase in reporter emission that is caused by cleavage of the probe during PCR, three normalizations are applied to the raw emission data. First, emission intensity of a buffer blank is subtracted for each wavelength. Second, emission intensity of the reporter is

TABLE 1 Sequences of Oligonucleotides

Name	Type	Sequence
F119	primer	ACCCACAGGAACTGATCACCACTC
R119	primer	ATGTCGCGTTCCGGCTGACGTTCTGC
P2	probe	TCGCATTACTGATCGTTGCCAACCAGTp
P2C	complement	GTACTGGTTGGCAACGATCAGTAATGCGATG
P5	probe	CGGATTTGCTGGTATCTATGACAAGGATp
P5C	complement	TTCATCCTTGTCATAGATACCAGCAAATCCG
AFP	primer	TCACCCACACTGTGCCCATCTACGA
ARP	primer	CAGCGGAACCGCTCATTGCCAATGG
A1	probe	ATGCCCTCCCCCATGCCATCCTGCGTp
A1C	complement	AGACGCAGGATGGCATGGGGGAGGGCATAC
A3	probe	CGCCCTGGACTTCGAGCAAGAGATp
A3C	complement	CCATCTCTTGCTCGAAGTCCAGGGCGAC

For each oligonucleotide used in this study, the nucleic acid sequence is given, written in the 5′ → 3′ direction. There are three types of oligonucleotides: PCR primer, fluorogenic probe used in the 5′ nuclease assay, and complement used to hybridize to the corresponding probe. For the probes, the underlined base indicates a position where LAN with TAMRA attached was substituted for a T. (p) The presence of a 3′ phosphate on each probe.

PAGE 3/7 * RCVD AT 10/24/2005 5:55:20 PM [Pacific Daylight Time] * SVR:SVCS01/0 * DNIS:6034 * CSID:(613) 991-5695 * DURATION (mm-ss):05-46

A1-2	RAQGCCCTCCCCCATGCCATCCTGCGTp
A1-7	RATGCCCQCCCCCATGCCATCCTGCGTp
A1-14	RATGCCCTCCCCCAQGCCATCCTGCGTp
A1-19	RATGCCCTCCCCCATGCCAQCCTGCGTp
A1-22	RATGCCCTCCCCCATGCCATCCQGCGTp
A1-26	RATGCCCTCCCCCATGCCATCCTGCGQp

Probe	518 nm		582 nm		RQ-	RQ+	ΔRQ
	no temp.	+ temp.	no temp.	+ temp.			
A1-2	25.5 ± 2.1	32.7 ± 1.9	38.2 ± 3.0	38.2 ± 2.0	0.67 ± 0.01	0.86 ± 0.06	0.19 ± 0.06
A1-7	53.5 ± 4.3	395.1 ± 21.4	108.5 ± 6.3	110.3 ± 5.3	0.49 ± 0.03	3.58 ± 0.17	3.09 ± 0.18
A1-14	127.0 ± 4.9	403.5 ± 19.1	109.7 ± 5.3	93.1 ± 6.3	1.16 ± 0.02	4.34 ± 0.15	3.18 ± 0.15
A1-19	187.5 ± 17.9	422.7 ± 7.7	70.3 ± 7.4	73.0 ± 2.8	2.67 ± 0.05	5.80 ± 0.15	3.13 ± 0.16
A1-22	224.6 ± 9.4	482.2 ± 43.6	100.0 ± 4.0	96.2 ± 9.6	2.25 ± 0.03	5.02 ± 0.11	2.77 ± 0.12
A1-26	160.2 ± 8.9	454.1 ± 18.4	93.1 ± 5.4	90.7 ± 3.2	1.72 ± 0.02	5.01 ± 0.08	3.29 ± 0.08

FIGURE 2 Results of 5′ nuclease assay comparing β-actin probes with TAMRA at different nucleotide positions. As described in Materials and Methods, PCR amplifications containing the indicated probes were performed, and the fluorescence emission was measured at 518 and 582 nm. Reported values are the average ± 1 S.D. for six reactions run without added template (no temp.) and six reactions run with template (+temp.). The RQ ratio was calculated for each individual reaction and averaged to give the reported RQ^- and RQ^+ values.

divided by the emission intensity of the quencher to give an RQ ratio for each reaction tube. This normalizes for well-to-well variations in probe concentration and fluorescence measurement. Finally, ΔRQ is calculated by subtracting the RQ value of the no-template control (RQ^-) from the RQ value for the complete reaction including template (RQ^+).

RESULTS

A series of probes with increasing distances between the fluorescein reporter and rhodamine quencher were tested to investigate the minimum and maximum spacing that would give an acceptable performance in the 5′ nuclease PCR assay. These probes hybridize to a target sequence in the human β-actin gene. Figure 2 shows the results of an experiment in which these probes were included in PCR that amplified a segment of the β-actin gene containing the target sequence. Performance in the 5′ nuclease PCR assay is monitored by the magnitude of ΔRQ, which is a measure of the increase in reporter fluorescence caused by PCR amplification of the probe target. Probe A1-2 has a ΔRQ value that is close to zero, indicating that the probe was not cleaved appreciably during the amplification reaction. This suggests that with the quencher dye on the second nucleotide from the 5′ end, there is insufficient room for *Taq* polymerase to cleave efficiently between the reporter and quencher. The other five probes exhibited comparable ΔRQ values that are clearly different from zero. Thus, all five probes are being cleaved during PCR amplification resulting in a similar increase in reporter fluorescence. It should be noted that complete digestion of a probe produces a much larger increase in reporter fluorescence than that observed in Figure 2 (data not shown). Thus, even in reactions where amplification occurs, the majority of probe molecules remain uncleaved. It is mainly for this reason that the fluorescence intensity of the quencher dye TAMRA changes little with amplification of the target. This is what allows us to use the 582-nm fluorescence reading as a normalization factor.

The magnitude of RQ^- depends mainly on the quenching efficiency inherent in the specific structure of the probe and the purity of the oligonucleotide. Thus, the larger RQ^- values indicate that probes A1-14, A1-19, A1-22, and A1-26 probably have reduced quenching as compared with A1-7. Still, the degree of quenching is sufficient to detect a highly significant increase in reporter fluorescence when each of these probes is cleaved during PCR.

To further investigate the ability of TAMRA on the 3′ end to quench 6-FAM on the 5′ end, three additional pairs of probes were tested in the 5′ nuclease PCR assay. For each pair, one probe has TAMRA attached to an internal nucleotide and the other has TAMRA attached to the 3′ end nucleotide. The results are shown in Table 2. For all three sets, the probe with the 3′ quencher exhibits a ΔRQ value that is considerably higher than for the probe with the internal quencher. The RQ^- values suggest that differences in quenching are not as great as those observed with some of the A1 probes. These results demonstrate that a quencher dye on the 3′ end of an oligonucleotide can quench efficiently the

TABLE 2 Results of 5′ Nuclease Assay Comparing Probes with TAMRA Attached to an Internal or 3′-terminal Nucleotide

Probe	518 nm		582 nm		RQ^-	RQ^+	ΔRQ
	no temp.	+ temp.	no temp.	+ temp.			
A3-6	54.6 ± 3.2	84.8 ± 3.7	116.2 ± 6.4	115.6 ± 2.5	0.47 ± 0.02	0.73 ± 0.03	0.26 ± 0.04
A3-24	72.1 ± 2.9	236.5 ± 11.1	84.2 ± 4.0	90.2 ± 3.8	0.86 ± 0.02	2.62 ± 0.05	1.76 ± 0.05
P2-7	82.8 ± 4.4	384.0 ± 34.1	105.1 ± 6.4	120.4 ± 10.2	0.79 ± 0.02	3.19 ± 0.16	2.40 ± 0.16
P2-27	113.4 ± 6.6	555.4 ± 14.1	140.7 ± 8.5	118.7 ± 4.8	0.81 ± 0.01	4.68 ± 0.10	3.88 ± 0.10
P5-10	77.5 ± 6.5	244.4 ± 15.9	86.7 ± 4.3	95.8 ± 6.7	0.89 ± 0.05	2.55 ± 0.06	1.66 ± 0.08
P5-28	64.0 ± 5.2	333.6 ± 12.1	100.6 ± 6.1	94.7 ± 6.3	0.63 ± 0.02	3.53 ± 0.12	2.89 ± 0.13

Reactions containing the indicated probes and calculations were performed as described in Material and Methods and in the legend to Fig. 2.

PAGE 4/7 * RCVD AT 10/24/2005 5:55:20 PM [Pacific Daylight Time] * SVR:SVCS01/0 * DNIS:6034 * CSID:(613) 991-5695 * DURATION (mm-ss):05-46

fluorescence of a reporter dye on the 5′ end. The degree of quenching is sufficient for this type of oligonucleotide to be used as a probe in the 5′ nuclease PCR assay.

To test the hypothesis that quenching by a 3′ TAMRA depends on the flexibility of the oligonucleotide, fluorescence was measured for probes in the single-stranded and double-stranded states. Table 3 reports the fluorescence observed at 518 and 582 nm. The relative degree of quenching is assessed by calculating the RQ ratio. For probes with TAMRA 6–10 nucleotides from the 5′ end, there is little difference in the RQ values when comparing single-stranded with double-stranded oligonucleotides. The results for probes with TAMRA at the 3′ end are much different. For these probes, hybridization to a complementary strand causes a dramatic increase in RQ. We propose that this loss of quenching is caused by the rigid structure of double-stranded DNA, which prevents the 5′ and 3′ ends from being in proximity.

When TAMRA is placed toward the 3′ end, there is a marked Mg^{2+} effect on quenching. Figure 3 shows a plot of observed RQ values for the A1 series of probes as a function of Mg^{2+} concentration. With TAMRA attached near the 5′ end (probe A1-2 or A1-7), the RQ value at 0 mM Mg^{2+} is only slightly higher than RQ at 10 mM Mg^{2+}. For probes A1-19, A1-22, and A1-26, the RQ values at 0 mM Mg^{2+} are very high, indicating a much reduced quenching efficiency. For each of these probes, there is a marked decrease in RQ at 1 mM Mg^{2+} followed by a gradual decline as the Mg^{2+} concentration increases to 10 mM. Probe A1-14 shows an intermediate RQ value at 0 mM Mg^{2+} with a gradual decline at higher Mg^{2+} concentrations. In a low-salt environment with no Mg^{2+} present, a single-stranded oligonucleotide would be expected to adopt an extended conformation because of electrostatic repulsion. The binding of Mg^{2+} ions acts to shield the negative charge of the phosphate backbone so that the oligonucleotide can adopt conformations where the 3′ end is close to the 5′ end. Therefore, the observed Mg^{2+} effects support the notion that quenching of a 5′ reporter dye by TAMRA at or near the 3′ end depends on the flexibility of the oligonucleotide.

DISCUSSION

The striking finding of this study is that it seems the rhodamine dye TAMRA, placed at any position in an oligonucleotide, can quench the fluorescent emission of a fluorescein (6-FAM) placed at the 5′ end. This implies that a single-stranded, double-labeled oligonucleotide must be able to adopt conformations where the TAMRA is close to the 5′ end. It should be noted that the decay of 6-FAM in the excited state requires a certain amount of time. Therefore, what matters for quenching is not the average distance between 6-FAM and TAMRA but, rather, how close TAMRA can get to 6-FAM during the lifetime of the 6-FAM excited state. As long as the decay time of the excited state is relatively long compared with the molecular motions of the oligonucleotide, quenching can occur. Thus, we propose that TAMRA at the 3′ end, or any other position, can quench 6-FAM at the 5′ end because TAMRA is in proximity to 6-FAM often enough to be able to accept energy transfer from an excited 6-FAM.

Details of the fluorescence measurements remain puzzling. For example, Table 3 shows that hybridization of probes A1-26, A3-24, and P5-28 to their complementary strands not only causes a large increase in 6-FAM fluorescence at 518 nm but also causes a modest increase in TAMRA fluorescence at 582 nm. If TAMRA is being excited by energy transfer from quenched 6-FAM, then loss of quenching attributable to hybridization should cause a decrease in the fluorescence emission of TAMRA. The fact that the fluorescence emission of TAMRA increases indicates that the situation is more complex. For example, we have anecdotal evidence that the bases of the oligonucleotide, especially G, quench the fluorescence of both 6-FAM and TAMRA to some degree. When double-stranded, base-pairing may reduce the ability of the bases to quench. The primary factor causing the quenching of 6-FAM in an intact probe is the TAMRA dye. Evidence for the importance of TAMRA is that 6-FAM fluorescence remains relatively unchanged when probes labeled only with 6-FAM are used in the 5′ nuclease PCR assay (data not shown). Secondary effectors of fluorescence, both before and after cleavage of the probe, need to be explored further.

Regardless of the physical mechanism, the relative independence of position and quenching greatly simplifies the design of probes for the 5′ nuclease PCR assay. There are three main factors that determine the performance of a double-labeled fluorescent probe in the 5′ nuclease PCR assay. The first factor is the degree of quenching observed in the intact probe. This is characterized by the value of RQ^-, which is the ratio of reporter to quencher fluorescent emissions for a no template control PCR. Influences on the value of RQ^- include the particular reporter and quencher

TABLE 3 Comparison of Fluorescence Emissions of Single-stranded and Double-stranded Fluorogenic Probes

	518 nm		582 nm		RQ	
Probe	ss	ds	ss	ds	ss	ds
A1-7	27.75	68.53	61.08	138.18	0.45	0.50
A1-26	43.31	509.38	53.50	93.86	0.81	5.43
A3-6	16.75	62.88	39.33	165.57	0.43	0.38
A3-24	30.05	578.64	67.72	140.25	0.45	3.21
P2-7	35.02	70.13	54.63	121.09	0.64	0.58
P2-27	39.89	320.47	65.10	61.13	0.61	5.25
P5-10	27.34	144.85	61.95	165.54	0.44	0.87
P5-28	33.65	462.29	72.39	104.61	0.46	4.43

(ss) Single-stranded. The fluorescence emissions at 518 or 582 nm for solutions containing a final concentration of 50 nM indicated probe, 10 mM Tris-HCl (pH 8.3), 50 mM KCl, and 10 mM $MgCl_2$. (ds) Double-stranded. The solutions contained, in addition, 100 nM A1C for probes A1-7 and A1-26, 100 nM A3C for probes A3-6 and A3-24, 100 nM P2C for probes P2-7 and P2-27, or 100 nM P5C for probes P5-10 and P5-28. Before the addition of $MgCl_2$, 120 μl of each sample was heated at 95°C for 5 min. Following the addition of 80 μl of 25 mM $MgCl_2$, each sample was allowed to cool to room temperature and the fluorescence emissions were measured. Reported values are the average of three determinations.

PAGE 5/7 * RCVD AT 10/24/2005 5:55:20 PM [Pacific Daylight Time] * SVR:SVCS01/0 * DNIS:6034 * CSID:(613) 991-5695 * DURATION (mm-ss):05-46

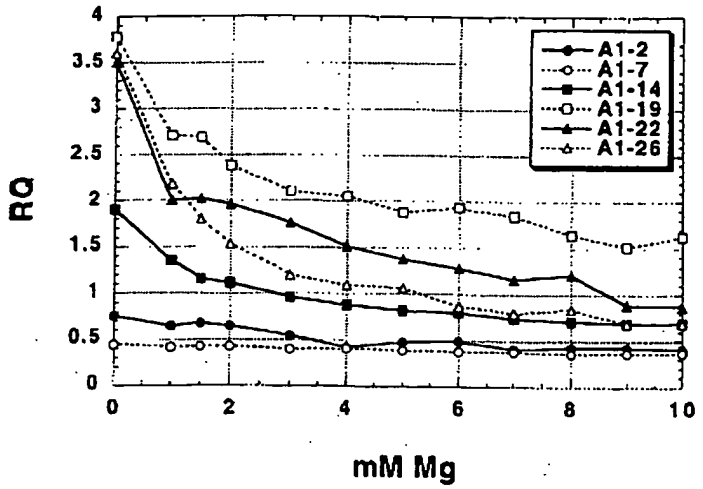

FIGURE 3 Effect of Mg^{2+} concentration on RQ ratio for the A1 series of probes. The fluorescence emission intensity at 518 and 582 nm was measured for solutions containing 50 nM probe, 10 mM Tris-HCl (pH 8.3), 50 mM KCl, and varying amounts (0–10 mM) of $MgCl_2$. The calculated RQ ratios (518 nm intensity divided by 582 nm intensity) are plotted vs. $MgCl_2$ concentration (mM Mg). The key (*upper right*) shows the probes examined.

dyes used, spacing between reporter and quencher dyes, nucleotide sequence context effects, presence of structure or other factors that reduce flexibility of the oligonucleotide, and purity of the probe. The second factor is the efficiency of hybridization, which depends on probe T_m, presence of secondary structure in probe or template, annealing temperature, and other reaction conditions. The third factor is the efficiency at which *Taq* DNA polymerase cleaves the bound probe between the reporter and quencher dyes. This cleavage is dependent on sequence complementarity between probe and template as shown by the observation that mismatches in the segment between reporter and quencher dyes drastically reduce the cleavage of probe.[1]

The rise in RQ^- values for the A1 series of probes seems to indicate that the degree of quenching is reduced somewhat as the quencher is placed toward the 3′ end. The lowest apparent quenching is observed for probe A1-19 (see Fig. 3) rather than for the probe where the TAMRA is at the 3′ end (A1-26). This is understandable, as the conformation of the 3′ end position would be expected to be less restricted than the conformation of an internal position. In effect, a quencher at the 3′ end is freer to adopt conformations close to the 5′ reporter dye than is an internally placed quencher. For the other three sets of probes, the interpretation of RQ^- values is less clear-cut. The A3 probes show the same trend as A1, with the 3′ TAMRA probe having a larger RQ^- than the internal TAMRA probe. For the P2 pair, both probes have about the same RQ^- value. For the P5 probes, the RQ^- for the 3′ probe is less than for the internally labeled probe. Another factor that may explain some of the observed variation is that purity affects the RQ^- value. Although all probes are HPLC purified, a small amount of contamination with unquenched reporter can have a large effect on RQ^-.

Although there may be a modest effect on degree of quenching, the position of the quencher apparently can have a large effect on the efficiency of probe cleavage. The most drastic effect is observed with probe A1-2, where placement of the TAMRA on the second nucleotide reduces the efficiency of cleavage to almost zero. For the A3, P2, and P5 probes, ΔRQ is much greater for the 3′ TAMRA probes as compared with the internal TAMRA probes. This is explained most easily by assuming that probes with TAMRA at the 3′ end are more likely to be cleaved between reporter and quencher than are probes with TAMRA attached internally. For the A1 probes, the cleavage efficiency of probe A1-7 must already be quite high, as ΔRQ does not increase when the quencher is placed closer to the 3′ end. This illustrates the importance of being able to use probes with a quencher on the 3′ end in the 5′ nuclease PCR assay. In this assay, an increase in the intensity of reporter fluorescence is observed only when the probe is cleaved between the reporter and quencher dyes. By placing the reporter and quencher dyes on the opposite ends of an oligonucleotide probe, any cleavage that occurs will be detected. When the quencher is attached to an internal nucleotide, sometimes the probe works well (A1-7) and other times not so well (A3-6). The relatively poor performance of probe A3-6 presumably means the probe is being cleaved 3′ to the quencher rather than between the reporter and quencher. Therefore, the best chance of having a probe that reliably detects accumulation of PCR product in the 5′ nuclease PCR assay is to use a probe with the reporter and quencher dyes on opposite ends.

Placing the quencher dye on the 3′ end may also provide a slight benefit in terms of hybridization efficiency. The presence of a quencher attached to an internal nucleotide might be expected to disrupt base-pairing and reduce the T_m of a probe. In fact, a 2°C–3°C reduction in T_m has been observed for two probes with internally attached TAMRAs.[9] This disruptive effect would be minimized by placing the quencher at the 3′ end. Thus, probes with 3′ quenchers might exhibit slightly higher hybridization efficiencies than probes with internal quenchers.

The combination of increased cleavage and hybridization efficiencies means that probes with 3′ quenchers probably will be more tolerant of mismatches between probe and target as compared with internally labeled probes. This tolerance of mismatches can be advantageous, as when trying to use a single probe to detect PCR-amplified products from samples of different species. Also, it means that cleavage of probe during PCR is less sensitive to alterations in annealing temperature or other reaction conditions. The one application where tolerance of mismatches may be a disadvantage is for allelic discrimination. Lee et al.[1] demonstrated that allele-specific probes were cleaved between reporter and quencher only when hybridized to a perfectly complementary target. This allowed them to distinguish the normal human cystic fibrosis allele from the *ΔF508* mutant. Their probes had TAMRA attached to the seventh nucleotide from

PAGE 6/7 * RCVD AT 10/24/2005 5:55:20 PM [Pacific Daylight Time] * SVR:SVCS01/0 * DNIS:6034 * CSID:(613) 991-5695 * DURATION (mm-ss):05-46

the 5′ end and were designed so that any mismatches were between the reporter and quencher. Increasing the distance between reporter and quencher would lessen the disruptive effect of mismatches and allow cleavage of the probe on the incorrect target. Thus, probes with a quencher attached to an internal nucleotide may still be useful for allelic discrimination.

In this study loss of quenching upon hybridization was used to show that quenching by a 3′ TAMRA is dependent on the flexibility of a single-stranded oligonucleotide. The increase in reporter fluorescence intensity, though, could also be used to determine whether hybridization has occurred or not. Thus, oligonucleotides with reporter and quencher dyes attached at opposite ends should also be useful as hybridization probes. The ability to detect hybridization in real time means that these probes could be used to measure hybridization kinetics. Also, this type of probe could be used to develop homogeneous hybridization assays for diagnostics or other applications. Bagwell et al.[10] describe just this type of homogeneous assay where hybridization of a probe causes an increase in fluorescence caused by a loss of quenching. However, they utilized a complex probe design that requires adding nucleotides to both ends of the probe sequence to form two imperfect hairpins. The results presented here demonstrate that the simple addition of a reporter dye to one end of an oligonucleotide and a quencher dye to the other end generates a fluorogenic probe that can detect hybridization or PCR amplification.

ACKNOWLEDGMENTS

We acknowledge Lincoln McBride of Perkin-Elmer for his support and encouragement on this project and Mitch Winnik of the University of Toronto for helpful discussions on time-resolved fluorescence.

REFERENCES

1. Lee, L.G., C.R. Connell, and W. Bloch. 1993. Allelic discrimination by nick-translation PCR with fluorogenic probes. *Nucleic Acids Res.* **21:** 3761–3766.
2. Holland, P.M., R.D. Abramson, R. Watson, and D.H. Gelfand. 1991. Detection of specific polymerase chain reaction product by utilizing the 5′ to 3′ exonuclease activity of *Thermus aquaticus* DNA polymerase. *Proc. Natl. Acad. Sci.* **88:** 7276–7280.
3. Lyamichev, V., M.A.D. Brow, and J.E. Dahlberg. 1993. Structure-specific endonucleolytic cleavage of nucleic acids by eubacterial DNA polymerases. *Science* **260:** 778–783.
4. Förster, V.Th. 1948. Zwischenmolekulare Energiewanderung und Fluoreszenz. *Ann. Phys. (Leipzig)* **2:** 55–75.
5. Lakowicz, J.R. 1983. Energy transfer. In *Principles of fluorescent spectroscopy*, pp. 303–339. Plenum Press, New York, NY.
6. Stryer, L. and R.P. Haugland. 1967. Energy transfer: A spectroscopic ruler. *Proc. Natl. Acad. Sci.* **58:** 719–726.
7. Nakajima-Iijima, S., H. Hamada, P. Reddy, and T. Kakunaga. 1985. Molecular structure of the human cytoplasmic beta-actin gene: Inter-species homology of sequences in the introns. *Proc. Natl. Acad. Sci.* **82:** 6133–6137.
8. du Breuil, R.M., J.M. Patel, and B.V. Mendelow. 1993. Quantitation of β-actin-specific mRNA transcripts using xeno-competitive PCR. *PCR Methods Applic.* **3:** 57–59.
9. Livak, K.J. (unpubl.).
10. Bagwell, C.B., M.E. Munson, R.L. Christensen, and E.J. Lovett. 1994. A new homogeneous assay system for specific nucleic acid sequences: Poly-dA and poly-A detection. *Nucleic Acids Res.* **22:** 2424–2425.

Received December 20, 1994; accepted in revised form March 6, 1995.

PAGE 7/7 * RCVD AT 10/24/2005 5:55:20 PM [Pacific Daylight Time] * SVR:SVCS01/0 * DNIS:6034 * CSID:(613) 991-5695 * DURATION (mm-ss):05-46

THIS MATERIAL MAY BE PROTECTED
BY COPYRIGHT LAW (17 U.S. CODE)

GENOME METHODS

Real Time Quantitative PCR

Christian A. Heid,[1] Junko Stevens,[2] Kenneth J. Livak,[2] and P. Mickey Williams[1,3]

[1]BioAnalytical Technology Department, Genentech, Inc., South San Francisco, California 94080;
[2]Applied BioSystems Division of Perkin Elmer Corp., Foster City, California 94404

We have developed a novel "real time" quantitative PCR method. The method measures PCR product accumulation through a dual-labeled fluorogenic probe (i.e., TaqMan Probe). This method provides very accurate and reproducible quantitation of gene copies. Unlike other quantitative PCR methods, real-time PCR does not require post-PCR sample handling, preventing potential PCR product carry-over contamination and resulting in much faster and higher throughput assays. The real-time PCR method has a very large dynamic range of starting target molecule determination (at least five orders of magnitude). Real-time quantitative PCR is extremely accurate and less labor-intensive than current quantitative PCR methods.

Quantitative nucleic acid sequence analysis has had an important role in many fields of biological research. Measurement of gene expression (RNA) has been used extensively in monitoring biological responses to various stimuli (Tan et al. 1994; Huang et al. 1995a,b; Prud'homme et al. 1995). Quantitative gene analysis (DNA) has been used to determine the genomic quantity of a particular gene, as in the case of the human *HER2* gene, which is amplified in ~30% of breast tumors (Slamon et al. 1987). Gene and genome quantitation (DNA and RNA) also have been used for analysis of human immunodeficiency virus (HIV) burden demonstrating changes in the levels of virus throughout the different phases of the disease (Connor et al. 1993; Piatak et al. 1993b; Furtado et al. 1995).

Many methods have been described for the quantitative analysis of nucleic acid sequences (both for RNA and DNA; Southern 1975; Sharp et al. 1980; Thomas 1980). Recently, PCR has proven to be a powerful tool for quantitative nucleic acid analysis. PCR and reverse transcriptase (RT)–PCR have permitted the analysis of minimal starting quantities of nucleic acid (as little as one cell equivalent). This has made possible many experiments that could not have been performed with traditional methods. Although PCR has provided a powerful tool, it is imperative that it be used properly for quantitation (Raeymaekers 1995). Many early reports of quantitative PCR and RT–PCR described quantitation of the PCR product but did not measure the initial target sequence quantity. It is essential to design proper controls for the quantitation of the initial target sequences (Ferre 1992; Clementi et al. 1993).

Researchers have developed several methods of quantitative PCR and RT–PCR. One approach measures PCR product quantity in the log phase of the reaction before the plateau (Kellogg et al. 1990; Pang et al. 1990). This method requires that each sample has equal input amounts of nucleic acid and that each sample under analysis amplifies with identical efficiency up to the point of quantitative analysis. A gene sequence (contained in all samples at relatively constant quantities, such as β-actin) can be used for sample amplification efficiency normalization. Using conventional methods of PCR detection and quantitation (gel electrophoresis or plate capture hybridization), it is extremely laborious to assure that all samples are analyzed during the log phase of the reaction (for both the target gene and the normalization gene). Another method, quantitative competitive (QC)–PCR, has been developed and is used widely for PCR quantitation. QC–PCR relies on the inclusion of an internal control competitor in each reaction (Becker-Andre 1991; Piatak et al. 1993a,b). The efficiency of each reaction is normalized to the internal competitor. A known amount of internal competitor can be

[3]Corresponding author.

added to each sample. To obtain relative quantitation, the unknown target PCR product is compared with the known competitor PCR product. Success of a quantitative competitive PCR assay relies on developing an internal control that amplifies with the same efficiency as the target molecule. The design of the competitor and the validation of amplification efficiencies require a dedicated effort. However, because QC–PCR does not require that PCR products be analyzed during the log phase of the amplification, it is the easier of the two methods to use.

Several detection systems are used for quantitative PCR and RT–PCR analysis: (1) agarose gels, (2) fluorescent labelling of PCR products and detection with laser-induced fluorescence using capillary electrophoresis (Fasco et al. 1995; Williams et al. 1996) or acrylamide gels, and (3) plate capture and sandwich probe hybridization (Mulder et al. 1994). Although these methods proved successful, each method requires post-PCR manipulations that add time to the analysis and may lead to laboratory contamination. The sample throughput of these methods is limited (with the exception of the plate capture approach), and, therefore, these methods are not well suited for uses demanding high sample throughput (i.e., screening of large numbers of biomolecules or analyzing samples for diagnostics or clinical trials).

Here we report the development of a novel assay for quantitative DNA analysis. The assay is based on the use of the 5′ nuclease assay first described by Holland et al. (1991). The method uses the 5′ nuclease activity of *Taq* polymerase to cleave a nonextendible hybridization probe during the extension phase of PCR. The approach uses dual-labeled fluorogenic hybridization probes (Lee et al. 1993; Bassler et al. 1995; Livak et al. 1995a,b). One fluorescent dye serves as a reporter [FAM (i.e., 6-carboxyfluorescein)] and its emission spectra is quenched by the second fluorescent dye, TAMRA (i.e., 6-carboxy-tetramethylrhodamine). The nuclease degradation of the hybridization probe releases the quenching of the FAM fluorescent emission, resulting in an increase in peak fluorescent emission at 518 nm. The use of a sequence detector (ABI Prism) allows measurement of fluorescent spectra of all 96 wells of the thermal cycler continuously during the PCR amplification. Therefore, the reactions are monitored in real time. The output data is described and quantitative analysis of input target DNA sequences is discussed below.

RESULTS

PCR Product Detection in Real Time

The goal was to develop a high-throughput, sensitive, and accurate gene quantitation assay for use in monitoring lipid mediated therapeutic gene delivery. A plasmid encoding human factor VIII gene sequence, pIHTM (see Methods), was used as a model therapeutic gene. The assay uses fluorescent Taqman methodology and an instrument capable of measuring fluorescence in real time (ABI Prism 7700 Sequence Detector). The Taqman reaction requires a hybridization probe labeled with two different fluorescent dyes. One dye is a reporter dye (FAM), the other is a quenching dye (TAMRA). When the probe is intact, fluorescent energy transfer occurs and the reporter dye fluorescent emission is absorbed by the quenching dye (TAMRA). During the extension phase of the PCR cycle, the fluorescent hybridization probe is cleaved by the 5′–3′ nucleolytic activity of the DNA polymerase. On cleavage of the probe, the reporter dye emission is no longer transferred efficiently to the quenching dye, resulting in an increase of the reporter dye fluorescent emission spectra. PCR primers and probes were designed for the human factor VIII sequence and human β-actin gene (as described in Methods). Optimization reactions were performed to choose the appropriate probe and magnesium concentrations yielding the highest intensity of reporter fluorescent signal without sacrificing specificity. The instrument uses a charge-coupled device (i.e., CCD camera) for measuring the fluorescent emission spectra from 500 to 650 nm. Each PCR tube was monitored sequentially for 25 msec with continuous monitoring throughout the amplification. Each tube was re-examined every 8.5 sec. Computer software was designed to examine the fluorescent intensity of both the reporter dye (FAM) and the quenching dye (TAMRA). The fluorescent intensity of the quenching dye, TAMRA, changes very little over the course of the PCR amplification (data not shown). Therefore, the intensity of TAMRA dye emission serves as an internal standard with which to normalize the reporter dye (FAM) emission variations. The software calculates a value termed ΔRn (or ΔRQ) using the following equation: $\Delta Rn = (Rn^+) - (Rn^-)$, where Rn^+ = emission intensity of reporter/emission intensity of quencher at any given time in a reaction tube, and Rn^- = emission intensity of re-

porter/emission intensity of quencher measured prior to PCR amplification in that same reaction tube. For the purpose of quantitation, the last three data points (ΔRns) collected during the extension step for each PCR cycle were analyzed. The nucleolytic degradation of the hybridization probe occurs during the extension phase of PCR, and, therefore, reporter fluorescent emission increases during this time. The three data points were averaged for each PCR cycle and the mean value for each was plotted in an "amplification plot" shown in Figure 1A. The ΔRn mean value is plotted on the *y*-axis, and time, represented by cycle number, is plotted on the *x*-axis. During the early cycles of the PCR amplification, the ΔRn value remains at base line. When sufficient hybridization probe has been cleaved by the *Taq* polymerase nuclease activity, the intensity of reporter fluorescent emission increases. Most PCR amplifications reach a plateau phase of reporter fluorescent emission if the reaction is carried out to high cycle numbers. The amplification plot is examined early in the reaction, at a point that represents the log phase of product accumulation. This is done by assigning an arbitrary threshold that is based on the variability of the base-line data. In Figure 1A, the threshold was set at 10 standard deviations above the mean of base line emission calculated from cycles 1 to 15. Once the threshold is chosen, the point at which

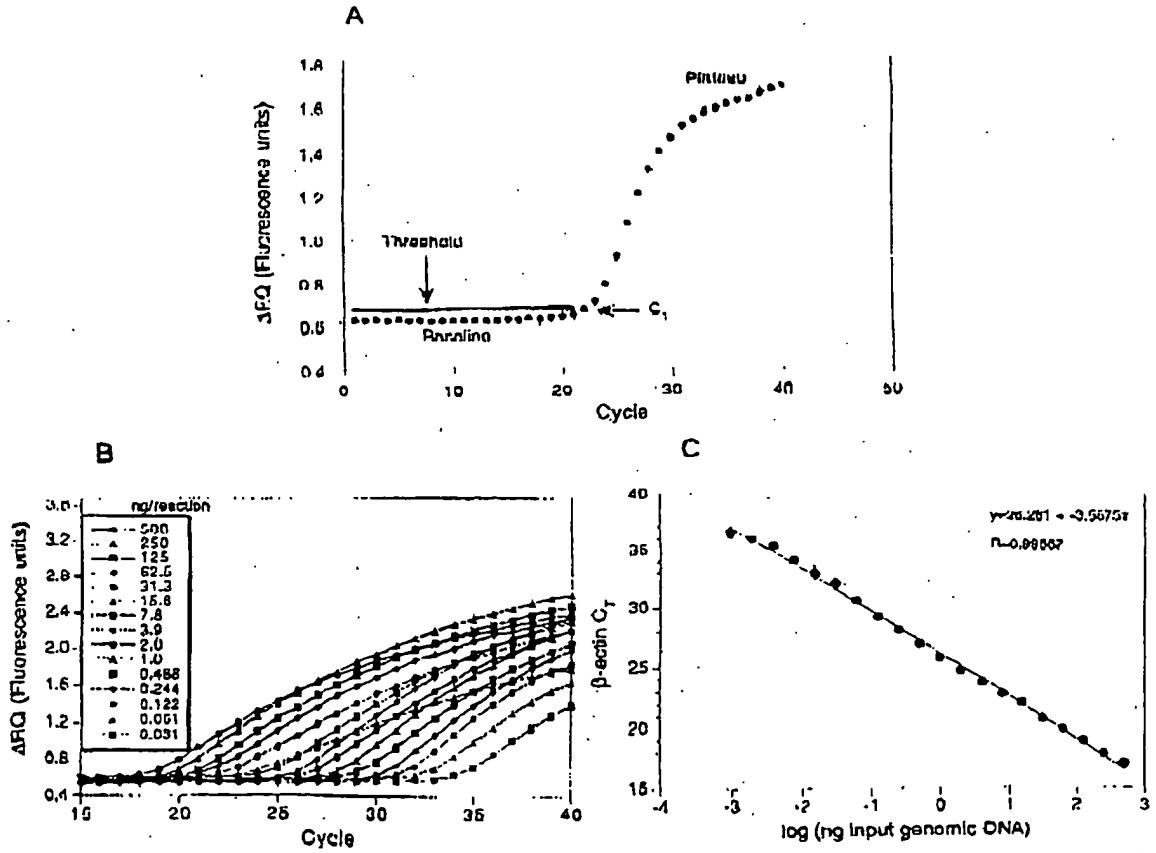

Figure 1 PCR product detection in real time. (*A*) The Model 7700 software will construct amplification plots from the extension phase fluorescent emission data collected during the PCR amplification. The standard deviation is determined from the data points collected from the base line of the amplification plot. C_T values are calculated by determining the point at which the fluorescence exceeds a threshold limit (usually 10 times the standard deviation of the base line). (*B*) Overlay of amplification plots of serially (1:2) diluted human genomic DNA samples amplified with β-actin primers. (*C*) Input DNA concentration of the samples plotted versus C_T. All

the amplification plot crosses the threshold is defined as C_T. C_T is reported as the cycle number at this point. As will be demonstrated, the C_T value is predictive of the quantity of input target.

C_T Values Provide a Quantitative Measurement of Input Target Sequences

Figure 1B shows amplification plots of 15 different PCR amplifications overlaid. The amplifications were performed on a 1:2 serial dilution of human genomic DNA. The amplified target was human β actin. The amplification plots shift to the right (to higher threshold cycles) as the input target quantity is reduced. This is expected because reactions with fewer starting copies of the target molecule require greater amplification to degrade enough probe to attain the threshold fluorescence. An arbitrary threshold of 10 standard deviations above the base line was used to determine the C_T values. Figure 1C represents the C_T values plotted versus the sample dilution value. Each dilution was amplified in triplicate PCR amplifications and plotted as mean values with error bars representing one standard deviation. The C_T values decrease linearly with increasing target quantity. Thus, C_T values can be used as a quantitative measurement of the input target number. It should be noted that the amplification plot for the 15.6-ng sample shown in Figure 1B does not reflect the same fluorescent rate of increase exhibited by most of the other samples. The 15.6-ng sample also achieves endpoint plateau at a lower fluorescent value than would be expected based on the input DNA. This phenomenon has been observed occasionally with other samples (data not shown) and may be attributable to late cycle inhibition; this hypothesis is still under investigation. It is important to note that the flattened slope and early plateau do not impact significantly the calculated C_T value as demonstrated by the fit on the line shown in Figure 1C. All triplicate amplifications resulted in very similar C_T values—the standard deviation did not exceed 0.5 for any dilution. This experiment contains a >100,000-fold range of input target molecules. Using C_T values for quantitation permits a much larger assay range than directly using total fluorescent emission intensity for quantitation. The linear range of fluorescent intensity measurement of the ABI Prism 7700 Sequence Detection System is only about 1,000-fold. Thus, the C_T value permits the analysis of experiments over a very large range of relative starting target quantities.

Sample Preparation Validation

Several parameters influence the efficiency of PCR amplification: magnesium and salt concentrations, reaction conditions (i.e., time and temperature), PCR target size and composition, primer sequences, and sample purity. All of the above factors are common to a single PCR assay except sample to sample purity. In an effort to validate the method of sample preparation for the factor VIII assay, PCR amplification reproducibility and efficiency of 10 replicate sample preparations were examined. After genomic DNA was prepared from the 10 replicate samples, the DNA was quantitated by ultraviolet spectroscopy. Amplifications were performed analyzing β-actin gene content in 100 and 25 ng of total genomic DNA. Each PCR amplification was performed in triplicate. Comparison of C_T values for each triplicate sample show minimal variation based on standard deviation and coefficient of variance (Table 1). Therefore, each of the triplicate PCR amplifications was highly reproducible, demonstrating that real time PCR using this instrumentation introduces minimal variation into the quantitative PCR analysis. Comparison of the mean C_T values of the 10 replicate sample preparations also showed minimal variability, indicating that each sample preparation yielded similar results for β-actin gene quantity. The highest C_T difference between any of the samples was 0.8 and 0.71 for the 100 and 25 ng samples, respectively. Additionally, the amplification of each sample exhibited an equivalent rate of fluorescent emission intensity change per amount of DNA target analyzed as indicated by similar slopes derived from the sample dilutions (Fig. 2). Any sample containing an excess of a PCR inhibitor would exhibit a greater measured β-actin C_T value for a given quantity of DNA. In addition, the inhibitor would be diluted along with the sample in the dilution analysis (Fig. 2), altering the expected C_T value change. Each sample amplification yielded a similar result in the analysis, demonstrating that this method of sample preparation is highly reproducible with regard to sample purity.

Quantitative Analysis of a Plasmid After

ORIGINAL

Table 1. Reproducibility of Sample Preparation Method

	100 ng				25 ng			
Sample no.	C_T	mean	standard deviation	CV	C_T	mean	standard deviation	CV
1	18.24				20.48			
	18.23				20.55			
	18.33	18.27	0.06	0.32	20.5	20.51	0.03	0.17
2	18.33				20.61			
	18.35				20.59			
	18.44	18.37	0.06	0.32	20.41	20.54	0.11	0.54
3	18.3				20.54			
	18.3				20.6			
	18.42	18.34	0.07	0.36	20.49	20.54	0.06	0.28
4	18.15				20.48			
	18.23				20.44			
	18.32	18.23	0.08	0.46	20.38	20.43	0.05	0.26
5	18.4				20.68			
	18.38				20.87			
	18.46	18.42	0.04	0.23	20.63	20.73	0.13	0.61
6	18.54				21.09			
	18.67				21.04			
	19	18.74	0.24	1.26	21.01	21.06	0.03	0.15
7	18.28				20.67			
	18.36				20.73			
	18.52	18.39	0.12	0.66	20.65	20.68	0.04	0.2
8	18.45				20.98			
	18.7				20.84			
	18.73	18.63	0.16	0.83	20.75	20.86	0.12	0.57
9	18.18				20.46			
	18.34				20.54			
	18.36	18.29	0.1	0.55	20.48	20.51	0.07	0.32
10	18.42				20.79			
	18.57				20.78			
	18.66	18.55	0.12	0.65	20.62	20.73	0.1	0.46
Mean	(1–10)	18.42	0.17	0.90		20.66	0.19	0.94

for containing a partial cDNA for human factor VIII, pF8TM. A series of transfections was set up using a decreasing amount of the plasmid (40, 4, 0.5, and 0.1 μg). Twenty-four hours post-transfection, total DNA was purified from each flask of cells. β-Actin gene quantity was chosen as a value for normalization of genomic DNA concentration from each sample. In this experiment, β-actin gene content should remain constant relative to total genomic DNA. Figure 3 shows the result of the β-actin DNA measurement (100 ng total DNA determined by ultraviolet spectroscopy) of each sample. Each sample was analyzed in triplicate and the mean β-actin C_T values of the triplicates were plotted (error bars represent one standard deviation). The highest difference between any two sample means was 0.95 C_T. Ten nanograms of total DNA of each sample were also examined for β-actin. The results again showed that very similar amounts of genomic DNA were present; the maximum mean β-actin C_T value difference was 1.0. As figure 3 shows, the rate of β-actin C_T change between the 100- and 10-ng samples was similar (slope values range between −3.56 and −3.45). This verifies again that the method of sample preparation yields samples of identical PCR integrity (i.e., no sample contained an excessive amount of a PCR inhibitor). However, these results indicate that each sample contained slight differences in the actual amount of genomic DNA analyzed. Determination of actual genomic DNA concentration was accomplished

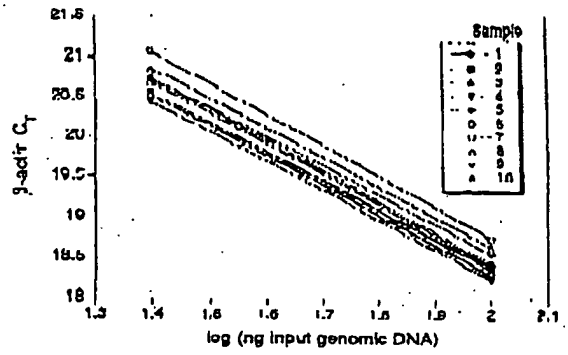

Figure 2 Sample preparation purity. The replicate samples shown in Table 1 were also amplified in tripicate using 25 ng of each DNA sample. The figure shows the input DNA concentration (100 and 25 ng) vs. C_T. In the figure, the 100 and 25 ng points for each sample are connected by a line.

by plotting the mean β-actin C_T value obtained for each 100-ng sample on a β-actin standard curve (shown in Fig. 4C). The actual genomic DNA concentration of each sample, *a*, was obtained by extrapolation to the *x*-axis.

Figure 4A shows the measured (i.e., non-normalized) quantities of factor VIII plasmid DNA (pF8TM) from each of the four transient cell transfections. Each reaction contained 100 ng of total sample DNA (as determined by UV spectroscopy). Each sample was analyzed in triplicate

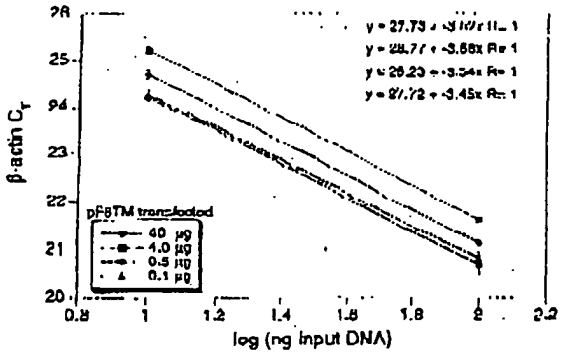

Figure 3 Analysis of transfected cell DNA quantity and purity. The DNA preparations of the four 293 cell transfections (40, 4, 0.5, and 0.1 µg of pF8TM) were analyzed for the β-actin gene. 100 and 10 ng (determined by ultraviolet spectroscopy) of each sample were amplified in triplicate. For each amount of pF8TM that was transfected, the β-actin C_T values are plotted versus the total input DNA concentration.

PCR amplifications. As shown, pF8TM purified from the 293 cells decreases (mean C_T values increase) with decreasing amounts of plasmid transfected. The mean C_T values obtained for pF8TM in Figure 4A were plotted on a standard curve comprised of serially diluted pF8TM, shown in Figure 4B. The quantity of pF8TM, *b*, found in each of the four transfections was determined by extrapolation to the *x* axis of the standard curve in Figure 4B. These uncorrected values, *b*, for pF8TM were normalized to determine the actual amount of pF8TM found per 100 ng of genomic DNA by using the equation:

$$\frac{b \times 100\ \text{ng}}{a} = \text{actual pF8TM copies per 100 ng of genomic DNA}$$

where *a* = actual genomic DNA in a sample and *b* = pF8TM copies from the standard curve. The normalized quantity of pF8TM per 100 ng of genomic DNA for each of the four transfections is shown in Figure 4D. These results show that the quantity of factor VIII plasmid associated with the 293 cells, 24 hr after transfection, decreases with decreasing plasmid concentration used in the transfection. The quantity of pF8TM associated with 293 cells, after transfection with 40 µg of plasmid, was 35 pg per 100 ng genomic DNA. This results in ~520 plasmid copies per cell.

DISCUSSION

We have described a new method for quantitating gene copy numbers using real-time analysis of PCR amplifications. Real-time PCR is compatible with either of the two PCR (RT–PCR) approaches: (1) quantitative competitive where an internal competitor for each target sequence is used for normalization (data not shown) or (2) quantitative comparative PCR using a normalization gene contained within the sample (i.e., β-actin) or a "housekeeping" gene for RT–PCR. If equal amounts of nucleic acid are analyzed for each sample and if the amplification efficiency before quantitative analysis is identical for each sample, the internal control (normalization gene or competitor) should give equal signals for all samples.

The real-time PCR method offers several advantages over the other two methods currently employed (see the Introduction). First, the real-time PCR method is performed in a closed-tube system and requires no post-PCR manipulation

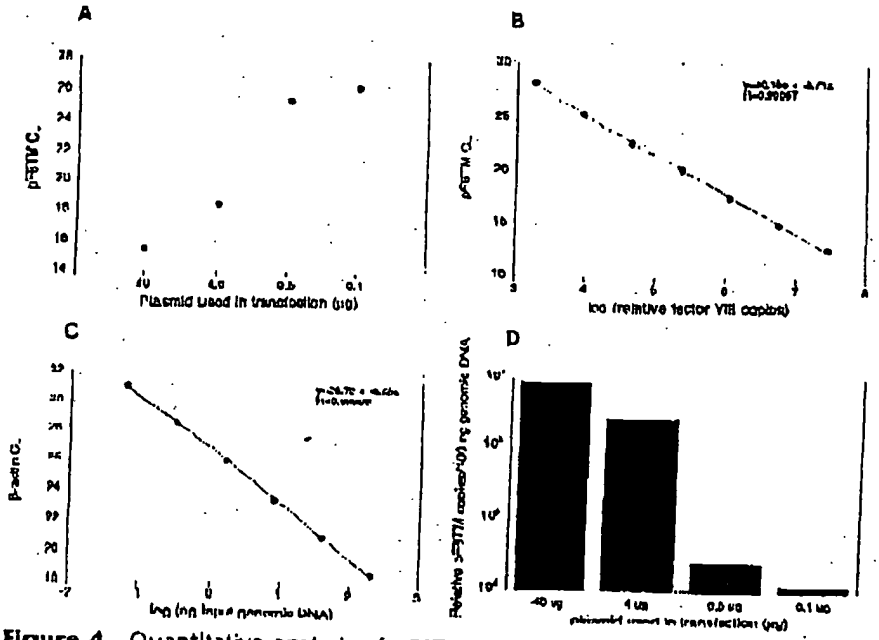

Figure 4 Quantitative analysis of pF8TM in transfected cells. (*A*) Amount of plasmid DNA used for the transfection plotted against the mean C_T value determined for pF8TM remaining 24 hr after transfection. (*B*,*C*) Standard curves of pF8TM and β-actin, respectively. pF8TM DNA (*B*) and genomic DNA (*C*) were diluted serially 1:5 before amplification with the appropriate primers. The β-actin standard curve was used to normalize the results of *A* to 100 ng of genomic DNA. (*D*) The amount of pF8TM present per 100 ng of genomic DNA.

of sample. Therefore, the potential for PCR contamination in the laboratory is reduced because amplified products can be analyzed and disposed of without opening the reaction tubes. Second, this method supports the use of a normalization gene (i.e., β-actin) for quantitative PCR or housekeeping genes for quantitative RT–PCR controls. Analysis is performed in real time during the log phase of product accumulation. Analysis during log phase permits many different genes (over a wide input target range) to be analyzed simultaneously, without concern of reaching reaction plateau at different cycles. This will make multigene analysis assays much easier to develop, because individual internal competitors will not be needed for each gene under analysis. Third, sample throughput will increase dramatically with the new method because there is no post-PCR processing time. Additionally, working in a 96-well format is highly compatible with automation technology.

The real-time PCR method is highly reproducible. Replicate amplifications can be analyzed for each sample minimizing potential error. The system allows for a very large assay dynamic range (approaching 1,000,000-fold starting target). Using a standard curve for the target of interest, relative copy number values can be determined for any unknown sample. Fluorescent threshold values, C_T, correlate linearly with relative DNA copy numbers. Real time quantitative RT-PCR methodology (Gibson et al., this issue) has also been developed. Finally, real time quantitative PCR methodology can be used to develop high-throughput screening assays for a variety of applications [quantitative gene expression (RT–PCR), gene copy assays (Her2, HIV, etc.), genotyping (knockout mouse analysis), and immuno-PCR].

Real-time PCR may also be performed using intercalating dyes (Higuchi et al. 1992) such as ethidium bromide. The fluorogenic probe method offers a major advantage over intercalating dyes—greater specificity (i.e., primer dimers and nonspecific PCR products are not detected).

METHODS

Generation of a Plasmid Containing a Partial cDNA for Human Factor VIII

Total RNA was harvested (RNAzol B from Tel Test, Inc., Friendswood, TX) from cells transfected with a factor VIII expression vector, pCIS2.8c251 (Eaton et al. 1986; Gorman et al. 1990). A factor VIII partial cDNA sequence was generated by RT PCR [GeneAmp EZ rTth RNA PCR Kit (part N808-0179, PE Applied Biosystems, Foster City, CA)] using the PCR primers F8for and F8rev (primer sequences are shown below). The amplicon was reamplified using modified F8for and F8rev primers (appended with *Bam*H I and *Hin*dIII restriction site sequences at the 5' end) and cloned into pGEM-3Z (Promega Corp., Madison, WI). The resulting clone, pF8TM, was used for transient transfection of 293 cells.

Amplification of Target DNA and Detection of Amplicon Factor VIII Plasmid DNA

(pF8TM) was amplified with the primers F8for 5'-CCCGTCCCAAGAGTGACATTGTC-3' and F8rev 5'-AAACCTTCACGCCTGGATGGTAGC-3'. The reaction produced a 422-bp PCR product. The forward primer was designed to recognize a unique sequence found in the 5' untranslated region of the parent pCIS2.8c251 plasmid and therefore does not recognize and amplify the human factor VIII gene. Primers were chosen with the assistance of the computer program Oligo 4.0 (National Biosciences, Inc., Plymouth, MN). The human β-actin gene was amplified with the primers β-actin forward primer 5'-TCACCCACACTGTGCCCATCTACGA-3' and β-actin reverse primer 5'-CAGCGGAACCGCTCATTGCCAATGG-3'. The reaction produced a 295-bp PCR product.

Amplification reactions (50 µl) contained a DNA sample, 10× PCR Buffer II (5 µl), 200 µM dATP, dCTP, dGTP, and 400 µM dUTP, 4 mM $MgCl_2$, 1.25 Units AmpliTaq DNA polymerase, 0.5 unit AmpErase uracil *N*-glycosylase (UNG), 60 pmole of each factor VIII primer, and 15 pmole of each β actin primer. The reactions also contained one of the following detection probes (100 nM each): F8probe 5'(FAM)ACGCTCTTCCACCTTGCTTTCTTTCTGTGCGTT(TAMRA)p 3' and β-actin probe 5' (FAM)ATGCCCX(TAMRA)CCCCCATGCCATCp-3' where p indicates phosphorylation and X indicates a linker arm nucleotide. Reaction tubes were MicroAmp Optical Tubes (part number N801 0933, Perkin Elmer) that were frosted (at Perkin Elmer) to prevent light from reflecting. Tube caps were similar to MicroAmp Caps but specially designed to prevent light scattering. All of the PCR consumables were supplied by PE Applied Biosystems (Foster City, CA) except the factor VIII primers, which were synthesized at Genentech, Inc. (South San Francisco, CA). Probes were designed using the Oligo 4.0 software, following guidelines suggested in the Model 7700 Sequence Detector Instrument manual. Briefly, probe T_m should be at least 5°C higher than the annealing temperature used during thermal cycling; primers should not form stable duplexes with the probe.

The thermal cycling conditions included 2 min at 50°C and 10 min at 95°C. Thermal cycling proceeded with reactions were performed in the Model 7700 Sequence Detector (PE Applied Biosystems), which contains a GeneAmp PCR System 9600. Reaction conditions were programmed on a Power Macintosh 7100 (Apple Computer, Santa Clara, CA) linked directly to the Model 7700 Sequence Detector. Analysis of data was also performed on the Macintosh computer. Collection and analysis software was developed at PE Applied Biosystems.

Transfection of Cells with Factor VIII Construct

Four T175 flasks of 293 cells (ATCC CRL 1573), a human fetal kidney suspension cell line, were grown to 80% confluency and transfected pF8TM. Cells were grown in the following media: 50% HAM'S F12 without GHT, 50% low glucose Dulbecco's modified Eagle medium (DMEM) without glycine with sodium bicarbonate, 10% fetal bovine serum, 2 mM L-glutamine, and 1% penicillin-streptomycin. The media was changed 30 min before the transfection. pF8TM DNA amounts of 40, 4, 0.5, and 0.1 µg were added to 1.5 ml of a solution containing 0.125 M $CaCl_2$ and 1× HEPES. The four mixtures were left at room temperature for 10 min and then added dropwise to the cells. The flasks were incubated at 37°C and 5% CO_2 for 24 hr, washed with PBS, and resuspended in PBS. The resuspended cells were divided into aliquots and DNA was extracted immediately using the QIAamp Blood Kit (Qiagen, Chatsworth, CA). DNA was eluted into 200 µl of 10 mM Tris-HCl at pH 8.0.

ACKNOWLEDGMENTS

We thank Genentech's DNA Synthesis Group for primer synthesis and Genentech's Graphics Group for assistance with the figures.

The publication costs of this article were defrayed in part by payment of page charges. This article must therefore be hereby marked "advertisement" in accordance with 18 USC section 1734 solely to indicate this fact.

REFERENCES

Bassler, H.A., S.J. Flood, K.J. Livak, J. Marmaro, R. Knorr, and C.A. Batt. 1995. Use of a fluorogenic probe in a PCR-based assay for the detection of Listeria monocytogenes. *App. Environ. Microbiol.* 61: 3724–3728.

Becker-Andre, M. 1991. Quantitative evaluation of IRBNA levels. *Meth. Mol. Cell. Biol.* 2: 189–201.

Clementi, M., S. Menzo, P. Bagnarelli, A. Manzin, A. Valenza, and P.E. Varaldo. 1993. Quantitative PCR and RT-PCR in virology. [Review]. *PCR Methods Applic.* 2: 191–196.

Connor, R.I., H. Mohri, Y. Cao, and D.D. Ho. 1993. Increased viral burden and cytopathicity correlate temporally with CD4+ T-lymphocyte decline and clinical progression in human immunodeficiency virus type 1-infected individuals. *J. Virol.* 67: 1772–1777.

Eaton, D.L., W.I. Wood, D. Eaton, P.E. Hass, P.

Venar, and C. Gorman. 1986. Construction and characterization of an active factor VIII variant lacking the central one third of the molecule. *Biochemistry* 25: 8343–8347.

Fasco, M.J., C.P. Treanor, S. Spivack, H.L. Pigge, and L.S. Kaminsky. 1995. Quantitative RNA-polymerase chain reaction-DNA analysis by capillary electrophoresis and laser-induced fluorescence. *Anal. Biochem.* 224: 140–147.

Ferre, F. 1992. Quantitative or semi-quantitative PCR: Reality versus myth. *PCR Methods Applic.* 2: 1–9.

Furtado, M.R., L.A. Kingsley, and S.M. Wolinsky. 1995. Changes in the viral mRNA expression pattern correlate with a rapid rate of CD4+ T-cell number decline in human immunodeficiency virus type 1-infected individuals. *J. Virol.* 69: 2092–2100.

Gibson, U.E.M., C.A. Heid, and P.M. Williams. 1996. A novel method for real time quantitative competitive RT–PCR. *Genome Res.* (this issue).

Gorman, C.M., D.R. Gies, and G. McCray. 1990. Transient production of proteins using an adenovirus transformed cell line. *DNA Prot. Engin. Tech.* 2: 3–10.

Higuchi, R., G. Dollinger, P.S. Walsh, and R. Griffith. 1992. Simultaneous amplification and detection of specific DNA sequences. *Biotechnology* 10: 413–417.

Holland, P.M., R.D. Abramson, R. Watson, and D.H. Gelfand. 1991. Detection of specific polymerase chain reaction product by utilizing the 5′—3′ exonuclease activity of Thermus aquaticus DNA polymerase. *Proc. Natl. Acad. Sci.* 88: 7276–7280.

Huang, S.K., H.Q. Xiao, T.J. Kleine, G. Pacciotti, D.G. Marsh, L.M. Lichtenstein, and M.C. Liu. 1995a. IL-13 expression at the sites of allergen challenge in patients with asthma. *J. Immun.* 155: 2688–2694.

Huang, S.K., M. Yi, E. Palmer, and D.G. Marsh. 1995b. A dominant T cell receptor beta-chain in response to a short ragweed allergen, Amb a 5. *J. Immun.* 154: 6157–6162.

Kellogg, D.E., J.J. Sninsky, and S. Kwok. 1990. Quantitation of HIV-1 proviral DNA relative to cellular DNA by the polymerase chain reaction. *Anal. Biochem.* 189: 202–208.

Lee, L.G., C.R. Connell, and W. Bloch. 1993. Allelic discrimination by nick-translation PCR with fluorogenic probes. *Nucleic Acids Res.* 21: 3761–3766.

Livak, K.J., S.J. Flood, J. Marmaro, W. Giusti, and K. Deetz. 1995a. Oligonucleotides with fluorescent dyes at opposite ends provide a quenched probe system useful for detecting PCR product and nucleic acid hybridization. *PCR Methods Applic.* 4: 357–362.

Livak, K.J., J. Marmaro, and J.A. Todd. 1995b. Towards fully automated genome-wide polymorphism screening [Letter]. *Nature Genet.* 9: 341–342.

Mulder, J., N. McKinney, C. Christopherson, J. Sninsky, L. Greenfield, and S. Kwok. 1994. Rapid and simple PCR assay for quantitation of human immunodeficiency virus type 1 RNA in plasma: Application to acute retroviral infection. *J. Clin. Microbiol.* 32: 292–300.

Pang, S., Y. Koyanagi, S. Miles, C. Wiley, H.V. Vinters, and I.S. Chen. 1990. High levels of unintegrated HIV-1 DNA in brain tissue of AIDS dementia patients. *Nature* 343: 85–89.

Piatak, M.J., K.C. Luk, B. Williams, and J.D. Lifson. 1993a. Quantitative competitive polymerase chain reaction for accurate quantitation of HIV DNA and RNA species. *BioTechniques* 14: 70–81.

Piatak, M.J., M.S. Saag, L.C. Yang, S.J. Clark, J.C. Kappes, K.C. Luk, B.H. Hahn, G.M. Shaw, and J.D. Lifson. 1993b. High levels of HIV-1 in plasma during all stages of infection determined by competitive PCR [see Comments]. *Science* 259: 1749–1754.

Prud'homme, G.J., D.H. Kono, and A.N. Theofilopoulos. 1995. Quantitative polymerase chain reaction analysis reveals marked overexpression of interleukin-1 beta, interleukin-4 and interferon-gamma mRNA in the lymph nodes of lupus-prone mice. *Mol. Immunol.* 32: 495–503.

Raeymaekers, L. 1995. A commentary on the practical applications of competitive PCR. *Genome Res.* 5: 91–94.

Sharp, P.A., A.J. Berk, and S.M. Berget. 1980. Transcription maps of adenovirus. *Methods Enzymol.* 65: 750–768.

Slamon, D.J., G.M. Clark, S.G. Wong, W.J. Levin, A. Ullrich, and W.L. McGuire. 1987. Human breast cancer: Correlation of relapse and survival with amplification of the HER-2/neu oncogene. *Science* 235: 177–182.

Southern, E.M. 1975. Detection of specific sequences among DNA fragments separated by gel electrophoresis. *J. Mol. Biol.* 98: 503–517.

Tan, X., X. Sun, C.P. Gonzalez, and W. Hsueh. 1994. PAF and TNF increase the precursor of NF-kappa B p50 mRNA in mouse intestine: Quantitative analysis by competitive PCR. *Biochim. Biophys. Acta* 1215: 157–162.

Thomas, P.S. 1980. Hybridization of denatured RNA and small DNA fragments transferred to nitrocellulose. *Proc. Natl. Acad. Sci.* 77: 5201–5205.

Williams, S., C. Schwer, A. Krishnarao, C. Heid, B. Karger, and P.M. Williams. 1996. Quantitative competitive PCR: Analysis of amplified products of the HIV-1 gag gene by capillary electrophoresis with laser induced fluorescence detection. *Anal. Biochem.* (in press).

Received June 3, 1996; accepted in revised form July 29, 1996.

Proc. Natl. Acad. Sci. USA
Vol. 95, pp. 14717–14722, December 1998
Cell Biology, Medical Sciences.

WISP genes are members of the connective tissue growth factor family that are up-regulated in Wnt-1-transformed cells and aberrantly expressed in human colon tumors

DIANE PENNICA*†, TODD A. SWANSON*, JAMES W. WELSH*, MARGARET A. ROY‡, DAVID A. LAWRENCE*, JAMES LEE‡, JENNIFER BRUSH‡, LISA A. TANEYHILL§, BETHANNE DEUEL‡, MICHAEL LEW¶, COLIN WATANABE‖, ROBERT L. COHEN*, MONA F. MELHEM**, GENE G. FINLEY**, PHIL QUIRKE††, AUDREY D. GODDARD‡, KENNETH J. HILLAN¶, AUSTIN L. GURNEY‡, DAVID BOTSTEIN‡,‡‡, AND ARNOLD J. LEVINE§

Departments of *Molecular Oncology, ‡Molecular Biology, §Scientific Computing, and ¶Pathology, Genentech Inc., 1 DNA Way, South San Francisco, CA 94080; **University of Pittsburgh School of Medicine, Veterans Administration Medical Center, Pittsburgh, PA 15240; ††University of Leeds, Leeds, LS29JT United Kingdom; ‡‡Department of Genetics, Stanford University, Palo Alto, CA 94305; and §Department of Molecular Biology, Princeton University, Princeton, NJ 08544

Contributed by David Botstein and Arnold J. Levine, October 21, 1998

ABSTRACT **Wnt family members are critical to many developmental processes, and components of the Wnt signaling pathway have been linked to tumorigenesis in familial and sporadic colon carcinomas. Here we report the identification of two genes, *WISP-1* and *WISP-2*, that are up-regulated in the mouse mammary epithelial cell line C57MG transformed by Wnt-1, but not by Wnt-4. Together with a third related gene, *WISP-3*, these proteins define a subfamily of the connective tissue growth factor family. Two distinct systems demonstrated *WISP* induction to be associated with the expression of Wnt-1. These included (*i*) C57MG cells infected with a Wnt-1 retroviral vector or expressing Wnt-1 under the control of a tetracyline repressible promoter, and (*ii*) Wnt-1 transgenic mice. The *WISP-1* gene was localized to human chromosome 8q24.1–8q24.3. *WISP-1* genomic DNA was amplified in colon cancer cell lines and in human colon tumors and its RNA overexpressed (2- to >30-fold) in 84% of the tumors examined compared with patient-matched normal mucosa. *WISP-3* mapped to chromosome 6q22–6q23 and also was overexpressed (4- to >40-fold) in 63% of the colon tumors analyzed. In contrast, *WISP-2* mapped to human chromosome 20q12–20q13 and its DNA was amplified, but RNA expression was reduced (2- to >30-fold) in 79% of the tumors. These results suggest that the *WISP* genes may be downstream of Wnt-1 signaling and that aberrant levels of *WISP* expression in colon cancer may play a role in colon tumorigenesis.**

Wnt-1 is a member of an expanding family of cysteine-rich, glycosylated signaling proteins that mediate diverse developmental processes such as the control of cell proliferation, adhesion, cell polarity, and the establishment of cell fates (1, 2). Wnt-1 originally was identified as an oncogene activated by the insertion of mouse mammary tumor virus in virus-induced mammary adenocarcinomas (3, 4). Although Wnt-1 is not expressed in the normal mammary gland, expression of Wnt-1 in transgenic mice causes mammary tumors (5).

In mammalian cells, Wnt family members initiate signaling by binding to the seven-transmembrane spanning Frizzled receptors and recruiting the cytoplasmic protein Dishevelled (Dsh) to the cell membrane (1, 2, 6). Dsh then inhibits the kinase activity of the normally constitutively active glycogen synthase kinase-3β (GSK-3β) resulting in an increase in β-catenin levels. Stabilized β-catenin interacts with the transcription factor TCF/Lef1, forming a complex that appears in the nucleus and binds TCF/Lef1 target DNA elements to activate transcription (7, 8). Other experiments suggest that the adenomatous polyposis coli (APC) tumor suppressor gene also plays an important role in Wnt signaling by regulating β-catenin levels (9). APC is phosphorylated by GSK-3β, binds to β-catenin, and facilitates its degradation. Mutations in either APC or β-catenin have been associated with colon carcinomas and melanomas, suggesting these mutations contribute to the development of these types of cancer, implicating the Wnt pathway in tumorigenesis (1).

Although much has been learned about the Wnt signaling pathway over the past several years, only a few of the transcriptionally activated downstream components activated by Wnt have been characterized. Those that have been described cannot account for all of the diverse functions attributed to Wnt signaling. Among the candidate Wnt target genes are those encoding the nodal-related 3 gene, *Xnr3*, a member of the transforming growth factor (TGF)-β superfamily, and the homeobox genes, *engrailed*, *goosecoid*, *twin* (*Xtwn*), and *siamois* (2). A recent report also identifies c-*myc* as a target gene of the Wnt signaling pathway (10).

To identify additional downstream genes in the Wnt signaling pathway that are relevant to the transformed cell phenotype, we used a PCR-based cDNA subtraction strategy, suppression subtractive hybridization (SSH) (11), using RNA isolated from C57MG mouse mammary epithelial cells and C57MG cells stably transformed by a Wnt-1 retrovirus. Overexpression of Wnt-1 in this cell line is sufficient to induce a partially transformed phenotype, characterized by elongated and refractile cells that lose contact inhibition and form a multilayered array (12, 13). We reasoned that genes differentially expressed between these two cell lines might contribute to the transformed phenotype.

In this paper, we describe the cloning and characterization of two genes up-regulated in Wnt-1 transformed cells, *WISP-1* and *WISP-2*, and a third related gene, *WISP-3*. The *WISP* genes are members of the CCN family of growth factors, which includes connective tissue growth factor (CTGF), Cyr61, and *nov*, a family not previously linked to Wnt signaling.

MATERIALS AND METHODS

SSH. SSH was performed by using the PCR-Select cDNA Subtraction Kit (CLONTECH). Tester double-stranded

The publication costs of this article were defrayed in part by page charge payment. This article must therefore be hereby marked "*advertisement*" in accordance with 18 U.S.C. §1734 solely to indicate this fact.

© 1998 by The National Academy of Sciences 0027-8424/98/9514717-6$2.00/0
PNAS is available online at www.pnas.org.

Abbreviations: TGF, transforming growth factor; CTGF, connective tissue growth factor; SSH, suppression subtractive hybridization; VWC, von Willebrand factor type C module.

Data deposition: The sequences reported in this paper have been deposited in the Genbank database (accession nos. AF100777, AF100778, AF100779, AF100780, and AF100781).

†To whom reprint requests should be addressed. e-mail: diane@gene.com.

cDNA was synthesized from 2 μg of poly(A)$^+$ RNA isolated from the C57MG/Wnt-1 cell line and driver cDNA from 2 μg of poly(A)$^+$ RNA from the parent C57MG cells. The subtracted cDNA library was subcloned into a pGEM-T vector for further analysis.

cDNA Library Screening. Clones encoding full-length mouse *WISP-1* were isolated by screening a λgt10 mouse embryo cDNA library (CLONTECH) with a 70-bp probe from the original partial clone 568 sequence corresponding to amino acids 128–169. Clones encoding full-length human *WISP-1* were isolated by screening λgt10 lung and fetal kidney cDNA libraries with the same probe at low stringency. Clones encoding full-length mouse and human *WISP-2* were isolated by screening a C57MG/Wnt-1 or human fetal lung cDNA library with a probe corresponding to nucleotides 1463–1512. Full-length cDNAs encoding *WISP-3* were cloned from human bone marrow and fetal kidney libraries.

Expression of Human *WISP* RNA. PCR amplification of first-strand cDNA was performed with human Multiple Tissue cDNA panels (CLONTECH) and 300 μM of each dNTP at 94°C for 1 sec, 62°C for 30 sec, 72°C for 1 min, for 22–32 cycles. *WISP* and glyceraldehyde-3-phosphate dehydrogenase primer sequences are available on request.

***In Situ* Hybridization.** ^{33}P-labeled sense and antisense riboprobes were transcribed from an 897-bp PCR product corresponding to nucleotides 601–1440 of mouse *WISP-1* or a 294-bp PCR product corresponding to nucleotides 82–375 of mouse *WISP-2*. All tissues were processed as described (40).

Radiation Hybrid Mapping. Genomic DNA from each hybrid in the Stanford G3 and Genebridge4 Radiation Hybrid Panels (Research Genetics, Huntsville, AL) and human and hamster control DNAs were PCR-amplified, and the results were submitted to the Stanford or Massachusetts Institute of Technology web servers.

Cell Lines, Tumors, and Mucosa Specimens. Tissue specimens were obtained from the Department of Pathology (University of Pittsburgh) for patients undergoing colon resection and from the University of Leeds, United Kingdom. Genomic DNA was isolated (Qiagen) from the pooled blood of 10 normal human donors, surgical specimens, and the following ATCC human cell lines: SW480, COLO 320DM, HT-29, WiDr, and SW403 (colon adenocarcinomas), SW620 (lymph node metastasis, colon adenocarcinoma), HCT 116 (colon carcinoma), SK-CO-1 (colon adenocarcinoma, ascites), and HM7 (a variant of ATCC colon adenocarcinoma cell line LS 174T). DNA concentration was determined by using Hoechst dye 33258 intercalation fluorimetry. Total RNA was prepared by homogenization in 7 M GuSCN followed by centrifugation over CsCl cushions or prepared by using RNAzol.

Gene Amplification and RNA Expression Analysis. Relative gene amplification and RNA expression of *WISP*s and c-*myc* in the cell lines, colorectal tumors, and normal mucosa were determined by quantitative PCR. Gene-specific primers and fluorogenic probes (sequences available on request) were designed and used to amplify and quantitate the genes. The relative gene copy number was derived by using the formula $2^{(\Delta Ct)}$ where ΔCt represents the difference in amplification cycles required to detect the *WISP* genes in peripheral blood lymphocyte DNA compared with colon tumor DNA or colon tumor RNA compared with normal mucosal RNA. The ∂-method was used for calculation of the SE of the gene copy number or RNA expression level. The *WISP*-specific signal was normalized to that of the glyceraldehyde-3-phosphate dehydrogenase housekeeping gene. All TaqMan assay reagents were obtained from Perkin–Elmer Applied Biosystems.

RESULTS

Isolation of *WISP-1* and *WISP-2* by SSH. To identify Wnt-1-inducible genes, we used the technique of SSH using the mouse mammary epithelial cell line C57MG and C57MG cells that stably express Wnt-1 (11). Candidate differentially expressed cDNAs (1,384 total) were sequenced. Thirty-nine percent of the sequences matched known genes or homologues, 32% matched expressed sequence tags, and 29% had no match. To confirm that the transcript was differentially expressed, semiquantitative reverse transcription–PCR and Northern analysis were performed by using mRNA from the C57MG and C57MG/Wnt-1 cells.

Two of the cDNAs, *WISP-1* and *WISP-2*, were differentially expressed, being induced in the C57MG/Wnt-1 cell line, but not in the parent C57MG cells or C57MG cells overexpressing Wnt-4 (Fig. 1 *A* and *B*). Wnt-4, unlike Wnt-1, does not induce the morphological transformation of C57MG cells and has no effect on β-catenin levels (13, 14). Expression of *WISP-1* was up-regulated approximately 3-fold in the C57MG/Wnt-1 cell line and *WISP-2* by approximately 5-fold by both Northern analysis and reverse transcription–PCR.

An independent, but similar, system was used to examine *WISP* expression after Wnt-1 induction. C57MG cells expressing the *Wnt-1* gene under the control of a tetracycline-repressible promoter produce low amounts of Wnt-1 in the repressed state but show a strong induction of *Wnt-1* mRNA and protein within 24 hr after tetracycline removal (8). The levels of Wnt-1 and *WISP* RNA isolated from these cells at various times after tetracycline removal were assessed by quantitative PCR. Strong induction of Wnt-1 mRNA was seen as early as 10 hr after tetracycline removal. Induction of *WISP* mRNA (2- to 6-fold) was seen at 48 and 72 hr (data not shown). These data support our previous observations that show that *WISP* induction is correlated with Wnt-1 expression. Because the induction is slow, occurring after approximately 48 hr, the induction of *WISP*s may be an indirect response to Wnt-1 signaling.

cDNA clones of human *WISP-1* were isolated and the sequence compared with mouse *WISP-1*. The cDNA sequences of mouse and human *WISP-1* were 1,766 and 2,830 bp in length, respectively, and encode proteins of 367 aa, with predicted relative molecular masses of ≈40,000 (M_r 40 K). Both have hydrophobic N-terminal signal sequences, 38 conserved cysteine residues, and four potential N-linked glycosylation sites and are 84% identical (Fig. 2*A*).

Full-length cDNA clones of mouse and human *WISP-2* were 1,734 and 1,293 bp in length, respectively, and encode proteins of 251 and 250 aa, respectively, with predicted relative molecular masses of ≈27,000 (M_r 27 K) (Fig. 2*B*). Mouse and human *WISP-2* are 73% identical. Human *WISP-2* has no potential N-linked glycosylation sites, and mouse *WISP-2* has one at

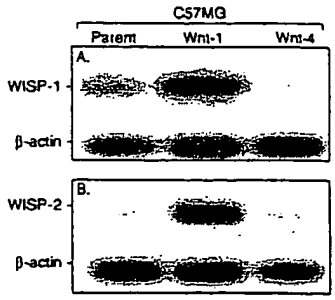

FIG. 1. *WISP-1* and *WISP-2* are induced by Wnt-1, but not Wnt-4, expression in C57MG cells. Northern analysis of *WISP-1* (*A*) and *WISP-2* (*B*) expression in C57MG, C57MG/Wnt-1, and C57MG/Wnt-4 cells. Poly(A)$^+$ RNA (2 μg) was subjected to Northern blot analysis and hybridized with a 70-bp mouse *WISP-1*-specific probe (amino acids 278–300) or a 190-bp *WISP-2*-specific probe (nucleotides 1438–1627) in the 3′ untranslated region. Blots were rehybridized with human β-actin probe.

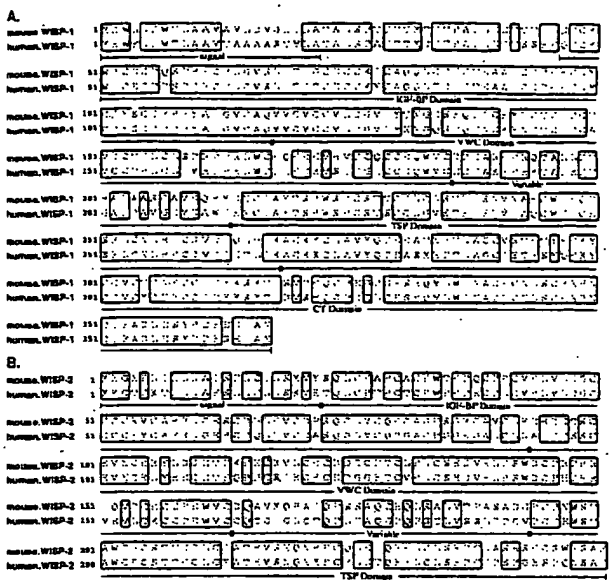

FIG. 2. Encoded amino acid sequence alignment of mouse and human *WISP-1* (*A*) and mouse and human *WISP-2* (*B*). The potential signal sequence, insulin-like growth factor-binding protein (IGF-BP), VWC, thrombospondin (TSP), and C-terminal (CT) domains are underlined.

position 197. *WISP-2* has 28 cysteine residues that are conserved among the 38 cysteines found in *WISP-1*.

Identification of *WISP-3*. To search for related proteins, we screened expressed sequence tag (EST) databases with the WISP-1 protein sequence and identified several ESTs as potentially related sequences. We identified a homologous protein that we have called WISP-3. A full-length human *WISP-3* cDNA of 1,371 bp was isolated corresponding to those ESTs that encode a 354-aa protein with a predicted molecular mass of 39,293. WISP-3 has two potential N-linked glycosylation sites and 36 cysteine residues. An alignment of the three human WISP proteins shows that WISP-1 and WISP-3 are the most similar (42% identity), whereas WISP-2 has 37% identity with WISP-1 and 32% identity with WISP-3 (Fig. 3*A*).

***WISPs* Are Homologous to the CTGF Family of Proteins.** Human *WISP-1*, *WISP-2*, and *WISP-3* are novel sequences; however, mouse *WISP-1* is the same as the recently identified *Elm1* gene. *Elm1* is expressed in low, but not high, metastatic mouse melanoma cells, and suppresses the *in vivo* growth and metastatic potential of K-1735 mouse melanoma cells (15). Human and mouse *WISP-2* are homologous to the recently described rat gene, *rCop-1* (16). Significant homology (36–44%) was seen to the CCN family of growth factors. This family includes three members, CTGF, Cyr61, and the protooncogene *nov*. CTGF is a chemotactic and mitogenic factor for fibroblasts that is implicated in wound healing and fibrotic disorders and is induced by TGF-β (17). Cyr61 is an extracellular matrix signaling molecule that promotes cell adhesion, proliferation, migration, angiogenesis, and tumor growth (18, 19). *nov* (nephroblastoma overexpressed) is an immediate early gene associated with quiescence and found altered in Wilms tumors (20). The proteins of the CCN family share functional, but not sequence, similarity to Wnt-1. All are secreted, cysteine-rich heparin binding glycoproteins that associate with the cell surface and extracellular matrix.

WISP proteins exhibit the modular architecture of the CCN family, characterized by four conserved cysteine-rich domains (Fig. 3*B*) (21). The N-terminal domain, which includes the first 12 cysteine residues, contains a consensus sequence (GCGCCXXC) conserved in most insulin-like growth factor (IGF)-binding proteins (BP). This sequence is conserved in WISP-2 and WISP-3, whereas WISP-1 has a glutamine in the third position instead of a glycine. CTGF recently has been shown to specifically bind IGF (22) and a truncated *nov* protein lacking the IGF-BP domain is oncogenic (23). The von Willebrand factor type C module (VWC), also found in certain collagens and mucins, covers the next 10 cysteine residues, and is thought to participate in protein complex formation and oligomerization (24). The VWC domain of WISP-3 differs from all CCN family members described previously, in that it contains only six of the 10 cysteine residues (Fig. 3 *A* and *B*). A short variable region follows the VWC domain. The third module, the thrombospondin (TSP) domain is involved in binding to sulfated glycoconjugates and contains six cysteine residues and a conserved WSxCSxxCG motif first identified in thrombospondin (25). The C-terminal (CT) module containing the remaining 10 cysteines is thought to be involved in dimerization and receptor binding (26). The CT domain is present in all CCN family members described to date but is absent in WISP-2 (Fig. 3 *A* and *B*). The existence of a putative signal sequence and the absence of a transmembrane domain suggest that WISPs are secreted proteins, an observation supported by an analysis of their expression and secretion from mammalian cell and baculovirus cultures (data not shown).

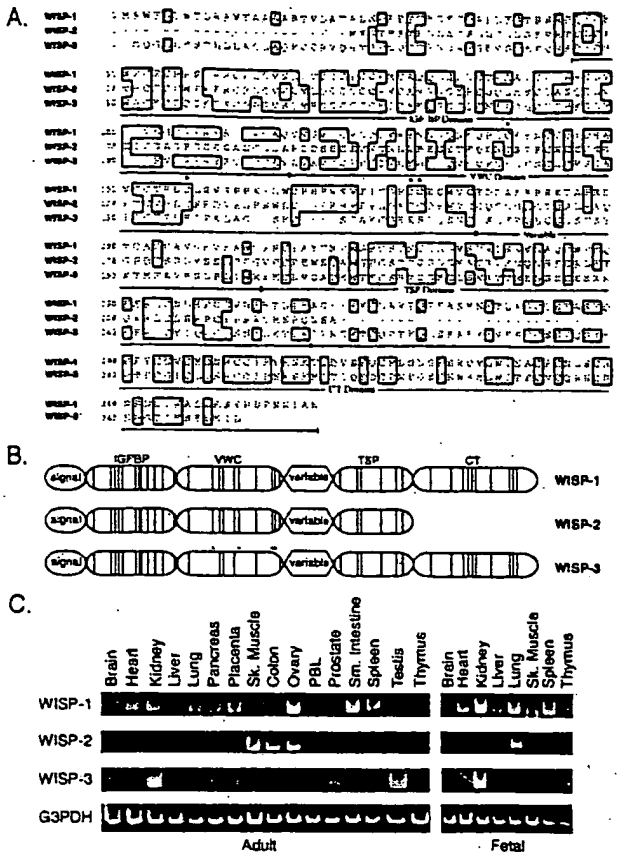

FIG. 3. (*A*) Encoded amino acid sequence alignment of human WISPs. The cysteine residues of WISP-1 and WISP-2 that are not present in WISP-3 are indicated with a dot. (*B*) Schematic representation of the WISP proteins showing the domain structure and cysteine residues (vertical lines). The four cysteine residues in the VWC domain that are absent in WISP-3 are indicated with a dot. (*C*) Expression of *WISP* mRNA in human tissues. PCR was performed on human multiple-tissue cDNA panels (CLONTECH) from the indicated adult and fetal tissues.

Expression of *WISP* mRNA in Human Tissues. Tissue-specific expression of human *WISP*s was characterized by PCR

analysis on adult and fetal multiple tissue cDNA panels. *WISP-1* expression was seen in the adult heart, kidney, lung, pancreas, placenta, ovary, small intestine, and spleen (Fig. 3*C*). Little or no expression was detected in the brain, liver, skeletal muscle, colon, peripheral blood leukocytes, prostate, testis, or thymus. *WISP-2* had a more restricted tissue expression and was detected in adult skeletal muscle, colon, ovary, and fetal lung. Predominant expression of *WISP-3* was seen in adult kidney and testis and fetal kidney. Lower levels of *WISP-3* expression were detected in placenta, ovary, prostate, and small intestine.

***In Situ* Localization of *WISP-1* and *WISP-2*.** Expression of *WISP-1* and *WISP-2* was assessed by *in situ* hybridization in mammary tumors from Wnt-1 transgenic mice. Strong expression of *WISP-1* was observed in stromal fibroblasts lying within the fibrovascular tumor stroma (Fig. 4 *A–D*). However, low-level *WISP-1* expression also was observed focally within tumor cells (data not shown). No expression was observed in normal breast. Like *WISP-1*, *WISP-2* expression also was seen in the tumor stroma in breast tumors from Wnt-1 transgenic animals (Fig. 4 *E–H*). However, *WISP-2* expression in the stroma was in spindle-shaped cells adjacent to capillary vessels, whereas the predominant cell type expressing *WISP-1* was the stromal fibroblasts.

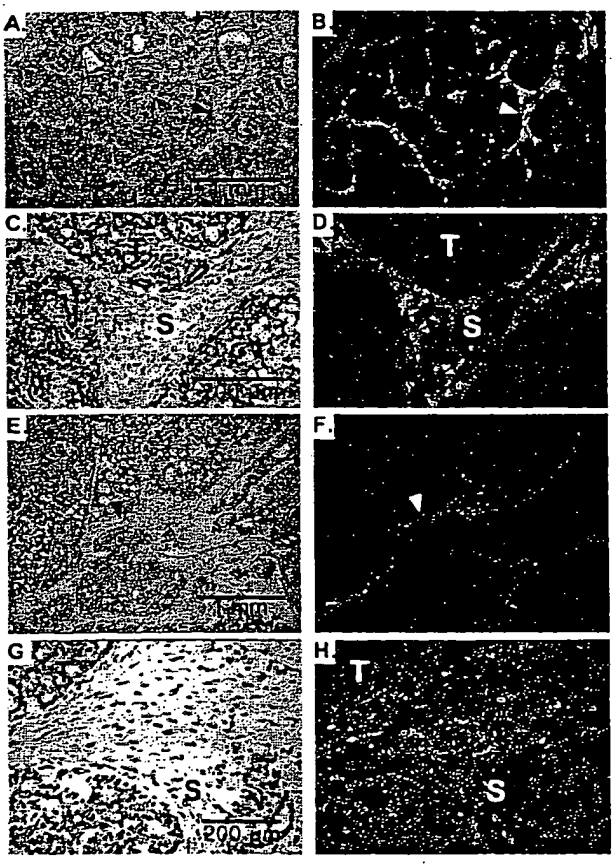

FIG. 4. (*A*, *C*, *E*, and *G*) Representative hematoxylin/eosin-stained images from breast tumors in Wnt-1 transgenic mice. The corresponding dark-field images showing *WISP-1* expression are shown in *B* and *D*. The tumor is a moderately well-differentiated adenocarcinoma showing evidence of adenoid cystic change. At low power (*A* and *B*), expression of *WISP-1* is seen in the delicate branching fibrovascular tumor stroma (arrowhead). At higher magnification, expression is seen in the stromal(s) fibroblasts (*C* and *D*), and tumor cells are negative. Focal expression of *WISP-1*, however, was observed in tumor cells in some areas. Images of *WISP-2* expression are shown in *E–H*. At low power (*E* and *F*), expression of WISP-2 is seen in cells lying within the fibrovascular tumor stroma. At higher magnification, these cells appeared to be adjacent to capillary vessels whereas tumor cells are negative (*G* and *H*).

Chromosome Localization of the *WISP* Genes. The chromosomal location of the human *WISP* genes was determined by radiation hybrid mapping panels. *WISP-1* is approximately 3.48 cR from the meiotic marker AFM259xc5 [logarithm of odds (lod) score 16.31] on chromosome 8q24.1 to 8q24.3, in the same region as the human locus of the *nov*H family member (27) and roughly 4 Mbs distal to c-*myc* (28). Preliminary fine mapping indicates that *WISP-1* is located near D8S1712 STS. *WISP-2* is linked to the marker SHGC-33922 (lod = 1,000) on chromosome 20q12–20q13.1. Human *WISP-3* mapped to chromosome 6q22–6q23 and is linked to the marker AFM211ze5 (lod = 1,000). *WISP-3* is approximately 18 Mbs proximal to CTGF and 23 Mbs proximal to the human cellular oncogene *MYB* (27, 29).

Amplification and Aberrant Expression of *WISPs* in Human Colon Tumors. Amplification of protooncogenes is seen in many human tumors and has etiological and prognostic significance. For example, in a variety of tumor types, c-*myc* amplification has been associated with malignant progression and poor prognosis (30). Because *WISP-1* resides in the same general chromosomal location (8q24) as c-*myc*, we asked whether it was a target of gene amplification, and, if so, whether this amplification was independent of the c-*myc* locus. Genomic DNA from human colon cancer cell lines was assessed by quantitative PCR and Southern blot analysis. (Fig. 5 *A* and *B*). Both methods detected similar degrees of *WISP-1* amplification. Most cell lines showed significant (2- to 4-fold) amplification, with the HT-29 and WiDr cell lines demonstrating an 8-fold increase. Significantly, the pattern of amplification observed did not correlate with that observed for c-*myc*, indicating that the c-*myc* gene is not part of the amplicon that involves the *WISP-1* locus.

We next examined whether the *WISP* genes were amplified in a panel of 25 primary human colon adenocarcinomas. The relative *WISP* gene copy number in each colon tumor DNA was compared with pooled normal DNA from 10 donors by quantitative PCR (Fig. 6). The copy number of *WISP-1* and *WISP-2* was significantly greater than one, approximately 2-fold for *WISP-1* in about 60% of the tumors and 2- to 4-fold for *WISP-2* in 92% of the tumors ($P < 0.001$ for each). The copy number for *WISP-3* was indistinguishable from one ($P = 0.166$). In addition, the copy number of *WISP-2* was significantly higher than that of *WISP-1* ($P < 0.001$).

The levels of *WISP* transcripts in RNA isolated from 19 adenocarcinomas and their matched normal mucosa were

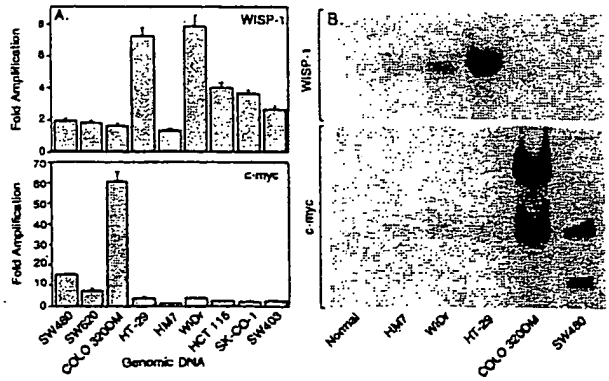

FIG. 5. Amplification of *WISP-1* genomic DNA in colon cancer cell lines. (*A*) Amplification in cell line DNA was determined by quantitative PCR. (*B*) Southern blots containing genomic DNA (10 μg) digested with *Eco*RI (*WISP-1*) or *Xba*I (c-*myc*) were hybridized with a 100-bp human *WISP-1* probe (amino acids 186–219) or a human c-*myc* probe (located at bp 1901–2000). The *WISP* and *myc* genes are detected in normal human genomic DNA after a longer film exposure.

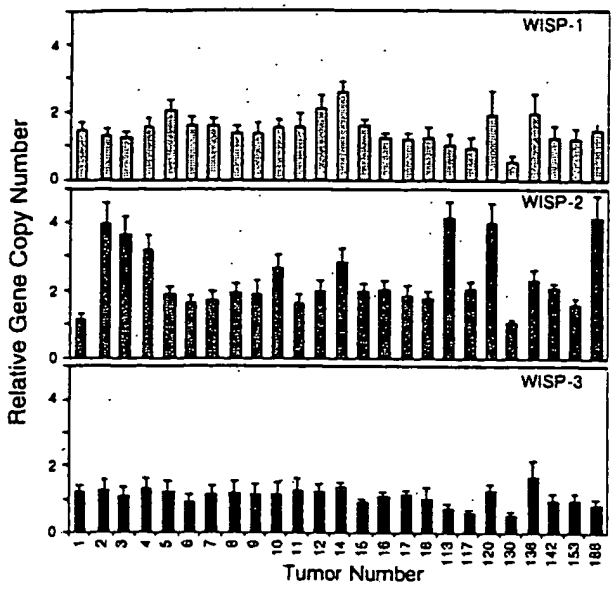

FIG. 6. Genomic amplification of *WISP* genes in human colon tumors. The relative gene copy number of the *WISP* genes in 25 adenocarcinomas was assayed by quantitative PCR, by comparing DNA from primary human tumors with pooled DNA from 10 healthy donors. The data are means ± SEM from one experiment done in triplicate. The experiment was repeated at least three times.

assessed by quantitative PCR (Fig. 7). The level of *WISP-1* RNA present in tumor tissue varied but was significantly increased (2- to >25-fold) in 84% (16/19) of the human colon tumors examined compared with normal adjacent mucosa. Four of 19 tumors showed greater than 10-fold overexpression. In contrast, in 79% (15/19) of the tumors examined, *WISP-2* RNA expression was significantly lower in the tumor than the mucosa. Similar to *WISP-1*, *WISP-3* RNA was overexpressed in 63% (12/19) of the colon tumors compared with the normal

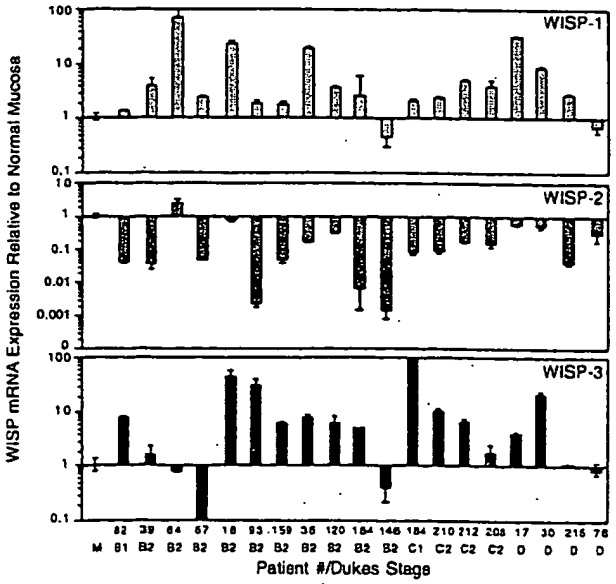

FIG. 7. *WISP* RNA expression in primary human colon tumors relative to expression in normal mucosa from the same patient. Expression of *WISP* mRNA in 19 adenocarcinomas was assayed by quantitative PCR. The Dukes stage of the tumor is listed under the sample number. The data are means ± SEM from one experiment done in triplicate. The experiment was repeated at least twice.

mucosa. The amount of overexpression of *WISP-3* ranged from 4- to >40-fold.

DISCUSSION

One approach to understanding the molecular basis of cancer is to identify differences in gene expression between cancer cells and normal cells. Strategies based on assumptions that steady-state mRNA levels will differ between normal and malignant cells have been used to clone differentially expressed genes (31). We have used a PCR-based selection strategy, SSH, to identify genes selectively expressed in C57MG mouse mammary epithelial cells transformed by Wnt-1.

Three of the genes isolated, *WISP-1*, *WISP-2*, and *WISP-3*, are members of the CCN family of growth factors, which includes CTGF, Cyr61, and *nov*, a family not previously linked to Wnt signaling.

Two independent experimental systems demonstrated that *WISP* induction was associated with the expression of Wnt-1. The first was C57MG cells infected with a Wnt-1 retroviral vector or C57MG cells expressing Wnt-1 under the control of a tetracyline-repressible promoter, and the second was in Wnt-1 transgenic mice, where breast tissue expresses Wnt-1, whereas normal breast tissue does not. No *WISP* RNA expression was detected in mammary tumors induced by polyoma virus middle T antigen (data not shown). These data suggest a link between Wnt-1 and *WISP*s in that in these two situations, *WISP* induction was correlated with Wnt-1 expression.

It is not clear whether the *WISP*s are directly or indirectly induced by the downstream components of the Wnt-1 signaling pathway (i.e., β-catenin-TCF-1/Lef1). The increased levels of *WISP* RNA were measured in Wnt-1-transformed cells, hours or days after Wnt-1 transformation. Thus, *WISP* expression could result from Wnt-1 signaling directly through β-catenin transcription factor regulation or alternatively through Wnt-1 signaling turning on a transcription factor, which in turn regulates *WISP*s.

The *WISP*s define an additional subfamily of the CCN family of growth factors. One striking difference observed in the protein sequence of WISP-2 is the absence of a CT domain, which is present in CTGF, Cyr61, *nov*, WISP-1, and WISP-3. This domain is thought to be involved in receptor binding and dimerization. Growth factors, such as TGF-β, platelet-derived growth factor, and nerve growth factor, which contain a cystine knot motif exist as dimers (32). It is tempting to speculate that WISP-1 and WISP-3 may exist as dimers, whereas WISP-2 exists as a monomer. If the CT domain is also important for receptor binding, WISP-2 may bind its receptor through a different region of the molecule than the other CCN family members. No specific receptors have been identified for CTGF or *nov*. A recent report has shown that integrin $\alpha_v\beta_3$ serves as an adhesion receptor for Cyr61 (33).

The strong expression of *WISP-1* and *WISP-2* in cells lying within the fibrovascular tumor stroma in breast tumors from Wnt-1 transgenic animals is consistent with previous observations that transcripts for the related CTGF gene are primarily expressed in the fibrous stroma of mammary tumors (34). Epithelial cells are thought to control the proliferation of connective tissue stroma in mammary tumors by a cascade of growth factor signals similar to that controlling connective tissue formation during wound repair. It has been proposed that mammary tumor cells or inflammatory cells at the tumor interstitial interface secrete TGF-β1, which is the stimulus for stromal proliferation (34). TGF-β1 is secreted by a large percentage of malignant breast tumors and may be one of the growth factors that stimulates the production of CTGF and WISPs in the stroma.

It was of interest that *WISP-1* and *WISP-2* expression was observed in the stromal cells that surrounded the tumor cells

(epithelial cells) in the Wnt-1 transgenic mouse sections of breast tissue. This finding suggests that paracrine signaling could occur in which the stromal cells could supply WISP-1 and WISP-2 to regulate tumor cell growth on the WISP extracellular matrix. Stromal cell-derived factors in the extracellular matrix have been postulated to play a role in tumor cell migration and proliferation (35). The localization of *WISP-1* and *WISP-2* in the stromal cells of breast tumors supports this paracrine model.

An analysis of *WISP-1* gene amplification and expression in human colon tumors showed a correlation between DNA amplification and overexpression, whereas overexpression of *WISP-3* RNA was seen in the absence of DNA amplification. In contrast, *WISP-2* DNA was amplified in the colon tumors, but its mRNA expression was significantly reduced in the majority of tumors compared with the expression in normal colonic mucosa from the same patient. The gene for human *WISP-2* was localized to chromosome 20q12–20q13, at a region frequently amplified and associated with poor prognosis in node negative breast cancer and many colon cancers, suggesting the existence of one or more oncogenes at this locus (36–38). Because the center of the 20q13 amplicon has not yet been identified, it is possible that the apparent amplification observed for *WISP-2* may be caused by another gene in this amplicon.

A recent manuscript on *rCop-1*, the rat orthologue of *WISP-2*, describes the loss of expression of this gene after cell transformation, suggesting it may be a negative regulator of growth in cell lines (16). Although the mechanism by which *WISP-2* RNA expression is down-regulated during malignant transformation is unknown, the reduced expression of *WISP-2* in colon tumors and cell lines suggests that it may function as a tumor suppressor. These results show that the *WISP* genes are aberrantly expressed in colon cancer and suggest that their altered expression may confer selective growth advantage to the tumor.

Members of the Wnt signaling pathway have been implicated in the pathogenesis of colon cancer, breast cancer, and melanoma, including the tumor suppressor gene adenomatous polyposis coli and β-catenin (39). Mutations in specific regions of either gene can cause the stabilization and accumulation of cytoplasmic β-catenin, which presumably contributes to human carcinogenesis through the activation of target genes such as the *WISP*s. Although the mechanism by which Wnt-1 transforms cells and induces tumorigenesis is unknown, the identification of *WISP*s as genes that may be regulated downstream of Wnt-1 in C57MG cells suggests they could be important mediators of Wnt-1 transformation. The amplification and altered expression patterns of the *WISP*s in human colon tumors may indicate an important role for these genes in tumor development.

We thank the DNA synthesis group for oligonucleotide synthesis, T. Baker for technical assistance, P. Dowd for radiation hybrid mapping, K. Willert and R. Nusse for the tet-repressible C57MG/Wnt-1 cells, V. Dixit for discussions, and D. Wood and A. Bruce for artwork.

1. Cadigan, K. M. & Nusse, R. (1997) *Genes Dev.* **11**, 3286–3305.
2. Dale, T. C. (1998) *Biochem. J.* **329**, 209–223.
3. Nusse, R. & Varmus, H. E. (1982) *Cell* **31**, 99–109.
4. van Ooyen, A. & Nusse, R. (1984) *Cell* **39**, 233–240.
5. Tsukamoto, A. S., Grosschedl, R., Guzman, R. C., Parslow, T. & Varmus, H. E. (1988) *Cell* **55**, 619–625.
6. Brown, J. D. & Moon, R. T. (1998) *Curr. Opin. Cell. Biol.* **10**, 182–187.
7. Molenaar, M., van de Wetering, M., Oosterwegel, M., Peterson-Maduro, J., Godsave, S., Korinek, V., Roose, J., Destree, O. & Clevers, H. (1996) *Cell* **86**, 391–399.
8. Korinek, V., Barker, N., Willert, K., Molenaar, M., Roose, J., Wagenaar, G., Markman, M., Lamers, W., Destree, O. & Clevers, H. (1998) *Mol. Cell. Biol.* **18**, 1248–1256.
9. Munemitsu, S., Albert, I., Souza, B., Rubinfeld, B. & Polakis, P. (1995) *Proc. Natl. Acad. Sci. USA* **92**, 3046–3050.
10. He, T. C., Sparks, A. B., Rago, C., Hermeking, H., Zawel, L., da Costa, L. T., Morin, P. J., Vogelstein, B. & Kinzler, K. W. (1998) *Science* **281**, 1509–1512.
11. Diatchenko, L., Lau, Y. F., Campbell, A. P., Chenchik, A., Moqadam, F., Huang, B., Lukyanov, S., Lukyanov, K., Gurskaya, N., Sverdlov, E. D. & Siebert, P. D. (1996) *Proc. Natl. Acad. Sci. USA* **93**, 6025–6030.
12. Brown, A. M., Wildin, R. S., Prendergast, T. J. & Varmus, H. E. (1986) *Cell* **46**, 1001–1009.
13. Wong, G. T., Gavin, B. J. & McMahon, A. P. (1994) *Mol. Cell. Biol.* **14**, 6278–6286.
14. Shimizu, H., Julius, M. A., Giarre, M., Zheng, Z., Brown, A. M. & Kitajewski, J. (1997) *Cell Growth Differ.* **8**, 1349–1358.
15. Hashimoto, Y., Shindo-Okada, N., Tani, M., Nagamachi, Y., Takeuchi, K., Shiroishi, T., Toma, H. & Yokota, J. (1998) *J. Exp. Med.* **187**, 289–296.
16. Zhang, R., Averboukh, L., Zhu, W., Zhang, H., Jo, H., Dempsey, P. J., Coffey, R. J., Pardee, A. B. & Liang, P. (1998) *Mol. Cell. Biol.* **18**, 6131–6141.
17. Grotendorst, G. R. (1997) *Cytokine Growth Factor Rev.* **8**, 171–179.
18. Kireeva, M. L., Mo, F. E., Yang, G. P. & Lau, L. F. (1996) *Mol. Cell. Biol.* **16**, 1326–1334.
19. Babic, A. M., Kireeva, M. L., Kolesnikova, T. V. & Lau, L. F. (1998) *Proc. Natl. Acad. Sci. USA* **95**, 6355–6360.
20. Martinerie, C., Huff, V., Joubert, I., Badzioch, M., Saunders, G., Strong, L. & Perbal, B. (1994) *Oncogene* **9**, 2729–2732.
21. Bork, P. (1993) *FEBS Lett.* **327**, 125–130.
22. Kim, H. S., Nagalla, S. R., Oh, Y., Wilson, E., Roberts, C. T., Jr. & Rosenfeld, R. G. (1997) *Proc. Natl. Acad. Sci. USA* **94**, 12981–12986.
23. Joliot, V., Martinerie, C., Dambrine, G., Plassiart, G., Brisac, M., Crochet, J. & Perbal, B. (1992) *Mol. Cell. Biol.* **12**, 10–21.
24. Mancuso, D. J., Tuley, E. A., Westfield, L. A., Worrall, N. K., Shelton-Inloes, B. B., Sorace, J. M., Alevy, Y. G. & Sadler, J. E. (1989) *J. Biol. Chem.* **264**, 19514–19527.
25. Holt, G. D., Pangburn, M. K. & Ginsburg, V. (1990) *J. Biol. Chem.* **265**, 2852–2855.
26. Voorberg, J., Fontijn, R., Calafat, J., Janssen, H., van Mourik, J. A. & Pannekoek, H. (1991) *J. Cell. Biol.* **113**, 195–205.
27. Martinerie, C., Viegas-Pequignot, E., Guenard, I., Dutrillaux, B., Nguyen, V. C., Bernheim, A. & Perbal, B. (1992) *Oncogene* **7**, 2529–2534.
28. Takahashi, E., Hori, T., O'Connell, P., Leppert, M. & White, R. (1991) *Cytogenet. Cell. Genet.* **57**, 109–111.
29. Meese, E., Meltzer, P. S., Witkowski, C. M. & Trent, J. M. (1989) *Genes Chromosomes Cancer* **1**, 88–94.
30. Garte, S. J. (1993) *Crit. Rev. Oncog.* **4**, 435–449.
31. Zhang, L., Zhou, W., Velculescu, V. E., Kern, S. E., Hruban, R. H., Hamilton, S. R., Vogelstein, B. & Kinzler, K. W. (1997) *Science* **276**, 1268–1272.
32. Sun, P. D. & Davies, D. R. (1995) *Annu. Rev. Biophys. Biomol. Struct.* **24**, 269–291.
33. Kireeva, M. L., Lam, S. C. T. & Lau, L. F. (1998) *J. Biol. Chem.* **273**, 3090–3096.
34. Frazier, K. S. & Grotendorst, G. R. (1997) *Int. J. Biochem. Cell. Biol.* **29**, 153–161.
35. Wernert, N. (1997) *Virchows Arch.* **430**, 433–443.
36. Tanner, M. M., Tirkkonen, M., Kallioniemi, A., Collins, C., Stokke, T., Karhu, R., Kowbel, D., Shadravan, F., Hintz, M., Kuo, W. L., *et al.* (1994) *Cancer Res.* **54**, 4257–4260.
37. Brinkmann, U., Gallo, M., Polymeropoulos, M. H. & Pastan, I. (1996) *Genome Res.* **6**, 187–194.
38. Bischoff, J. R., Anderson, L., Zhu, Y., Mossie, K., Ng, L., Souza, B., Schryver, B., Flanagan, P., Clairvoyant, F., Ginther, C., *et al.* (1998) *EMBO J.* **17**, 3052–3065.
39. Morin, P. J., Sparks, A. B., Korinek, V., Barker, N., Clevers, H., Vogelstein, B. & Kinzler, K. W. (1997) *Science* **275**, 1787–1790.
40. Lu, L. H. & Gillett, N. (1994) *Cell Vision* **1**, 169–176.

methods. Peptides AENK or AEQK were dissolved in water, made isotonic with NaCl and diluted into RPMI growth medium. T-cell-proliferation assays were done essentially as described[20,21]. Briefly, after antigen pulsing (30 μg ml^{-1} TTCF) with tetrapeptides (1–2 mg ml^{-1}), PBMCs or EBV-B cells were washed in PBS and fixed for 45 s in 0.05% glutaraldehyde. Glycine was added to a final concentration of 0.1 M and the cells were washed five times in RPMI 1640 medium containing 1% FCS before co-culture with T-cell clones in round-bottom 96-well microtitre plates. After 48 h, the cultures were pulsed with 1 μCi of ^{3}H-thymidine and harvested for scintillation counting 16 h later. Predigestion of native TTCF was done by incubating 200 μg TTCF with 0.25 μg pig kidney legumain in 500 μl 50 mM citrate buffer, pH 5.5, for 1 h at 37 °C.

Glycopeptide digestions. The peptides HIDNEEDI, HIDN(*N*-glucosamine) EEDI and HIDNESDI, which are based on the TTCF sequence, and QQQHLFGSNVTDCSGNFCLFR(KKK), which is based on human transferrin, were obtained by custom synthesis. The three C-terminal lysine residues were added to the natural sequence to aid solubility. The transferrin glycopeptide QQQHLFGSNVTDCSGNFCLFR was prepared by tryptic (Promega) digestion of 5 mg reduced, carboxy-methylated human transferrin followed by concanavalin A chromatography[11]. Glycopeptides corresponding to residues 622–642 and 421–452 were isolated by reverse-phase HPLC and identified by mass spectrometry and N-terminal sequencing. The lyophilized transferrin-derived peptides were redissolved in 50 mM sodium acetate, pH 5.5, 10 mM dithiothreitol, 20% methanol. Digestions were performed for 3 h at 30 °C with 5–50 mU ml^{-1} pig kidney legumain or B-cell AEP. Products were analysed by HPLC or MALDI-TOF mass spectrometry using a matrix of 10 mg ml^{-1} α-cyanocinnamic acid in 50% acetonitrile/0.1% TFA and a PerSeptive Biosystems Elite STR mass spectrometer set to linear or reflector mode. Internal standardization was obtained with a matrix ion of 568.13 mass units.

Received 29 September; accepted 3 November 1998.

1. Chen, J. M. *et al.* Cloning, isolation, and characterisation of mammalian legumain, an asparaginyl endopeptidase. *J. Biol. Chem.* 272, 8090–8098 (1997).
2. Kembhavi, A. A., Buttle, D. J., Knight, C. G. & Barrett, A. J. The two cysteine endopeptidases of legume seeds: purification and characterization by use of specific fluorometric assays. *Arch. Biochem. Biophys.* 303, 208–213 (1993).
3. Dalton, J. P., Hola Jamriska, L. & Bridley, P. J. Asparaginyl endopeptidase activity in adult *Schistosoma mansoni*. *Parasitology* 111, 575–580 (1995).
4. Bennett, K. *et al.* Antigen processing for presentation by class II major histocompatibility complex requires cleavage by cathespin E. *Eur. J. Immunol.* 22, 1519–1524 (1992).
5. Riese, R. J. *et al.* Essential role for cathepsin S in MHC class II-associated invariant chain processing and peptide loading. *Immunity* 4, 357–366 (1996).
6. Rodriguez, G. M. & Diment, S. Role of cathepsin D in antigen presentation of ovalbumin. *J. Immunol.* 149, 2894–2898 (1992).
7. Hewitt, E. W. *et al.* Natural processing sites for human cathepsin E and cathepsin D in tetanus toxin: implications for T cell epitope generation. *J. Immunol.* 159, 4693–4699 (1997).
8. Watts, C. Capture and processing of exogenous antigens for presentation on MHC molecules. *Annu. Rev. Immunol.* 15, 821–850 (1997).
9. Chapman, H. A. Endosomal proteases and MHC class II function. *Curr. Opin. Immunol.* 10, 93–102 (1998).
10. Fineschi, B. & Miller, J. Endosomal proteases and antigen processing. *Trends Biochem. Sci.* 22, 377–382 (1997).
11. Lu, J. & van Halbeek, H. Complete ^{1}H and ^{13}C resonance assignments of a 21-amino acid glycopeptide prepared from human serum transferrin. *Carbohydr. Res.* 296, 1–21 (1996).
12. Fearon, D. T. & Locksley, R. M. The instructive role of innate immunity in the acquired immune response. *Science* 272, 50–54 (1996).
13. Medzhitov, R. & Janeway, C. A. J. Innate immunity: the virtues of a nonclonal system of recognition. *Cell* 91, 295–298 (1997).
14. Wyatt, R. *et al.* The antigenic structure of the HIV gp120 envelope glycoprotein. *Nature* 393, 705–711 (1998).
15. Botarelli, P. *et al.* N-glycosylation of HIV gp120 may constrain recognition by T lymphocytes. *J. Immunol.* 147, 3128–3132 (1991).
16. Davidson, H. W., West, M. A. & Watts, C. Endocytosis, intracellular trafficking, and processing of membrane IgG and monovalent antigen/membrane IgG complexes in B lymphocytes. *J. Immunol.* 144, 4101–4109 (1990).
17. Barrett, A. J. & Kirschke, H. Cathepsin B, cathepsin H and cathepsin L. *Methods Enzymol.* 80, 535–559 (1981).
18. Makoff, A. J., Ballantine, S. P., Smallwood, A. E. & Fairweather, N. F. Expression of tetanus toxin fragment C in *E. coli*: its purification and potential use as a vaccine. *Biotechnology* 7, 1043–1046 (1989).
19. Lane, D. P. & Harlow, E. *Antibodies: A Laboratory Manual* (Cold Spring Harbor Laboratory Press, 1988).
20. Lanzavecchia, A. Antigen-specific interaction between T and B cells. *Nature* 314, 537–539 (1985).
21. Pond, L. & Watts, C. Characterization of transport of newly assembled, T cell-stimulatory MHC class II-peptide complexes from MHC class II compartments to the cell surface. *J. Immunol.* 159, 543–553 (1997).

Acknowledgements. We thank M. Ferguson for helpful discussions and advice; E. Smythe and L. Grayson for advice and technical assistance; B. Spruce, A. Knight and the BTS (Ninewells Hospital) for help with blood monocyte preparation; and our colleagues for many helpful comments on the manuscript. This work was supported by the Wellcome Trust and by an EMBO Long-term fellowship to B. M.

Correspondence and requests for materials should be addressed to C.W. (e-mail: c.watts@dundee.ac.uk).

Genomic amplification of a decoy receptor for Fas ligand in lung and colon cancer

Robert M. Pitti*†, Scot A. Marsters*†, David A. Lawrence*†, Margaret Roy*, Frank C. Kischkel*, Patrick Dowd*, Arthur Huang*, Christopher J. Donahue*, Steven W. Sherwood*, Daryl T. Baldwin*, Paul J. Godowski*, William I. Wood*, Austin L. Gurney*, Kenneth J. Hillan*, Robert L. Cohen*, Audrey D. Goddard*, David Botstein‡ & Avi Ashkenazi*

** Departments of Molecular Oncology, Molecular Biology, and Immunology, Genentech Inc., 1 DNA Way, South San Francisco, California 94080, USA*
‡ Department of Genetics, Stanford University, Stanford, California 94305, USA
† These authors contributed equally to this work

Fas ligand (FasL) is produced by activated T cells and natural killer cells and it induces apoptosis (programmed cell death) in target cells through the death receptor Fas/Apo1/CD95 (ref. 1). One important role of FasL and Fas is to mediate immune-cytotoxic killing of cells that are potentially harmful to the organism, such as virus-infected or tumour cells[1]. Here we report the discovery of a soluble decoy receptor, termed decoy receptor 3 (DcR3), that binds to FasL and inhibits FasL-induced apoptosis. The DcR3 gene was amplified in about half of 35 primary lung and colon tumours studied, and DcR3 messenger RNA was expressed in malignant tissue. Thus, certain tumours may escape FasL-dependent immune-cytotoxic attack by expressing a decoy receptor that blocks FasL.

By searching expressed sequence tag (EST) databases, we identified a set of related ESTs that showed homology to the tumour necrosis factor (TNF) receptor (TNFR) gene superfamily[2]. Using the overlapping sequence, we isolated a previously unknown full-length complementary DNA from human fetal lung. We named the protein encoded by this cDNA decoy receptor 3 (DcR3). The cDNA encodes a 300-amino-acid polypeptide that resembles members of the TNFR family (Fig. 1a): the amino terminus contains a leader sequence, which is followed by four tandem cysteine-rich domains (CRDs). Like one other TNFR homologue, osteoprotegerin (OPG)[3], DcR3 lacks an apparent transmembrane sequence, which indicates that it may be a secreted, rather than a membrane-asscociated, molecule. We expressed a recombinant, histidine-tagged form of DcR3 in mammalian cells; DcR3 was secreted into the cell culture medium, and migrated on polyacrylamide gels as a protein of relative molecular mass 35,000 (data not shown). DcR3 shares sequence identity in particular with OPG (31%) and TNFR2 (29%), and has relatively less homology with Fas (17%). All of the cysteines in the four CRDs of DcR3 and OPG are conserved; however, the carboxy-terminal portion of DcR3 is 101 residues shorter.

We analysed expression of DcR3 mRNA in human tissues by northern blotting (Fig. 1b). We detected a predominant 1.2-kilobase transcript in fetal lung, brain, and liver, and in adult spleen, colon and lung. In addition, we observed relatively high DcR3 mRNA expression in the human colon carcinoma cell line SW480.

To investigate potential ligand interactions of DcR3, we generated a recombinant, Fc-tagged DcR3 protein. We tested binding of DcR3–Fc to human 293 cells transfected with individual TNF-family ligands, which are expressed as type 2 transmembrane proteins (these transmembrane proteins have their N termini in the cytosol). DcR3–Fc showed a significant increase in binding to cells transfected with FasL[4] (Fig. 2a), but not to cells transfected with TNF[5], Apo2L/TRAIL[6,7], Apo3L/TWEAK[8,9], or OPGL/TRANCE/

Nature © Macmillan Publishers Ltd 1998

RANKL[10-12] (data not shown). DcR3–Fc immunoprecipitated shed FasL from FasL-transfected 293 cells (Fig. 2b) and purified soluble FasL (Fig. 2c), as did the Fc-tagged ectodomain of Fas but not TNFR1. Gel-filtration chromatography showed that DcR3–Fc and soluble FasL formed a stable complex (Fig. 2d). Equilibrium analysis indicated that DcR3–Fc and Fas–Fc bound to soluble FasL with a comparable affinity ($K_d = 0.8 \pm 0.2$ and 1.1 ± 0.1 nM, respectively; Fig. 2e), and that DcR3–Fc could block nearly all of the binding of soluble FasL to Fas–Fc (Fig. 2e, inset). Thus, DcR3 competes with Fas for binding to FasL.

To determine whether binding of DcR3 inhibits FasL activity, we tested the effect of DcR3–Fc on apoptosis induction by soluble FasL in Jurkat T leukaemia cells, which express Fas (Fig. 3a). DcR3–Fc and Fas–Fc blocked soluble-FasL-induced apoptosis in a similar dose-dependent manner, with half-maximal inhibition at ~0.1 μg ml^{-1}. Time-course analysis showed that the inhibition did not merely delay cell death, but rather persisted for at least 24 hours (Fig. 3b). We also tested the effect of DcR3–Fc on activation-induced cell death (AICD) of mature T lymphocytes, a FasL-dependent process[1]. Consistent with previous results[13], activation of interleukin-2-stimulated CD4-positive T cells with anti-CD3 antibody increased the level of apoptosis twofold, and Fas–Fc blocked this effect substantially (Fig. 3c); DcR3–Fc blocked the induction of apoptosis to a similar extent. Thus, DcR3 binding blocks apoptosis induction by FasL.

FasL-induced apoptosis is important in elimination of virus-infected cells and cancer cells by natural killer cells and cytotoxic T lymphocytes; an alternative mechanism involves perforin and granzymes[1,14–16]. Peripheral blood natural killer cells triggered marked cell death in Jurkat T leukaemia cells (Fig. 3d); DcR3–Fc and Fas–Fc each reduced killing of target cells from ~65% to ~30%, with half-maximal inhibition at ~1 μg ml^{-1}; the residual killing was probably mediated by the perforin/granzyme pathway. Thus, DcR3 binding blocks FasL-dependent natural killer cell activity. Higher DcR3–Fc and Fas–Fc concentrations were required to block natural killer cell activity compared with those required to block soluble FasL activity, which is consistent with the greater potency of membrane-associated FasL compared with soluble FasL[17].

Given the role of immune-cytotoxic cells in elimination of tumour cells and the fact that DcR3 can act as an inhibitor of FasL, we proposed that DcR3 expression might contribute to the ability of some tumours to escape immune-cytotoxic attack. As genomic amplification frequently contributes to tumorigenesis, we investigated whether the DcR3 gene is amplified in cancer. We analysed DcR3 gene-copy number by quantitative polymerase chain

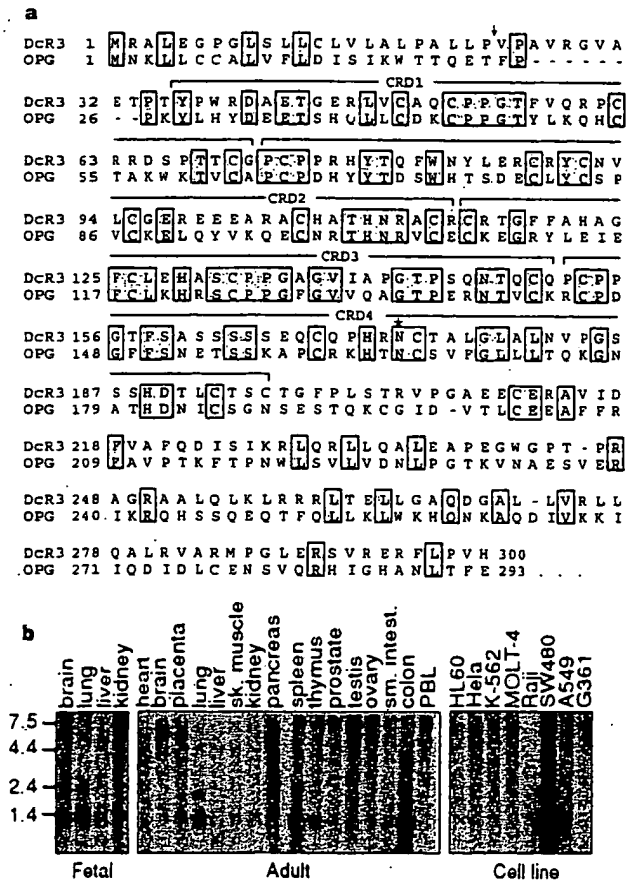

Figure 1 Primary structure and expression of human DcR3. a, Alignment of the amino-acid sequences of DcR3 and of osteoprotegerin (OPG); the C-terminal 101 residues of OPG are not shown. The putative signal cleavage site (arrow), the cysteine-rich domains (CRD 1-4), and the *N*-linked glycosylation site (asterisk) are shown. b, Expression of DcR3 mRNA. Northern hybridization analysis was done using the DcR3 cDNA as a probe and blots of poly(A)$^+$ RNA (Clontech) from human fetal and adult tissues or cancer cell lines. PBL, peripheral blood lymphocyte.

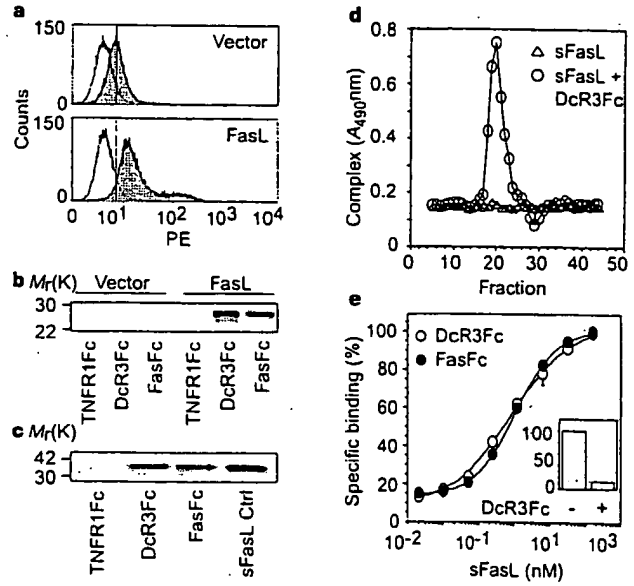

Figure 2 Interaction of DcR3 with FasL. a, 293 cells were transfected with pRK5 vector (top) or with pRK5 encoding full-length FasL (bottom), incubated with DcR3-Fc (solid line, shaded area), TNFR1-Fc (dotted line) or buffer control (dashed line) (the dashed and dotted lines overlap), and analysed for binding by FACS. Statistical analysis showed a significant difference ($P < 0.001$) between the binding of DcR3-Fc to cells transfected with FasL or pRK5. PE, phycoerythrin-labelled cells. b, 293 cells were transfected as in a and metabolically labelled, and cell supernatants were immunoprecipitated with Fc-tagged TNFR1, DcR3 or Fas. c, Purified soluble FasL (sFasL) was immunoprecipitated with TNFR1-Fc, DcR3-Fc or Fas-Fc and visualized by immunoblot with anti-FasL antibody. sFasL was loaded directly for comparison in the right-hand lane. d, Flag-tagged sFasL was incubated with DcR3-Fc or with buffer and resolved by gel filtration; column fractions were analysed in an assay that detects complexes containing DcR3-Fc and sFasL-Flag. e, Equilibrium binding of DcR3-Fc or Fas-Fc to sFasL-Flag. Inset, competition of DcR3-Fc with Fas-Fc for binding to sFasL-Flag.

Nature © Macmillan Publishers Ltd 1998

reaction (PCR)[18] in genomic DNA from 35 primary lung and colon tumours, relative to pooled genomic DNA from peripheral blood leukocytes (PBLs) of 10 healthy donors. Eight of 18 lung tumours and 9 of 17 colon tumours showed DcR3 gene amplification, ranging from 2- to 18-fold (Fig. 4a, b). To confirm this result, we analysed the colon tumour DNAs with three more, independent sets of DcR3-based PCR primers and probes; we observed nearly the same amplification (data not shown).

We then analysed DcR3 mRNA expression in primary tumour tissue sections by *in situ* hybridization. We detected DcR3 expression in 6 out of 15 lung tumours, 2 out of 2 colon tumours, 2 out of 5 breast tumours, and 1 out of 1 gastric tumour (data not shown). A section through a squamous-cell carcinoma of the lung is shown in Fig. 4c. DcR3 mRNA was localized to infiltrating malignant epithelium, but was essentially absent from adjacent stroma, indicating tumour-specific expression. Although the individual tumour specimens that we analysed for mRNA expression and gene amplification were different, the *in situ* hybridization results are consistent with the finding that the DcR3 gene is amplified frequently in tumours. SW480 colon carcinoma cells, which showed abundant DcR3 mRNA expression (Fig. 1b), also had marked DcR3 gene amplification, as shown by quantitative PCR (fourfold) and by Southern blot hybridization (fivefold) (data not shown).

If DcR3 amplification in cancer is functionally relevant, then DcR3 should be amplified more than neighbouring genomic regions that are not important for tumour survival. To test this, we mapped the human DcR3 gene by radiation-hybrid analysis; DcR3 showed linkage to marker AFM218xe7 (T160), which maps to chromosome position 20q13. Next, we isolated from a bacterial artificial chromosome (BAC) library a human genomic clone that carries DcR3, and sequenced the ends of the clone's insert. We then determined, from the nine colon tumours that showed twofold or greater amplification of DcR3, the copy number of the DcR3-flanking sequences (reverse and forward) from the BAC, and of seven genomic markers that span chromosome 20 (Fig. 4d). The DcR3-linked reverse marker showed an average amplification of roughly threefold, slightly less than the approximately fourfold amplification of DcR3; the other markers showed little or no amplification. These data indicate that DcR3 may be at the 'epicentre' of a distal chromosome 20 region that is amplified in colon cancer, consistent with the possibility that DcR3 amplification promotes tumour survival.

Our results show that DcR3 binds specifically to FasL and inhibits FasL activity. We did not detect DcR3 binding to several other TNF-ligand-family members; however, this does not rule out the possibility that DcR3 interacts with other ligands, as do some other TNFR family members, including OPG[2,19].

FasL is important in regulating the immune response; however, little is known about how FasL function is controlled. One mechanism involves the molecule cFLIP, which modulates apoptosis signalling downstream of Fas[20]. A second mechanism involves proteolytic shedding of FasL from the cell surface[17]. DcR3 competes with Fas for

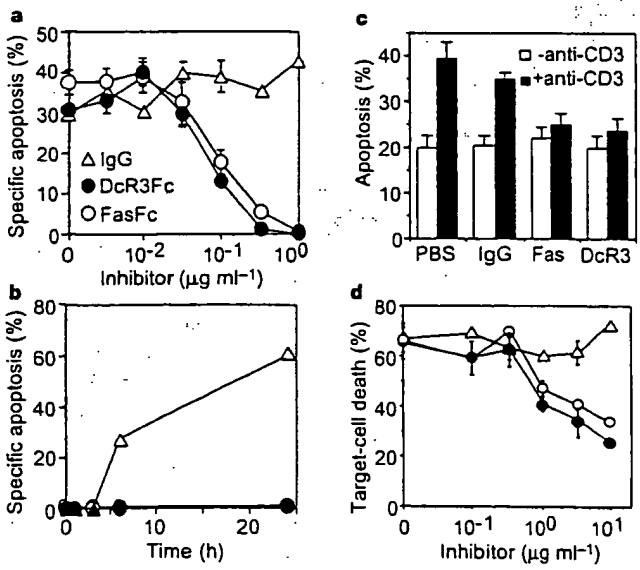

Figure 3 Inhibition of FasL activity by DcR3. **a**, Human Jurkat T leukaemia cells were incubated with Flag-tagged soluble FasL (sFasL; 5 ng ml^{-1}) oligomerized with anti-Flag antibody (0.1 μg ml^{-1}) in the presence of the proposed inhibitors DcR3-Fc, Fas-Fc or human IgG1 and assayed for apoptosis (mean ± s.e.m. of triplicates). **b**, Jurkat cells were incubated with sFasL-Flag plus anti-Flag antibody as in **a**, in presence of 1 μg ml^{-1} DcR3-Fc (filled circles), Fas-Fc (open circles) or human IgG1 (triangles), and apoptosis was determined at the indicated time points. **c**, Peripheral blood T cells were stimulated with PHA and interleukin-2, followed by control (white bars) or anti-CD3 antibody (filled bars), together with phosphate-buffered saline (PBS), human IgG1, Fas-Fc, or DcR3-Fc (10 μg ml^{-1}). After 16 h, apoptosis of CD4$^+$ cells was determined (mean ± s.e.m. of results from five donors). **d**, Peripheral blood natural killer cells were incubated with ^{51}Cr-labelled Jurkat cells in the presence of DcR3-Fc (filled circles), Fas-Fc (open circles) or human IgG1 (triangles), and target-cell death was determined by release of ^{51}Cr (mean ± s.d. for two donors, each in triplicate).

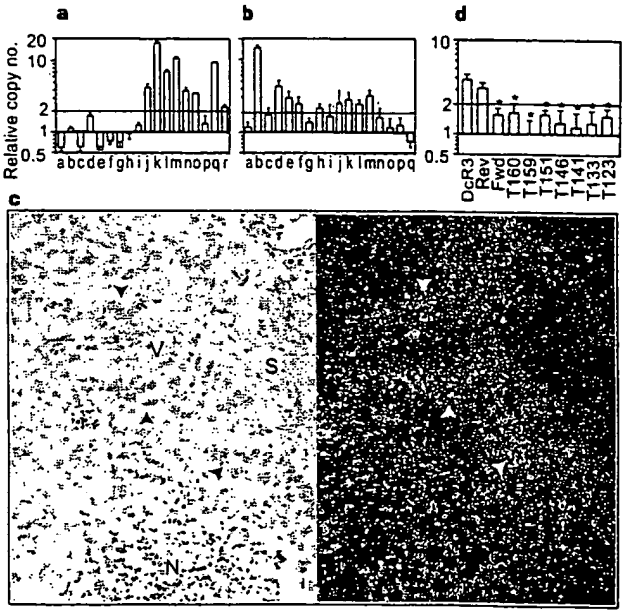

Figure 4 Genomic amplification of DcR3 in tumours. **a**, Lung cancers, comprising eight adenocarcinomas (c, d, f, g, h, j, k, r), seven squamous-cell carcinomas (a, e, m, n, o, p, q), one non-small-cell carcinoma (b), one small-cell carcinoma (i), and one bronchial adenocarcinoma (l). The data are means ± s.d. of 2 experiments done in duplicate. **b**, Colon tumours, comprising 17 adenocarcinomas. Data are means ± s.e.m. of five experiments done in duplicate. **c**, *In situ* hybridization analysis of DcR3 mRNA expression in a squamous-cell carcinoma of the lung. A representative bright-field image (left) and the corresponding dark-field image (right) show DcR3 mRNA over infiltrating malignant epithelium (arrowheads). Adjacent non-malignant stroma (S), blood vessel (V) and necrotic tumour tissue (N) are also shown. **d**, Average amplification of DcR3 compared with amplification of neighbouring genomic regions (reverse and forward, Rev and Fwd), the DcR3-linked marker T160, and other chromosome-20 markers, in the nine colon tumours showing DcR3 amplification of twofold or more (**b**). Data are from two experiments done in duplicate. Asterisk indicates $P < 0.01$ for a Student's *t*-test comparing each marker with DcR3.

Nature © Macmillan Publishers Ltd 1998

FasL binding; hence, it may represent a third mechanism of extracellular regulation of FasL activity. A decoy receptor that modulates the function of the cytokine interleukin-1 has been described[21]. In addition, two decoy receptors that belong to the TNFR family, DcR1 and DcR2, regulate the FasL-related apoptosis-inducing molecule Apo2L[22]. Unlike DcR1 and DcR2, which are membrane-associated proteins, DcR3 is directly secreted into the extracellular space. One other secreted TNFR-family member is OPG[3], which shares greater sequence homology with DcR3 (31%) than do DcR1 (17%) or DcR2 (19%); OPG functions as a third decoy for Apo2L[19]. Thus, DcR3 and OPG define a new subset of TNFR-family members that function as secreted decoys to modulate ligands that induce apoptosis. Pox viruses produce soluble TNFR homologues that neutralize specific TNF-family ligands, thereby modulating the antiviral immune response[2]. Our results indicate that a similar mechanism, namely, production of a soluble decoy receptor for FasL, may contribute to immune evasion by certain tumours. □

Methods

Isolation of DcR3 cDNA. Several overlapping ESTs in GenBank (accession numbers AA025672, AA025673 and W67560) and in Lifeseq™ (Incyte Pharmaceuticals; accession numbers 1339238, 1533571, 1533650, 1542861, 1789372 and 2207027) showed similarity to members of the TNFR family. We screened human cDNA libraries by PCR with primers based on the region of EST consensus; fetal lung was positive for a product of the expected size. By hybridization to a PCR-generated probe based on the ESTs, one positive clone (DNA30942) was identified. When searching for potential alternatively spliced forms of DcR3 that might encode a transmembrane protein, we isolated 50 more clones; the coding regions of these clones were identical in size to that of the initial clone (data not shown).

Fc-fusion proteins (immunoadhesins). The entire DcR3 sequence, or the ectodomain of Fas or TNFR1, was fused to the hinge and Fc region of human IgG1, expressed in insect SF9 cells or in human 293 cells, and purified as described[23].

Fluorescence-activated cell sorting (FACS) analysis. We transfected 293 cells using calcium phosphate or Effectene (Qiagen) with pRK5 vector or pRK5 encoding full-length human FasL[4] (2 μg), together with pRK5 encoding CrmA (2 μg) to prevent cell death. After 16 h, the cells were incubated with biotinylated DcR3–Fc or TNFR1–Fc and then with phycoerythrin-conjugated streptavidin (GibcoBRL), and were assayed by FACS. The data were analysed by Kolmogorov–Smirnov statistical analysis. There was some detectable staining of vector-transfected cells by DcR3–Fc; as these cells express little FasL (data not shown), it is possible that DcR3 recognized some other factor that is expressed constitutively on 293 cells.

Immunoprecipitation. Human 293 cells were transfected as above, and metabolically labelled with [^{35}S]cysteine and [^{35}S]methionine (0.5 mCi; Amersham). After 16 h of culture in the presence of z-VAD-fmk (10 μM), the medium was immunoprecipitated with DcR3–Fc, Fas–Fc or TNFR1–Fc (5 μg), followed by protein A–Sepharose (Repligen). The precipitates were resolved by SDS–PAGE and visualized on a phosphorimager (Fuji BAS2000). Alternatively, purified, Flag-tagged soluble FasL (1 μg) (Alexis) was incubated with each Fc-fusion protein (1 μg), precipitated with protein A–Sepharose, resolved by SDS–PAGE and visualized by immunoblotting with rabbit anti-FasL antibody (Oncogene Research).

Analysis of complex formation. Flag-tagged soluble FasL (25 μg) was incubated with buffer or with DcR3–Fc (40 μg) for 1.5 h at 24 °C. The reaction was loaded onto a Superdex 200 HR 10/30 column (Pharmacia) and developed with PBS; 0.6-ml fractions were collected. The presence of DcR3–Fc–FasL complex in each fraction was analysed by placing 100 μl aliquots into microtitre wells precoated with anti-human IgG (Boehringer) to capture DcR3–Fc, followed by detection with biotinylated anti-Flag antibody Bio M2 (Kodak) and streptavidin–horseradish peroxidase (Amersham). Calibration of the column indicated an apparent relative molecular mass of the complex of 420K (data not shown), which is consistent with a stoichiometry of two DcR3–Fc homodimers to two soluble FasL homotrimers.

Equilibrium binding analysis. Microtitre wells were coated with anti-human IgG, blocked with 2% BSA in PBS. DcR3–Fc or Fas–Fc was added, followed by serially diluted Flag-tagged soluble FasL. Bound ligand was detected with anti-Flag antibody as above. In the competition assay, Fas–Fc was immobilized as above; and the wells were blocked with excess IgG1 before addition of Flag-tagged soluble FasL plus DcR3–Fc.

T-cell AICD. CD3$^+$ lymphocytes were isolated from peripheral blood of individual donors using anti-CD3 magnetic beads (Miltenyi Biotech), stimulated with phytohaemagglutinin (PHA; 2 μg ml^{-1}) for 24 h, and cultured in the presence of interleukin-2 (100 U ml^{-1}) for 5 days. The cells were plated in wells coated with anti-CD3 antibody (Pharmingen) and analysed for apoptosis 16 h later by FACS analysis of annexin-V-binding of CD4$^+$ cells[24].

Natural killer cell activity. Natural killer cells were isolated from peripheral blood of individual donors using anti-CD56 magnetic beads (Miltenyi Biotech), and incubated for 16 h with ^{51}Cr-loaded Jurkat cells at an effector-to-target ratio of 1:1 in the presence of DcR3–Fc, Fas–Fc or human IgG1. Target-cell death was determined by release of ^{51}Cr in effector–target co-cultures relative to release of ^{51}Cr by detergent lysis of equal numbers of Jurkat cells.

Gene-amplification analysis. Surgical specimens were provided by J. Kern (lung tumours) and P. Quirke (colon tumours). Genomic DNA was extracted (Qiagen) and the concentration was determined using Hoechst dye 33258 intercalation fluorometry. Amplification was determined by quantitative PCR[18] using a TaqMan instrument (ABI). The method was validated by comparison of PCR and Southern hybridization data for the Myc and HER-2 oncogenes (data not shown). Gene-specific primers and fluorogenic probes were designed on the basis of the sequence of DcR3 or of nearby regions identified on a BAC carrying the human DcR3 gene; alternatively, primers and probes were based on Stanford Human Genome Center marker AFM218xe7 (T160), which is linked to DcR3 (likelihood score = 5.4), SHGC-36268 (T159), the nearest available marker which maps to ~500 kilobases from T160, and five extra markers that span chromosome 20. The DcR3-specific primer sequences were 5′-CTTCTTCGCGCACGCTG-3′ and 5′-ATCACGCCGGCACCAG-3′ and the fluorogenic probe sequence was 5′-(FAM-ACACGATGCGTGCTCCAAGCAG AAp-(TAMARA), where FAM is 5′-fluorescein phosphoramidite. Relative gene-copy numbers were derived using the formula $2^{(\Delta CT)}$, where ΔCT is the difference in amplification cycles required to detect DcR3 in peripheral blood lymphocyte DNA compared to test DNA.

Received 24 September; accepted 6 November 1998.

1. Nagata, S. Apoptosis by death factor. *Cell* 88, 355–365 (1997).
2. Smith, C. A., Farrah, T. & Goodwin, R. G. The TNF receptor superfamily of cellular and viral proteins: activation, costimulation, and death. *Cell* 76, 959–962 (1994).
3. Simonet, W. S. *et al.* Osteoprotegerin: a novel secreted protein involved in the regulation of bone density. *Cell* 89, 309–319 (1997).
4. Suda, T., Takahashi, T., Golstein, P. & Nagata, S. Molecular cloning and expression of Fas ligand, a novel member of the TNF family. *Cell* 75, 1169–1178 (1993).
5. Pennica, D. *et al.* Human tumour necrosis factor: precursor structure, expression and homology to lymphotoxin. *Nature* 312, 724–729 (1984).
6. Pitti, R. M. *et al.* Induction of apoptosis by Apo-2 ligand, a new member of the tumor necrosis factor receptor family. *J. Biol. Chem.* 271, 12687–12690 (1996).
7. Wiley, S. R. *et al.* Identification and characterization of a new member of the TNF family that induces apoptosis. *Immunity* 3, 673–682 (1995).
8. Marsters, S. A. *et al.* Identification of a ligand for the death-domain-containing receptor Apo3. *Curr. Biol.* 8, 525–528 (1998).
9. Chicheportiche, Y. *et al.* TWEAK, a new secreted ligand in the TNF family that weakly induces apoptosis. *J. Biol. Chem.* 272, 32401–32410 (1997).
10. Wong, B. R. *et al.* TRANCE is a novel ligand of the TNFR family that activates c-Jun-N-terminal kinase in T cells. *J. Biol. Chem.* 272, 25190–25194 (1997).
11. Anderson, D. M. *et al.* A homolog of the TNF receptor and its ligand enhance T-cell growth and dendritic-cell function. *Nature* 390, 175–179 (1997).
12. Lacey, D. L. *et al.* Osteoprotegerin ligand is a cytokine that regulates osteoclast differentiation and activation. *Cell* 93, 165–176 (1998).
13. Dhein, J., Walczak, H., Baumler, C., Debatin, K. M. & Krammer, P. H. Autocrine T-cell suicide mediated by Apo1/(Fas/CD95). *Nature* 373, 438–441 (1995).
14. Arase, H., Arase, N. & Saito, T. Fas-mediated cytotoxicity by freshly isolated natural killer cells. *J. Exp. Med.* 181, 1235–1238 (1995).
15. Medvedev, A. E. *et al.* Regulation of Fas and Fas ligand expression in NK cells by cytokines and the involvement of Fas ligand in NK/LAK cell-mediated cytotoxicity. *Cytokine* 9, 394–404 (1997).
16. Moretta, A. Mechanisms in cell-mediated cytotoxicity. *Cell* 90, 13–18 (1997).
17. Tanaka, M., Itai, T., Adachi, M. & Nagata, S. Downregualtion of Fas ligand by shedding. *Nature Med.* 4, 31–36 (1998).
18. Gelmini, S. *et al.* Quantitative PCR-based homogeneous assay with fluorogenic probes to measure c-erbB-2 oncogene amplification. *Clin. Chem.* 43, 752–758 (1997).
19. Emery, J. G. *et al.* Osteoprotegerin is a receptor for the cytotoxic ligand TRAIL. *J. Biol. Chem.* 273, 14363–14367 (1998).
20. Wallach, D. Placing death under control. *Nature* 388, 123–125 (1997).
21. Colotta, F. *et al.* Interleukin-1 type II receptor: a decoy target for IL-1 that is regulated by IL-4. *Science* 261, 472–475 (1993).

Nature © Macmillan Publishers Ltd 1998

22. Ashkenazi, A. & Dixit, V. M. Death receptors: signaling and modulation. *Science* 281, 1305–1308 (1998).
23. Ashkenazi, A. & Chamow, S. M. Immunoadhesins as research tools and therapeutic agents. *Curr. Opin. Immunol.* 9, 195–200 (1997).
24. Marsden, S. *et al.* Activation of apoptosis by Apo-2 ligand is independent of FADD but blocked by CrmA. *Curr. Biol.* 6, 750–752 (1996).

Acknowledgements. We thank C. Clark, D. Pennica and V. Dixit for comments, and J. Kern and P. Quirke for tumour specimens.

Correspondence and requests for materials should be addressed to A.A. (e-mail: aa@gene.com). The GenBank accession number for the DcR3 cDNA sequence is AF104419.

Crystal structure of the ATP-binding subunit of an ABC transporter

Li-Wei Hung*, Iris Xiaoyan Wang†, Kishiko Nikaido†, Pei-Qi Liu†, Giovanna Ferro-Luzzi Ames† & Sung-Hou Kim*‡

* *E. O. Lawrence Berkeley National Laboratory,* † *Department of Molecular and Cell Biology, and* ‡ *Department of Chemistry, University of California at Berkeley, Berkeley, California 94720, USA*

ABC transporters (also known as traffic ATPases) form a large family of proteins responsible for the translocation of a variety of compounds across membranes of both prokaryotes and eukaryotes[1]. The recently completed *Escherichia coli* genome sequence revealed that the largest family of paralogous *E. coli* proteins is composed of ABC transporters[2]. Many eukaryotic proteins of medical significance belong to this family, such as the cystic fibrosis transmembrane conductance regulator (CFTR), the P-glycoprotein (or multidrug-resistance protein) and the heterodimeric transporter associated with antigen processing (Tap1–Tap2). Here we report the crystal structure at 1.5 Å resolution of HisP, the ATP-binding subunit of the histidine permease, which is an ABC transporter from *Salmonella typhimurium*. We correlate the details of this structure with the biochemical, genetic and biophysical properties of the wild-type and several mutant HisP proteins. The structure provides a basis for understanding properties of ABC transporters and of defective CFTR proteins.

ABC transporters contain four structural domains: two nucleotide-binding domains (NBDs), which are highly conserved throughout the family, and two transmembrane domains[1]. In prokaryotes these domains are often separate subunits which are assembled into a membrane-bound complex; in eukaryotes the domains are generally fused into a single polypeptide chain. The periplasmic histidine permease of *S. typhimurium* and *E. coli*[1,3–8] is a well-characterized ABC transporter that is a good model for this superfamily. It consists of a membrane-bound complex, $HisQMP_2$, which comprises integral membrane subunits, HisQ and HisM, and two copies of HisP, the ATP-binding subunit. HisP, which has properties intermediate between those of integral and peripheral membrane proteins[9], is accessible from both sides of the membrane, presumably by its interaction with HisQ and HisM[6]. The two HisP subunits form a dimer, as shown by their cooperativity in ATP hydrolysis[5], the requirement for both subunits to be present for activity[8], and the formation of a HisP dimer upon chemical cross-linking. Soluble HisP also forms a dimer[3]. HisP has been purified and characterized in an active soluble form[3] which can be reconstituted into a fully active membrane-bound complex[8].

The overall shape of the crystal structure of the HisP monomer is that of an 'L' with two thick arms (arm I and arm II); the ATP-binding pocket is near the end of arm I (Fig. 1). A six-stranded β-sheet (β3 and β8–β12) spans both arms of the L, with a domain of a α- plus β-type structure (β1, β2, β4–β7, α1 and α2) on one side (within arm I) and a domain of mostly α-helices (α3–α9) on the

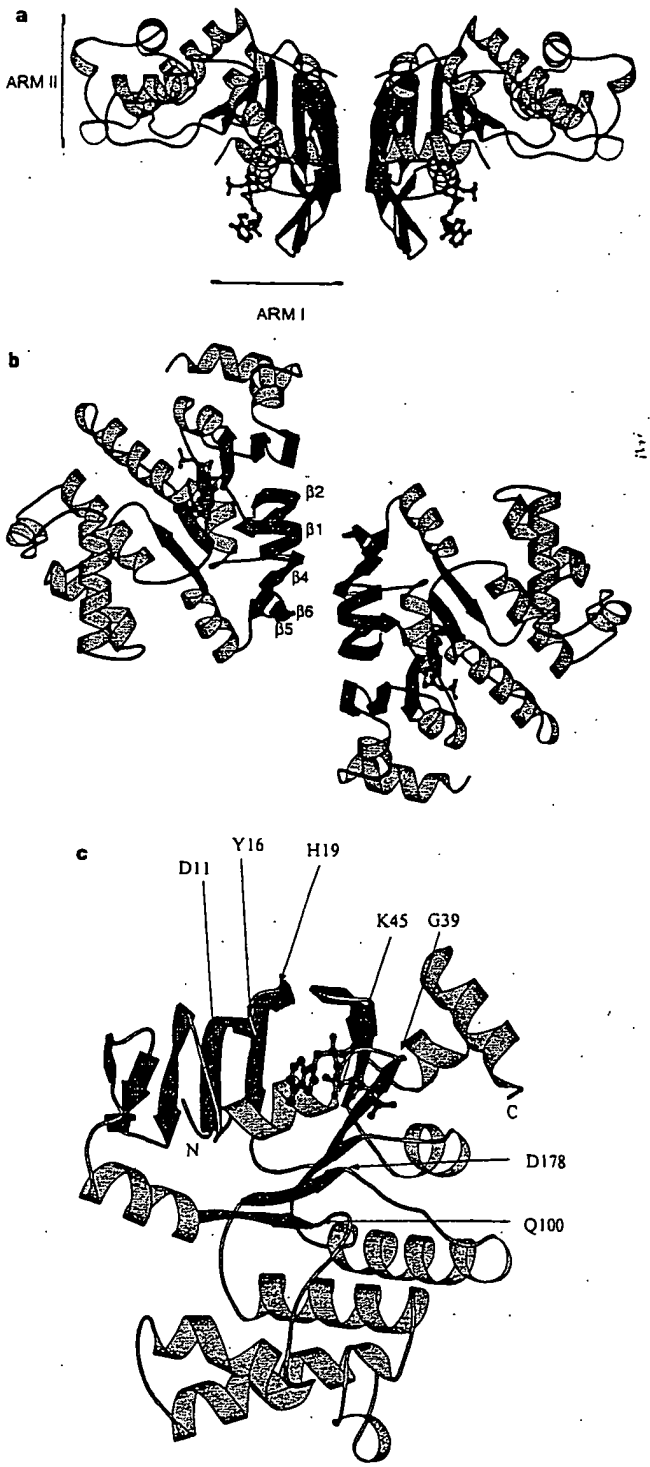

Figure 1 Crystal structure of HisP. **a**, View of the dimer along an axis perpendicular to its two-fold axis. The top and bottom of the dimer are suggested to face towards the periplasmic and cytoplasmic sides, respectively (see text). The thickness of arm II is about 25 Å, comparable to that of membrane. α-Helices are shown in orange and β-sheets in green. **b**, View along the two-fold axis of the HisP dimer, showing the relative displacement of the monomers not apparent in **a**. The β-strands at the dimer interface are labelled. **c**, View of one monomer from the bottom of arm I, as shown in **a**, towards arm II, showing the ATP-binding pocket. **a**–**c**, The protein and the bound ATP are in 'ribbon' and 'ball-and-stick' representations, respectively. Key residues discussed in the text are indicated in **c**. These figures were prepared with MOLSCRIPT[28]. N, amino terminus; C, C terminus.

Nature © Macmillan Publishers Ltd 1998

Int. J. Cancer: 78, 661–666 (1998)
© 1998 Wiley-Liss, Inc.

Publication of the International Union Against Cancer
Publication de l'Union Internationale Contre le Cancer

NOVEL APPROACH TO QUANTITATIVE POLYMERASE CHAIN REACTION USING REAL-TIME DETECTION: APPLICATION TO THE DETECTION OF GENE AMPLIFICATION IN BREAST CANCER

Ivan BIÈCHE[1,2], Martine OLIVI[1], Marie-Hélène CHAMPÈME[2], Dominique VIDAUD[1], Rosette LIDEREAU[2] and Michel VIDAUD[1]*

[1]*Laboratoire de Génétique Moléculaire, Faculté des Sciences Pharmaceutiques et Biologiques de Paris, Paris, France*
[2]*Laboratoire d'Oncogénétique, Centre René Huguenin, St-Cloud, France*

Gene amplification is a common event in the progression of human cancers, and amplified oncogenes have been shown to have diagnostic, prognostic and therapeutic relevance. A kinetic quantitative polymerase-chain-reaction (PCR) method, based on fluorescent TaqMan methodology and a new instrument (ABI Prism 7700 Sequence Detection System) capable of measuring fluorescence in real-time, was used to quantify gene amplification in tumor DNA. Reactions are characterized by the point during cycling when PCR amplification is still in the exponential phase, rather than the amount of PCR product accumulated after a fixed number of cycles. None of the reaction components is limited during the exponential phase, meaning that values are highly reproducible in reactions starting with the same copy number. This greatly improves the precision of DNA quantification. Moreover, real-time PCR does not require post-PCR sample handling, thereby preventing potential PCR-product carry-over contamination; it possesses a wide dynamic range of quantification and results in much faster and higher sample throughput. The real-time PCR method, was used to develop and validate a simple and rapid assay for the detection and quantification of the 3 most frequently amplified genes (*myc, ccnd1* and *erbB2*) in breast tumors. Extra copies of *myc, ccnd1* and *erbB2* were observed in 10, 23 and 15%, respectively, of 108 breast-tumor DNA; the largest observed numbers of gene copies were 4.6, 18.6 and 15.1, respectively. These results correlated well with those of Southern blotting. The use of this new semi-automated technique will make molecular analysis of human cancers simpler and more reliable, and should find broad applications in clinical and research settings. *Int. J. Cancer* 78:661–666, 1998.
© *1998 Wiley-Liss, Inc.*

Gene amplification plays an important role in the pathogenesis of various solid tumors, including breast cancer, probably because over-expression of the amplified target genes confers a selective advantage. The first technique used to detect genomic amplification was cytogenetic analysis. Amplification of several chromosome regions, visualized either as extrachromosomal double minutes (dmins) or as integrated homogeneously staining regions (HSRs), are among the main visible cytogenetic abnormalities in breast tumors. Other techniques such as comparative genomic hybridization (CGH) (Kallioniemi *et al.*, 1994) have also been used in broad searches for regions of increased DNA copy numbers in tumor cells, and have revealed some 20 amplified chromosome regions in breast tumors. Positional cloning efforts are underway to identify the critical gene(s) in each amplified region. To date, genes known to be amplified frequently in breast cancers include *myc* (8q24), *ccnd*1 (11q13), and *erb*B2 (17q12-q21) (for review, see Bièche and Lidereau, 1995).

Amplification of the *myc, ccnd1,* and *erb*B2 proto-oncogenes should have clinical relevance in breast cancer, since independent studies have shown that these alterations can be used to identify sub-populations with a worse prognosis (Berns *et al.*, 1992; Schuuring *et al.*, 1992; Slamon *et al.*, 1987). Muss *et al.* (1994) suggested that these gene alterations may also be useful for the prediction and assessment of the efficacy of adjuvant chemotherapy and hormone therapy.

However, published results diverge both in terms of the frequency of these alterations and their clinical value. For instance, over 500 studies in 10 years have failed to resolve the controversy surrounding the link suggested by Slamon *et al.* (1987) between *erb*B2 amplification and disease progression. These discrepancies are partly due to the clinical, histological and ethnic heterogeneity of breast cancer, but technical considerations are also probably involved.

Specific genes (DNA) were initially quantified in tumor cells by means of blotting procedures such as Southern and slot blotting. These batch techniques require large amounts of DNA (5–10 µg/reaction) to yield reliable quantitative results. Furthermore, meticulous care is required at all stages of the procedures to generate blots of sufficient quality for reliable dosage analysis. Recently, PCR has proven to be a powerful tool for quantitative DNA analysis, especially with minimal starting quantities of tumor samples (small, early-stage tumors and formalin-fixed, paraffin-embedded tissues).

Quantitative PCR can be performed by evaluating the amount of product either after a given number of cycles (end-point quantitative PCR) or after a varying number of cycles during the exponential phase (kinetic quantitative PCR). In the first case, an internal standard distinct from the target molecule is required to ascertain PCR efficiency. The method is relatively easy but implies generating, quantifying and storing an internal standard for each gene studied. Nevertheless, it is the most frequently applied method to date.

One of the major advantages of the kinetic method is its rapidity in quantifying a new gene, since no internal standard is required (an external standard curve is sufficient). Moreover, the kinetic method has a wide dynamic range (at least 5 orders of magnitude), giving an accurate value for samples differing in their copy number. Unfortunately, the method is cumbersome and has therefore been rarely used. It involves aliquot sampling of each assay mix at regular intervals and quantifying, for each aliquot, the amplification product. Interest in the kinetic method has been stimulated by a novel approach using fluorescent TaqMan methodology and a new instrument (ABI Prism 7700 Sequence Detection System) capable of measuring fluorescence in real time (Gibson *et al.*, 1996; Heid *et al.*, 1996). The TaqMan reaction is based on the 5′ nuclease assay first described by Holland *et al.* (1991). The latter uses the 5′ nuclease activity of Taq polymerase to cleave a specific fluorogenic oligonucleotide probe during the extension phase of PCR. The approach uses dual-labeled fluorogenic hybridization probes (Lee *et al.*, 1993). One fluorescent dye, co-valently linked to the 5′ end of the oligonucleotide, serves as a reporter [FAM (*i.e.*, 6-carboxy-fluorescein)] and its emission spectrum is quenched by a second fluorescent dye, TAMRA (*i.e.*, 6-carboxy-tetramethyl-rhodamine) attached to the 3′ end. During the extension phase of the PCR

Grant sponsors: Association Pour la Recherche sur le Cancer and Ministère de l'Enseignement Supérieur et de la Recherche.

*Correspondence to: Laboratoire de Génétique Moléculaire, Faculté des Sciences Pharmaceutiques et Biologiques de Paris, 4 Avenue de l'Observatoire, F-75006 Paris, France. Fax: (33)1-4407-1754.
E-mail: mvidaud@teaser.fr

Received 2 May 1998; Revised 30 June 1998

cycle, the fluorescent hybridization probe is hydrolyzed by the 5′-3′ nucleolytic activity of DNA polymerase. Nuclease degradation of the probe releases the quenching of FAM fluorescence emission, resulting in an increase in peak fluorescence emission. The fluorescence signal is normalized by dividing the emission intensity of the reporter dye (FAM) by the emission intensity of a reference dye (*i.e.*, ROX, 6-carboxy-X-rhodamine) included in TaqMan buffer, to obtain a ratio defined as the Rn (normalized reporter) for a given reaction tube. The use of a sequence detector enables the fluorescence spectra of all 96 wells of the thermal cycler to be measured continuously during PCR amplification.

The real-time PCR method offers several advantages over other current quantitative PCR methods (Celi *et al.*, 1994): *(i)* the probe-based homogeneous assay provides a real-time method for detecting only specific amplification products, since specific hybridation of both the primers and the probe is necessary to generate a signal; *(ii)* the C_t (threshold cycle) value used for quantification is measured when PCR amplification is still in the log phase of PCR product accumulation. This is the main reason why C_t is a more reliable measure of the starting copy number than are end-point measurements, in which a slight difference in a limiting component can have a drastic effect on the amount of product; *(iii)* use of C_t values gives a wider dynamic range (at least 5 orders of magnitude), reducing the need for serial dilution; *(iv)* The real-time PCR method is run in a closed-tube system and requires no post-PCR sample handling, thus avoiding potential contamination; *(v)* the system is highly automated, since the instrument continuously measures fluorescence in all 96 wells of the thermal cycler during PCR amplification and the corresponding software processes, and analyzes the fluorescence data; *(vi)* the assay is rapid, as results are available just one minute after thermal cycling is complete; *(vii)* the sample throughput of the method is high, since 96 reactions can be analyzed in 2 hr.

Here, we applied this semi-automated procedure to determine the copy numbers of the 3 most frequently amplified genes in breast tumors (*myc*, *ccnd1* and *erb*B2), as well as 2 genes (*alb* and *app*) located in a chromosome region in which no genetic changes have been observed in breast tumors. The results for 108 breast tumors were compared with previous Southern-blot data for the same samples.

MATERIAL AND METHODS

Tumor and blood samples

Samples were obtained from 108 primary breast tumors removed surgically from patients at the Centre René Huguenin; none of the patients had undergone radiotherapy or chemotherapy. Immediately after surgery, the tumor samples were placed in liquid nitrogen until extraction of high-molecular-weight DNA. Patients were included in this study if the tumor sample used for DNA preparation contained more than 60% of tumor cells (histological analysis). A blood sample was also taken from 18 of the same patients.

DNA was extracted from tumor tissue and blood leukocytes according to standard methods.

Real-time PCR

Theoretical basis. Reactions are characterized by the point during cycling when amplification of the PCR product is first detected, rather than by the amount of PCR product accumulated after a fixed number of cycles. The higher the starting copy number of the genomic DNA target, the earlier a significant increase in fluorescence is observed. The parameter C_t (threshold cycle) is defined as the fractional cycle number at which the fluorescence generated by cleavage of the probe passes a fixed threshold above baseline. The target gene copy number in unknown samples is quantified by measuring C_t and by using a standard curve to determine the starting copy number. The precise amount of genomic DNA (based on optical density) and its quality (*i.e.*, lack of extensive degradation) are both difficult to assess. We therefore also quantified a control gene *(alb)* mapping to chromosome region 4q11-q13, in which no genetic alterations have been found in breast-tumor DNA by means of CGH (Kallioniemi *et al.*, 1994).

Thus, the ratio of the copy number of the target gene to the copy number of the *alb* gene normalizes the amount and quality of genomic DNA. The ratio defining the level of amplification is termed "N", and is determined as follows:

$$N = \frac{\text{copy number of target gene } (\textit{app}, \textit{myc}, \textit{ccnd1}, \textit{erb}\text{B2})}{\text{copy number of reference gene } (\textit{alb})}.$$

Primers, probes, reference human genomic DNA and PCR consumables. Primers and probes were chosen with the assistance of the computer programs Oligo 4.0 (National Biosciences, Plymouth, MN), EuGene (Daniben Systems, Cincinnati, OH) and Primer Express (Perkin-Elmer Applied Biosystems, Foster City, CA).

Primers were purchased from DNAgency (Malvern, PA) and probes from Perkin-Elmer Applied Biosystems.

Nucleotide sequences for the oligonucleotide hybridization probes and primers are available on request.

The TaqMan PCR Core reagent kit, MicroAmp optical tubes, and MicroAmp caps were from Perkin-Elmer Applied Biosystems.

Standard-curve construction. The kinetic method requires a standard curve. The latter was constructed with serial dilutions of specific PCR products, according to Piatak *et al.* (1993). In practice, each specific PCR product was obtained by amplifying 20 ng of a standard human genomic DNA (Boehringer, Mannheim, Germany) with the same primer pairs as those used later for real-time quantitative PCR. The 5 PCR products were purified using MicroSpin S-400 HR columns (Pharmacia, Uppsala, Sweden) electrophorezed through an acrylamide gel and stained with ethidium bromide to check their quality. The PCR products were then quantified spectrophotometrically and pooled, and serially diluted 10-fold in mouse genomic DNA (Clontech, Palo Alto, CA) at a constant concentration of 2 ng/µl. The standard curve used for real-time quantitative PCR was based on serial dilutions of the pool of PCR products ranging from 10^{-7} (10^5 copies of each gene) to 10^{-10} (10^2 copies). This series of diluted PCR products was aliquoted and stored at −80°C until use.

The standard curve was validated by analyzing 2 known quantities of calibrator human genomic DNA (20 ng and 50 ng).

PCR amplification. Amplification mixes (50 µl) contained the sample DNA (around 20 ng, around 6600 copies of disomic genes), 10× TaqMan buffer (5 µl), 200 µM dATP, dCTP, dGTP, and 400 µM dUTP, 5 mM $MgCl_2$, 1.25 units of AmpliTaq Gold, 0.5 units of AmpErase uracil N-glycosylase (UNG), 200 nM each primer and 100 nM probe. The thermal cycling conditions comprised 2 min at 50°C and 10 min at 95°C. Thermal cycling consisted of 40 cycles at 95°C for 15 s and 65°C for 1 min. Each assay included: a standard curve (from 10^5 to 10^2 copies) in duplicate, a no-template control, 20 ng and 50 ng of calibrator human genomic DNA (Boehringer) in triplicate, and about 20 ng of unknown genomic DNA in triplicate (26 samples can thus be analyzed on a 96-well microplate). All samples with a coefficient of variation (CV) higher than 10% were retested.

All reactions were performed in the ABI Prism 7700 Sequence Detection System (Perkin-Elmer Applied Biosystems), which detects the signal from the fluorogenic probe during PCR.

Equipment for real-time detection. The 7700 system has a built-in thermal cycler and a laser directed via fiber optical cables to each of the 96 sample wells. A charge-coupled-device (CDD) camera collects the emission from each sample and the data are analyzed automatically. The software accompanying the 7700 system calculates C_t and determines the starting copy number in the samples.

Determination of gene amplification. Gene amplification was calculated as described above. Only samples with an N value higher than 2 were considered to be amplified.

RESULTS

To validate the method, real-time PCR was performed on genomic DNA extracted from 108 primary breast tumors, and 18 normal leukocyte DNA samples from some of the same patients. The target genes were the *myc*, *ccnd1* and *erb*B2 proto-oncogenes, and the β-amyloid precursor protein gene (*app*), which maps to a chromosome region (21q21.2) in which no genetic alterations have been found in breast tumors (Kallioniemi *et al.*, 1994). The reference disomic gene was the albumin gene (*alb*, chromosome 4q11-q13).

Validation of the standard curve and dynamic range of real-time PCR

The standard curve was constructed from PCR products serially diluted in genomic mouse DNA at a constant concentration of 2 ng/µl. It should be noted that the 5 primer pairs chosen to analyze the 5 target genes do not amplify genomic mouse DNA (data not shown). Figure 1 shows the real-time PCR standard curve for the *alb* gene. The dynamic range was wide (at least 4 orders of magnitude), with samples containing as few as 10^2 copies or as many as 10^5 copies.

*Copy-number ratio of the 2 reference genes (*app *and* alb*)*

The *app* to *alb* copy-number ratio was determined in 18 normal leukocyte DNA samples and all 108 primary breast-tumor DNA

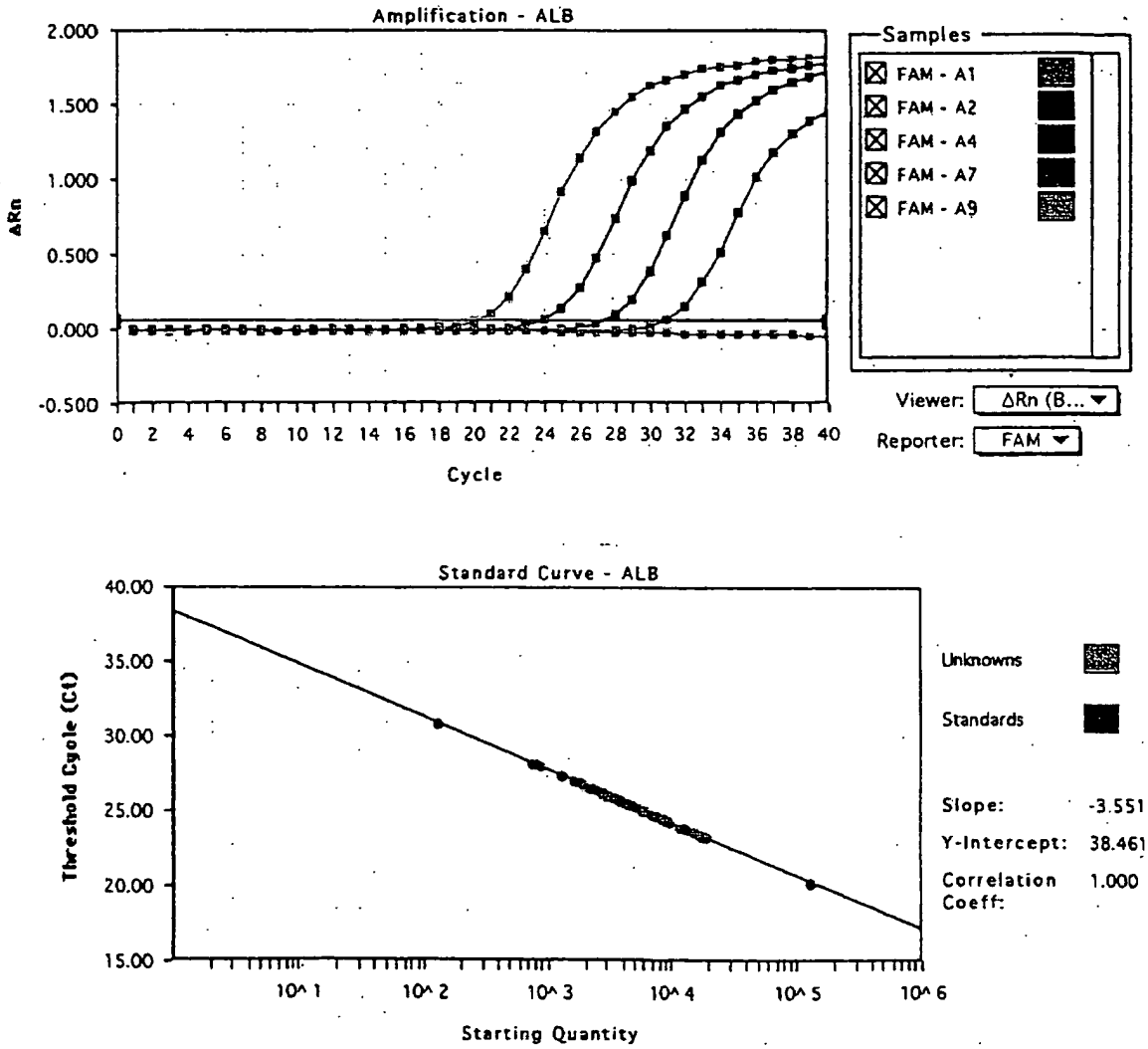

FIGURE 1 – Albumin (*alb*) gene dosage by real-time PCR. Top: Amplification plots for reactions with starting *alb* gene copy number ranging from 10^5 (A9), 10^4 (A7), 10^3 (A4) to 10^2 (A2) and a no-template control (A1). Cycle number is plotted *vs.* change in normalized reporter signal (ΔRn). For each reaction tube, the fluorescence signal of the reporter dye (FAM) is divided by the fluorescence signal of the passive reference dye (ROX), to obtain a ratio defined as the normalized reporter signal (Rn). ΔRn represents the normalized reporter signal (Rn) minus the baseline signal established in the first 15 PCR cycles. ΔRn increases during PCR as *alb* PCR product copy number increases until the reaction reaches a plateau. C_t (threshold cycle) represents the fractional cycle number at which a significant increase in Rn above a baseline signal (horizontal black line) can first be detected. Two replicate plots were performed for each standard sample, but the data for only one are shown here. Bottom: Standard curve plotting log starting copy number *vs.* C_t (threshold cycle). The black dots represent the data for standard samples plotted in duplicate and the red dots the data for unknown genomic DNA samples plotted in triplicate. The standard curve shows 4 orders of linear dynamic range.

samples. We selected these 2 genes because they are located in 2 chromosome regions (*app*, 21q21.2; *alb*, 4q11-q13) in which no obvious genetic changes (including gains or losses) have been observed in breast cancers (Kallioniemi *et al.*, 1994). The ratio for the 18 normal leukocyte DNA samples fell between 0.7 and 1.3 (mean 1.02 ± 0.21), and was similar for the 108 primary breast-tumor DNA samples (0.6 to 1.6, mean 1.06 ± 0.25), confirming that *alb* and *app* are appropriate reference disomic genes for breast-tumor DNA. The low range of the ratios also confirmed that the nucleotide sequences chosen for the primers and probes were not polymorphic, as mismatches of their primers or probes with the subject's DNA would have resulted in differential amplification.

myc, ccnd1 *and* erb*B2 gene dose in normal leukocyte DNA*

To determine the cut-off point for gene amplification in breast-cancer tissue, 18 normal leukocyte DNA samples were tested for the gene dose (N), calculated as described in "Material and Methods". The N value of these samples ranged from 0.5 to 1.3 (mean 0.84 ± 0.22) for *myc*; 0.7 to 1.6 (mean 1.06 ± 0.23) for *ccnd1* and 0.6 to 1.3 (mean 0.91 ± 0.19) for *erb*B2. Since N values for *myc*, *ccnd1* and *erb*B2 in normal leukocyte DNA consistently fell between 0.5 and 1.6, values of 2 or more were considered to represent gene amplification in tumor DNA.

myc, ccnd1 *and* erb*B2 gene dose in breast-tumor DNA*

myc, *ccnd1* and *erb*B2 gene copy numbers in the 108 primary breast tumors are reported in Table I. Extra copies of *ccnd1* were more frequent (23%, 25/108) than extra copies of *erb*B2 (15%, 16/108) and *myc* (10%, 11/108), and ranged from 2 to 18.6 for *ccnd1*, 2 to 15.1 for *erb*B2, and only 2 to 4.6 for the *myc* gene. Figure 2 and Table II represent tumors in which the *ccnd1* gene was amplified 16-fold (T145), 6-fold (T133) and non-amplified (T118). The 3 genes were never found to be co-amplified in the same tumor. *erb*B2 and *ccnd1* were co-amplified in only 3 cases, *myc* and *ccnd1* in 2 cases and *myc* and *erb*B2 in 1 case. This favors the hypothesis that gene amplifications are independent events in breast cancer. Interestingly, 5 tumors showed a decrease of at least 50% in the *erb*B2 copy number ($N < 0.5$), suggesting that they bore deletions of the 17q21 region (the site of *erb*B2). No such decrease in copy number was observed with the other 2 proto-oncogenes.

Comparison of gene dose determined by real-time quantitative PCR and Southern-blot analysis

Southern-blot analysis of *myc*, *ccnd1* and *erb*B2 amplifications had previously been done on the same 108 primary breast tumors. A perfect correlation between the results of real-time PCR and Southern blot was obtained for tumors with high copy numbers ($N \geq 5$). However, there were cases (1 *myc*, 6 *ccnd1* and 4 *erb*B2) in which real-time PCR showed gene amplification whereas Southern-blot did not, but these were mainly cases with low extra copy numbers (N from 2 to 2.9).

DISCUSSION

The clinical applications of gene amplification assays are currently limited, but would certainly increase if a simple, standardized and rapid method were perfected. Gene amplification status has been studied mainly by means of Southern blotting, but this method is not sensitive enough to detect low-level gene amplification nor accurate enough to quantify the full range of amplification values. Southern blotting is also time-consuming, uses radioactive reagents and requires relatively large amounts of high-quality genomic DNA, which means it cannot be used routinely in many laboratories. An amplification step is therefore required to determine the copy number of a given target gene from minimal quantities of tumor DNA (small early-stage tumors, cytopuncture specimens or formalin-fixed, paraffin-embedded tissues).

In this study, we validated a PCR method developed for the quantification of gene over-representation in tumors. The method, based on real-time analysis of PCR amplification, has several advantages over other PCR-based quantitative assays such as competitive quantitative PCR (Celi *et al.*, 1994). First, the real-time PCR method is performed in a closed-tube system, avoiding the risk of contamination by amplified products. Re-amplification of carryover PCR products in subsequent experiments can also be prevented by using the enzyme uracil N-glycosylase (UNG) (Longo *et al.*, 1990). The second advantage is the simplicity and rapidity of sample analysis, since no post-PCR manipulations are required. Our results show that the automated method is reliable. We found it possible to determine, in triplicate, the number of copies of a target gene in more than 100 tumors per day. Third, the system has a linear dynamic range of at least 4 orders of magnitude, meaning that samples do not have to contain equal starting amounts of DNA. This technique should therefore be suitable for analyzing formalin-fixed, paraffin-embedded tissues. Fourth, and above all, real-time PCR makes DNA quantification much more precise and reproducible, since it is based on C_t values rather than end-point measurement of the amount of accumulated PCR product. Indeed, the ABI Prism 7700 Sequence Detection System enables C_t to be calculated when PCR amplification is still in the exponential phase and when none of the reaction components is rate-limiting. The within-run CV of the C_t value for calibrator human DNA (5 replicates) was always below 5%, and the between-assay precision in 5 different runs was always below 10% (data not shown). In addition, the use of a standard curve is not absolutely necessary, since the copy number can be determined simply by comparing the C_t ratio of the target gene with that of reference genes. The results obtained by the 2 methods (with and without a standard curve) are similar in our experiments (data not shown). Moreover, unlike competitive quantitative PCR, real-time PCR does not require an internal control (the design and storage of internal controls and the validation of their amplification efficiency is laborious).

The only potential disavantage of real-time PCR, like all other PCR-based methods and solid-matrix blotting techniques (Southern blots and dot blots) is that is cannot avoid dilution artifacts inherent in the extraction of DNA from tumor cells contained in heterogeneous tissue specimens. Only FISH and immunohistochemistry can measure alterations on a cell-by-cell basis (Pauletti *et al.*, 1996; Slamon *et al.*, 1989). However, FISH requires expensive equipment and trained personnel and is also time-consuming. Moreover, FISH does not assess gene expression and therefore cannot detect cases in which the gene product is over-expressed in the absence of gene amplification, which will be possible in the future by real-time quantitative RT-PCR. Immunohistochemistry is subject to considerable variations in the hands of different teams, owing to alterations of target proteins during the procedure, the different primary antibodies and fixation methods used and the criteria used to define positive staining.

The results of this study are in agreement with those reported in the literature. (*i*) Chromosome regions 4q11-q13 and 21q21.2 (which bear *alb* and *app*, respectively) showed no genetic alterations in the breast-cancer samples studied here, in keeping with the results of CGH (Kallioniemi *et al.*, 1994). (*ii*) We found that amplifications of these 3 oncogenes were independent events, as reported by other teams (Berns *et al.*, 1992; Borg *et al.*, 1992). (*iii*) The frequency and degree of *myc* amplification in our breast tumor DNA series were lower than those of *ccnd1* and *erb*B2 amplification, confirming the findings of Borg *et al.* (1992) and Courjal *et al.* (1997). (*iv*) The maxima of *ccnd1* and *erb*B2 over-representation were 18-fold and 15-fold, also in keeping with earlier results (about

TABLE I – DISTRIBUTION OF AMPLIFICATION LEVEL (N) FOR *myc*, *ccnd1* AND *erb*B2 GENES IN 108 HUMAN BREAST TUMORS

Gene	Amplification level (N)			
	<0.5	0.5–1.9	2–4.9	≥5
myc	0	97 (89.8%)	11 (10.2%)	0
ccnd1	0	83 (76.9%)	17 (15.7%)	8 (7.4%)
*erb*B2	5 (4.6%)	87 (80.6%)	8 (7.4%)	8 (7.4%)

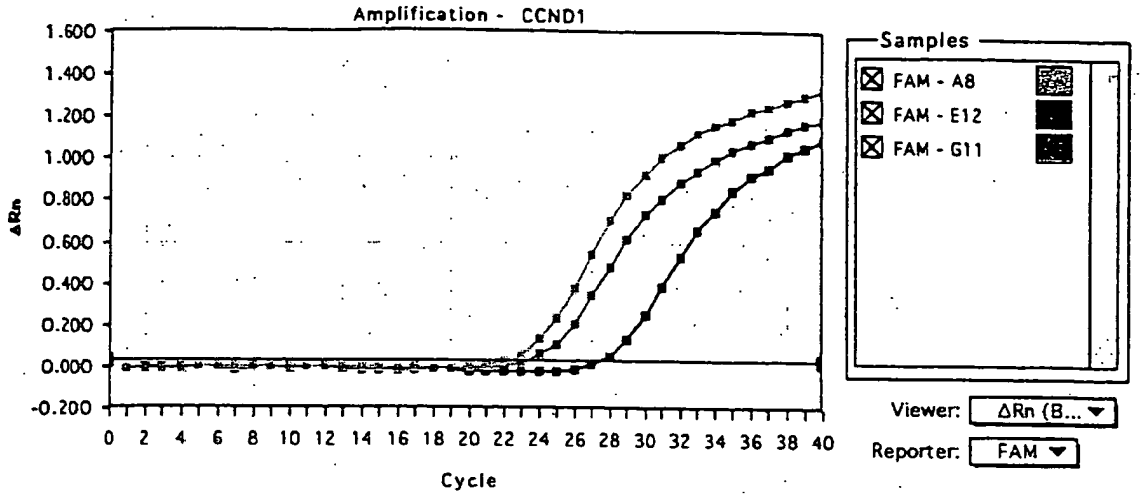

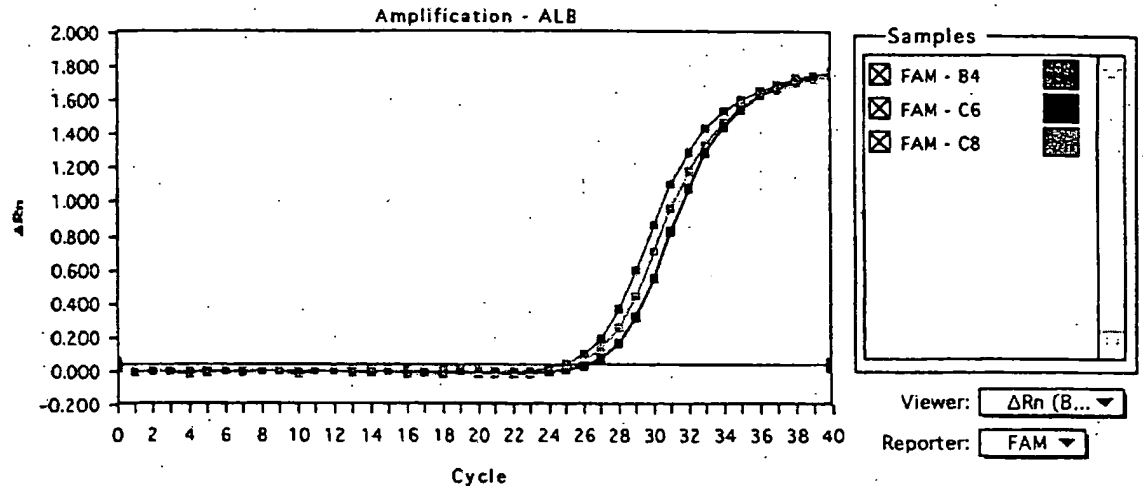

Tumor	CCND1 C_t	CCND1 Copy number	ALB C_t	ALB Copy number
T118	27.3	4605	26.5	4365
T133	23.2	61659	25.2	10092
T145	22.1	125892	25.6	7762

FIGURE 2 – *ccnd1* and alb gene dosage by real-time PCR in 3 breast tumor samples: T118 (E12, C6, black squares), T133 (G11, B4, red squares) and T145 (A8, C8, blue squares). Given the C_t of each sample, the initial copy number is inferred from the standard curve obtained during the same experiment. Triplicate plots were performed for each tumor sample, but the data for only one are shown here. The results are shown in Table II.

30-fold maximum) (Berns *et al.*, 1992; Borg *et al.*, 1992; Courjal *et al.*, 1997). (*v*) The *erb*B2 copy numbers obtained with real-time PCR were in good agreement with data obtained with other quantitative PCR-based assays in terms of the frequency and degree of amplification (An *et al.*, 1995; Deng *et al.*, 1996; Valeron *et al.*, 1996). Our results also correlate well with those recently published by Gelmini *et al.* (1997), who used the TaqMan system to measure *erb*B2 amplification in a small series of breast tumors (n = 25), but with an instrument (LS-50B luminescence spectrometer, Perkin-Elmer Applied Biosystems) which only allows end-

TABLE II – EXAMPLES OF *ccnd1* GENE DOSAGE RESULTS FROM 3 BREAST TUMORS[1]

Tumor	*ccnd1*			*alb*			Nccnd1/alb
	Copy number	Mean	SD	Copy number	Mean	SD	
T118	4525			4223			
	4605	4603	77	4365	4325	89	1.06
	4678			4387			
T133	59821			9787			
	61659	61100	1111	10092	10137	375	6.03
	61821			10533			
T145	128563			7321			
	125892	125392	3448	7762	7672	316	16.34
	121722			7933			

[1]For each sample, 3 replicate experiments were performed and the mean and the standard deviation (SD) was determined. The level of *ccnd1* gene amplification (*Nccnd1/alb*) is determined by dividing the average *ccnd1* copy number value by the average *alb* copy number value.

point measurement of fluorescence intensity. Here we report *myc* and *ccnd1* gene dosage in breast cancer by means of quantitative PCR. (vi) We found a high degree of concordance between real-time quantitative PCR and Southern blot analysis in terms of gene amplification, especially for samples with high copy numbers (≥5-fold). The slightly higher frequency of gene amplification (especially *ccnd1* and *erb*B2) observed by means of real-time quantitative PCR as compared with Southern-blot analysis may be explained by the higher sensitivity of the former method. However, we cannot rule out the possibility that some tumors with a few extra gene copies observed in real-time PCR had additional copies of an arm or a whole chromosome (trisomy, tetrasomy or polysomy) rather than true gene amplification. These 2 types of genetic alteration (polysomy and gene amplification) could be easily distinguished in the future by using an additional probe located on the same chromosome arm, but some distance from the target gene. It is noteworthy that high gene copy numbers have the greatest prognostic significance in breast carcinoma (Borg *et al.*, 1992; Slamon *et al.*, 1987).

Finally, this technique can be applied to the detection of gene deletion as well as gene amplification. Indeed, we found a decreased copy number of *erb*B2 (but not of the other 2 proto-oncogenes) in several tumors; *erb*B2 is located in a chromosome region (17q21) reported to contain both deletions and amplifications in breast cancer (Bièche and Lidereau, 1995).

In conclusion, gene amplification in various cancers can be used as a marker of pre-neoplasia, also for early diagnosis of cancer, staging, prognostication and choice of treatment. Southern blotting is not sufficiently sensitive, and FISH is lengthy and complex. Real-time quantitative PCR overcomes both these limitations, and is a sensitive and accurate method of analyzing large numbers of samples in a short time. It should find a place in routine clinical gene dosage.

ACKNOWLEDGEMENTS

RL is a research director at the Institut National de la Santé et de la Recherche Médicale (INSERM). We thank the staff of the Centre René Huguenin for assistance in specimen collection and patient care.

REFERENCES

AN, H.X., NIEDERACHER, D., BECKMANN, M.W., GÖHRING, U.J., SCHARL, A., PICARD, F., VAN ROEYEN, C., SCHNÜRCH, H.G. and BENDER, H.G., *erb*B2 gene amplification detected by fluorescent differential polymerase chain reaction in paraffin-embedded breast carcinoma tissues. *Int. J. Cancer (Pred. Oncol.)*, **64**, 291–297 (1995).

BERNS, E.M.J.J., KLIJN, J.G.M., VAN PUTTEN, W.L.J., VAN STAVEREN, I.L., PORTENGEN, H. and FOEKENS, J.A., c-*myc* amplification is a better prognostic factor than HER2/*neu* amplification in primary breast cancer. *Cancer Res.*, **52**, 1107–1113 (1992).

BIÈCHE, I. and LIDEREAU, R., Genetic alterations in breast cancer. *Genes Chrom. Cancer*, **14**, 227–251 (1995).

BORG, A., BALDETORP, B., FERNO, M., OLSSON, H. and SIGURDSSON, H., c-*myc* amplification is an independent prognostic factor in post-menopausal breast cancer. *Int. J. Cancer*, **51**, 687–691 (1992).

CELI, F.S., COHEN, M.M., ANTONARAKIS, S.E., WERTHEIMER, E., ROTH, J. and SHULDINER, A.R., Determination of gene dosage by a quantitative adaptation of the polymerase chain reaction (gd-PCR): rapid detection of deletions and duplications of gene sequences. *Genomics*, **21**, 304–310 (1994).

COURJAL, F., CUNY, M., SIMONY-LAFONTAINE, J., LOUASSON, G., SPEISER, P., ZEILLINGER, R., RODRIGUEZ, C. and THEILLET, C., Mapping of DNA amplifications at 15 chromosomal localizations in 1875 breast tumors: definition of phenotypic groups. *Cancer Res.*, **57**, 4360–4367 (1997).

DENG, G., YU, M., CHEN, L.C., MOORE, D., KURISU, W., KALLIONIEMI, A., WALDMAN, F.M., COLLINS, C. and SMITH, H.S., Amplifications of oncogene *erb*B-2 and chromosome 20q in breast cancer determined by differentially competitive polymerase chain reaction. *Breast Cancer Res. Treat.*, **40**, 271–281 (1996).

GELMINI, S., ORIANDO, C., SESTINI, R., VONA, G., PINZANI, P., RUOCCO, L. and PAZZAGLI, M., Quantitative polymerase chain reaction-based homogeneous assay with fluorogenic probes to measure c-*erB*-2 oncogene amplification. *Clin. Chem.*, **43**, 752–758 (1997).

GIBSON, U.E.M., HEID, C.A. and WILLIAMS, P.M., A novel method for real-time quantitative RT-PCR. *Genome Res.*, **6**, 995–1001 (1996).

HEID, C.A., STEVENS, J., LIVAK, K.J. and WILLIAMS, P.M., Real-time quantitative PCR. *Genome Res.*, **6**, 986–994 (1996).

HOLLAND, P.M., ABRAMSON, R.D., WATSON, R. and GELFAND, D.H., Detection of specific polymerase chain reaction product by utilizing the 5′ to 3′ exonuclease activity of *Thermus aquaticus* DNA polymerase. *Proc. nat. Acad. Sci. (Wash.)*, **88**, 7276–7280 (1991).

KALLIONIEMI, A., KALLIONIEMI, O.P., PIPER, J., TANNER, M., STOKKES, T., CHEN, L., SMITH, H.S., PINKEL, D., GRAY, J.W. and WALDMAN, F.M., Detection and mapping of amplified DNA sequences in breast cancer by comparative genomic hybridization. *Proc. nat. Acad. Sci. (Wash.)*, **91**, 2156–2160 (1994).

LEE, L.G., CONNELL, C.R. and BIOCH, W., Allelic discrimination by nick-translation PCR with fluorogenic probe. *Nucleic Acids Res.*, **21**, 3761–3766 (1993).

LONGO, N., BERNINGER, N.S. and HARTLEY, J.L., Use of uracil DNA glycosylase to control carry-over contamination in polymerase chain reactions. *Gene*, **93**, 125–128 (1990).

MUSS, H.B., THOR, A.D., BERRY, D.A., KUTE, T., LIU, E.T., KOERNER, F., CIRRINCIONE, C.T., BUDMAN, D.R., WOOD, W.C., BARCOS, M. and HENDERSON, I.C., c-*erb*B-2 expression and response to adjuvant therapy in women with node-positive early breast cancer. *New Engl. J. Med.*, **330**, 1260–1266 (1994).

PAULETTI, G., GODOLPHIN, W., PRESS, M.F. and SALMON, D.J., Detection and quantification of HER-2/*neu* gene amplification in human breast cancer archival material using fluorescence *in situ* hybridization. *Oncogene*, **13**, 63–72 (1996).

PIATAK, M., LUK, K.C., WILLIAMS, B. and LIFSON, J.D., Quantitative competitive polymerase chain reaction for accurate quantitation of HIV DNA and RNA species. *Biotechniques*, **14**, 70–80 (1993).

SCHUURING, E., VERHOEVEN, E., VAN TINTEREN, H., PETERSE, J.L., NUNNIK, B., THUNNISSEN, F.B.J.M., DEVILEE, P., CORNELISSE, C.J., VAN DE VIJVER, M.J., MOOI, W.J. and MICHALIDES, R.J.A.M., Amplification of genes within the chromosome 11q13 region is indicative of poor prognosis in patients with operable breast cancer. *Cancer Res.*, **52**, 5229–5234 (1992).

SLAMON, D.J., CLARK, G.M., WONG, S.G., LEVIN, W.S., ULLRICH, A. and MCGUIRE, W.L., Human breast cancer: correlation of relapse and survival with amplification of the HER-2/*neu* oncogene. *Science*, **235**, 177–182 (1987).

SLAMON, D.J., GODOLPHIN, W., JONES, L.A., HOLT, J.A., WONG, S.G., KEITH, D.E., LEVIN, W.J., STUART, S.G., UDOVE, J., ULLRICH, A. and PRESS, M.F., Studies of the HER-2/*neu* proto-oncogene in human breast and ovarian cancer. *Science*, **244**, 707–712 (1989).

VALERON, P.F., CHIRINO, R., FERNANDEZ, L., TORRES, S., NAVARRO, D., AGUIAR, J., CABRERA, J.J., DIAZ-CHICO, B.N. and DIAZ-CHICO, J.C., Validation of a differential PCR and an ELISA procedure in studying HER-2/*neu* status in breast cancer. *Int. J. Cancer*, **65**, 129–133 (1996).

IN THE UNITED STATES PATENT AND TRADEMARK OFFICE

Applicant	:	Ashkenazi et al.
App. No.	:	09/903,925
Filed	:	July 11, 2001
For	:	SECRETED AND TRANSMEMBRANE POLYPEPTIDES AND NUCLEIC ACIDS ENCODING THE SAME
Examiner	:	Hamud, Fozia M

Group Art Unit 1647

CERTIFICATE OF EXPRESS MAILING

I hereby certify that this correspondence is being deposited with the United States Postal Service with sufficient postage as first class mail in an envelope addressed to Commissioner of Patents, Washington D.C. 20231 on:

_____
(Date)

_____

Commissioner of Patents
P.O. Box 1450
Alexandria, VA 22313-1450

DECLARATION OF AVI ASHKENAZI, Ph.D UNDER 37 C.F.R. § 1.132

I, Avi Ashkenazi, Ph.D. declare and say as follows: -

1. I am Director and Staff Scientist at the Molecular Oncology Department of Genentech, Inc., South San Francisco, CA 94080.

2. I joined Genentech in 1988 as a postdoctoral fellow. Since then, I have investigated a variety of cellular signal transduction mechanisms, including apoptosis, and have developed technologies to modulate such mechanisms as a means of therapeutic intervention in cancer and autoimmune disease. I am currently involved in the investigation of a series of secreted proteins over-expressed in tumors, with the aim to identify useful targets for the development of therapeutic antibodies for cancer treatment.

3. My scientific Curriculum Vitae, including my list of publications, is attached to and forms part of this Declaration (Exhibit A).

4. Gene amplification is a process in which chromosomes undergo changes to contain multiple copies of certain genes that normally exist as a single copy, and is an important factor in the pathophysiology of cancer. Amplification of certain genes (e.g., Myc or Her2/Neu)

gives cancer cells a growth or survival advantage relative to normal cells, and might also provide a mechanism of tumor cell resistance to chemotherapy or radiotherapy.

5. If gene amplification results in over-expression of the mRNA and the corresponding gene product, then it identifies that gene product as a promising target for cancer therapy, for example by the therapeutic antibody approach. Even in the absence of over-expression of the gene product, amplification of a cancer marker gene - as detected, for example, by the reverse transcriptase TaqMan® PCR or the fluorescence *in situ* hybridization (FISH) assays -is useful in the diagnosis or classification of cancer, or in predicting or monitoring the efficacy of cancer therapy. An increase in gene copy number can result not only from intrachromosomal changes but also from chromosomal aneuploidy. It is important to understand that detection of gene amplification can be used for cancer diagnosis even if the determination includes measurement of chromosomal aneuploidy. Indeed, as long as a significant difference relative to normal tissue is detected, it is irrelevant if the signal originates from an increase in the number of gene copies per chromosome and/or an abnormal number of chromosomes.

6. I understand that according to the Patent Office, absent data demonstrating that the increased copy number of a gene in certain types of cancer leads to increased expression of its product, gene amplification data are insufficient to provide substantial utility or well established utility for the gene product (the encoded polypeptide), or an antibody specifically binding the encoded polypeptide. However, even when amplification of a cancer marker gene does not result in significant over-expression of the corresponding gene product, this very absence of gene product over-expression still provides significant information for cancer diagnosis and treatment. Thus, if over-expression of the gene product does not parallel gene amplification in certain tumor types but does so in others, then parallel monitoring of gene amplification and gene product over-expression enables more accurate tumor classification and hence better determination of suitable therapy. In addition, absence of over-expression is crucial information for the practicing clinician. If a gene is amplified but the corresponding gene product is not over-expressed, the clinician accordingly will decide not to treat a patient with agents that target that gene product.

7. I hereby declare that all statements made herein of my own knowledge are true and that all statements made on information or belief are believed to be true, and further that these statements were made with the knowledge that willful false statements and the like so

made are punishable by fine or imprisonment, or both, under Section 1001 of Title 18 of the United States Code and that such willful statements may jeopardize the validity of the application or any patent issued thereon.

By: Avi Ashkenazi
Avi Ashkenazi, Ph.D.

Date: 9/15/03

SV 455281 v1
9/12/03 3:06 PM (39780.7000)

CURRICULUM VITAE

Avi Ashkenazi

July 2003

Personal:

Date of birth:	29 November, 1956
Address:	1456 Tarrytown Street, San Mateo, CA 94402
Phone:	(650) 578-9199 (home); (650) 225-1853 (office)
Fax:	(650) 225-6443 (office)
Email:	aa@gene.com

Education:

1983:	B.S. in Biochemistry, with honors, Hebrew University, Israel
1986:	Ph.D. in Biochemistry, Hebrew University, Israel

Employment:

1983-1986:	Teaching assistant, undergraduate level course in Biochemistry
1985-1986:	Teaching assistant, graduate level course on Signal Transduction
1986 - 1988:	Postdoctoral fellow, Hormone Research Dept., UCSF, and Developmental Biology Dept., Genentech, Inc., with J. Ramachandran
1988 - 1989:	Postdoctoral fellow, Molecular Biology Dept., Genentech, Inc., with D. Capon
1989 - 1993:	Scientist, Molecular Biology Dept., Genentech, Inc.
1994 -1996:	Senior Scientist, Molecular Oncology Dept., Genentech, Inc.
1996-1997:	Senior Scientist and Interim director, Molecular Oncology Dept., Genentech, Inc.
1997-1990:	Senior Scientist and preclinical project team leader, Genentech, Inc.
1999 -2002:	Staff Scientist in Molecular Oncology, Genentech, Inc.
2002-present:	Staff Scientist and Director in Molecular Oncology, Genentech, Inc.

Awards:

1988:	First prize, The Boehringer Ingelheim Award

Editorial:

Editorial Board Member: Current Biology

Associate Editor, Clinical Cancer Research.

Associate Editor, Cancer Biology and Therapy.

Refereed papers:

1. Gertler, A., Ashkenazi, A., and Madar, Z. Binding sites for human growth hormone and ovine and bovine prolactins in the mammary gland and liver of the lactating cow. *Mol. Cell. Endocrinol.* **34**, 51-57 (1984).
2. Gertler, A., Shamay, A., Cohen, N., Ashkenazi, A., Friesen, H., Levanon, A., Gorecki, M., Aviv, H., Hadari, D., and Vogel, T. Inhibition of lactogenic activities of ovine prolactin and human growth hormone (hGH) by a novel form of a modified recombinant hGH. *Endocrinology* **118**, 720-726 (1986).
3. Ashkenazi, A., Madar, Z., and Gertler, A. Partial purification and characterization of bovine mammary gland prolactin receptor. *Mol. Cell. Endocrinol.* **50**, 79-87 (1987).
4. Ashkenazi, A., Pines, M., and Gertler, A. Down-regulation of lactogenic hormone receptors in Nb2 lymphoma cells by cholera toxin. *Biochemistry Internatl.* **14**, 1065-1072 (1987).
5. Ashkenazi, A., Cohen, R., and Gertler, A. Characterization of lactogen receptors in lactogenic hormone-dependent and independent Nb2 lymphoma cell lines. *FEBS Lett.* **210**, 51-55 (1987).
6. Ashkenazi, A., Vogel, T., Barash, I., Hadari, D., Levanon, A., Gorecki, M., and Gertler, A. Comparative study on in vitro and in vivo modulation of lactogenic and somatotropic receptors by native human growth hormone and its modified recombinant analog. *Endocrinology* **121**, 414-419 (1987).
7. Peralta, E., Winslow, J., Peterson, G., Smith, D., Ashkenazi, A., Ramachandran, J., Schimerlik, M., and Capon, D. Primary structure and biochemical properties of an M2 muscarinic receptor. *Science* **236**, 600-605 (1987).
8. Peralta, E. Ashkenazi, A., Winslow, J., Smith, D., Ramachandran, J., and Capon, D. J. Distincnt primary structures, ligand-binding properties and tissue-specific expression of four human muscarinic acetylcholine receptors. *EMBO J.* **6**, 3923-3929 (1987).
9. Ashkenazi, A., Winslow, J., Peralta, E., Peterson, G., Schimerlik, M., Capon, D., and Ramachandran, J. An M2 muscarinic receptor subtype coupled to both adenylyl cyclase and phosphoinositide turnover. *Science* **238**, 672-675 (1987).

10. Pines, M., Ashkenazi, A., Cohen-Chapnik, N., Binder, L., and Gertler, A. Inhibition of the proliferation of Nb2 lymphoma cells by femtomolar concentrations of cholera toxin and partial reversal of the effect by 12-o-tetradecanoyl-phorbol-13-acetate. *J. Cell. Biochem.* **37**, 119-129 (1988).

11. Peralta, E. Ashkenazi, A., Winslow, J. Ramachandran, J., and Capon, D. Differential regulation of PI hydrolysis and adenylyl cyclase by muscarinic receptor subtypes. *Nature* **334**, 434-437 (1988).

12. Ashkenazi., A. Peralta, E., Winslow, J., Ramachandran, J., and Capon, D. Functionally distinct G proteins couple different receptors to PI hydrolysis in the same cell. *Cell* **56**, 487-493 (1989).

13. Ashkenazi, A., Ramachandran, J., and Capon, D. Acetylcholine analogue stimulates DNA synthesis in brain-derived cells via specific muscarinic acetylcholine receptor subtypes. *Nature* **340**, 146-150 (1989).

14. Lammare, D., Ashkenazi, A., Fleury, S., Smith, D., Sekaly, R., and Capon, D. The MHC-binding and gp120-binding domains of CD4 are distinct and separable. *Science* **245**, 743-745 (1989).

15. Ashkenazi., A., Presta, L., Marsters, S., Camerato, T., Rosenthal, K., Fendly, B., and Capon, D. Mapping the CD4 binding site for human immunodefficiency virus type 1 by alanine-scanning mutagenesis. *Proc. Natl. Acad. Sci. USA.* **87**, 7150-7154 (1990).

16. Chamow, S., Peers, D., Byrn, R., Mulkerrin, M., Harris, R., Wang, W., Bjorkman, P., Capon, D., and Ashkenazi, A. Enzymatic cleavage of a CD4 immunoadhesin generates crystallizable, biologically active Fd-like fragments. *Biochemistry* **29**, 9885-9891 (1990).

17. Ashkenazi, A., Smith, D., Marsters, S., Riddle, L., Gregory, T., Ho, D., and Capon, D. Resistance of primary isolates of human immunodefficiency virus type 1 to soluble CD4 is independent of CD4-rgp120 binding affinity. *Proc. Natl. Acad. Sci. USA.* **88**, 7056-7060 (1991).

18. Ashkenazi, A., Marsters, S., Capon, D., Chamow, S., Figari., I., Pennica, D., Goeddel., D., Palladino, M., and Smith, D. Protection against endotoxic shock by a tumor necrosis factor receptor immunoadhesin. *Proc. Natl. Acad. Sci. USA.* **88**, 10535-10539 (1991).

19. Moore, J., McKeating, J., Huang, Y., Ashkenazi, A., and Ho, D. Virions of primary HIV-1 isolates resistant to sCD4 neutralization differ in sCD4 affinity and glycoprotein gp120 retention from sCD4-sensitive isolates. *J. Virol.* **66**, 235-243 (1992).

20. Jin, H., Oksenberg, D., Ashkenazi, A., Peroutka, S., Duncan, A., Rozmahel., R., Yang, Y., Mengod, G., Palacios, J., and O'Dowd, B. Characterization of the human 5-hydroxytryptamine$_{1B}$ receptor. *J. Biol. Chem.* **267**, 5735-5738 (1992).

21. Marsters, A., Frutkin, A., Simpson, N., Fendly, B. and Ashkenazi, A. Identification of cysteine-rich domains of the type 1 tumor necrosis receptor involved in ligand binding. *J. Biol. Chem.* **267**, 5747-5750 (1992).

22. Chamow, S., Kogan, T., Peers, D., Hastings, R., Byrn, R., and Ashkenazi, A. Conjugation of sCD4 without loss of biological activity via a novel carbohydrate-directed cross-linking reagent. *J. Biol. Chem.* **267**, 15916-15922 (1992).

23. Oksenberg, D., Marsters, A., O'Dowd, B., Jin, H., Havlik, S., Peroutka, S., and Ashkenazi, A. A single amino-acid difference confers major pharmacologic variation between human and rodent 5-HT$_{1B}$ receptors. *Nature* **360**, 161-163 (1992).

24. Haak-Frendscho, M., Marsters, S., Chamow, S., Peers, D., Simpson, N., and Ashkenazi, A. Inhibition of interferon γ by an interferon γ receptor immunoadhesin. *Immunology* **79**, 594-599 (1993).

25. Penica, D., Lam, V., Weber, R., Kohr, W., Basa, L., Spellman, M., Ashkenazi, Shire, S., and Goeddel, D. Biochemical characterization of the extracellular domain of the 75-kd tumor necrosis factor receptor. *Biochemistry* **32**, 3131-3138. (1993).

26. Barfod, L., Zheng, Y., Kuang, W., Hart, M., Evans, T., Cerione, R., and Ashkenazi, A. Cloning and expression of a human CDC42 GTPase Activating Protein reveals a functional SH3-binding domain. *J. Biol. Chem.* **268**, 26059-26062 (1993).

27. Chamow, S., Zhang, D., Tan, X., Mhtre, S., Marsters, S., Peers, D., Byrn, R., Ashkenazi, A., and Yunghans, R. A humanized bispecific immunoadhesin-antibody that retargets CD3+ effectors to kill HIV-1-infected cells. *J. Immunol.* **153**, 4268-4280 (1994).

28. Means, R., Krantz, S., Luna, J., Marsters, S., and Ashkenazi, A. Inhibition of murine erythroid colony formation in vitro by iterferon γ and correction by interferon γ receptor immunoadhesin. *Blood* **83**, 911-915 (1994).

29. Haak-Frendscho, M., Marsters, S., Mordenti, J., Gillet, N., Chen, S., andAshkenazi, A. Inhibition of TNF by a TNF receptor immunoadhesin: comparison with an anti-TNF mAb. *J. Immunol.* **152**, 1347-1353 (1994).

30. Chamow, S., Kogan, T., Venuti, M., Gadek, T., Peers, D., Mordenti, J., Shak, S., and Ashkenazi, A. Modification of CD4 immunoadhesin with monomethoxy-PEG aldehyde via reductive alkilation. *Bioconj. Chem.* 5, 133-140 (1994).

31. Jin, H., Yang, R., Marsters, S., Bunting, S., Wurm, F., Chamow, S., and Ashkenazi, A. Protection against rat endotoxic shock by p55 tumor necrosis factor (TNF) receptor immunoadhesin: comparison to anti-TNF monoclonal antibody. *J. Infect. Diseases* 170, 1323-1326 (1994).

32. Beck, J., Marsters, S., Harris, R., Ashkenazi, A., and Chamow, S. Generation of soluble interleukin-1 receptor from an immunoadhesin by specific cleavage. *Mol. Immunol.* 31, 1335-1344 (1994).

33. Pitti, B., Marsters, M., Haak-Frendscho, M., Osaka, G., Mordenti, J., Chamow, S., and Ashkenazi, A. Molecular and biological properties of an interleukin-1 receptor immunoadhesin. *Mol. Immunol.* 31, 1345-1351 (1994).

34. Oksenberg, D., Havlik, S., Peroutka, S., and Ashkenazi, A. The third intracellular loop of the 5-HT2 receptor specifies effector coupling. *J. Neurochem.* 64, 1440-1447 (1995).

35. Bach, E., Szabo, S., Dighe, A., Ashkenazi, A., Aguet, M., Murphy, K., and Schreiber, R. Ligand-induced autoregulation of IFN-γ receptor β chain expression in T helper cell subsets. *Science* 270, 1215-1218 (1995).

36. Jin, H., Yang, R., Marsters, S., Ashkenazi, A., Bunting, S., Marra, M., Scott, R., and Baker, J. Protection against endotoxic shock by bactericidal/permeability-increasing protein in rats. *J. Clin. Invest.* 95, 1947-1952 (1995).

37. Marsters, S., Penica, D., Bach, E., Schreiber, R., and Ashkenazi, A. Interferon γ signals via a high-affinity multisubunit receptor complex that contains two types of polypeptide chain. *Proc. Natl. Acad. Sci. USA.* 92, 5401-5405 (1995).

38. Van Zee, K., Moldawer, L., Oldenburg, H., Thompson, W., Stackpole, S., Montegut, W., Rogy, M., Meschter, C., Gallati, H., Schiller, C., Richter, W., Loetcher, H., Ashkenazi, A., Chamow, S., Wurm, F., Calvano, S., Lowry, S., and Lesslauer, W. Protection against lethal E. coli bacteremia in baboons by pretreatment with a 55-kDa TNF receptor-Ig fusion protein, Ro45-2081. *J. Immunol.* 156, 2221-2230 (1996).

39. Pitti, R., Marsters, S., Ruppert, S., Donahue, C., Moore, A., and Ashkenazi, A. Induction of apoptosis by Apo-2 Ligand, a new member of the tumor necrosis factor cytokine family. *J. Biol. Chem.* 271, 12687-12690 (1996).

40. Marsters, S., Pitti, R., Donahue, C., Rupert, S., Bauer, K., and Ashkenazi, A. Activation of apoptosis by Apo-2 ligand is independent of FADD but blocked by CrmA. *Curr. Biol.* **6**, 1669-1676 (1996).

41. Marsters, S., Skubatch, M., Gray, C., and Ashkenazi, A. Herpesvirus entry mediator, a novel member of the tumor necrosis factor receptor family, activates the NF-κB and AP-1 transcription factors. *J. Biol. Chem.* **272**, 14029-14032 (1997).

42. Sheridan, J., Marsters, S., Pitti, R., Gurney, A., Skubatch, M., Baldwin, D., Ramakrishnan, L., Gray, C., Baker, K., Wood, W.I., Goddard, A., Godowski, P., and Ashkenazi, A. Control of TRAIL-induced apoptosis by a family of signaling and decoy receptors. *Science* **277**, 818-821 (1997).

43. Marsters, S., Sheridan, J., Pitti, R., Gurney, A., Skubatch, M., Balswin, D., Huang, A., Yuan, J., Goddard, A., Godowski, P., and Ashkenazi, A. A novel receptor for Apo2L/TRAIL contains a truncated death domain. *Curr. Biol.* **7**, 1003-1006 (1997).

44. Marsters, A., Sheridan, J., Pitti, R., Brush, J., Goddard, A., and Ashkenazi, A. Identification of a ligand for the death-domain-containing receptor Apo3. *Curr. Biol.* **8**, 525-528 (1998).

45. Rieger, J., Naumann, U., Glaser, T., Ashkenazi, A., and Weller, M. Apo2 ligand: a novel weapon against malignant glioma? *FEBS Lett.* **427**, 124-128 (1998).

46. Pender, S., Fell, J., Chamow, S., Ashkenazi, A., and MacDonald, T. A p55 TNF receptor immunoadhesin prevents T cell mediated intestinal injury by inhibiting matrix metalloproteinase production. *J. Immunol.* **160**, 4098-4103 (1998).

47. Pitti, R., Marsters, S., Lawrence, D., Roy, Kischkel, F., M., Dowd, P., Huang, A., Donahue, C., Sherwood, S., Baldwin, D., Godowski, P., Wood, W., Gurney, A., Hillan, K., Cohen, R., Goddard, A., Botstein, D., and Ashkenazi, A. Genomic amplification of a decoy receptor for Fas ligand in lung and colon cancer. *Nature* **396**, 699-703 (1998).

48. Mori, S., Marakami-Mori, K., Nakamura, S., Ashkenazi, A., and Bonavida, B. Sensitization of AIDS Kaposi's sarcoma cells to Apo-2 ligand-induced apoptosis by actinomycin D. *J. Immunol.* **162**, 5616-5623 (1999).

49. Gurney, A. Marsters, S., Huang, A., Pitti, R., Mark, M., Baldwin, D., Gray, A., Dowd, P., Brush, J., Heldens, S., Schow, P., Goddard, A., Wood, W., Baker, K., Godowski, P., and Ashkenazi, A. Identification of a new member of the tumor necrosis factor family and its receptor, a human ortholog of mouse GITR. *Curr. Biol.* 9, 215-218 (1999).

50. Ashkenazi, A., Pai, R., Fong, s., Leung, S., Lawrence, D., Marsters, S., Blackie, C., Chang, L., McMurtrey, A., Hebert, A., DeForge, L., Khoumenis, I., Lewis, D., Harris, L., Bussiere, J., Koeppen, H., Shahrokh, Z., and Schwall, R. Safety and anti-tumor activity of recombinant soluble Apo2 ligand. *J. Clin. Invest.* **104**, 155-162 (1999).

51. Chuntharapai, A., Gibbs, V., Lu, J., Ow, A., Marsters, S., Ashkenazi, A., De Vos, A., Kim, K.J. Determination of residues involved in ligand binding and signal transmissiion in the human IFN-α receptor 2. *J. Immunol.* **163**, 766-773 (1999).

52. Johnsen, A.-C., Haux, J., Steinkjer, B., Nonstad, U., Egeberg, K., Sundan, A., Ashkenazi, A., and Espevik, T. Regulation of Apo2L/TRAIL expression in NK cells – involvement in NK cell-mediated cytotoxicity. *Cytokine* **11**, 664-672 (1999).

53. Roth, W., Isenmann, S., Naumann, U., Kugler, S., Bahr, M., Dichgans, J., Ashkenazi, A., and Weller, M. Eradication of intracranial human malignant glioma xenografts by Apo2L/TRAIL. *Biochem. Biophys. Res. Commun.* **265**, 479-483 (1999).

54. Hymowitz, S.G., Christinger, H.W., Fuh, G., Ultsch, M., O'Connell, M., Kelley, R.F., Ashkenazi, A. and de Vos, A.M. Triggering Cell Death: The Crystal Structure of Apo2L/TRAIL in a Complex with Death Receptor 5. *Molec. Cell* **4**, 563–571 (1999).

55. Hymowitz, S.G., O'Connel, M.P., Utsch, M.H., Hurst, A., Totpal, K., Ashkenazi, A., de Vos, A.M., Kelley, R.F. A unique zinc-binding site revealed by a high-resolution X-ray structure of homotrimeric Apo2L/TRAIL. *Biochemistry* **39**, 633-640 (2000).

56. Zhou, Q., Fukushima, P., DeGraff, W., Mitchell, J.B., Stetler-Stevenson, M., Ashkenazi, A., and Steeg, P.S. Radiation and the Apo2L/TRAIL apoptotic pathway preferentially inhibit the colonization of premalignant human breast cancer cells overexpressing cyclin D1. *Cancer Res.* **60**, 2611-2615 (2000).

57. Kischkel, F.C., Lawrence, D. A., Chuntharapai, A., Schow, P., Kim, J., and Ashkenazi, A. Apo2L/TRAIL-dependent recruitment of endogenous FADD and Caspase-8 to death receptors 4 and 5. *Immunity* **12**, 611-620 (2000).

58. Yan, M., Marsters, S.A., Grewal, I.S., Wang, H., *Ashkenazi, A., and *Dixit, V.M. Identification of a receptor for BlyS demonstrates a crucial role in humoral immunity. *Nature Immunol.* **1**, 37-41 (2000).

59. Marsters, S.A., Yan, M., Pitti, R.M., Haas, P.E., Dixit, V.M., and Ashkenazi, A. Interaction of the TNF homologues BLyS and APRIL with the TNF receptor homologues BCMA and TACI. *Curr. Biol.* **10**, 785-788 (2000).

60. Kischkel, F.C., and Ashkenazi, A. Combining enhanced metabolic labeling with immunoblotting to detect interactions of endogenous cellular proteins. *Biotechniques* **29**, 506-512 (2000).

61. Lawrence, D., Shahrokh, Z., Marsters, S., Achilles, K., Shih, D. Mounho, B., Hillan, K., Totpal, K. DeForge, L., Schow, P., Hooley, J., Sherwood, S., Pai, R., Leung, S., Khan, L., Gliniak, B., Bussiere, J., Smith, C., Strom, S., Kelley, S., Fox, J., Thomas, D., and Ashkenazi, A. Differential hepatocyte toxicity of recombinant Apo2L/TRAIL versions. *Nature Med.* **7**, 383-385 (2001).

62. Chuntharapai, A., Dodge, K., Grimmer, K., Schroeder, K., Martsters, S.A., Koeppen, H., Ashkenazi, A., and Kim, K.J. Isotype-dependent inhibition of tumor growth in vivo by monoclonal antibodies to death receptor 4. *J. Immunol.* **166**, 4891-4898 (2001).

63. Pollack, I.F., Erff, M., and Ashkenazi, A. Direct stimulation of apoptotic signaling by soluble Apo2L/tumor necrosis factor-related apoptosis-inducing ligand leads to selective killing of glioma cells. *Clin. Cancer Res.* **7**, 1362-1369 (2001).

64. Wang, H., Marsters, S.A., Baker, T., Chan, B., Lee, W.P., Fu, L., Tumas, D., Yan, M., Dixit, V.M., *Ashkenazi, A., and *Grewal, I.S. TACI-ligand interactions are required for T cell activation and collagen-induced arthritis in mice. *Nature Immunol.* 2, 632-637 (2001).

65. Kischkel, F.C., Lawrence, D. A., Tinel, A., Virmani, A., Schow, P., Gazdar, A., Blenis, J., Arnott, D., and Ashkenazi, A. Death receptor recruitment of endogenous caspase-10 and apoptosis initiation in the absence of caspase-8. *J. Biol. Chem.* 276, 46639-46646 (2001).

66. LeBlanc, H., Lawrence, D.A., Varfolomeev, E., Totpal, K., Morlan, J., Schow, P., Fong, S., Schwall, R., Sinicropi, D., and Ashkenazi, A Tumor cell resistance to death receptor induced apoptosis through mutational inactivation of the proapoptotitc Bcl-2 homolog Bax. *Nature Med.* 8, 274-281 (2002).

67. Miller, K., Meng, G., Liu, J., Hurst, A., Hsei, V., Wong, W-L., Ekert, R., Lawrence, D., Sherwood, S., DeForge, L., Gaudreault., Keller, G., Sliwkowski, M., Ashkenazi, A., and Presta, L. Design, Construction, and analyses of multivalent antibodies. *J. Immunol.* 170, 4854-4861 (2003).

68. Varfolomeev, E., Kischkel, F., Martin, F., Wanh, H., Lawrence, D., Olsson, C., Tom, L., Erickson, S., French, D., Schow, P., Grewal, I. and Ashkenazi, A. Immune system development in APRIL knockout mice. Submitted.

Review articles:

1. Ashkenazi, A., Peralta, E., Winslow, J., Ramachandran, J., and Capon, D., J. Functional role of muscarinic acetylcholine receptor subtype diversity. *Cold Spring Harbor Symposium on Quantitative Biology*. LIII, 263-272 (1988).
2. Ashkenazi, A., Peralta, E., Winslow, J., Ramachandran, J., and Capon, D. Functional diversity of muscarinic receptor subtypes in cellular signal transduction and growth. *Trends Pharmacol. Sci.* Dec Supplement, 12-21 (1989).
3. Chamow, S., Duliege, A., Ammann, A., Kahn, J., Allen, D., Eichberg, J., Byrn, R., Capon, D., Ward, R., and Ashkenazi, A. CD4 immunoadhesins in anti-HIV therapy: new developments. *Int. J. Cancer* Supplement 7, 69-72 (1992).
4. Ashkenazi, A., Capon, and D. Ward, R. Immunoadhesins. *Int. Rev. Immunol.* **10**, 217-225 (1993).
5. Ashkenazi, A., and Peralta, E. Muscarinic Receptors. In *Handbook of Receptors and Channels*. (S. Peroutka, ed.), CRC Press, Boca Raton, Vol. I, p. 1-27, (1994).
6. Krantz, S. B., Means, R. T., Jr., Lina, J., Marsters, S. A., and Ashkenazi, A. Inhibition of erythroid colony formation in vitro by gamma interferon. In *Molecular Biology of Hematopoiesis* (N. Abraham, R. Shadduck, A. Levine F. Takaku, eds.) Intercept Ltd. Paris, Vol. 3, p. 135-147 (1994).
7. Ashkenazi, A. Cytokine neutralization as a potential therapeutic approach for SIRS and shock. *J. Biotechnology in Healthcare* **1**, 197-206 (1994).
8. Ashkenazi, A., and Chamow, S. M. Immunoadhesins: an alternative to human monoclonal antibodies. *Immunomethods: A companion to Methods in Enzimology* **8**, 104-115 (1995).
9. Chamow, S., and Ashkenazi, A. Immunoadhesins: Principles and Applications. *Trends Biotech.* **14**, 52-60 (1996).
10. Ashkenazi, A., and Chamow, S. M. Immunoadhesins as research tools and therapeutic agents. *Curr. Opin. Immunol.* 9, 195-200 (1997).
11. Ashkenazi, A., and Dixit, V. Death receptors: signaling and modulation. *Science* 281, 1305-1308 (1998).
12. Ashkenazi, A., and Dixit, V. Apoptosis control by death and decoy receptors. *Curr. Opin. Cell. Biol.* 11, 255-260 (1999).

13. Ashkenazi, A. Chapters on Apo2L/TRAIL; DR4, DR5, DcR1, DcR2; and DcR3. Online Cytokine Handbook (www.apnet.com/cytokinereference/).
14. Ashkenazi, A. Targeting death and decoy receptors of the tumor necrosis factor superfamily. *Nature Rev. Cancer* 2, 420-430 (2002).
15. LeBlanc, H. and Ashkenazi, A. Apoptosis signaling by Apo2L/TRAIL. *Cell Death and Differentiation* 10, 66-75 (2003).
16. Almasan, A. and Ashkenazi, A. Apo2L/TRAIL: apoptosis signaling, biology, and potential for cancer therapy. Cytokine and Growth Factor Reviews 14, 337-348 (2003).

Book:

Antibody Fusion Proteins (Chamow, S., and Ashkenazi, A., eds., John Wiley and Sons Inc.) (1999).

Talks:

1. Resistance of primary HIV isolates to CD4 is independent of CD4-gp120 binding affinity. UCSD Symposium, HIV Disease: Pathogenesis and Therapy. Greenelefe, FL, March 1991.
2. Use of immuno-hybrids to extend the half-life of receptors. IBC conference on Biopharmaceutical Halflife Extension. New Orleans, LA, June 1992.
3. Results with TNF receptor Immunoadhesins for the Treatment of Sepsis. IBC conference on Endotoxemia and Sepsis. Philadelphia, PA, June 1992.
4. Immunoadhesins: an alternative to human antibodies. IBC conference on Antibody Engineering. San Diego, CA, December 1993.
5. Tumor necrosis factor receptor: a potential therapeutic for human septic shock. American Society for Microbiology Meeting, Atlanta, GA, May 1993.
6. Protective efficiacy of TNF receptor immunoadhesin vs anti-TNF monoclonal antibody in a rat model for endotoxic shock. 5th International Congress on TNF. Asilomar, CA, May 1994.
7. Interferon-γ signals via a multisubunit receptor complex that contains two types of polypeptide chain. American Association of Immunologists Conference. San Franciso, CA, July 1995.
8. Immunoadhesins: Principles and Applications. Gordon Research Conference on Drug Delivery in Biology and Medicine. Ventura, CA, February 1996.

9. Apo-2 Ligand, a new member of the TNF family that induces apoptosis in tumor cells. Cambridge Symposium on TNF and Related Cytokines in Treatment of Cancer. Hilton-Head, NC, March 1996.
10. Induction of apoptosis by Apo2 Ligand. American Society for Biochemistry and Molecular Biology, Symposium on Growth Factors and Cytokine Receptors. New Orleans, LA, June, 1996.
11. Apo2 ligand, an extracellular trigger of apoptosis. 2nd Clontech Symposium, Palo Alto, CA, October 1996.
12. Regulation of apoptosis by members of the TNF ligand and receptor families. Stanford University School of Medicine, Palo Alto, CA, December 1996.
13. Apo-3: anovel receptor that regulates cell death and inflammation. 4th International Congress on Immune Consequences of Trauma, Shock, and Sepsis. Munich, Germany, March 1997.
14. New members of the TNF ligand and receptor families that regulate apoptosis, inflammation, and immunity. UCLA School of Medicine, LA, CA, March 1997.
15. Immunoadhesins: an alternative to monoclonal antibodies. 5th World Conference on Bispecific Antibodies. Volendam, Holland, June 1997.
16. Control of Apo2L signaling. Cold Spring Harbor Laboratory Symposium on Programmed Cell Death. Cold Spring Harbor, New York. September, 1997.
17. Chairman and speaker, Apoptosis Signaling session. IBC's 4th Annual Conference on Apoptosis. San Diego, CA., October 1997.
18. Control of Apo2L signaling by death and decoy receptors. American Association for the Advancement of Science. Philladelphia, PA, February 1998.
19. Apo2 ligand and its receptors. American Society of Immunologists. San Francisco, CA, April 1998.
20. Death receptors and ligands. 7th International TNF Congress. Cape Cod, MA, May 1998.
21. Apo2L as a potential therapeutic for cancer. UCLA School of Medicine. LA, CA, June 1998.
22. Apo2L as a potential therapeutic for cancer. Gordon Research Conference on Cancer Chemotherapy. New London, NH, July 1998.
23. Control of apoptosis by Apo2L. Endocrine Society Conference, Stevenson, WA, August 1998.
24. Control of apoptosis by Apo2L. International Cytokine Society Conference, Jerusalem, Israel, October 1998.

25. Apoptosis control by death and decoy receptors. American Association for Cancer Research Conference, Whistler, BC, Canada, March 1999.
26. Apoptosis control by death and decoy receptors. American Society for Biochemistry and Molecular Biology Conference, San Francisco, CA, May 1999.
27. Apoptosis control by death and decoy receptors. Gordon Research Conference on Apoptosis, New London, NH, June 1999.
28. Apoptosis control by death and decoy receptors. Arthritis Foundation Research Conference, Alexandria GA, Aug 1999.
29. Safety and anti-tumor activity of recombinant soluble Apo2L/TRAIL. Cold Spring Harbor Laboratory Symposium on Programmed Cell Death. . Cold Spring Harbor, NY, September 1999.
30. The Apo2L/TRAIL system: therapeutic potential. American Association for Cancer Research, Lake Tahoe, NV, Feb 2000.
31. Apoptosis and cancer therapy. Stanford University School of Medicine, Stanford, CA, Mar 2000.
32. Apoptosis and cancer therapy. University of Pennsylvania School of Medicine, Philladelphia, PA, Apr 2000.
33. Apoptosis signaling by Apo2L/TRAIL. International Congress on TNF. Trondheim, Norway, May 2000.
34. The Apo2L/TRAIL system: therapeutic potential. Cap-CURE summit meeting. Santa Monica, CA, June 2000.
35. The Apo2L/TRAIL system: therapeutic potential. MD Anderson Cancer Center. Houston, TX, June 2000.
36. Apoptosis signaling by Apo2L/TRAIL. The Protein Society, 14th Symposium. San Diego, CA, August 2000.
37. Anti-tumor activity of Apo2L/TRAIL. AAPS annual meeting. Indianapolis, IN Aug 2000.
38. Apoptosis signaling and anti-cancer potential of Apo2L/TRAIL. Cancer Research Institute, UC San Francisco, CA, September 2000.
39. Apoptosis signaling by Apo2L/TRAIL. Kenote address, TNF family Minisymposium, NIH. Bethesda, MD, September 2000.
40. Death receptors: signaling and modulation. Keystone symposium on the Molecular basis of cancer. Taos, NM, Jan 2001.
41. Preclinical studies of Apo2L/TRAIL in cancer. Symposium on Targeted therapies in the treatment of lung cancer. Aspen, CO, Jan 2001.

42. Apoptosis signaling by Apo2L/TRAIL. Wiezmann Institute of Science, Rehovot, Israel, March 2001.
43. Apo2L/TRAIL: Apoptosis signaling and potential for cancer therapy. Weizmann Institute of Science, Rehovot, Israel, March 2001.
44. Targeting death receptors in cancer with Apo2L/TRAIL. Cell Death and Disease conference, North Falmouth, MA, Jun 2001.
45. Targeting death receptors in cancer with Apo2L/TRAIL. Biotechnology Organization conference, San Diego, CA, Jun 2001.
46. Apo2L/TRAIL signaling and apoptosis resistance mechanisms. Gordon Research Conference on Apoptosis, Oxford, UK, July 2001.
47. Apo2L/TRAIL signaling and apoptosis resistance mechanisms. Cleveland Clinic Foundation, Cleveland, OH, Oct 2001.
48. Apoptosis signaling by death receptors: overview. International Society for Interferon and Cytokine Research conference, Cleveland, OH, Oct 2001.
49. Apoptosis signaling by death receptors. American Society of Nephrology Conference. San Francisco, CA, Oct 2001.
50. Targeting death receptors in cancer. Apoptosis: commercial opportunities. San Diego, CA, Apr 2002.
51. Apo2L/TRAIL signaling and apoptosis resistance mechanisms. Kimmel Cancer Research Center, Johns Hopkins University, Baltimore MD. May 2002.
52. Apoptosis control by Apo2L/TRAIL. (Keynote Address) University of Alabama Cancer Center Retreat, Birmingham, Ab. October 2002.
53. Apoptosis signaling by Apo2L/TRAIL. (Session co-chair) TNF international conference. San Diego, CA. October 2002.
54. Apoptosis signaling by Apo2L/TRAIL. Swiss Institute for Cancer Research (ISREC). Lausanne, Swizerland. Jan 2003.
55. Apoptosis induction with Apo2L/TRAIL. Conference on New Targets and Innovative Strategies in Cancer Treatment. Monte Carlo. February 2003.
56. Apoptosis signaling by Apo2L/TRAIL. Hermelin Brain Tumor Center Symposium on Apoptosis. Detroit, MI. April 2003.
57. Targeting apoptosis through death receptors. Sixth Annual Conference on Targeted Therapies in the Treatment of Breast Cancer. Kona, Hawaii. July 2003.
58. Targeting apoptosis through death receptors. Second International Conference on Targeted Cancer Therapy. Washington, DC. Aug 2003.

Issued Patents:

1. Ashkenazi, A., Chamow, S. and Kogan, T. Carbohydrate-directed crosslinking reagents. US patent 5,329,028 (Jul 12, 1994).
2. Ashkenazi, A., Chamow, S. and Kogan, T. Carbohydrate-directed crosslinking reagents. US patent 5,605,791 (Feb 25, 1997).
3. Ashkenazi, A., Chamow, S. and Kogan, T. Carbohydrate-directed crosslinking reagents. US patent 5,889,155 (Jul 27, 1999).
4. Ashkenazi, A., APO-2 Ligand. US patent 6,030,945 (Feb 29, 2000).
5. Ashkenazi, A., Chuntharapai, A., Kim, J., APO-2 ligand antibodies. US patent 6, 046, 048 (Apr 4, 2000).
6. Ashkenazi, A., Chamow, S. and Kogan, T. Carbohydrate-directed crosslinking reagents. US patent 6,124,435 (Sep 26, 2000).
7. Ashkenazi, A., Chuntharapai, A., Kim, J., Method for making monoclonal and cross-reactive antibodies. US patent 6,252,050 (Jun 26, 2001).
8. Ashkenazi, A. APO-2 Receptor. US patent 6,342,369 (Jan 29, 2002).
9. Ashkenazi, A. Fong, S., Goddard, A., Gurney, A., Napier, M., Tumas, D., Wood, W. A-33 polypeptides. US patent 6,410,708 (Jun 25, 2002).
10. Ashkenazi, A. APO-3 Receptor. US patent 6,462,176 B1 (Oct 8, 2002).
11. Ashkenazi, A. APO-2LI and APO-3 polypeptide antibodies. US patent 6,469,144 B1 (Oct 22, 2002).
12. Ashkenazi, A., Chamow, S. and Kogan, T. Carbohydrate-directed crosslinking reagents. US patent 6,582,928B1 (Jun 24, 2003).

DECLARATION OF PAUL POLAKIS, Ph.D.

I, Paul Polakis, Ph.D., declare and say as follows:

1. I was awarded a Ph.D. by the Department of Biochemistry of the Michigan State University in 1984. My scientific Curriculum Vitae is attached to and forms part of this Declaration (Exhibit A).

2. I am currently employed by Genentech, Inc. where my job title is Staff Scientist. Since joining Genentech in 1999, one of my primary responsibilities has been leading Genentech's Tumor Antigen Project, which is a large research project with a primary focus on identifying tumor cell markers that find use as targets for both the diagnosis and treatment of cancer in humans.

3. As part of the Tumor Antigen Project, my laboratory has been analyzing differential expression of various genes in tumor cells relative to normal cells. The purpose of this research is to identify proteins that are abundantly expressed on certain tumor cells and that are either (i) not expressed, or (ii) expressed at lower levels, on corresponding normal cells. We call such differentially expressed proteins "tumor antigen proteins". When such a tumor antigen protein is identified, one can produce an antibody that recognizes and binds to that protein. Such an antibody finds use in the diagnosis of human cancer and may ultimately serve as an effective therapeutic in the treatment of human cancer.

4. In the course of the research conducted by Genentech's Tumor Antigen Project, we have employed a variety of scientific techniques for detecting and studying differential gene expression in human tumor cells relative to normal cells, at genomic DNA, mRNA and protein levels. An important example of one such technique is the well known and widely used technique of microarray analysis which has proven to be extremely useful for the identification of mRNA molecules that are differentially expressed in one tissue or cell type relative to another. In the course of our research using microarray analysis, we have identified approximately 200 gene transcripts that are present in human tumor cells at significantly higher levels than in corresponding normal human cells. To date, we have generated antibodies that bind to about 30 of the tumor antigen proteins expressed from these differentially expressed gene transcripts and have used these antibodies to quantitatively determine the level of production of these tumor antigen proteins in both human cancer cells and corresponding normal cells. We have then compared the levels of mRNA and protein in both the tumor and normal cells analyzed.

5. From the mRNA and protein expression analyses described in paragraph 4 above, we have observed that there is a strong correlation between changes in the level of mRNA present in any particular cell type and the level of protein

expressed from that mRNA in that cell type. In approximately 80% of our observations we have found that increases in the level of a particular mRNA correlates with changes in the level of protein expressed from that mRNA when human tumor cells are compared with their corresponding normal cells.

6. Based upon my own experience accumulated in more than 20 years of research, including the data discussed in paragraphs 4 and 5 above and my knowledge of the relevant scientific literature, it is my considered scientific opinion that for human genes, an increased level of mRNA in a tumor cell relative to a normal cell typically correlates to a similar increase in abundance of the encoded protein in the tumor cell relative to the normal cell. In fact, it remains a central dogma in molecular biology that increased mRNA levels are predictive of corresponding increased levels of the encoded protein. While there have been published reports of genes for which such a correlation does not exist, it is my opinion that such reports are exceptions to the commonly understood general rule that increased mRNA levels are predictive of corresponding increased levels of the encoded protein.

7. I hereby declare that all statements made herein of my own knowledge are true and that all statements made on information or belief are believed to be true, and further that these statements were made with the knowledge that willful false statements and the like so made are punishable by fine or imprisonment, or both, under Section 1001 of Title 18 of the United States Code and that such willful statements may jeopardize the validity of the application or any patent issued thereon.

Dated: 5/07/04

By: Paul Polakis

Paul Polakis, Ph.D.

SV 2031808 v1

[CANCER RESEARCH 62, 6240–6245, November 1, 2002]

Impact of DNA Amplification on Gene Expression Patterns in Breast Cancer[1,2]

Elizabeth Hyman,[3] Päivikki Kauraniemi,[3] Sampsa Hautaniemi, Maija Wolf, Spyro Mousses, Ester Rozenblum, Markus Ringnér, Guido Sauter, Outi Monni, Abdel Elkahloun, Olli-P. Kallioniemi, and Anne Kallioniemi[4]

Howard Hughes Medical Institute-NIH Research Scholar, Bethesda, Maryland 20892 [E. H.]; Cancer Genetics Branch, National Human Genome Research Institute, NIH, Bethesda, Maryland 20892 [E. H., P. K., S. H., M. W., S. M., E. R., M. R., A. E., O. K., A. K.]; Laboratory of Cancer Genetics, Institute of Medical Technology, University of Tampere and Tampere University Hospital, FIN-33520 Tampere, Finland [P. K., A. K.]; Signal Processing Laboratory, Tampere University of Technology, FIN-33101 Tampere, Finland [S. H.]; Institute of Pathology, University of Basel, CH-4003 Basel, Switzerland [G. S.]; and Biomedicum Biochip Center, Helsinki University Hospital, Biomedicum Helsinki, FIN-00014 Helsinki, Finland [O. M.]

ABSTRACT

Genetic changes underlie tumor progression and may lead to cancer-specific expression of critical genes. Over 1100 publications have described the use of comparative genomic hybridization (CGH) to analyze the pattern of copy number alterations in cancer, but very few of the genes affected are known. Here, we performed high-resolution CGH analysis on cDNA microarrays in breast cancer and directly compared copy number and mRNA expression levels of 13,824 genes to quantitate the impact of genomic changes on gene expression. We identified and mapped the boundaries of 24 independent amplicons, ranging in size from 0.2 to 12 Mb. Throughout the genome, both high- and low-level copy number changes had a substantial impact on gene expression, with 44% of the highly amplified genes showing overexpression and 10.5% of the highly overexpressed genes being amplified. Statistical analysis with random permutation tests identified 270 genes whose expression levels across 14 samples were systematically attributable to gene amplification. These included most previously described amplified genes in breast cancer and many novel targets for genomic alterations, including the *HOXB7* gene, the presence of which in a novel amplicon at 17q21.3 was validated in 10.2% of primary breast cancers and associated with poor patient prognosis. In conclusion, CGH on cDNA microarrays revealed hundreds of novel genes whose overexpression is attributable to gene amplification. These genes may provide insights to the clonal evolution and progression of breast cancer and highlight promising therapeutic targets.

INTRODUCTION

Gene expression patterns revealed by cDNA microarrays have facilitated classification of cancers into biologically distinct categories, some of which may explain the clinical behavior of the tumors (1–6). Despite this progress in diagnostic classification, the molecular mechanisms underlying gene expression patterns in cancer have remained elusive, and the utility of gene expression profiling in the identification of specific therapeutic targets remains limited.

Accumulation of genetic defects is thought to underlie the clonal evolution of cancer. Identification of the genes that mediate the effects of genetic changes may be important by highlighting transcripts that are actively involved in tumor progression. Such transcripts and their encoded proteins would be ideal targets for anticancer therapies, as demonstrated by the clinical success of new therapies against amplified oncogenes, such as *ERBB2* and *EGFR* (7, 8), in breast cancer and other solid tumors. Besides amplifications of known oncogenes, over 20 recurrent regions of DNA amplification have been mapped in breast cancer by CGH[5] (9, 10). However, these amplicons are often large and poorly defined, and their impact on gene expression remains unknown.

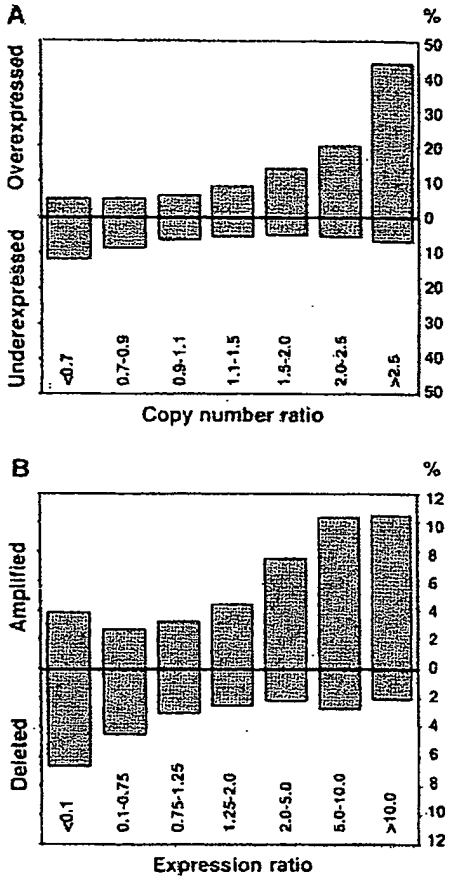

Fig. 1. Impact of gene copy number on global gene expression levels. *A*, percentage of over- and underexpressed genes (*Y axis*) according to copy number ratios (*X axis*). Threshold values used for over- and underexpression were >2.184 (global upper 7% of the cDNA ratios) and <0.4826 (global lower 7% of the expression ratios). *B*, percentage of amplified and deleted genes according to expression ratios. Threshold values for amplification and deletion were >1.5 and <0.7.

We hypothesized that genome-wide identification of those gene expression changes that are attributable to underlying gene copy number alterations would highlight transcripts that are actively involved in the causation or maintenance of the malignant phenotype. To identify such transcripts, we applied a combination of cDNA and CGH microarrays to: (*a*) determine the global impact that gene copy number variation plays in breast cancer development and progression; and (*b*) identify and characterize those genes whose mRNA expres-

Received 5/29/02; accepted 8/28/02.

The costs of publication of this article were defrayed in part by the payment of page charges. This article must therefore be hereby marked *advertisement* in accordance with 18 U.S.C. Section 1734 solely to indicate this fact.

[1] Supported in part by the Academy of Finland, Emil Aaltonen Foundation, the Finnish Cancer Society, the Pirkanmaa Cancer Society, the Pirkanmaa Cultural Foundation, the Finnish Breast Cancer Group, the Foundation for the Development of Laboratory Medicine, the Medical Research Fund of the Tampere University Hospital, the Foundation for Commercial and Technical Sciences, and the Swedish Research Council.

[2] Supplementary data for this article are available at Cancer Research Online (http://cancerres.aacrjournals.org).

[3] Contributed equally to this work.

[4] To whom requests for reprints should be addressed, at Laboratory of Cancer Genetics, Institute of Medical Technology, Lenkkeilijankatu 6, FIN-33520 Tampere, Finland. Phone: 358-3247-4125; Fax: 358-3247-4168; E-mail: anne.kallioniemi@uta.fi.

[5] The abbreviations used are: CGH, comparative genomic hybridization; FISH, fluorescence *in situ* hybridization; RT-PCR, reverse transcription-PCR.

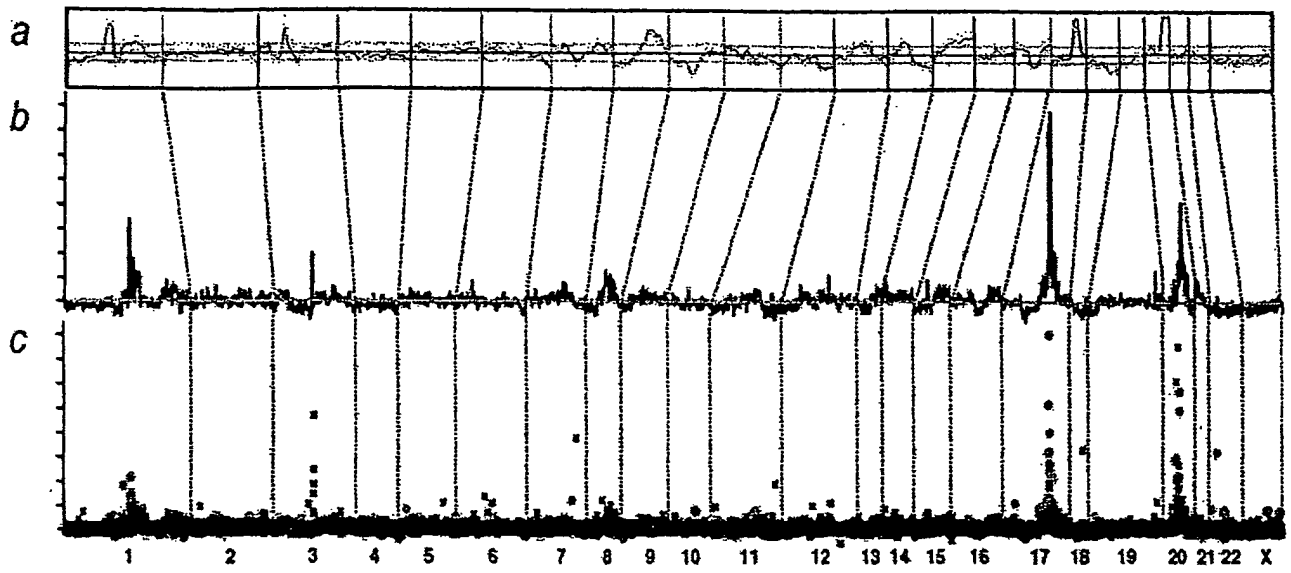

Fig. 2. Genome-wide copy number and expression analysis in the MCF-7 breast cancer cell line. *A*, chromosomal CGH analysis of MCF-7. The copy number ratio profile (*blue line*) across the entire genome from 1p telomere to Xq telomere is shown along with ±1 SD (*orange lines*). The *black horizontal line* indicates a ratio of 1.0; *red line*, a ratio of 0.8; and *green line*, a ratio of 1.2. *B–C*, genome-wide copy number analysis in MCF-7 by CGH on cDNA microarray. The copy number ratios were plotted as a function of the position of the cDNA clones along the human genome. In *B*, individual data points are connected with a line, and a moving median of 10 adjacent clones is shown. *Red horizontal line*, the copy number ratio of 1.0. In *C*, individual data points are labeled by color coding according to cDNA expression ratios. The *bright red dots* indicate the upper 2%, and *dark red dots*, the next 5% of the expression ratios in MCF-7 cells (overexpressed genes); *bright green dots* indicate the lowest 2%, and *dark green dots*, the next 5% of the expression ratios (underexpressed genes); the rest of the observations are shown with *black crosses*. The chromosome numbers are shown at the *bottom* of the figure, and chromosome boundaries are indicated with a *dashed line*.

sion is most significantly associated with amplification of the corresponding genomic template.

MATERIALS AND METHODS

Breast Cancer Cell Lines. Fourteen breast cancer cell lines (BT-20, BT-474, HCC1428, Hs578t, MCF7, MDA-361, MDA-436, MDA-453, MDA-468, SKBR-3, T-47D, UACC812, ZR-75-1, and ZR-75-30) were obtained from the American Type Culture Collection (Manassas, VA). Cells were grown under recommended culture conditions. Genomic DNA and mRNA were isolated using standard protocols.

Copy Number and Expression Analyses by cDNA Microarrays. The preparation and printing of the 13,824 cDNA clones on glass slides were performed as described (11–13). Of these clones, 244 represented uncharacterized expressed sequence tags, and the remainder corresponded to known genes. CGH experiments on cDNA microarrays were done as described (14, 15). Briefly, 20 μg of genomic DNA from breast cancer cell lines and normal human WBCs were digested for 14–18 h with *Alu*I and *Rsa*I (Life Technologies, Inc., Rockville, MD) and purified by phenol/chloroform extraction. Six μg of digested cell line DNAs were labeled with Cy3-dUTP (Amersham Pharmacia) and normal DNA with Cy5-dUTP (Amersham Pharmacia) using the Bioprime Labeling kit (Life Technologies, Inc.). Hybridization (14, 15) and posthybridization washes (13) were done as described. For the expression analyses, a standard reference (Universal Human Reference RNA; Stratagene, La Jolla, CA) was used in all experiments. Forty μg of reference RNA were labeled with Cy3-dUTP and 3.5 μg of test mRNA with Cy5-dUTP, and the labeled cDNAs were hybridized on microarrays as described (13, 15). For both microarray analyses, a laser confocal scanner (Agilent Technologies, Palo Alto, CA) was used to measure the fluorescence intensities at the target locations using the DEARRAY software (16). After background subtraction, average intensities at each clone in the test hybridization were divided by the average intensity of the corresponding clone in the control hybridization. For the copy number analysis, the ratios were normalized on the basis of the distribution of ratios of all targets on the array and for the expression analysis on the basis of 88 housekeeping genes, which were spotted four times onto the array. Low quality measurements (*i.e.*, copy number data with mean reference intensity <100 fluorescent units, and expression data with both test and reference intensity <100 fluorescent units and/or with spot size <50 units) were excluded from the analysis and were treated as missing values. The distributions of fluorescence ratios were used to define cutpoints for increased/decreased copy number. Genes with CGH ratio >1.43 (representing the upper 5% of the CGH ratios across all experiments) were considered to be amplified, and genes with ratio <0.73 (representing the lower 5%) were considered to be deleted.

Statistical Analysis of CGH and cDNA Microarray Data. To evaluate the influence of copy number alterations on gene expression, we applied the following statistical approach. CGH and cDNA calibrated intensity ratios were log-transformed and normalized using median centering of the values in each cell line. Furthermore, cDNA ratios for each gene across all 14 cell lines were median centered. For each gene, the CGH data were represented by a vector that was labeled 1 for amplification (ratio, >1.43) and 0 for no amplification. Amplification was correlated with gene expression using the signal-to-noise statistics (1). We calculated a weight, w_g, for each gene as follows:

$$w_g = \frac{m_{g1} - m_{g0}}{\sigma_{g1} + \sigma_{g0}}$$

where m_{g1}, σ_{g1} and m_{g0}, σ_{g0} denote the means and SDs for the expression levels for amplified and nonamplified cell lines, respectively. To assess the statistical significance of each weight, we performed 10,000 random permutations of the label vector. The probability that a gene had a larger or equal weight by random permutation than the original weight was denoted by α. A low α (<0.05) indicates a strong association between gene expression and amplification.

Genomic Localization of cDNA Clones and Amplicon Mapping. Each cDNA clone on the microarray was assigned to a Unigene cluster using the Unigene Build 141.[6] A database of genomic sequence alignment information for mRNA sequences was created from the August 2001 freeze of the University of California Santa Cruz's GoldenPath database.[7] The chromosome and bp positions for each cDNA clone were then retrieved by relating these data sets. Amplicons were defined as a CGH copy number ratio >2.0 in at least two adjacent clones in two or more cell lines or a CGH ratio >2.0 in at least three adjacent clones in a single cell line. The amplicon start and end positions were

[6] Internet address: http://research.nhgri.nih.gov/microarray/downloadable_cdna.html.
[7] Internet address: www.genome.ucsc.edu.

Table 1 *Summary of independent amplicons in 14 breast cancer cell lines by CGH microarray*

Location	Start (Mb)	End (Mb)	Size (Mb)
1p13	132.79	132.94	0.2
1q21	173.92	177.25	3.3
1q22	179.28	179.57	0.3
3p14	71.94	74.66	2.7
7p12.1–7p11.2	55.62	60.95	5.3
7q31	125.73	130.96	5.2
7q32	140.01	140.68	0.7
8q21.11–8q21.13	86.45	92.46	6.0
8q21.3	98.45	103.05	4.6
8q23.3–8q24.14	129.88	142.15	12.3
8q24.22	151.21	152.16	1.0
9p13	38.65	39.25	0.6
13q22–q31	77.15	81.38	4.2
16q22	86.70	87.62	0.9
17q11	29.30	30.85	1.6
17q12–q21.2	39.79	42.80	3.0
17q21.32–q21.33	52.47	55.80	3.3
17q22–q23.3	63.81	69.70	5.9
17q23.3–q24.3	69.93	74.99	5.1
19q13	40.63	41.40	0.8
20q11.22	34.59	35.85	1.3
20q13.12	44.00	45.62	1.6
20q13.12–q13.13	46.45	49.43	3.0
20q13.2–q13.32	51.32	59.12	7.8

extended to include neighboring nonamplified clones (ratio, <1.5). The amplicon size determination was partially dependent on local clone density.

FISH. Dual-color interphase FISH to breast cancer cell lines was done as described (17). Bacterial artificial chromosome clone RP11-361K8 was labeled with SpectrumOrange (Vysis, Downers Grove, IL), and SpectrumOrange-labeled probe for *EGFR* was obtained from Vysis. SpectrumGreen-labeled chromosome 7 and 17 centromere probes (Vysis) were used as a reference. A tissue microarray containing 612 formalin-fixed, paraffin-embedded primary breast cancers (17) was applied in FISH analyses as described (18). The use of these specimens was approved by the Ethics Committee of the University of Basel and by the NIH. Specimens containing a 2-fold or higher increase in the number of test probe signals, as compared with corresponding centromere signals, in at least 10% of the tumor cells were considered to be amplified. Survival analysis was performed using the Kaplan-Meier method and the log-rank test.

RT-PCR. The *HOXB7* expression level was determined relative to *GAPDH*. Reverse transcription and PCR amplification were performed using Access RT-PCR System (Promega Corp., Madison, WI) with 10 ng of mRNA as a template. *HOXB7* primers were 5′-GAGCAGAGGGACTCGGACTT-3′ and 5′-GCGTCAGGTAGCGATTGTAG-3′.

RESULTS

Global Effect of Copy Number on Gene Expression. 13,824 arrayed cDNA clones were applied for analysis of gene expression and gene copy number (CGH microarrays) in 14 breast cancer cell lines. The results illustrate a considerable influence of copy number on gene expression patterns. Up to 44% of the highly amplified transcripts (CGH ratio, >2.5) were overexpressed (*i.e.*, belonged to the global upper 7% of expression ratios), compared with only 6% for genes with normal copy number levels (Fig. 1A). Conversely, 10.5% of the transcripts with high-level expression (cDNA ratio, >10) showed increased copy number (Fig. 1*B*). Low-level copy number increases and decreases were also associated with similar, although less dramatic, outcomes on gene expression (Fig. 1).

Identification of Distinct Breast Cancer Amplicons. Base-pair locations obtained for 11,994 cDNAs (86.8%) were used to plot copy number changes as a function of genomic position (Fig. 2, Supplement Fig. A). The average spacing of clones throughout the genome was 267 kb. This high-resolution mapping identified 24 independent breast cancer amplicons, spanning from 0.2 to 12 Mb of DNA (Table 1). Several amplification sites detected previously by chromosomal CGH were validated, with 1q21, 17q12–q21.2, 17q22–q23, 20q13.1, and 20q13.2 regions being most commonly amplified. Furthermore, the boundaries of these amplicons were precisely delineated. In addition, novel amplicons were identified at 9p13 (38.65–39.25 Mb), and 17q21.3 (52.47–55.80 Mb).

Direct Identification of Putative Amplification Target Genes. The cDNA/CGH microarray technique enables the direct correlation of copy number and expression data on a gene-by-gene basis throughout the genome. We directly annotated high-resolution CGH plots with gene expression data using color coding. Fig. 2*C* shows that most of the amplified genes in the MCF-7 breast cancer cell line at 1p13, 17q22–q23, and 20q13 were highly overexpressed. A view of chromosome 7 in the MDA-468 cell line implicates *EGFR* as the most highly overexpressed and amplified gene at 7p11–p12 (Fig. 3*A*). In BT-474, the two known amplicons at 17q12 and 17q22–q23 contained numerous highly overexpressed genes (Fig. 3*B*). In addition, several genes, including the homeobox genes *HOXB2* and *HOXB7*, were highly amplified in a previously undescribed independent amplicon at 17q21.3. *HOXB7* was systematically amplified (as validated by FISH, Fig. 3*B*, *inset*) as well as overexpressed (as verified by RT-PCR, data not shown) in BT-474, UACC812, and ZR-75-30 cells. Furthermore, this novel

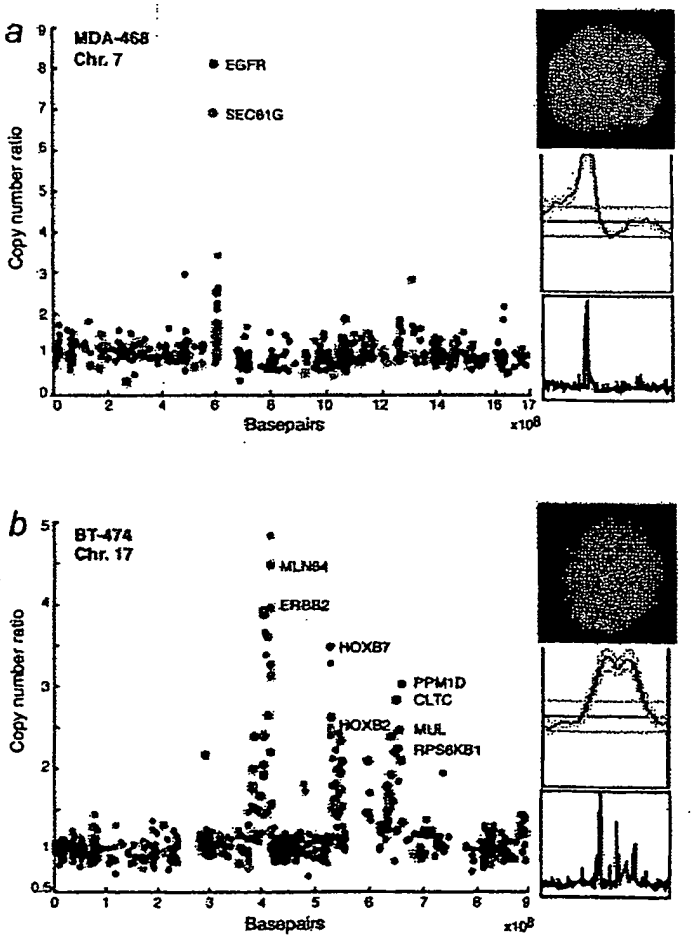

Fig. 3. Annotation of gene expression data on CGH microarray profiles. *A*, genes in the 7p11-p12 amplicon in the MDA-468 cell line are highly expressed (*red dots*) and include the *EGFR* oncogene. *B*, several genes in the 17q12, 17q21.3, and 17q23 amplicons in the BT-474 breast cancer cell line are highly overexpressed (*red*) and include the *HOXB7* gene. The data labels and color coding are as indicated for Fig. 2*C*. *Insets* show chromosomal CGH profiles for the corresponding chromosomes and validation of the increased copy number by interphase FISH using *EGFR* (*red*) and chromosome 7 centromere probe (*green*) to MDA-468 (*A*) and *HOXB7*-specific probe (*red*) and chromosome 17 centromere (*green*) to BT-474 cells (*B*).

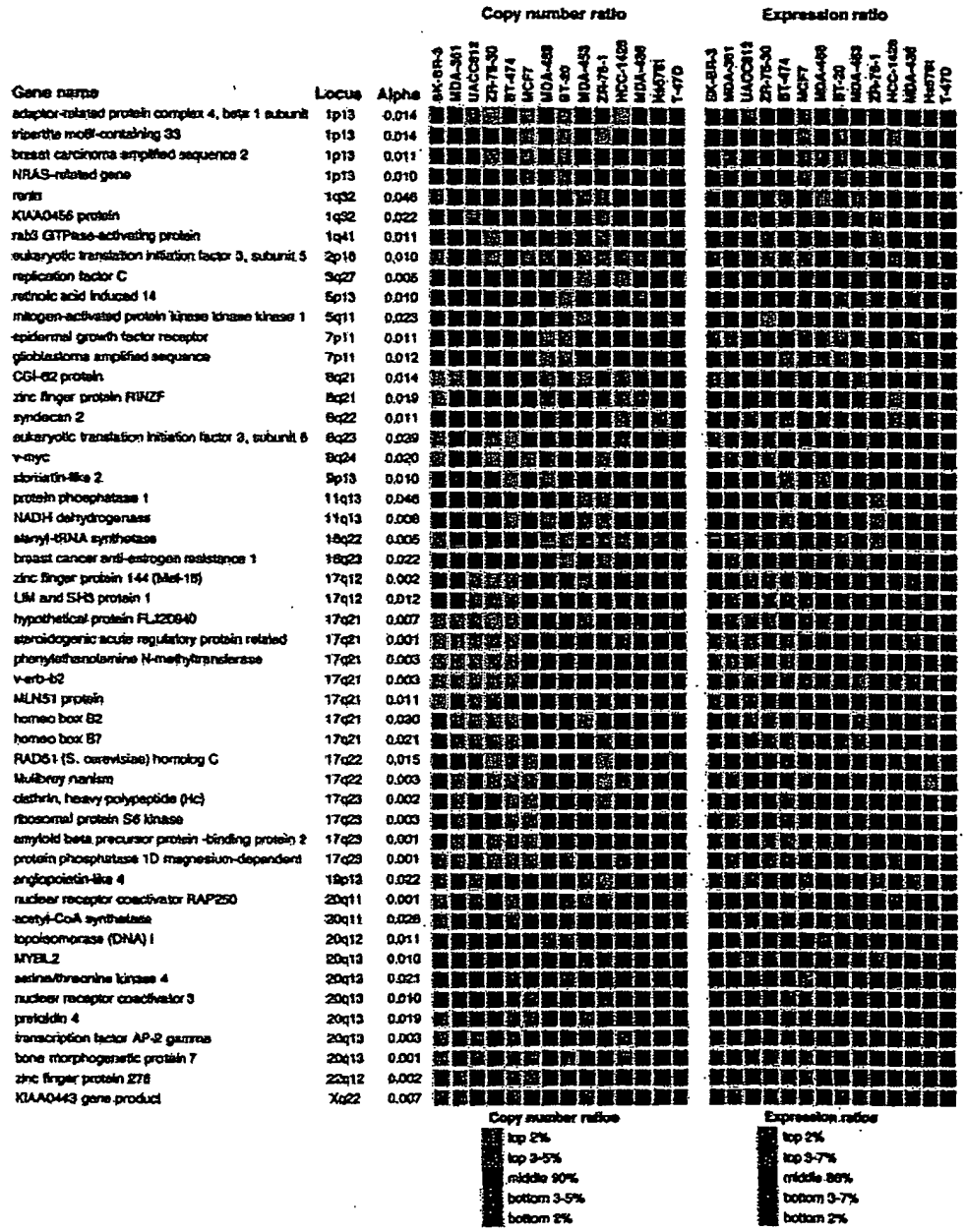

Gene name	Locus	Alpha
adaptor-related protein complex 4, beta 1 subunit	1p13	0.014
tripartite motif-containing 33	1p13	0.014
breast carcinoma amplified sequence 2	1p13	0.011
NRAS-related gene	1p13	0.010
renin	1q32	0.046
KIAA0456 protein	1q32	0.022
rab3 GTPase-activating protein	1q41	0.011
eukaryotic translation initiation factor 3, subunit 5	2p16	0.010
replication factor C	3q27	0.005
retinoic acid induced 14	5p13	0.010
mitogen-activated protein kinase kinase kinase 1	5q11	0.023
epidermal growth factor receptor	7p11	0.011
glioblastoma amplified sequence	7p11	0.012
CGI-62 protein	8q21	0.014
zinc finger protein RINZF	8q21	0.019
syndecan 2	8q22	0.011
eukaryotic translation initiation factor 3, subunit 6	8q23	0.029
v-myc	8q24	0.020
stonin-like 2	9p13	0.010
protein phosphatase 1	11q13	0.046
NADH dehydrogenase	11q13	0.008
alanyl-tRNA synthetase	16q22	0.005
breast cancer anti-estrogen resistance 1	16q23	0.022
zinc finger protein 144 (Mel-15)	17q12	0.002
LIM and SH3 protein 1	17q12	0.012
hypothetical protein FLJ20640	17q21	0.007
steroidogenic acute regulatory protein related	17q21	0.001
phenylethanolamine N-methyltransferase	17q21	0.003
v-erb-b2	17q21	0.003
MLN51 protein	17q21	0.011
homeo box B2	17q21	0.030
homeo box B7	17q21	0.021
RAD51 (S. cerevisiae) homolog C	17q22	0.015
Muirbrey nanism	17q22	0.003
clathrin, heavy polypeptide (Hc)	17q23	0.002
ribosomal protein S6 kinase	17q23	0.003
amyloid beta precursor protein -binding protein 2	17q23	0.001
protein phosphatase 1D magnesium-dependent	17q23	0.001
angiopoietin-like 4	19p13	0.022
nuclear receptor coactivator RAP250	20q11	0.001
acetyl-CoA synthetase	20q11	0.028
topoisomerase (DNA) I	20q12	0.011
MYBL2	20q13	0.010
serine/threonine kinase 4	20q13	0.023
nuclear receptor coactivator 3	20q13	0.010
prickldin 4	20q13	0.019
transcription factor AP-2 gamma	20q13	0.003
bone morphogenetic protein 7	20q13	0.001
zinc finger protein 276	22q12	0.002
KIAA0443 gene product	Xq22	0.007

Fig. 4. List of 50 genes with a statistically significant correlation (α value <0.05) between gene copy number and gene expression. Name, chromosomal location, and the α value for each gene are indicated. The genes have been ordered according to their position in the genome. The color maps on the *right* illustrate the copy number and expression ratio patterns in the 14 cell lines. The key to the color code is shown at the *bottom* of the graph. *Gray squares,* missing values. The complete list of 270 genes is shown in supplemental Fig. B.

amplification was validated to be present in 10.2% of 363 primary breast cancers by FISH to a tissue microarray and was associated with poor prognosis of the patients ($P = 0.001$).

Statistical Identification and Characterization of 270 Highly Expressed Genes in Amplicons. Statistical comparison of expression levels of all genes as a function of gene amplification identified 270 genes whose expression was significantly influenced by copy number across all 14 cell lines (Fig. 4, Supplemental Fig. B). According to the gene ontology data,[8] 91 of the 270 genes represented hypothetical proteins or genes with no functional annotation, whereas 179 had associated functional information available. Of these, 151 (84%) are implicated in apoptosis, cell proliferation, signal transduction, and transcription, whereas 28 (16%) had functional annotations that could not be directly linked with cancer.

DISCUSSION

The importance of recurrent gene and chromosome copy number changes in the development and progression of solid tumors has been characterized in >1000 publications applying CGH[9] (9, 10), as well as in a large number of other molecular cytogenetic, cytogenetic, and molecular genetic studies. The effects of these somatic genetic changes on gene expression levels have remained largely unknown, although a few studies have explored gene expression changes occurring in specific amplicons (15, 19–21). Here, we applied genome-wide cDNA microarrays to identify transcripts whose expression changes were attributable to underlying gene copy number alterations in breast cancer.

The overall impact of copy number on gene expression patterns was substantial with the most dramatic effects seen in the case of high-

[8] Internet address: http://www.geneontology.org/.

[9] Internet address: http://www.ncbi.nlm.nih.gov/entrez.

level copy number increase. Low-level copy number gains and losses also had a significant influence on expression levels of genes in the regions affected, but these effects were more subtle on a gene-by-gene basis than those of high-level amplifications. However, the impact of low-level gains on the dysregulation of gene expression patterns in cancer may be equally important if not more important than that of high-level amplifications. Aneuploidy and low-level gains and losses of chromosomal arms represent the most common types of genetic alterations in breast and other cancers and, therefore, have an influence on many genes. Our results in breast cancer extend the recent studies on the impact of aneuploidy on global gene expression patterns in yeast cells, acute myeloid leukemia, and a prostate cancer model system (22–24).

The CGH microarray analysis identified 24 independent breast cancer amplicons. We defined the precise boundaries for many amplicons detected previously by chromosomal CGH (9, 10, 25, 26) and also discovered novel amplicons that had not been detected previously, presumably because of their small size (only 1–2 Mb) or close proximity to other larger amplicons. One of these novel amplicons involved the homeobox gene region at 17q21.3 and led to the overexpression of the *HOXB7* and *HOXB2* genes. The homeodomain transcription factors are known to be key regulators of embryonic development and have been occasionally reported to undergo aberrant expression in cancer (27, 28). *HOXB7* transfection induced cell proliferation in melanoma, breast, and ovarian cancer cells and increased tumorigenicity and angiogenesis in breast cancer (29–32). The present results imply that gene amplification may be a prominent mechanism for overexpressing *HOXB7* in breast cancer and suggest that *HOXB7* contributes to tumor progression and confers an aggressive disease phenotype in breast cancer. This view is supported by our finding of amplification of *HOXB7* in 10% of 363 primary breast cancers, as well as an association of amplification with poor prognosis of the patients.

We carried out a systematic search to identify genes whose expression levels across all 14 cell lines were attributable to amplification status. Statistical analysis revealed 270 such genes (representing ~2% of all genes on the array), including not only previously described amplified genes, such as *HER-2*, *MYC*, *EGFR*, ribosomal protein s6 kinase, and *AIB3*, but also numerous novel genes such as *NRAS-related gene* (1p13), *syndecan-2* (8q22), and *bone morphogenic protein* (20q13.1), whose activation by amplification may similarly promote breast cancer progression. Most of the 270 genes have not been implicated previously in breast cancer development and suggest novel pathogenetic mechanisms. Although we would not expect all of them to be causally involved, it is intriguing that 84% of the genes with associated functional information were implicated in apoptosis, cell proliferation, signal transduction, transcription, or other cellular processes that could directly imply a possible role in cancer progression. Therefore, a detailed characterization of these genes may provide biological insights to breast cancer progression and might lead to the development of novel therapeutic strategies.

In summary, we demonstrate application of cDNA microarrays to the analysis of both copy number and expression levels of over 12,000 transcripts throughout the breast cancer genome, roughly once every 267 kb. This analysis provided: (*a*) evidence of a prominent global influence of copy number changes on gene expression levels; (*b*) a high-resolution map of 24 independent amplicons in breast cancer; and (*c*) identification of a set of 270 genes, the overexpression of which was statistically attributable to gene amplification. Characterization of a novel amplicon at 17q21.3 implicated amplification and overexpression of the *HOXB7* gene in breast cancer, including a clinical association between *HOXB7* amplification and poor patient prognosis. Overall, our results illustrate how the identification of genes activated by gene amplification provides a powerful approach to highlight genes with an important role in cancer as well as to prioritize and validate putative targets for therapy development.

REFERENCES

1. Golub, T. R., Slonim, D. K., Tamayo, P., Huard, C., Gaasenbeek, M., Mesirov, J. P., Coller, H., Loh, M. L., Downing, J. R., Caligiuri, M. A., Bloomfield, C. D., and Lander, E. S. Molecular classification of cancer: class discovery and class prediction by gene expression monitoring. Science (Wash. DC), *286:* 531–537, 1999.
2. Alizadeh, A. A., Eisen, M. B., Davis, R. E., Ma, C., Lossos, I. S., Rosenwald, A., Boldrick, J. C., Sabet, H., Tran, T., Yu, X., *et al.* Distinct types of diffuse large B-cell lymphoma identified by gene expression profiling. Nature (Lond.), *403:* 503–511, 2000.
3. Bittner, M., Meltzer, P., Chen, Y., Jiang, Y., Seftor, E., Hendrix, M., Radmacher, M., Simon, R., Yakhini, Z., Ben-Dor, A., *et al.* Molecular classification of cutaneous malignant melanoma by gene expression profiling. Nature (Lond.), *406:* 536–540, 2000.
4. Perou, C. M., Sorlie, T., Eisen, M. B., van de Rijn, M., Jeffrey, S. S., Rees, C. A., Pollack, J. R., Ross, D. T., Johnsen, H., Akslen, L. A., *et al.* Molecular portraits of human breast tumours. Nature (Lond.), *406:* 747–752, 2000.
5. Dhanasekaran, S. M., Barrette, T. R., Ghosh, D., Shah, R., Varambally, S., Kurachi, K., Pienta, K. J., Rubin, M. A., and Chinnaiyan, A. M. Delineation of prognostic biomarkers in prostate cancer. Nature (Lond.), *412:* 822–826, 2001.
6. Sorlie, T., Perou, C. M., Tibshirani, R., Aas, T., Geisler, S., Johnsen, H., Hastie, T., Eisen, M. B., van de Rijn, M., Jeffrey, S. S., *et al.* Gene expression patterns of breast carcinomas distinguish tumor subclasses with clinical implications. Proc. Natl. Acad. Sci. USA, *98:* 10869–10874, 2001.
7. Ross, J. S., and Fletcher, J. A. The *HER-2/neu* oncogene: prognostic factor, predictive factor and target for therapy. Semin. Cancer Biol., *9:* 125–138, 1999.
8. Arteaga, C. L. The epidermal growth factor receptor: from mutant oncogene in nonhuman cancers to therapeutic target in human neoplasia. J. Clin. Oncol., *19:* 32–40, 2001.
9. Knuutila, S., Bjorkqvist, A. M., Autio, K., Tarkkanen, M., Wolf, M., Monni, O., Szymanska, J., Larramendy, M. L., Tapper, J., Pere, H., El-Rifai, W., *et al.* DNA copy number amplifications in human neoplasms: review of comparative genomic hybridization studies. Am. J. Pathol., *152:* 1107–1123, 1998.
10. Knuutila S., Autio K., and Aalto Y. Online access to CGH data of DNA sequence copy number changes. Am. J. Pathol., *157:* 689, 2000.
11. DeRisi, J., Penland, L., Brown, P. O., Bittner, M. L., Meltzer, P. S., Ray, M., Chen, Y., Su, Y. A., and Trent, J. M. Use of a cDNA microarray to analyse gene expression patterns in human cancer. Nat. Genet., *14:* 457–460, 1996.
12. Shalon, D., Smith, S. J., and Brown, P. O. A DNA microarray system for analyzing complex DNA samples using two-color fluorescent probe hybridization. Genome Res., *6:* 639–645, 1996.
13. Mousses, S., Bittner, M. L., Chen, Y., Dougherty, E. R., Baxevanis, A., Meltzer, P. S., and Trent, J. M. Gene expression analysis by cDNA microarrays. *In:* F. J. Livesey and S. P. Hunt (eds.), Functional Genomics, pp. 113–137. Oxford: Oxford University Press, 2000.
14. Pollack, J. R., Perou, C. M., Alizadeh, A. A., Eisen, M. B., Pergamenschikov, A., Williams, C. F., Jeffrey, S. S., Botstein, D., and Brown, P. O. Genome-wide analysis of DNA copy-number changes using cDNA microarrays. Nat. Genet., *23:* 41–46, 1999.
15. Monni, O., Bärlund, M., Mousses, S., Kononen, J., Sauter, G., Heiskanen, M., Paavola, P., Avela, K., Chen, Y., Bittner, M. L., and Kallioniemi, A. Comprehensive copy number and gene expression profiling of the 17q23 amplicon in human breast cancer. Proc. Natl. Acad. Sci. USA, *98:* 5711–5716, 2001.
16. Chen, Y., Dougherty, E. R., and Bittner, M. L. Ratio-based decisions and the quantitative analysis of cDNA microarray images. J. Biomed. Optics, *2:* 364–374, 1997.
17. Bärlund, M., Forozan, F., Kononen, J., Bubendorf, L., Chen, Y., Bittner, M. L., Torhorst, J., Haas, P., Bucher, C., Sauter, G., *et al.* Detecting activation of ribosomal protein S6 kinase by complementary DNA and tissue microarray analysis. J. Natl. Cancer Inst., *92:* 1252–1259, 2000.
18. Andersen, C. L., Hostetter, G., Grigoryan, A., Sauter, G., and Kallioniemi, A. Improved procedure for fluorescence *in situ* hybridization on tissue microarrays. Cytometry, *45:* 83–86, 2001.
19. Kauraniemi, P., Bärlund, M., Monni, O., and Kallioniemi, A. New amplified and highly expressed genes discovered in the ERBB2 amplicon in breast cancer by cDNA microarrays. Cancer Res., *61:* 8235–8240, 2001.
20. Clark, J., Edwards, S., John, M., Flohr, P., Gordon, T., Maillard, K., Giddings, I., Brown, C., Bagherzadeh, A., Campbell, C., Shipley, J., Wooster, R., and Cooper, C. S. Identification of amplified and expressed genes in breast cancer by comparative hybridization onto microarrays of randomly selected cDNA clones. Genes Chromosomes Cancer, *34:* 104–114, 2002.
21. Varis, A., Wolf, M., Monni, O., Vakkari, M. L., Kokkola, A., Moskaluk, C., Frierson, H., Powell, S. M., Knuutila, S., Kallioniemi, A., and El-Rifai, W. Targets of gene amplification and overexpression at 17q in gastric cancer. Cancer Res., *62:* 2625–2629, 2002.
22. Hughes, T. R., Roberts, C. J., Dai, H., Jones, A. R., Meyer, M. R., Slade, D., Burchard, J., Dow, S., Ward, T. R., Kidd, M. J., Friend, S. H., and Marton M. J.

Widespread aneuploidy revealed by DNA microarray expression profiling. Nat. Genet., *25:* 333–337, 2000.

23. Virtaneva, K., Wright, F. A., Tanner, S. M., Yuan, B., Lemon, W. J., Caligiuri, M. A., Bloomfield, C. D., de La Chapelle, A., and Krahe, R. Expression profiling reveals fundamental biological differences in acute myeloid leukemia with isolated trisomy 8 and normal cytogenetics. Proc. Natl. Acad. Sci. USA, *98:* 1124–1129, 2001.
24. Phillips, J. L., Hayward, S. W., Wang, Y., Vasselli, J., Pavlovich, C., Padilla-Nash, H., Pezullo, J. R., Ghadimi, B. M., Grossfeld, G. D., Rivera, A., Linehan, W. M., Cunha, G. R., and Ried, T. The consequences of chromosomal aneuploidy on gene expression profiles in a cell line model for prostate carcinogenesis. Cancer Res., *61:* 8143–8149, 2001.
25. Bärlund, M., Tirkkonen, M., Forozan, F., Tanner, M. M., Kallioniemi, O. P., and Kallioniemi, A. Increased copy number at 17q22–q24 by CGH in breast cancer is due to high-level amplification of two separate regions. Genes Chromosomes Cancer, *20:* 372–376, 1997.
26. Tanner, M. M., Tirkkonen, M., Kallioniemi, A., Isola, J., Kuukasjärvi, T., Collins, C., Kowbel, D., Guan, X. Y., Trent, J., Gray, J. W., Meltzer, P., and Kallioniemi O. P. Independent amplification and frequent co-amplification of three nonsyntenic regions on the long arm of chromosome 20 in human breast cancer. Cancer Res., *56:* 3441–3445, 1996.
27. Cillo, C., Faiella, A., Cantile, M., and Boncinelli, E. Homeobox genes and cancer. Exp. Cell Res., *248:* 1–9, 1999.
28. Cillo, C., Cantile, M., Faiella, A., and Boncinelli, E. Homeobox genes in normal and malignant cells. J. Cell. Physiol., *188:* 161–169, 2001.
29. Care, A., Silvani, A., Meccia, E., Mattia, G., Stoppacciaro, A., Parmiani, G., Peschle, C., and Colombo, M. P. HOXB7 constitutively activates basic fibroblast growth factor in melanomas. Mol. Cell. Biol., *16:* 4842–4851, 1996.
30. Care, A., Silvani, A., Meccia, E., Mattia, G., Peschle, C., and Colombo, M. P. Transduction of the SkBr3 breast carcinoma cell line with the *HOXB7* gene induces bFGF expression, increases cell proliferation and reduces growth factor dependence. Oncogene, *16:* 3285–3289, 1998.
31. Care, A., Felicetti, F., Meccia, E., Bottero, L., Parenza, M., Stoppacciaro, A., Peschle, C., and Colombo, M. P. HOXB7: a key factor for tumor-associated angiogenic switch. Cancer Res., *61:* 6532–6539, 2001.
32. Naora, H., Yang, Y. Q., Montz, F. J., Seidman, J. D., Kurman, R. J., and Roden, R. B. A serologically identified tumor antigen encoded by a homeobox gene promotes growth of ovarian epithelial cells. Proc. Natl. Acad. Sci. USA, *98:* 4060–4065, 2001.

Microarray analysis reveals a major direct role of DNA copy number alteration in the transcriptional program of human breast tumors

Jonathan R. Pollack*†‡, Therese Sørlie§, Charles M. Perou¶, Christian A. Rees‖**, Stefanie S. Jeffrey††, Per E. Lonning‡‡, Robert Tibshirani§§, David Botstein‖, Anne-Lise Børresen-Dale§, and Patrick O. Brown†¶¶

Departments of *Pathology, ‖Genetics, ††Surgery, §§Health Research and Policy, and ¶¶Biochemistry, and †Howard Hughes Medical Institute, Stanford University School of Medicine, Stanford, CA 94305; §Department of Genetics, Norwegian Radium Hospital, Montebello, N-0310 Oslo, Norway; ‡‡Department of Medicine (Oncology), Haukeland University Hospital, N-5021 Bergen, Norway; and ¶Department of Genetics and Lineberger Comprehensive Cancer Center, University of North Carolina, Chapel Hill, NC 27599

Contributed by Patrick O. Brown, August 6, 2002

Genomic DNA copy number alterations are key genetic events in the development and progression of human cancers. Here we report a genome-wide microarray comparative genomic hybridization (array CGH) analysis of DNA copy number variation in a series of primary human breast tumors. We have profiled DNA copy number alteration across 6,691 mapped human genes, in 44 predominantly advanced, primary breast tumors and 10 breast cancer cell lines. While the overall patterns of DNA amplification and deletion corroborate previous cytogenetic studies, the high-resolution (gene-by-gene) mapping of amplicon boundaries and the quantitative analysis of amplicon shape provide significant improvement in the localization of candidate oncogenes. Parallel microarray measurements of mRNA levels reveal the remarkable degree to which variation in gene copy number contributes to variation in gene expression in tumor cells. Specifically, we find that 62% of highly amplified genes show moderately or highly elevated expression, that DNA copy number influences gene expression across a wide range of DNA copy number alterations (deletion, low-, mid- and high-level amplification), that on average, a 2-fold change in DNA copy number is associated with a corresponding 1.5-fold change in mRNA levels, and that overall, at least 12% of all the variation in gene expression among the breast tumors is directly attributable to underlying variation in gene copy number. These findings provide evidence that widespread DNA copy number alteration can lead directly to global deregulation of gene expression, which may contribute to the development or progression of cancer.

Conventional cytogenetic techniques, including comparative genomic hybridization (CGH) (1), have led to the identification of a number of recurrent regions of DNA copy number alteration in breast cancer cell lines and tumors (2–4). While some of these regions contain known or candidate oncogenes [e.g., FGFR1 (8p11), MYC (8q24), CCND1 (11q13), ERBB2 (17q12), and ZNF217 (20q13)] and tumor suppressor genes [RB1 (13q14) and TP53 (17p13)], the relevant gene(s) within other regions (e.g., gain of 1q, 8q22, and 17q22–24, and loss of 8p) remain to be identified. A high-resolution genome-wide map, delineating the boundaries of DNA copy number alterations in tumors, should facilitate the localization and identification of oncogenes and tumor suppressor genes in breast cancer. In this study, we have created such a map, using array-based CGH (5–7) to profile DNA copy number alteration in a series of breast cancer cell lines and primary tumors.

An unresolved question is the extent to which the widespread DNA copy number changes that we and others have identified in breast tumors alter expression of genes within involved regions. Because we had measured mRNA levels in parallel in the same samples (8), using the same DNA microarrays, we had an opportunity to explore on a genomic scale the relationship between DNA copy number changes and gene expression. From this analysis, we have identified a significant impact of widespread DNA copy number alteration on the transcriptional programs of breast tumors.

Materials and Methods

Tumors and Cell Lines. Primary breast tumors were predominantly large (>3 cm), intermediate-grade, infiltrating ductal carcinomas, with more than 50% being lymph node positive. The fraction of tumor cells within specimens averaged at least 50%. Details of individual tumors have been published (8, 9), and are summarized in Table 1, which is published as supporting information on the PNAS web site, www.pnas.org. Breast cancer cell lines were obtained from the American Type Culture Collection. Genomic DNA was isolated either using Qiagen genomic DNA columns, or by phenol/chloroform extraction followed by ethanol precipitation.

DNA Labeling and Microarray Hybridizations. Genomic DNA labeling and hybridizations were performed essentially as described in Pollack *et al.* (7), with slight modifications. Two micrograms of DNA was labeled in a total volume of 50 microliters and the volumes of all reagents were adjusted accordingly. "Test" DNA (from tumors and cell lines) was fluorescently labeled (Cy5) and hybridized to a human cDNA microarray containing 6,691 different mapped human genes (i.e., UniGene clusters). The "reference" (labeled with Cy3) for each hybridization was normal female leukocyte DNA from a single donor. The fabrication of cDNA microarrays and the labeling and hybridization of mRNA samples have been described (8).

Data Analysis and Map Positions. Hybridized arrays were scanned on a GenePix scanner (Axon Instruments, Foster City, CA), and fluorescence ratios (test/reference) calculated using SCANALYZE software (available at http://rana.lbl.gov). Fluorescence ratios were normalized for each array by setting the average log fluorescence ratio for all array elements equal to 0. Measurements with fluorescence intensities more than 20% above background were considered reliable. DNA copy number profiles that deviated significantly from background ratios measured in normal genomic DNA control hybridizations were interpreted as evidence of real DNA copy number alteration (see *Estimating Significance of Altered Fluorescence Ratios* in the supporting information). When indicated, DNA copy number profiles are displayed as a moving average (symmetric 5-nearest neighbors). Map positions for arrayed human cDNAs were assigned by

Abbreviation: CGH, comparative genomic hybridization.

†To whom reprint requests should be addressed at: Department of Pathology, Stanford University School of Medicine, CCSR Building, Room 3245A, 269 Campus Drive, Stanford, CA 94305-5176. E-mail: pollack1@stanford.edu.

**Present address: Zyomyx Inc., Hayward, CA 94545.

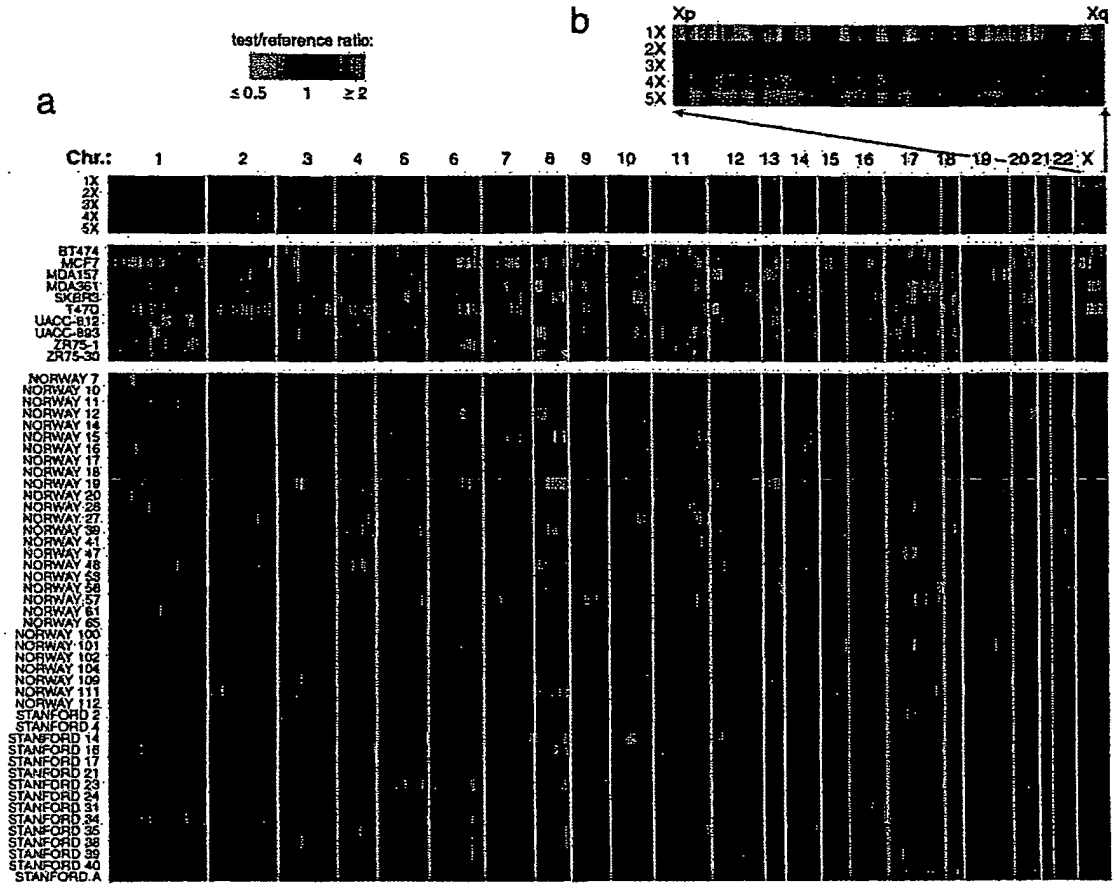

Fig. 1. Genome-wide measurement of DNA copy number alteration by array CGH. (*a*) DNA copy number profiles are illustrated for cell lines containing different numbers of X chromosomes, for breast cancer cell lines, and for breast tumors. Each row represents a different cell line or tumor, and each column represents one of 6,691 different mapped human genes present on the microarray, ordered by genome map position from 1pter through Xqter. Moving average (symmetric 5-nearest neighbors) fluorescence ratios (test/reference) are depicted using a $\log_2$-based pseudocolor scale (indicated), such that red luminescence reflects fold-amplification, green luminescence reflects fold-deletion, and black indicates no change (gray indicates poorly measured data). (*b*) Enlarged view of DNA copy number profiles across the X chromosome, shown for cell lines containing different numbers of X chromosomes.

identifying the starting position of the best and longest match of any DNA sequence represented in the corresponding UniGene cluster (10) against the "Golden Path" genome assembly (http://genome.ucsc.edu/; Oct 7, 2000 Freeze). For UniGene clusters represented by multiple arrayed elements, mean fluorescence ratios (for all elements representing the same UniGene cluster) are reported. For mRNA measurements, fluorescence ratios are "mean-centered" (i.e., reported relative to the mean ratio across the 44 tumor samples). The data set described here can be accessed in its entirety in the supporting information.

Results

We performed CGH on 44 predominantly locally advanced, primary breast tumors and 10 breast cancer cell lines, using cDNA microarrays containing 6,691 different mapped human genes (Fig. 1*a*; also see *Materials and Methods* for details of microarray hybridizations). To take full advantage of the improved spatial resolution of array CGH, we ordered (fluorescence ratios for) the 6,691 cDNAs according to the "Golden Path" (http://genome.ucsc.edu/) genome assembly of the draft human genome sequences (11). In so doing, arrayed cDNAs not only themselves represent genes of potential interest (e.g., candidate oncogenes within amplicons), but also provide precise genetic landmarks for chromosomal regions of amplification and deletion. Parallel analysis of DNA from cell lines containing different numbers of X chromosomes (Fig. 1*b*), as we did before (7), demonstrated the sensitivity of our method to detect single-copy loss (45, XO), and 1.5- (47,XXX), 2- (48,XXXX), or 2.5-fold (49,XXXXX) gains (also see Fig. 5, which is published as supporting information on the PNAS web site). Fluorescence ratios were linearly proportional to copy number ratios, which were slightly underestimated, in agreement with previous observations (7). Numerous DNA copy number alterations were evident in both the breast cancer cell lines and primary tumors (Fig. 1*a*), detected in the tumors despite the presence of euploid non-tumor cell types; the magnitudes of the observed changes were generally lower in the tumor samples. DNA copy-number alterations were found in every cancer cell line and tumor, and on every human chromosome in at least one sample. Recurrent regions of DNA copy number gain and loss were readily identifiable. For example, gains within 1q, 8q, 17q, and 20q were observed in a high proportion of breast cancer cell lines/tumors (90%/69%, 100%/47%, 100%/60%, and 90%/44%, respectively), as were losses within 1p, 3p, 8p, and 13q (80%/24%, 80%/22%, 80%/22%, and 70%/18%, respectively), consistent with published cytogenetic studies (refs. 2–4; a complete listing of gains/losses is provided in Tables 2 and 3, which are published as supporting information on the PNAS web site). The total

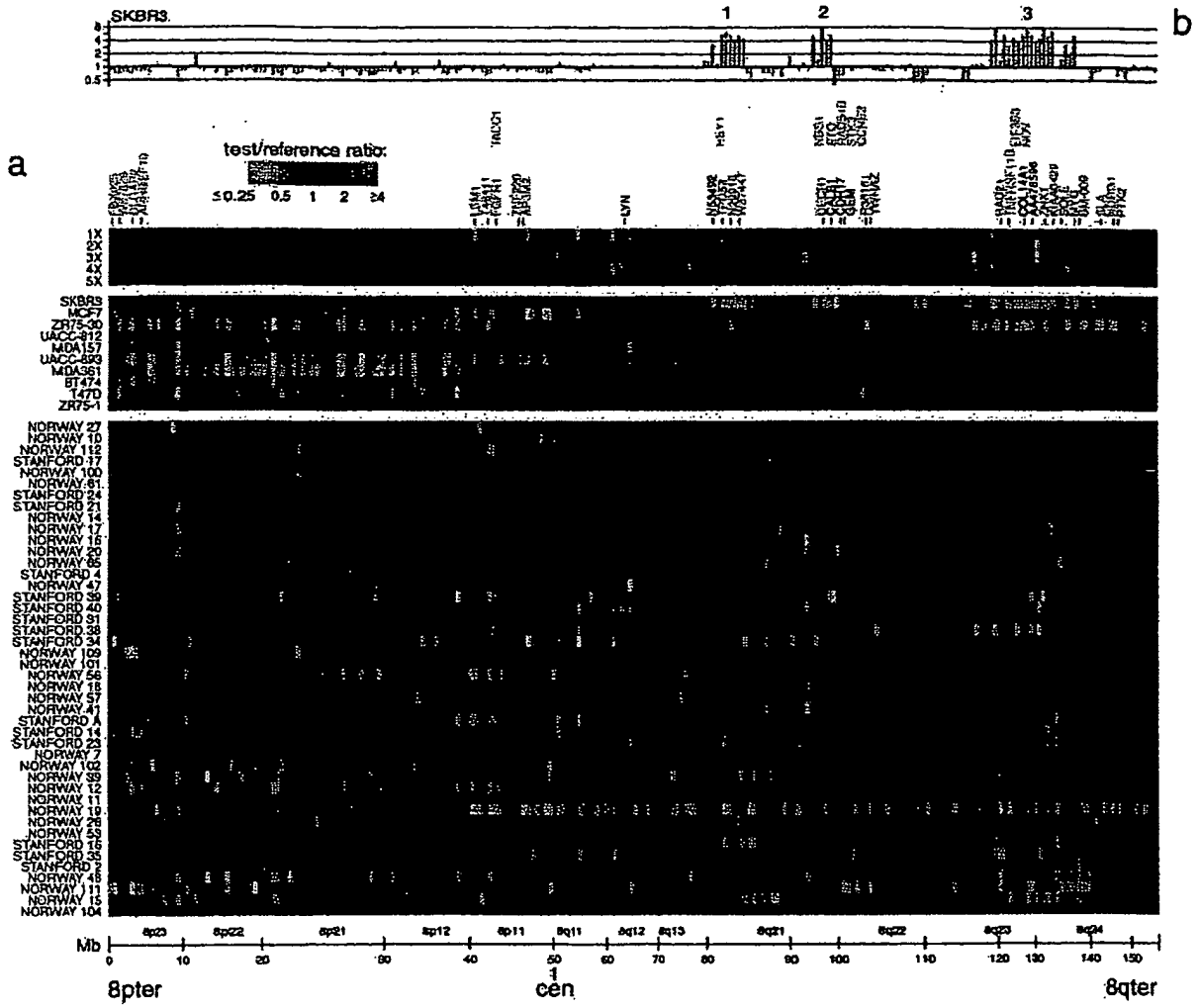

Fig. 2. DNA copy number alteration across chromosome 8 by array CGH. (*a*) DNA copy number profiles are illustrated for cell lines containing different numbers of X chromosomes, for breast cancer cell lines, and for breast tumors. Breast cancer cell lines and tumors are separately ordered by hierarchical clustering to highlight recurrent copy number changes. The 241 genes present on the microarrays and mapping to chromosome 8 are ordered by position along the chromosome. Fluorescence ratios (test/reference) are depicted by a $\log_2$ pseudocolor scale (indicated). Selected genes are indicated with color-coded text (red, increased; green, decreased; black, no change; gray, not well measured) to reflect correspondingly altered mRNA levels (observed in the majority of the subset of samples displaying the DNA copy number change). The map positions for genes of interest that are not represented on the microarray are indicated in the row above those genes represented on the array. (*b*) Graphical display of DNA copy number profile for breast cancer cell line SKBR3. Fluorescence ratios (tumor/normal) are plotted on a $\log_2$ scale for chromosome 8 genes, ordered along the chromosome.

number of genomic alterations (gains and losses) was found to be significantly higher in breast tumors that were high grade (P = 0.008), consistent with published CGH data (3), estrogen receptor negative (P = 0.04), and harboring TP53 mutations (P = 0.0006) (see Table 4, which is published as supporting information on the PNAS web site).

The improved spatial resolution of our array CGH analysis is illustrated for chromosome 8, which displayed extensive DNA copy number alteration in our series. A detailed view of the variation in the copy number of 241 genes mapping to chromosome 8 revealed multiple regions of recurrent amplification; each of these potentially harbors a different known or previously uncharacterized oncogene (Fig. 2*a*). The complexity of amplicon structure is most easily appreciated in the breast cancer cell line SKBR3. Although a conventional CGH analysis of 8q in SKBR3 identified only two distinct regions of amplification (12), we observed three distinct regions of high-level amplification (labeled 1–3 in Fig. 2*b*). For each of these regions we can define the boundaries of the interval recurrently amplified in the tumors we examined; in each case, known or plausible candidate oncogenes can be identified (a description of these regions, as well as the recurrently amplified regions on chromosomes 17 and 20, can be found in Figs. 6 and 7, which are published as supporting information on the PNAS web site).

For a subset of breast cancer cell lines and tumors (4 and 37, respectively), and a subset of arrayed genes (6,095), mRNA levels were quantitatively measured in parallel by using cDNA microarrays (8). The parallel assessment of mRNA levels is useful in the interpretation of DNA copy number changes. For example, the highly amplified genes that are also highly expressed are the strongest candidate oncogenes within an amplicon. Perhaps more significantly, our parallel analysis of DNA copy number changes and mRNA levels provides us the opportunity to assess the global impact of widespread DNA copy number alteration on gene expression in tumor cells.

A strong influence of DNA copy number on gene expression is evident in an examination of the pseudocolor representations

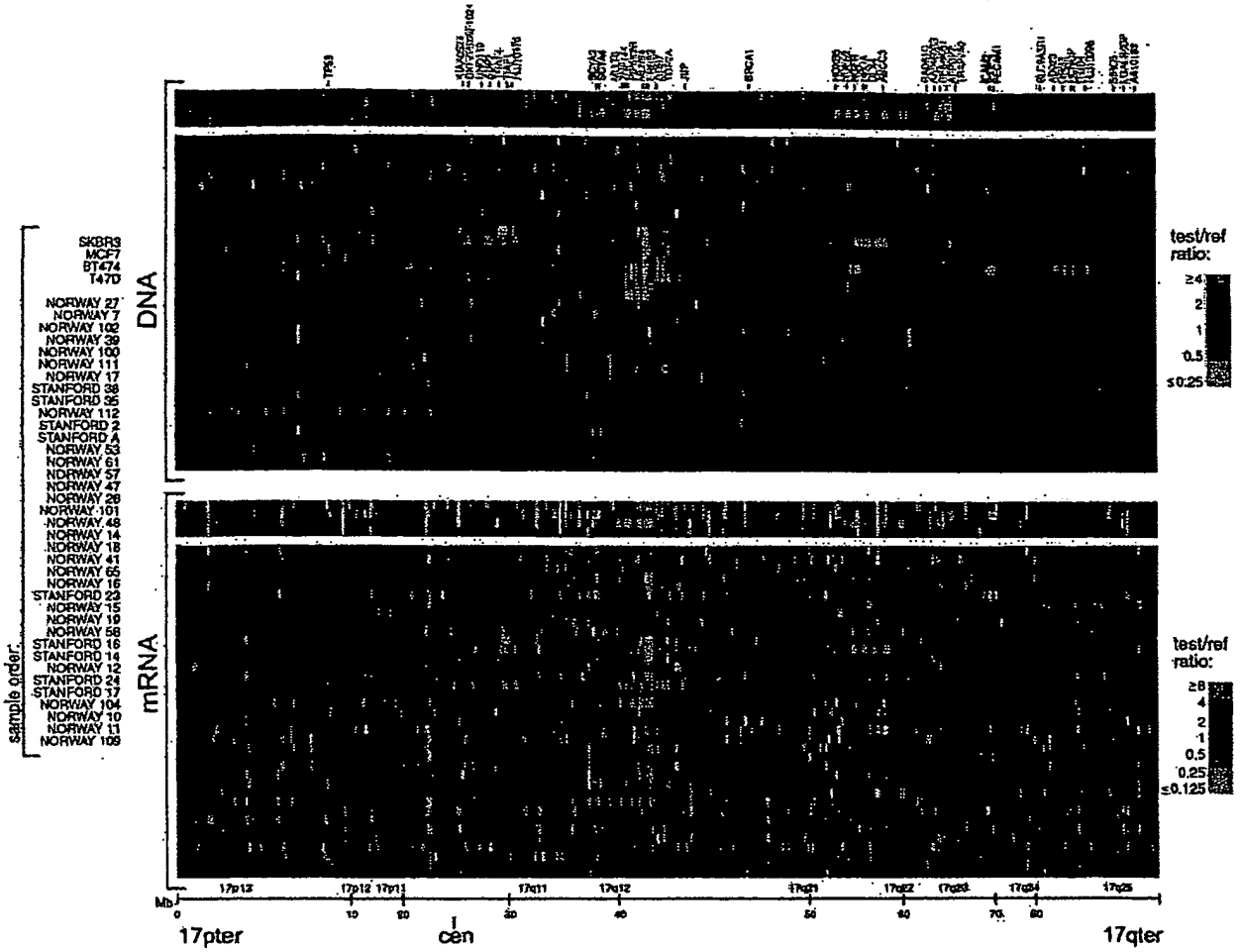

Fig. 3. Concordance between DNA copy number and gene expression across chromosome 17. DNA copy number alteration (*Upper*) and mRNA levels (*Lower*) are illustrated for breast cancer cell lines and tumors. Breast cancer cell lines and tumors are separately ordered by hierarchical clustering (*Upper*), and the identical sample order is maintained (*Lower*). The 354 genes present on the microarrays and mapping to chromosome 17, and for which both DNA copy number and mRNA levels were determined, are ordered by position along the chromosome; selected genes are indicated in color-coded text (see Fig. 2 legend). Fluorescence ratios (test/reference) are depicted by separate $\log_2$ pseudocolor scales (indicated).

of DNA copy number and mRNA levels for genes on chromosome 17 (Fig. 3). The overall patterns of gene amplification and elevated gene expression are quite concordant; i.e., a significant fraction of highly amplified genes appear to be correspondingly highly expressed. The concordance between high-level amplification and increased gene expression is not restricted to chromosome 17. Genome-wide, of 117 high-level DNA amplifications (fluorescence ratios >4, and representing 91 different genes), 62% (representing 54 different genes; see Table 5, which is published as supporting information on the PNAS web site) are found associated with at least moderately elevated mRNA levels (mean-centered fluorescence ratios >2), and 42% (representing 36 different genes) are found associated with comparably highly elevated mRNA levels (mean-centered fluorescence ratios >4).

To determine the extent to which DNA deletion and lower-level amplification (in addition to high-level amplification) are also associated with corresponding alterations in mRNA levels, we performed three separate analyses on the complete data set (4 cell lines and 37 tumors, across 6,095 genes). First, we determined the average mRNA levels for each of five classes of genes, representing DNA deletion, no change, and low-, medium-, and high-level amplification (Fig. 4*a*). For both the breast cancer cell lines and tumors, average mRNA levels tracked with DNA copy number across all five classes, in a statistically significant fashion (*P* values for pair-wise Student's *t* tests comparing adjacent classes: cell lines, 4×10^{-49}, 1×10^{-49}, 5×10^{-5}, 1×10^{-2}; tumors, 1×10^{-43}, 1×10^{-214}, 5×10^{-41}, 1×10^{-4}). A linear regression of the average log(DNA copy number), for each class, against average log(mRNA level) demonstrated that on average, a 2-fold change in DNA copy number was accompanied by 1.4- and 1.5-fold changes in mRNA level for the breast cancer cell lines and tumors, respectively (Fig. 4*a*, regression line not shown). Second, we characterized the distribution of the 6,095 correlations between DNA copy number and mRNA level, each across the 37 tumor samples (Fig. 4*b*). The distribution of correlations forms a normal-shaped curve, but with the peak markedly shifted in the positive direction from zero. This shift is statistically significant, as evidenced in a plot of observed vs. expected correlations (Fig. 4*c*), and reflects a pervasive global influence of DNA copy number alterations on gene expression. Notably, the highest correlations between DNA copy number and mRNA level (the right tail of the distribution in Fig. 4*b*) comprise both amplified and deleted genes (data not shown). Third, we used a linear regression model to estimate the fraction of all variation measured in mRNA levels among the 37

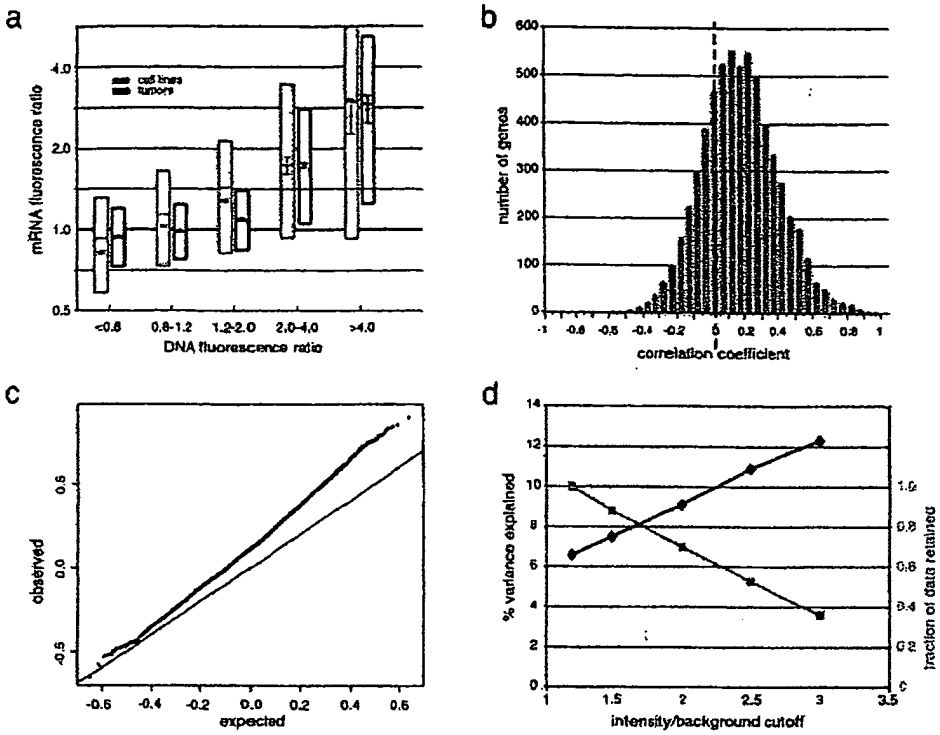

Fig. 4. Genome-wide influence of DNA copy number alterations on mRNA levels. (*a*) For breast cancer cell lines (gray) and tumor samples (black), both mean-centered mRNA fluorescence ratio ($\log_2$ scale) quartiles (box plots indicate 25th, 50th, and 75th percentile) and averages (diamonds; *Y*-value error bars indicate standard errors of the mean) are plotted for each of five classes of genes, representing DNA deletion (tumor/normal ratio < 0.8), no change (0.8–1.2), low- (1.2–2), medium- (2–4), and high-level (>4) amplification. *P* values for pair-wise Student's *t* tests, comparing averages between adjacent classes (moving left to right), are 4×10^{-49}, 1×10^{-49}, 5×10^{-5}, 1×10^{-2} (cell lines), and 1×10^{-43}, 1×10^{-214}, 5×10^{-41}, 1×10^{-4} (tumors). (*b*) Distribution of correlations between DNA copy number and mRNA levels, for 6,095 different human genes across 37 breast tumor samples. (*c*) Plot of observed versus expected correlation coefficients. The expected values were obtained by randomization of the sample labels in the DNA copy number data set. The line of unity is indicated. (*d*) Percent variance in gene expression (among tumors) directly explained by variation in gene copy number. Percent variance explained (black line) and fraction of data retained (gray line) are plotted for different fluorescence intensity/background (a rough surrogate for signal/noise) cutoff values. Fraction of data retained is relative to the 1.2 intensity/background cutoff. Details of the linear regression model used to estimate the fraction of variation in gene expression attributable to underlying DNA copy number alteration can be found in the supporting information (see *Estimating the Fraction of Variation in Gene Expression Attributable to Underlying DNA Copy Number Alteration*).

tumors that could be attributed to underlying variation in DNA copy number. From this analysis, we estimate that, overall, about 7% of all of the observed variation in mRNA levels can be explained directly by variation in copy number of the altered genes (Fig. 4*d*). We can reduce the effects of experimental measurement error on this estimate by using only that fraction of the data most reliably measured (fluorescence intensity/background >3); using that data, our estimate of the percent variation in mRNA levels directly attributed to variation in gene copy number increases to 12% (Fig. 4*d*). This still undoubtedly represents a significant underestimate, as the observed variation in global gene expression is affected not only by true variation in the expression programs of the tumor cells themselves, but also by the variable presence of non-tumor cell types within clinical samples.

Discussion

This genome-wide, array CGH analysis of DNA copy number alteration in a series of human breast tumors demonstrates the usefulness of defining amplicon boundaries at high resolution (gene-by-gene), and quantitatively measuring amplicon shape, to assist in locating and identifying candidate oncogenes. By analyzing mRNA levels in parallel, we have also discovered that changes in DNA copy number have a large, pervasive, direct effect on global gene expression patterns in both breast cancer cell lines and tumors. Although the DNA microarrays used in our analysis may display a bias toward characterized and/or highly expressed genes, because we are examining such a large fraction of the genome (approximately 20% of all human genes), and because, as detailed above, we are likely underestimating the contribution of DNA copy number changes to altered gene expression, we believe our findings are likely to be generalizable (but would nevertheless still be remarkable if only applicable to this set of ~6,100 genes).

In budding yeast, aneuploidy has been shown to result in chromosome-wide gene expression biases (13). Two recent studies have begun to examine the global relationship between DNA copy number and gene expression in cancer cells. In agreement with our findings, Phillips *et al.* (14) have shown that with the acquisition of tumorigenicity in an immortalized prostate epithelial cell line, new chromosomal gains and losses resulted in a statistically significant respective increase and decrease in the average expression level of involved genes. In contrast, Platzer *et al.* (15) recently reported that in metastatic colon tumors only ~4% of genes within amplified regions were found more highly (>2-fold) expressed, when compared with normal colonic epithelium. This report differs substantially from our finding that 62% of highly amplified genes in breast cancer exhibit at least 2-fold increased expression. These contrasting findings may reflect methodological differences between the

studies. For example, the study of Platzer *et al.* (15) may have systematically under-measured gene expression changes. In this regard it is remarkable that only 14 transcripts of many thousand residing within unamplified chromosomal regions were found to exhibit at least 4-fold altered expression in metastatic colon cancer. Additionally, their reliance on lower-resolution chromosomal CGH may have resulted in poorly delimiting the boundaries of high-complexity amplicons, effectively overcalling regions with amplification. Alternatively, the contrasting findings for amplified genes may represent real biological differences between breast and metastatic colon tumors; resolution of this issue will require further studies.

Our finding that widespread DNA copy number alteration has a large, pervasive and direct effect on global gene expression patterns in breast cancer has several important implications. First, this finding supports a high degree of copy number-dependent gene expression in tumors. Second, it suggests that most genes are not subject to specific autoregulation or dosage compensation. Third, this finding cautions that elevated expression of an amplified gene cannot alone be considered strong independent evidence of a candidate oncogene's role in tumorigenesis. In our study, fully 62% of highly amplified genes demonstrated moderately or highly elevated expression. This highlights the importance of high-resolution mapping of amplicon boundaries and shape [to identify the "driving" gene(s) within amplicons (16)], on a large number of samples, in addition to functional studies. Fourth, this finding suggests that analyzing the genomic distribution of expressed genes, even within existing microarray gene expression data sets, may permit the inference of DNA copy number aberration, particularly aneuploidy (where gene expression can be averaged across large chromosomal regions; see Fig. 3 and supporting information). Fifth, this finding implies that a substantial portion of the phenotypic uniqueness (and by extension, the heterogeneity in clinical behavior) among patients' tumors may be traceable to underlying variation in DNA copy number. Sixth, this finding supports a possible role for widespread DNA copy number alteration in tumorigenesis (17, 18), beyond the amplification of specific oncogenes and deletion of specific tumor suppressor genes. Widespread DNA copy number alteration, and the concomitant widespread imbalance in gene expression, might disrupt critical stochiometric relationships in cell metabolism and physiology (e.g., proteosome, mitotic spindle), possibly promoting further chromosomal instability and directly contributing to tumor development or progression. Finally, our findings suggest the possibility of cancer therapies that exploit specific or global imbalances in gene expression in cancer.

We thank the many members of the P.O.B. and D.B. labs for helpful discussions. J.R.P. was a Howard Hughes Medical Institute Physician Postdoctoral Fellow during a portion of this work. P.O.B. is a Howard Hughes Medical Institute Associate Investigator. This work was supported by grants from the National Institutes of Health, the Howard Hughes Medical Institute, the Norwegian Cancer Society, and the Norwegian Research Council.

1. Kallioniemi, A., Kallioniemi, O. P., Sudar, D., Rutovitz, D., Gray, J. W., Waldman, F. & Pinkel, D. (1992) *Science* 258, 818–821.
2. Kallioniemi, A., Kallioniemi, O. P., Piper, J., Tanner, M., Stokke, T., Chen, L., Smith, H. S., Pinkel, D., Gray, J. W. & Waldman, F. M. (1994) *Proc. Natl. Acad. Sci. USA* 91, 2156–2160.
3. Tirkkonen, M., Tanner, M., Karhu, R., Kallioniemi, A., Isola, J. & Kallioniemi, O. P. (1998) *Genes Chromosomes Cancer* 21, 177–184.
4. Forozan, F., Mahlamaki, E. H., Monni, O., Chen, Y., Veldman, R., Jiang, Y., Gooden, G. C., Ethier, S. P., Kallioniemi, A. & Kallioniemi, O. P. (2000) *Cancer Res.* 60, 4519–4525.
5. Solinas-Toldo, S., Lampel, S., Stilgenbauer, S., Nickolenko, J., Benner, A., Dohner, H., Cremer, T. & Lichter, P. (1997) *Genes Chromosomes Cancer* 20, 399–407.
6. Pinkel, D., Segraves, R., Sudar, D., Clark, S., Poole, I., Kowbel, D., Collins, C., Kuo, W. L., Chen, C., Zhai, Y., *et al.* (1998) *Nat. Genet.* 20, 207–211.
7. Pollack, J. R., Perou, C. M., Alizadeh, A. A., Eisen, M. B., Pergamenschikov, A., Williams, C. F., Jeffrey, S. S., Botstein, D. & Brown, P. O. (1999) *Nat. Genet.* 23, 41–46.
8. Perou, C. M., Sorlie, T., Eisen, M. B., van de Rijn, M., Jeffrey, S. S., Rees, C. A., Pollack, J. R., Ross, D. T., Johnsen, H., Akslen, L. A., *et al.* (2000) *Nature (London)* 406, 747–752.
9. Sorlie, T., Perou, C. M., Tibshirani, R., Aas, T., Geisler, S., Johnsen, H., Hastie, T., Eisen, M. B., van de Rijn, M., Jeffrey, S. S., *et al.* (2001) *Proc. Natl. Acad. Sci. USA* 98, 10869–10874.
10. Schuler, G. D. (1997) *J. Mol. Med.* 75, 694–698.
11. Lander, E. S., Linton, L. M., Birren, B., Nusbaum, C., Zody, M. C., Baldwin, J., Devon, K., Dewar, K., Doyle, M., FitzHugh, W., *et al.* (2001) *Nature (London)* 409, 860–921.
12. Fejzo, M. S., Godfrey, T., Chen, C., Waldman, F. & Gray, J. W. (1998) *Genes Chromosomes Cancer* 22, 105–113.
13. Hughes, T. R., Roberts, C. J., Dai, H., Jones, A. R., Meyer, M. R., Slade, D., Burchard, J., Dow, S., Ward, T. R., Kidd, M. J., *et al.* (2000) *Nat. Genet.* 25, 333–337.
14. Phillips, J. L., Hayward, S. W., Wang, Y., Vasselli, J., Pavlovich, C., Padilla-Nash, H., Pezullo, J. R., Ghadimi, B. M., Grossfeld, G. D., Rivera, A., *et al.* (2001) *Cancer Res.* 61, 8143–8149.
15. Platzer, P., Upender, M. B., Wilson, K., Willis, J., Lutterbaugh, J., Nosrati, A., Willson, J. K., Mack, D., Ried, T. & Markowitz, S. (2002) *Cancer Res.* 62, 1134–1138.
16. Albertson, D. G., Ylstra, B., Segraves, R., Collins, C., Dairkee, S. H., Kowbel, D., Kuo, W. L., Gray, J. W. & Pinkel, D. (2000) *Nat. Genet.* 25, 144–146.
17. Li, R., Yerganian, G., Duesberg, P., Kraemer, A., Willer, A., Rausch, C. & Hehlmann, R. (1997) *Proc. Natl. Acad. Sci. USA* 94, 14506–14511.
18. Rasnick, D. & Duesberg, P. H. (1999) *Biochem. J.* 340, 621–630.

TECHNICAL UPDATE

FROM YOUR LABORATORY SERVICES PROVIDER

HER-2/neu Breast Cancer Predictive Testing

Julie Sanford Hanna, Ph.D. and Dan Mornin, M.D.

EACH YEAR, OVER 182,000 WOMEN in the United States are diagnosed with breast cancer, and approximately 45,000 die of the disease.[1] Incidence appears to be increasing in the United States at a rate of roughly 2% per year. The reasons for the increase are unclear, but non-genetic risk factors appear to play a large role.[2]

Five-year survival rates range from approximately 65%-85%, depending on demographic group, with a significant percentage of women experiencing recurrence of their cancer within 10 years of diagnosis. One of the factors most predictive for recurrence once a diagnosis of breast cancer has been made is the number of axillary lymph nodes to which tumor has metastasized. Most node-positive women are given adjuvant therapy, which increases their survival. However, 20%-30% of patients without axillary node involvement also develop recurrent disease, and the difficulty lies in how to identify this high-risk subset of patients. These patients could benefit from increased surveillance, early intervention, and treatment.

Prognostic markers currently used in breast cancer recurrence prediction include tumor size, histological grade, steroid hormone receptor status, DNA ploidy, proliferative index, and cathepsin D status. Expression of growth factor receptors and over-expression of the HER-2/neu oncogene have also been identified as having value regarding treatment regimen and prognosis.

HER-2/neu (also known as c-erbB2) is an oncogene that encodes a transmembrane glycoprotein that is homologous to, but distinct from, the epidermal growth factor receptor. Numerous studies have indicated that high levels of expression of this protein are associated with rapid tumor growth, certain forms of therapy resistance, and shorter disease-free survival. The gene has been shown to be amplified and/or overexpressed in 10%-30% of invasive breast cancers and in 40%-60% of intraductal breast carcinoma.[3]

There are two distinct FDA-approved methods by which HER-2/neu status can be evaluated: immunohistochemistry (IHC, HercepTest™) and FISH (fluorescent in situ hybridization, PathVysion™ Kit). Both methods can be performed on archived and current specimens. The first method allows visual assessment of the amount of HER-2/neu protein present on the cell membrane. The latter method allows direct quantification of the level of gene amplification present in the tumor, enabling differentiation between low- versus high-amplification. At least one study has demonstrated a difference in recurrence risk in women younger than 40 years of age for low- versus high-amplified tumors (54.5% compared to 85.7%); this is compared to a recurrence rate of 16.7% for patients with no HER-2/neu gene amplification.[4] HER-2/neu status may be particularly important to establish in women with small ($\leq$1 cm) tumor size.

The choice of methodology for determination of HER-2/neu status depends in part on the clinical setting. FDA approval for the Vysis FISH test was granted based on clinical trials involving 1549 node-positive patients. Patients received one of three different treatments consisting of different doses of cyclophosphamide, Adriamycin, and 5-fluorouracil (CAF). The study showed that patients with amplified HER-2/neu benefited from treatment with higher doses of adriamycin-based therapy, while those with normal HER-2/neu levels did not. The study therefore identified a sub-set of women, who because they did not benefit from more aggressive treatment, did not need to be exposed to the associated side effects. In addition, other evidence indicates that HER-2/neu amplification in node-negative patients can be used as an independent prognostic indicator for early recurrence, recurrent disease at any time and disease-related death.[5] Demonstration of HER-2/neu gene amplification by FISH has also been shown to be of value in predicting response to chemotherapy in stage-2 breast cancer patients.

Selection of patients for Herceptin© (Trastuzumab) monoclonal antibody therapy, however, is based upon demonstration of HER-2/neu protein overexpression using HercepTest™. Studies using Herceptin© in patients with metastatic breast cancer show an increase in time to disease progression, increased response rate to chemotherapeutic agents and a small increase in overall survival rate. The FISH assays have not yet been approved for this purpose, and studies looking at response to Herceptin© in patients with or without gene amplification status determined by FISH are in progress.

In general, FISH and IHC results correlate well. However, subsets of tumors are found which show discordant results; i.e., protein overexpression without gene amplification or lack of protein overexpression with gene amplification. The clinical significance of such results is unclear. Based on the above considerations, HER-2/neu testing at SHMC/PAML will utilize immunohistochemistry (HercepTest©) as a screen, followed by FISH in IHC-negative cases. Alternatively, either method may be ordered individually depending on the clinical setting or clinician preference.

CPT code information

HER-2/neu via IHC

88342 (including interpretive report)

HER-2/neu via FISH

88271×2 Molecular cytogenetics, DNA probe, each
88274 Molecular cytogenetics, interphase in situ hybridization, analyze 25-99 cells
88291 Cytogenetics and molecular cytogenetics, interpretation and report

Procedural Information

Immunohistochemistry is performed using the FDA-approved DAKO antibody kit, Herceptest©. The DAKO kit contains reagents required to complete a two-step immunohistochemical staining procedure for routinely processed, paraffin-embedded specimens. Following incubation with the primary rabbit antibody to human HER-2/neu protein, the kit employs a ready-to-use dextran-based visualization reagent. This reagent consists of both secondary goat anti-rabbit antibody molecules with horseradish peroxidase molecules linked to a common dextran polymer backbone, thus eliminating the need for sequential application of link antibody and peroxidase conjugated antibody. Enzymatic conversion of the subsequently added chromogen results in formation of visible reaction product at the antigen site. The specimen is then counterstained; a pathologist using light-microscopy interprets results.

FISH analysis at SHMC/PAML is performed using the FDA-approved PathVysion™ HER-2/neu DNA probe kit, produced by Vysis, Inc. Formalin fixed, paraffin-embedded breast tissue is processed using routine histological methods, and then slides are treated to allow hybridization of DNA probes to the nuclei present in the tissue section. The Pathvysion™ kit contains two direct-labeled DNA probes, one specific for the alphoid repetitive DNA (CEP 17, spectrum orange) present at the chromosome 17 centromere and the second for the HER-2/neu oncogene located at 17q11.2-12 (spectrum green). Enumeration of the probes allows a ratio of the number of copies of chromosome 17 to the number of copies of HER-2/neu to be obtained; this enables quantification of low versus high amplification levels, and allows an estimate of the percentage of cells with HER-2/neu gene amplification. The clinically relevant distinction is whether the gene amplification is due to increased gene copy number on the two chromosome 17 homologues normally present or an increase in the number of chromosome 17s in the cells. In the majority of cases, ratio equivalents less than 2.0 are indicative of a normal/negative result, ratios of 2.1 and over indicate that amplification is present and to what degree. Interpretation of this data will be performed and reported from the Vysis-certified Cytogenetics laboratory at SHMC.

References

1. Wingo, P.A., Tong, T., Bolden, S., "Cancer Statistics", 1995;45:1:8-31.
2. "Cancer Rates and Risks", 4th ed., National Institutes of Health, National Cancer Institute, 1996, p. 120.
3. Slamon, D.J., Clark, G.M., Song, S.G., Levin, W.J., Ullrich, A., McGuire, W.L. "Human breast Cancer: Correlation of relapse and survival with amplification of the her-2/neu oncogene". Science, 235:177-182, 1987.
4. Xing, W.R., Gilchrist, K.W., Harris, C.P., Samson, W., Meisner, L.F. "FISH detection of HER-s/neu oncogene amplification in early onset breast cancer". Breast Cancer Res. And Treatment 39(2):203-212, 1996.
5. Press, M.F. Bernstein, L., Thomas, P.A., Meisner, L.F., Zhou, J.Y., Ma, Y., Hung, G., Robinson, R.A., Harris, C., El-Naggar, A., Slamon, D.J., Phillips, R.N., Ross, J.S., Wolman, S.R., Flom, K.J., "Her-2/neu gene amplification characterized by fluorescence in situ hybridization: poor prognosis in node-negative breast carcinomas", J. Clinical Oncology 15(8):2894-2904, 1997.

Provided for the clients of

PATHOLOGY ASSOCIATES MEDICAL LABORATORIES
PACLAB NETWORK LABORATORIES
TRI-CITIES LABORATORY
TREASURE VALLEY LABORATORY

For more information, please contact your local representative.

© 1999 by Pathology Associates Medical Laboratories.

Genome-wide Study of Gene Copy Numbers, Transcripts, and Protein Levels in Pairs of Non-invasive and Invasive Human Transitional Cell Carcinomas*

Torben F. Ørntoft‡§, Thomas Thykjaer¶, Frederic M. Waldman‖, Hans Wolf**, and Julio E. Celis‡‡

Gain and loss of chromosomal material is characteristic of bladder cancer, as well as malignant transformation in general. The consequences of these changes at both the transcription and translation levels is at present unknown partly because of technical limitations. Here we have attempted to address this question in pairs of non-invasive and invasive human bladder tumors using a combination of technology that included comparative genomic hybridization, high density oligonucleotide array-based monitoring of transcript levels (5600 genes), and high resolution two-dimensional gel electrophoresis. The results showed that there is a gene dosage effect that in some cases superimposes on other regulatory mechanisms. This effect depended ($p < 0.015$) on the magnitude of the comparative genomic hybridization change. In general (18 of 23 cases), chromosomal areas with more than 2-fold gain of DNA showed a corresponding increase in mRNA transcripts. Areas with loss of DNA, on the other hand, showed either reduced or unaltered transcript levels. Because most proteins resolved by two-dimensional gels are unknown it was only possible to compare mRNA and protein alterations in relatively few cases of well focused abundant proteins. With few exceptions we found a good correlation ($p < 0.005$) between transcript alterations and protein levels. The implications, as well as limitations, of the approach are discussed. *Molecular & Cellular Proteomics 1:37–45, 2002.*

Aneuploidy is a common feature of most human cancers (1), but little is known about the genome-wide effect of this phenomenon at both the transcription and translation levels. High throughput array studies of the breast cancer cell line BT474 has suggested that there is a correlation between DNA copy numbers and gene expression in highly amplified areas (2), and studies of individual genes in solid tumors have revealed a good correlation between gene dose and mRNA or protein levels in the case of c-erb-B2, *cyclin d1*, *ems1*, and N-myc (3–5). However, a high cyclin D1 protein expression has been observed without simultaneous amplification (4), and a low level of c-myc copy number increase was observed without concomitant c-myc protein overexpression (6).

In human bladder tumors, karyotyping, fluorescent *in situ* hybridization, and comparative genomic hybridization (CGH)[1] have revealed chromosomal aberrations that seem to be characteristic of certain stages of disease progression. In the case of non-invasive pTa transitional cell carcinomas (TCCs), this includes loss of chromosome 9 or parts of it, as well as loss of Y in males. In minimally invasive pT1 TCCs, the following alterations have been reported: 2q−, 11p−, 1q+, 11q13+, 17q+, and 20q+ (7–12). It has been suggested that these regions harbor tumor suppressor genes and oncogenes; however, the large chromosomal areas involved often contain many genes, making meaningful predictions of the functional consequences of losses and gains very difficult.

In this investigation we have combined genome-wide technology for detecting genomic gains and losses (CGH) with gene expression profiling techniques (microarrays and proteomics) to determine the effect of gene copy number on transcript and protein levels in pairs of non-invasive and invasive human bladder TCCs.

EXPERIMENTAL PROCEDURES

Material—Bladder tumor biopsies were sampled after informed consent was obtained and after removal of tissue for routine pathology examination. By light microscopy tumors 335 and 532 were staged by an experienced pathologist as pTa (superficial papillary),

From the ‡Department of Clinical Biochemistry, Molecular Diagnostic Laboratory and **Department of Urology, Aarhus University Hospital, Skejby, DK-8200 Aarhus N, Denmark, ¶AROS Applied Biotechnology ApS, Gustav Wiedsvej 10, DK-8000 Aarhus C, Denmark, ‖UCSF Cancer Center and Department of Laboratory Medicine, University of California, San Francisco, CA 94143-0808, and ‡‡Institute of Medical Biochemistry and Danish Centre for Human Genome Research, Ole Worms Allé 170, Aarhus University, DK-8000 Aarhus C, Denmark

Received, September 26, 2001, and in revised form, November 7, 2001

Published, MCP Papers in Press, November 13, 2001, DOI 10.1074/mcp.M100019-MCP200

[1] The abbreviations used are: CGH, comparative genomic hybridization; TCC, transitional cell carcinoma; LOH, loss of heterozygosity; PA-FABP, psoriasis-associated fatty acid-binding protein; 2D, two-dimensional.

© 2002 by The American Society for Biochemistry and Molecular Biology, Inc.
This paper is available on line at http://www.mcponline.org

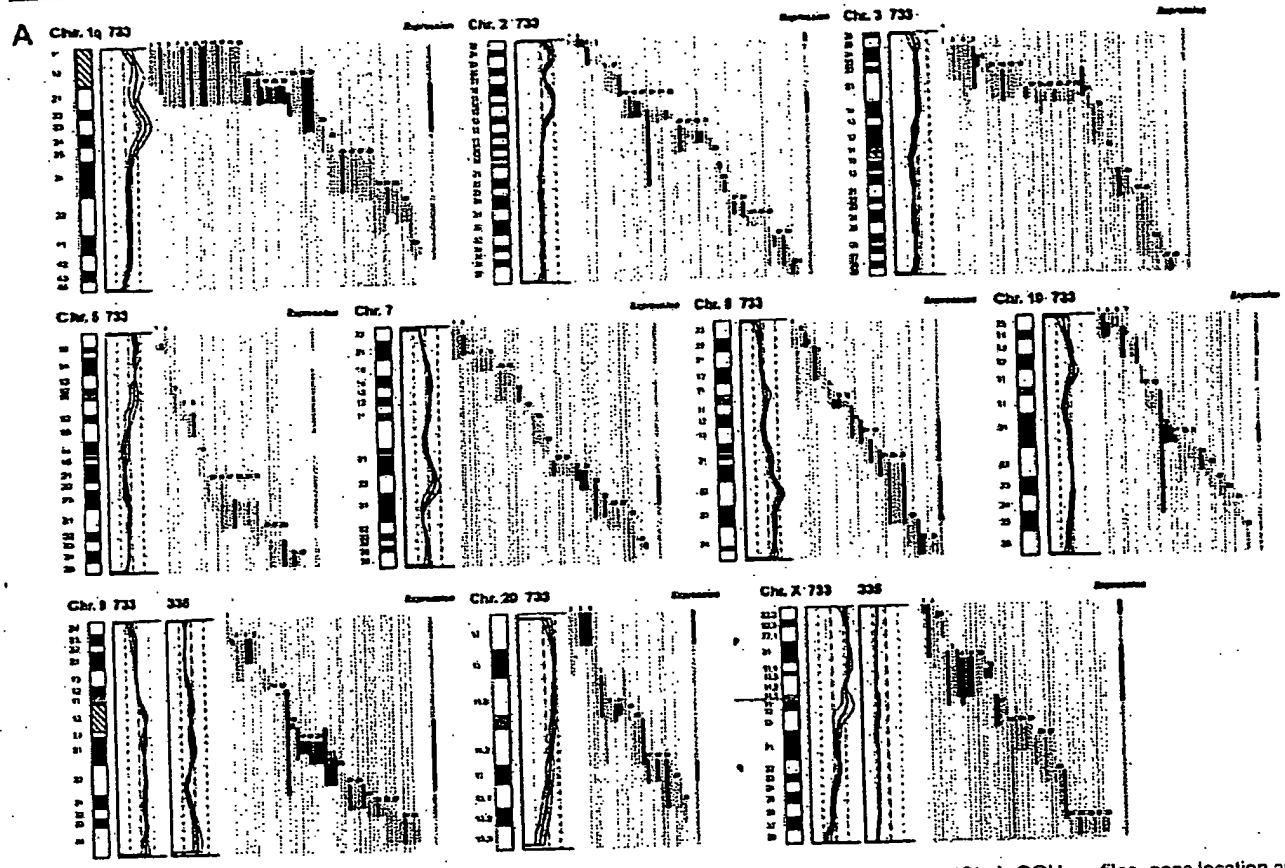

FIG. 1. **DNA copy number and mRNA expression level.** Shown from *left* to *right* are chromosome (*Chr.*), CGH profiles, gene location and expression level of specific genes, and overall expression level along the chromosome. *A*, expression of mRNA in invasive tumor 733 as compared with the non-invasive counterpart tumor 335. *B*, expression of mRNA in invasive tumor 827 compared with the non-invasive counterpart tumor 532. The average fluorescent signal ratio between tumor DNA and normal DNA is shown along the length of the chromosome (*left*). The *bold curve* in the ratio profile represents a mean of four chromosomes and is surrounded by *thin curves* indicating one standard deviation. The *central vertical line* (*broken*) indicates a ratio value of 1 (no change), and the *vertical lines* next to it (*dotted*) indicate a ratio of 0.5 (*left*) and 2.0 (*right*). In chromosomes where the non-invasive tumor 335 used for comparison showed alterations in DNA content, the ratio profile of that chromosome is shown to the *right* of the invasive tumor profile. The *colored bars* represents one gene each, identified by the running *numbers above* the *bars* (the name of the gene can be seen at www.MDL.DK/sdata.html). The *bars* indicate the purported location of the gene, and the *colors* indicate the expression level of the gene in the invasive tumor compared with the non-invasive counterpart; >2-fold increase (*black*), >2-fold decrease (*blue*), no significant change (*orange*). The *bar* to the *far right*, entitled *Expression* shows the resulting change in expression along the chromosome; the *colors* indicate that at least half of the genes were up-regulated (*black*), at least half of the genes down-regulated (*blue*), or more than half of the genes are unchanged (*orange*). If a gene was absent in one of the samples and present in another, it was regarded as more than a 2-fold change. A 2-fold level was chosen as this corresponded to one standard deviation in a double determination of ~1800 genes. Centromeres and heterochromatic regions were excluded from data analysis.

grade I and II, respectively, tumors 733 and 827 were staged as pT1 (invasive into submucosa), 733 was staged as solid, and 827 was staged as papillary, both grade III.

mRNA Preparation—Tissue biopsies, obtained fresh from surgery, were embedded immediately in a sodium-guanidinium thiocyanate solution and stored at −80 °C. Total RNA was isolated using the RNAzol B RNA isolation method (WAK-Chemie Medical GMBH). poly(A)$^+$ RNA was isolated by an oligo(dT) selection step (Oligotex mRNA kit; Qiagen).

cRNA Preparation—1 μg of mRNA was used as starting material. The first and second strand cDNA synthesis was performed using the SuperScript® choice system (Invitrogen) according to the manufacturer's instructions but using an oligo(dT) primer containing a T7 RNA polymerase binding site. Labeled cRNA was prepared using the MEGAscrip® *in vitro* transcription kit (Ambion). Biotin-labeled CTP and UTP (Enzo) was used, together with unlabeled NTPs in the reaction. Following the *in vitro* transcription reaction, the unincorporated nucleotides were removed using RNeasy columns (Qiagen).

Array Hybridization and Scanning—Array hybridization and scanning was modified from a previous method (13). 10 μg of cRNA was fragmented at 94 °C for 35 min in buffer containing 40 mM Tris acetate, pH 8.1, 100 mM KOAc, 30 mM MgOAc. Prior to hybridization, the fragmented cRNA in a 6× SSPE-T hybridization buffer (1 M NaCl, 10 mM Tris, pH 7.6, 0.005% Triton), was heated to 95 °C for 5 min, subsequently cooled to 40 °C, and loaded onto the Affymetrix probe array cartridge. The probe array was then incubated for 16 h at 40 °C at constant rotation (60 rpm). The probe array was exposed to 10 washes in 6× SSPE-T at 25 °C followed by 4 washes in 0.5× SSPE-T at 50 °C. The biotinylated cRNA was stained with a streptavidin-phycoerythrin conjugate, 10 μg/ml (Molecular Probes) in 6× SSPE-T

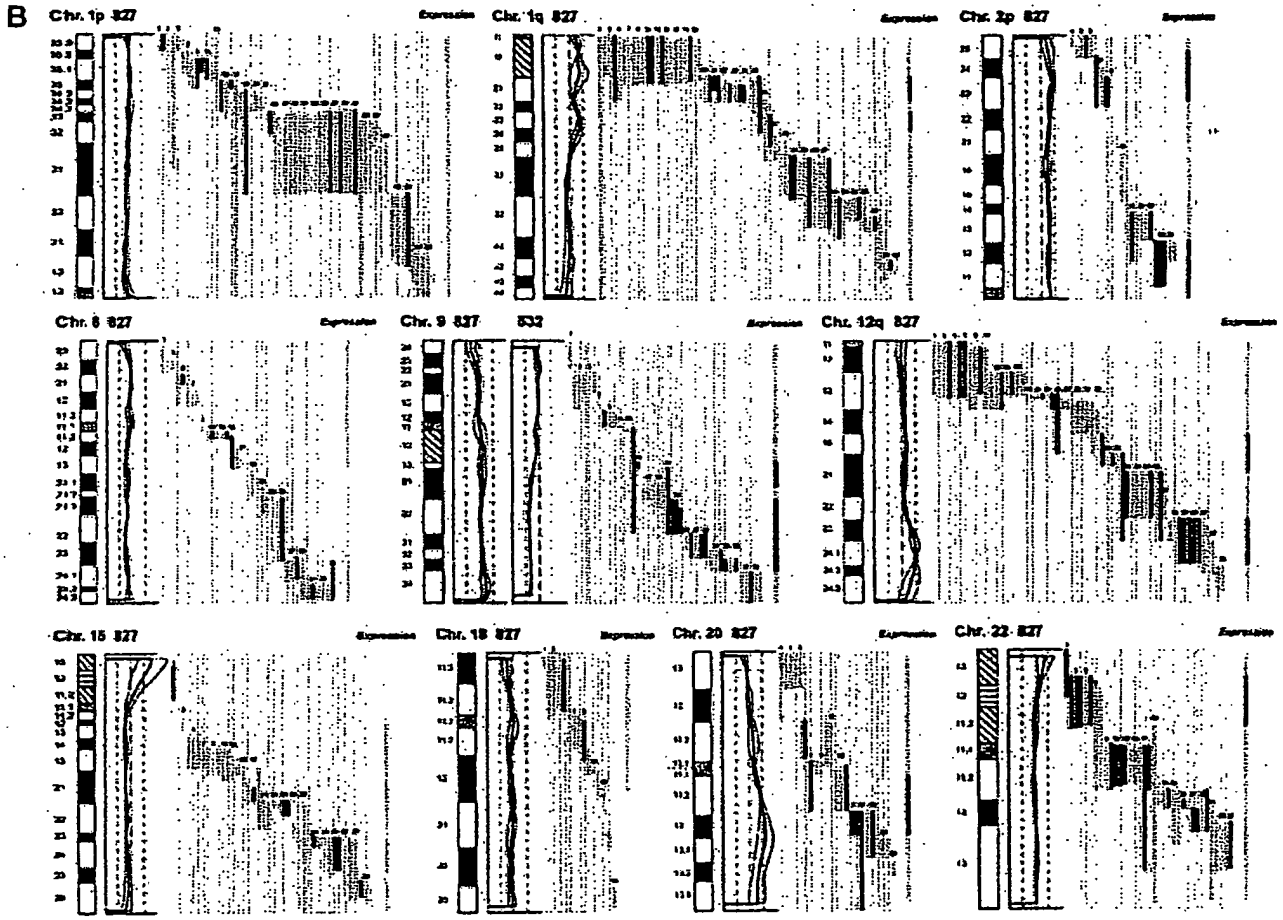

FIG. 1—*continued*

for 30 min at 25 °C followed by 10 washes in 6× SSPE-T at 25 °C. The probe arrays were scanned at 560 nm using a confocal laser scanning microscope (made for Affymetrix by Hewlett-Packard). The readings from the quantitative scanning were analyzed by Affymetrix gene expression analysis software.

Microsatellite Analysis—Microsatellite Analysis was performed as described previously (14). Microsatellites were selected by use of www.nobi.nlm.nih.gov/genemap98, and primer sequences were obtained from the genome data base at www.gdb.org. DNA was extracted from tumor and blood and amplified by PCR in a volume of 20 μl for 35 cycles. The amplicons were denatured and electrophoresed for 3 h in an ABI Prism 377. Data were collected in the Gene Scan program for fragment analysis. Loss of heterozygosity was defined as less than 33% of one allele detected in tumor amplicons compared with blood.

Proteomic Analysis—TCCs were minced into small pieces and homogenized in a small glass homogenizer in 0.5 ml of lysis solution. Samples were stored at −20 °C until use. The procedure for 2D gel electrophoresis has been described in detail elsewhere (15, 16). Gels were stained with silver nitrate and/or Coomassie Brilliant Blue. Proteins were identified by a combination of procedures that included microsequencing, mass spectrometry, two-dimensional gel Western immunoblotting, and comparison with the master two-dimensional gel image of human keratinocyte proteins; see biobase.dk/cgi-bin/celis.

CGH—Hybridization of differentially labeled tumor and normal DNA to normal metaphase chromosomes was performed as described previously (10). Fluorescein-labeled tumor DNA (200 ng), Texas Red-labeled reference DNA (200 ng), and human Cot-1 DNA (20 μg) were denatured at 37 °C for 5 min and applied to denatured normal metaphase slides. Hybridization was at 37 °C for 2 days. After washing, the slides were counterstained with 0.15 μg/ml 4,6-diamidino-2-phenylindole in an anti-fade solution. A second hybridization was performed for all tumor samples using fluorescein-labeled reference DNA and Texas Red-labeled tumor DNA (inverse labeling) to confirm the aberrations detected during the initial hybridization. Each CGH experiment also included a normal control hybridization using fluorescein- and Texas Red-labeled normal DNA. Digital image analysis was used to identify chromosomal regions with abnormal fluorescence ratios, indicating regions of DNA gains and losses. The average green:red fluorescence intensity ratio profiles were calculated using four images of each chromosome (eight chromosomes total) with normalization of the green:red fluorescence intensity ratio for the entire metaphase and background correction. Chromosome identification was performed based on 4,6-diamidino-2-phenylindole banding patterns. Only images showing uniform high intensity fluorescence with minimal background staining were analyzed. All centromeres, p arms of acrocentric chromosomes, and heterochromatic regions were excluded from the analysis.

RESULTS

Comparative Genomic Hybridization—The CGH analysis identified a number of chromosomal gains and losses in the

TABLE I

Correlation between alterations detected by CGH and by expression monitoring

Top, CGH used as independent variable (if CGH alteration – what expression ratio was found); bottom, altered expression used as independent variable (if expression alteration – what CGH deviation was found).

CGH alterations	Tumor 733 vs. 335 Expression change clusters	Concordance	CGH alterations	Tumor 827 vs. 532 Expression change clusters	Concordance
13 Gain	10 Up-regulation 0 Down-regulation 3 No change	77%	10 Gain	8 Up-regulation 0 Down-regulation 2 No change	80%
10 Loss	1 Up-regulation 5 Down-regulation 4 No change	50%	12 Loss	3 Up-regulation 2 Down regulation 7 No change	17%

Expression change clusters	Tumor 733 vs. 335 CGH alterations	Concordance	Expression change clusters	Tumor 827 vs. 532 CGH alterations	Concordance
16 Up-regulation	11 Gain 2 Loss 3 No change	69%	17 Up-regulation	10 Gain 5 Loss 2 No change	59%
21 Down-regulation	1 Gain 8 Loss 12 No change	38%	9 Down-regulation	0 Gain 3 Loss 6 No change	33%
15 No change	3 Gain 3 Loss 9 No change	60%	21 No change	1 Gain 3 Loss 17 No change	81%

two invasive tumors (stage pT1, TCCs 733 and 827), whereas the two non-invasive papillomas (stage pTa, TCCs 335 and 532) showed only 9p–, 9q22-q33–, and X–, and 7+, 9q–, and Y–, respectively. Both invasive tumors showed changes (1q22–24+, 2q14.1-qter–, 3q12-q13.3–, 6q12-q22–, 9q34+, 11q12-q13+, 17+, and 20q11.2-q12+) that are typical for their disease stage, as well as additional alterations, some of which are shown in Fig. 1. Areas with gains and losses deviated from the normal copy number to some extent, and the average numerical deviation from normal was 0.4-fold in the case of TCC 733 and 0.3-fold for TCC 827. The largest changes, amounting to at least a doubling of chromosomal content, were observed at 1q23 in TCC 733 (Fig. 1*A*) and 20q12 in TCC 827 (Fig. 1*B*).

mRNA Expression in Relation to DNA Copy Number—The mRNA levels from the two invasive tumors (TCCs 827 and 733) were compared with the two non-invasive counterparts (TCCs 532 and 335). This was done in two separate experiments in which we compared TCCs 733 to 335 and 827 to 532, respectively, using two different scaling settings for the arrays to rule out scaling as a confounding parameter. Approximately 1,800 genes that yielded a signal on the arrays were searched in the Unigene and Genemap data bases for chromosomal location, and those with a known location (1096) were plotted as bars covering their purported locus. In that way it was possible to construct a graphic presentation of DNA copy number and relative mRNA levels along the individual chromosomes (Fig. 1).

For each mRNA a ratio was calculated between the level in the invasive *versus* the non-invasive counterpart. Bars, which represent chromosomal location of a gene, were color-coded according to the expression ratio, and only differences larger than 2-fold were regarded as informative (Fig. 1). The density of genes along the chromosomes varied, and areas containing only one gene were excluded from the calculations. The resolution of the CGH method is very low, and some of the outlier data may be because of the fact that the boundaries of the chromosomal aberrations are not known at high resolution.

Two sets of calculations were made from the data. For the first set we used CGH alterations as the independent variable and estimated the frequency of expression alterations in these chromosomal areas. In general, areas with a strong gain of chromosomal material contained a cluster of genes having increased mRNA expression. For example, both chromosomes 1q21-q25, 2p and 9q, showed a relative gain of more than 100% in DNA copy number that was accompanied by increased mRNA expression levels in the two tumor pairs (Fig. 1). In most cases, chromosomal gains detected by CGH were accompanied by an increased level of transcripts in both TCCs 733 (77%) and 827 (80%) (Table I, *top*). Chromosomal losses, on the other hand, were not accompanied by decreased expression in several cases, and were often registered as having unaltered RNA levels (Table I, *top*). The inability to detect RNA expression changes in these cases was not because of fewer genes mapping to the lost regions (data not shown).

In the second set of calculations we selected expression alterations above 2-fold as the independent variable and estimated the frequency of CGH alterations in these areas. As above, we found that increased transcript expression correlated with gain of chromosomal material (TCC 733, 69% and TCC 827, 59%), whereas reduced expression was often detected in areas with unaltered CGH ratios (Table I, *bottom*). Furthermore, as a control we looked at areas with no alter-

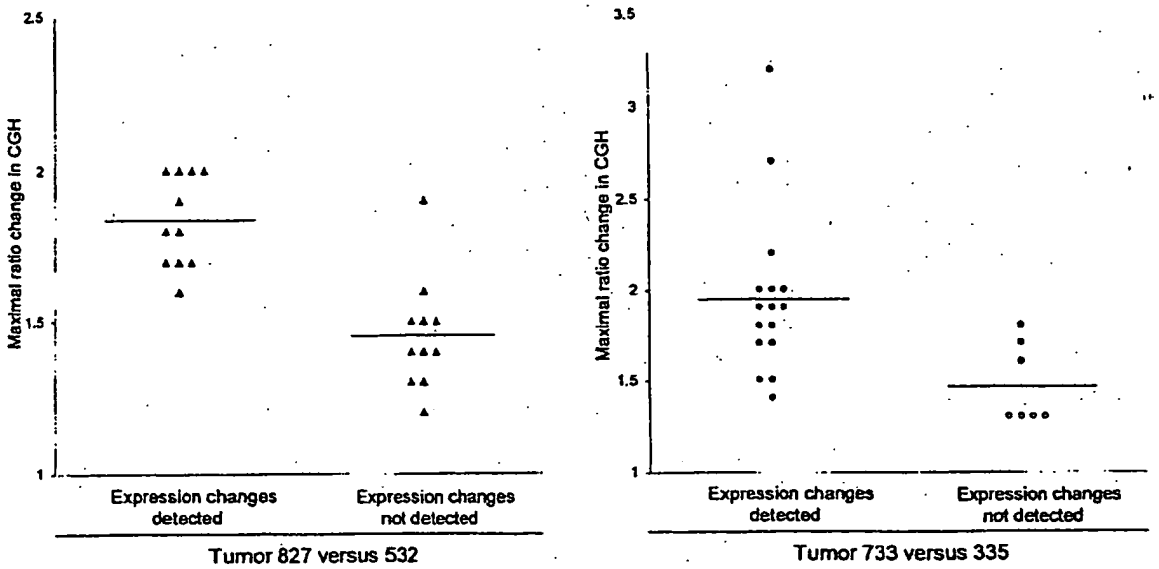

FIG. 2. **Correlation between maximum CGH aberration and the ability to detect expression change by oligonucleotide array monitoring.** The aberration is shown as a numerical -fold change in ratio between invasive tumors 827 (▲) and 733 (♦) and their non-invasive counterparts 532 and 335. The expression change was taken from the *Expression* line to the *right* in Fig. 1, which depicts the resulting expression change for a given chromosomal region. At least half of the mRNAs from a given region have to be either up- or down-regulated to be scored as an expression change. All chromosomal arms in which the CGH ratio plus or minus one standard deviation was outside the ratio value of one were included.

ation in expression. No alteration was detected by CGH in most of these areas (TCC 733, 60% and TCC 827, 81%; see Table I, *bottom*). Because the ability to observe reduced or increased mRNA expression clustering to a certain chromosomal area clearly reflected the extent of copy number changes, we plotted the maximum CGH aberrations in the regions showing CGH changes against the ability to detect a change in mRNA expression as monitored by the oligonucleotide arrays (Fig. 2). For both tumors TCC 733 ($p < 0.015$) and TCC 827 ($p < 0.00003$) a highly significant correlation was observed between the level of CGH ratio change (reflecting the DNA copy number) and alterations detected by the array based technology (Fig. 2). Similar data were obtained when areas with altered expression were used as independent variables. These areas correlated best with CGH when the CGH ratio deviated 1.6- to 2.0-fold (Table I, *bottom*) but mostly did not at lower CGH deviations. These data probably reflect that loss of an allele may only lead to a 50% reduction in expression level, which is at the cut-off point for detection of expression alterations. Gain of chromosomal material can occur to a much larger extent.

Microsatellite-based Detection of Minor Areas of Losses—In TCC 733, several chromosomal areas exhibiting DNA amplification were preceded or followed by areas with a normal CGH but reduced mRNA expression (see Fig. 1, TCC 733 chromosome 1q32, 2p21, and 7q21 and q32, 9q34, and 10q22). To determine whether these results were because of undetected loss of chromosomal material in these regions or because of other non-structural mechanisms regulating transcription, we examined two microsatellites positioned at chromosome 1q25–32 and two at chromosome 2p22. Loss of heterozygosity (LOH) was found at both 1q25 and at 2p22 indicating that minor deleted areas were not detected with the resolution of CGH (Fig. 3). Additionally, chromosome 2p in TCC 733 showed a CGH pattern of gain/no change/gain of DNA that correlated with transcript increase/decrease/increase. Thus, for the areas showing increased expression there was a correlation with the DNA copy number alterations (Fig. 1*A*). As indicated above, the mRNA decrease observed in the middle of the chromosomal gain was because of LOH, implying that one of the mechanisms for mRNA down-regulation may be regions that have undergone smaller losses of chromosomal material. However, this cannot be detected with the resolution of the CGH method.

In both TCC 733 and TCC 827, the telomeric end of chromosome 11p showed a normal ratio in the CGH analysis; however, clusters of five and three genes, respectively, lost their expression. Two microsatellites (D11S1760, D11S922) positioned close to MUC2, IGF2, and cathepsin D indicated LOH as the most likely mechanism behind the loss of expression (data not shown).

A reduced expression of mRNA observed in TCC 733 at chromosomes 3q24, 11p11, 12p12.2, 12q21.1, and 16q24 and in TCC 827 at chromosome 11p15.5, 12p11, 15q11.2, and 18q12 was also examined for chromosomal losses using microsatellites positioned as close as possible to the gene loci

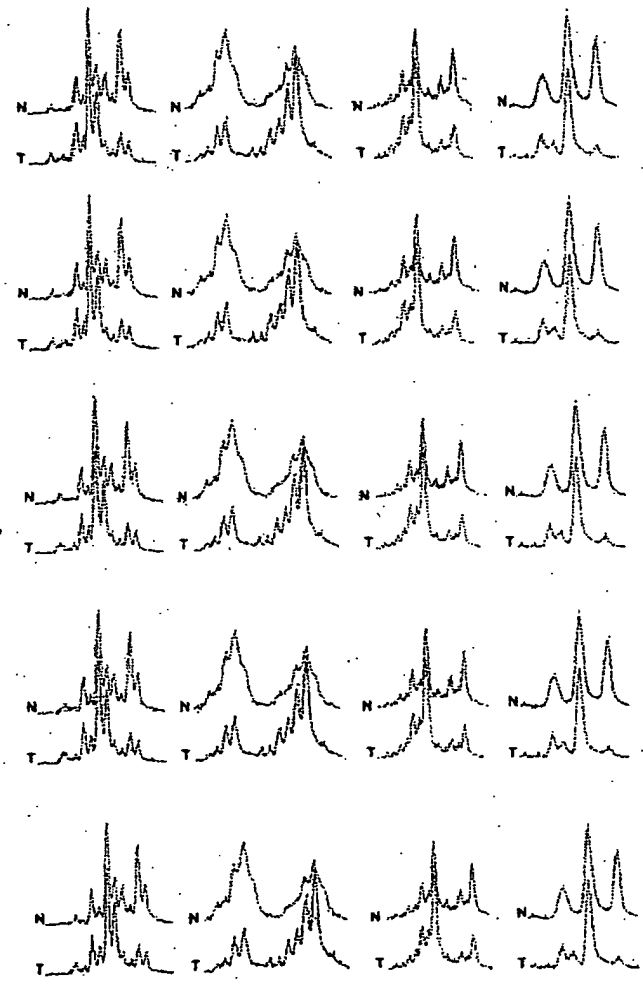

FIG. 3. **Microsatellite analysis of loss of heterozygosity.** Tumor 733 showing loss of heterozygosity at chromosome 1q25, detected (*a*) by D1S215 close to Hu class I histocompatibility antigen (gene number 38 in Fig. 1), (*b*) by D1S2735 close to cathepsin E (gene number 41 in Fig. 1), and (*c*) at chromosome 2p23 by D2S2251 close to general β-spectrin (gene number 11 on Fig. 1) and of (*d*) tumor 827 showing loss of heterozygosity at chromosome 18q12 by S18S1118 close to mitochondrial 3-oxoacyl-coenzyme A thiolase (gene number 12 in Fig. 1). The *upper curves* show the electropherogram obtained from normal DNA from leukocytes (*N*), and the *lower curves* show the electropherogram from tumor DNA (*T*). In all cases one allele is partially lost in the tumor amplicon.

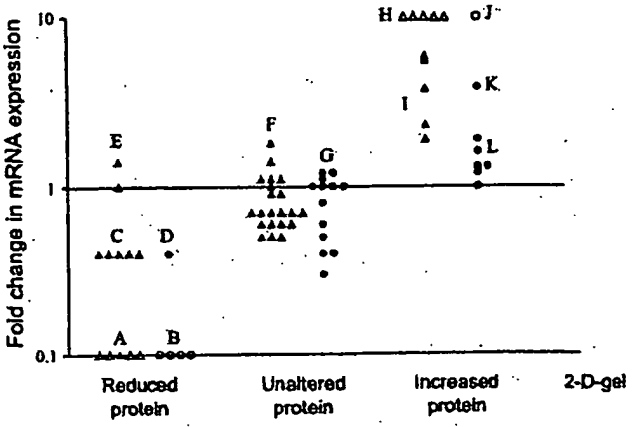

FIG. 4. **Correlation between protein levels as judged by 2D-PAGE and transcript ratio.** For comparison proteins were divided in three groups, unaltered in level or up- or down-regulated (*horizontal axis*). The mRNA ratio as determined by oligonucleotide arrays was plotted for each gene (*vertical axis*). ▲, mRNAs that were scored as present in both tumors used for the ratio calculation; Δ, mRNAs that were scored as absent in the invasive tumors (along *horizontal axis*) or as absent in non-invasive reference (*top* of figure). Two different scalings were used to exclude scaling as a confounder, TCCs 827 and 532 (▲Δ) were scaled with background suppression, and TCCs 733 and 335 (●○) were scaled without suppression. Both comparisons showed highly significant ($p < 0.005$) differences in mRNA ratios between the groups. Proteins shown were as follows: Group *A* (from *left*), phosphoglucomutase 1, glutathione transferase class μ number 4, fatty acid-binding protein homologue, cytokeratin 15, and cytokeratin 13; *B* (from *left*), fatty acid-binding protein homologue, 28-kDa heat shock protein, cytokeratin 13, and calcyclin; *C* (from *left*), α-enolase, hnRNP B1, 28-kDa heat shock protein, 14–3-3-ε, and pre-mRNA splicing factor; *D*, mesothelial keratin K7 (type II); *E* (from *top*), glutathione *S*-transferase-π and mesothelial keratin K7 (type II); *F* (from *top* and *left*), adenylyl cyclase-associated protein, E-cadherin, keratin 19, calgizzarin, phosphoglycerate mutase, annexin IV, cytoskeletal γ-actin, hnRNP A1, integral membrane protein calnexin (IP90), hnRNP H, brain-type clathrin light chain-a, hnRNP F, 70-kDa heat shock protein, heterogeneous nuclear ribonucleoprotein A/B, translationally controlled tumor protein, liver glyceraldehyde-3-phosphate dehydrogenase, keratin 8, aldehyde reductase, and Na,K-ATPase β-1 subunit; *G*, (from *top* and *left*), TCP20, calgizzarin, 70-kDa heat shock protein, calnexin, hnRNP H, cytokeratin 15, ATP synthase, keratin 19, triosephosphate isomerase, hnRNP F, liver glyceraldehyde-3-phosphatase dehydrogenase, glutathione *S*-transferase-π, and keratin 8; *H* (from *left*), plasma gelsolin, autoantigen calreticulin, thioredoxin, and NAD+-dependent 15 hydroxyprostaglandin dehydrogenase; *I* (from *top*), prolyl 4-hydroxylase β-subunit, cytokeratin 20, cytokeratin 17, prohibition, and fructose 1,6-biphosphatase; *J* annexin II; *K*, annexin IV; *L* (from *top* and *left*), 90-kDa heat shock protein, prolyl 4-hydroxylase β-subunit, α-enolase, GRP 78, cyclophilin, and cofilin.

showing reduced mRNA transcripts. Only the microsatellite positioned at 18q12 showed LOH (Fig. 3), suggesting that transcriptional down-regulation of genes in the other regions may be controlled by other mechanisms.

Relation between Changes in mRNA and Protein Levels—2D-PAGE analysis, in combination with Coomassie Brilliant Blue and/or silver staining, was carried out on all four tumors using fresh biopsy material. 40 well resolved abundant known proteins migrating in areas away from the edges of the pH gradient, and having a known chromosomal location, were selected for analysis in the TCC pair 827/532. Proteins were identified by a combination of methods (see "Experimental Procedures"). In general there was a highly significant correlation ($p < 0.005$) between mRNA and protein alterations (Fig. 4). Only one gene showed disagreement between transcript alteration and protein alteration. Except for a group of cyto-

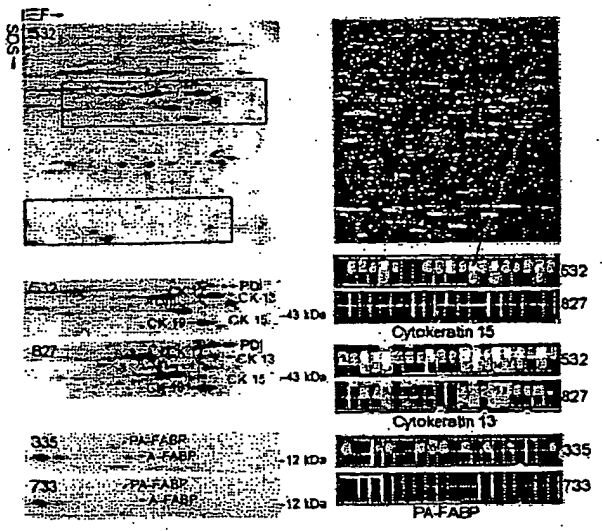

FIG. 5. **Comparison of protein and transcript levels in invasive and non-invasive TCCs.** The *upper part* of the figure shows a 2D gel (*left*) and the oligonucleotide array (*right*) of TCC 532. The *red rectangles* on the *upper gel* highlight the areas that are compared below. Identical areas of 2D gels of TCCs 532 and 827 are shown below. Clearly, cytokeratins 13 and 15 are strongly down-regulated in TCC 827 (*red annotation*). The tile on the array containing probes for cytokeratin 15 is enlarged *below* the array (*red arrow*) from TCC 532 and is compared with TCC 827. The *upper row* of *squares* in each tile corresponds to perfect match probes; the *lower row* corresponds to mismatch probes containing a mutation (used for correction for unspecific binding). Absence of signal is depicted as *black*, and the higher the signal the lighter the color. A high transcript level was detected in TCC 532 (6151 units) whereas a much lower level was detected in TCC 827 (absence of signals). For cytokeratin 13, a high transcript level was also present in TCC 532 (15659 units), and a much lower level was present in TCC 827 (623 units). The 2D gels at the *bottom* of the figure (*left*) show levels of PA-FABP and adipocyte-FABP in TCCs 335 and 733 (invasive), respectively. Both proteins are down-regulated in the invasive tumor. To the *right* we show the array tiles for the PA-FABP transcript. A medium transcript level was detected in the case of TCC 335 (1277 units) whereas very low levels were detected in TCC 733 (166 units). *IEF*, isoelectric focusing.

keratins encoded by genes on chromosome 17 (Fig. 5) the analyzed proteins did not belong to a particular family. 26 well focused proteins whose genes had a know chromosomal location were detected in TCCs 733 and 335, and of these 19 correlated ($p < 0.005$) with the mRNA changes detected using the arrays (Fig. 4). For example, PA-FABP was highly expressed in the non-invasive TCC 335 but lost in the invasive counterpart (TCC 733; see Fig. 5). The smaller number of proteins detected in both 733 and 335 was because of the smaller size of the biopsies that were available.

11 chromosomal regions where CGH showed aberrations that corresponded to the changes in transcript levels also showed corresponding changes in the protein level (Table II). These regions included genes that encode proteins that are found to be frequently altered in bladder cancer, namely cytokeratins 17 and 20, annexins II and IV, and the fatty acid-binding proteins PA-FABP and FBP1. Four of these proteins were encoded by genes in chromosome 17q, a frequently amplified chromosomal area in invasive bladder cancers.

DISCUSSION

Most human cancers have abnormal DNA content, having lost some chromosomal parts and gained others. The present study provides some evidence as to the effect of these gains and losses on gene expression in two pairs of non-invasive and invasive TCCs using high throughput expression arrays and proteomics, in combination with CGH. In general, the results showed that there is a clear individual regulation of the mRNA expression of single genes, which in some cases was superimposed by a DNA copy number effect. In most cases, genes located in chromosomal areas with gains often exhibited increased mRNA expression, whereas areas showing losses showed either no change or a reduced mRNA expression. The latter might be because of the fact that losses most often are restricted to loss of one allele, and the cut-off point for detection of expression alterations was a 2-fold change, thus being at the border of detection. In several cases, how-

TABLE II

Proteins whose expression level correlates with both mRNA and gene dose changes

Protein	Chromosomal location	Tumor TCC	CGH alteration	Transcript alteration[a]	Protein alteration
Annexin II	1q21	733	Gain	Abs to Pres[a]	Increase
Annexin IV	2p13	733	Gain	3.9-Fold up	Increase
Cytokeratin 17	17q12-q21	827	Gain	3.8-Fold up	Increase
Cytokeratin 20	17q21.1	827	Gain	5.6-Fold up	Increase
(PA-)FABP	8q21.2	827	Loss	10-Fold down	Decrease
FBP1	9q22	827	Gain	2.3-Fold up	Increase
Plasma gelsolin	9q31	827	Gain	Abs to Pres	Increase
Heat shock protein 28	15q12-q13	827	Loss	2.5-Fold up	Decrease
Prohibitin	17q21	827/733	Gain	3.7-/2.5-Fold up[b]	Increase
Prolyl-4-hydroxyl	17q25	827/733	Gain	5.7-/1.6-Fold up	Increase
hnRNPB1	7p15	827	Loss	2.5-Fold down	Decrease

[a] Abs, absent; Pres, present.
[b] In cases where the corresponding alterations were found in both TCCs 827 and 733 these are shown as 827/733.

ever, an increase or decrease in DNA copy number was associated with *de novo* occurrence or complete loss of transcript, respectively. Some of these transcripts could not be detected in the non-invasive tumor but were present at relatively high levels in areas with DNA amplifications in the invasive tumors (*e.g.* in TCC 733 transcript from cellular ligand of annexin II gene (chromosome 1q21) from absent to 2670 arbitrary units; in TCC 827 transcript from small proline-rich protein 1 gene (chromosome 1q12-q21.1) from absent to 1326 arbitrary units). It may be anticipated from these data that significant clustering of genes with an increased expression to a certain chromosomal area indicates an increased likelihood of gain of chromosomal material in this area.

Considering the many possible regulatory mechanisms acting at the level of transcription, it seems striking that the gene dose effects were so clearly detectable in gained areas. One hypothetical explanation may lie in the loss of controlled methylation in tumor cells (17–19). Thus, it may be possible that in chromosomes with increased DNA copy numbers two or more alleles could be demethylated simultaneously leading to a higher transcription level, whereas in chromosomes with losses the remaining allele could be partly methylated, turning off the process (20, 21). A recent report has documented a ploidy regulation of gene expression in yeast, but in this case all the genes were present in the same ratio (22), a situation that is not analogous to that of cancer cells, which show marked chromosomal aberrations, as well as gene dosage effects.

Several CGH studies of bladder cancer have shown that some chromosomal aberrations are common at certain stages of disease progression, often occurring in more than 1 of 3 tumors. In pTa tumors, these include 9p−, 9q−, 1q+, Y− (2, 6), and in pT1 tumors, 2q−,11p−, 11q−, 1q+, 5p+, 8q+, 17q+, and 20q+ (2–4, 6, 7). The pTa tumors studied here showed similar aberrations such as 9p− and 9q22-q33− and 9q− and Y−, respectively. Likewise, the two minimal invasive pT1 tumors showed aberrations that are commonly seen at that stage, and TCC 827 had a remarkable resemblance to the commonly seen pattern of losses and gains, such as 1q22–24 amplification (seen in both tumors), 11q14-q22 loss, the latter often linked to 17 q+ (both tumors), and 1q+ and 9p−, often linked to 20q+ and 11 q13+ (both tumors) (7–9). These observations indicate that the pairs of tumors used in this study exhibit chromosomal changes observed in many tumors, and therefore the findings could be of general importance for bladder cancer.

Considering that the mapping resolution of CGH is of about 20 megabases it is only possible to get a crude picture of chromosomal instability using this technique. Occasionally, we observed reduced transcript levels close to or inside regions with increased copy numbers. Analysis of these regions by positioning heterozygous microsatellites as close as possible to the locus showing reduced gene expression revealed loss of heterozygosity in several cases. It seems likely that multiple and different events occur along each chromosomal arm and that the use of cDNA microarrays for analysis of DNA copy number changes will reach a resolution that can resolve these changes, as has recently been proposed (2). The outlier data were not more frequent at the boundaries of the CGH aberrations. At present we do not know the mechanism behind chromosomal aneuploidy and cannot predict whether chromosomal gains will be transcribed to a larger extent than the two native alleles. A mechanism as genetic imprinting has an impact on the expression level in normal cells and is often reduced in tumors. However, the relation between imprinting and gain of chromosomal material is not known.

We regard it as a strength of this investigation that we were able to compare invasive tumors to benign tumors rather than to normal urothelium, as the tumors studied were biologically very close and probably may represent successive steps in the progression of bladder cancer. Despite the limited amount of fresh tissue available it was possible to apply three different state of the art methods. The observed correlation between DNA copy number and mRNA expression is remarkable when one considers that different pieces of the tumor biopsies were used for the different sets of experiments. This indicate that bladder tumors are relatively homogenous, a notion recently supported by CGH and LOH data that showed a remarkable similarity even between tumors and distant metastasis (10, 23).

In the few cases analyzed, mRNA and protein levels showed a striking correspondence although in some cases we found discrepancies that may be attributed to translational regulation, post-translational processing, protein degradation, or a combination of these. Some transcripts belong to undertranslated mRNA pools, which are associated with few translationally inactive ribosomes; these pools, however, seem to be rare (24). Protein degradation, for example, may be very important in the case of polypeptides with a short half-life (*e.g.* signaling proteins). A poor correlation between mRNA and protein levels was found in liver cells as determined by arrays and 2D-PAGE (25), and a moderate correlation was recently reported by Ideker *et al.* (26) in yeast.

Interestingly, our study revealed a much better correlation between gained chromosomal areas and increased mRNA levels than between loss of chromosomal areas and reduced mRNA levels. In general, the level of CGH change determined the ability to detect a change in transcript. One possible explanation could be that by losing one allele the change in mRNA level is not so dramatic as compared with gain of material, which can be rather unlimited and may lead to a severalfold increase in gene copy number resulting in a much higher impact on transcript level. The latter would be much easier to detect on the expression arrays as the cut-off point was placed at a 2-fold level so as not to be biased by noise on the array. Construction of arrays with a better signal to noise ratio may in the future allow detection of lesser than 2-fold alterations in transcript levels, a feature that may facilitate the analysis of the effect of loss of chromosomal areas on transcript levels.

In eleven cases we found a significant correlation between DNA copy number, mRNA expression, and protein level. Four of these proteins were encoded by genes located at a frequently amplified area in chromosome 17q. Whether DNA copy number is one of the mechanisms behind alteration of these eleven proteins is at present unknown and will have to be proved by other methods using a larger number of samples. One factor making such studies complicated is the large extent of protein modification that occurs after translation, requiring immunoidentification and/or mass spectrometry to correctly identify the proteins in the gels.

In conclusion, the results presented in this study exemplify the large body of knowledge that may be possible to gather in the future by combining state of the art techniques that follow the pathway from DNA to protein (26). Here, we used a traditional chromosomal CGH method, but in the future high resolution CGH based on microarrays with many thousand radiation hybrid-mapped genes will increase the resolution and information derived from these types of experiments (2). Combined with expression arrays analyzing transcripts derived from genes with known locations, and 2D gel analysis to obtain information at the post-translational level, a clearer and more developed understanding of the tumor genome will be forthcoming.

Acknowledgments—We thank Mie Madsen, Hanne Steen, Inge Lis Thorsen, Hans Lund, Vikolaj Ørntoft, and Lynn Bjerke for technical help and Thomas Gingeras, Christine Harrington, and Morten Østergaard for valuable discussions.

• This work was supported by grants from The Danish Cancer Society, the University of Aarhus, Aarhus County, Novo Nordic, the Danish Biotechnology Program, the Frenkels Foundation, the John and Birthe Meyer Foundation, and NCI, National Institutes of Health Grant CA47537. The costs of publication of this article were defrayed in part by the payment of page charges. This article must therefore be hereby marked "*advertisement*" in accordance with 18 U.S.C. Section 1734 solely to indicate this fact.

§ To whom correspondence should be addressed: Dept. of Clinical Biochemistry, Molecular Diagnostic Laboratory, Aarhus University Hospital, Skejby, DK-8200 Aarhus N, Denmark. Tel.: 45-89495100/45-86156201 (private); Fax: 45-89496018; E-mail: ortoft@kba.sks.au.dk.

REFERENCES

1. Lengauer, C., Kinzler, K. W., and Vogelstein, B. (1998) Genetic instabilities in human cancers. *Nature* **17**, 643–649
2. Pollack, J. R., Perou, C. M., Alizadeh, A. A., Eisen, M. B., Pergamenschikov, A., Williams, C. F., Jeffrey, S. S., Botstein, D., and Brown, P. O. (1999) Genome-wide analysis of DNA copy-number changes using cDNA microarrays. *Nat. Genet.* **23**, 41–46
3. de Cremoux, P., Martin, E. C., Vincent-Salomon, A., Dieras, V., Barbaroux, C., Liva, S., Pouillart, P., Sastre-Garau, X., and Magdelenat, H. (1999) Quantitative PCR analysis of c-erb B-2 (HER2/neu) gene amplification and comparison with p185(HER2/neu) protein expression in breast cancer drill biopsies. *Int. J. Cancer* **83**, 157–161
4. Brungier, P. P., Tamimi, Y., Shuuring, E., and Schalken, J. (1996) Expression of cyclin D1 and EMS1 in bladder tumors; relationship with chromosome 11q13 amplifications. *Oncogene* **12**, 1747–1753
5. Slavc, I., Ellenbogen, R., Jung, W. H., Vawter, G. F., Kretschmar, C., Grier, H., and Korf, B. R. (1990) *myc* gene amplification and expression in primary human neuroblastoma. *Cancer Res.* **50**, 1459–1463
6. Sauter, G., Carroll, P., Moch, H., Kallioniemi, A., Kerschmann, R., Narayan, P., Mihatsch, M. J., and Waldman, F. M. (1995) c-*myc* copy number gains in bladder cancer detected by fluorescence *in situ* hybridization. *Am J. Pathol.* **146**, 1131–1139
7. Richter, J., Jiang, F., Gorog, J. P., Sartorious, G., Egenter, C., Gasser, T. C., Moch, H., Mihatsch, M. J., and Sauter, G. (1997) Marked genetic differences between stage pTa and stage pT1 papillary bladder cancer detected by comparative genomic hybridization. *Cancer Res.* **57**, 2860–2864
8. Richter, J., Beffa, L., Wagner, U., Schraml, P., Gasser, T. C., Moch, H., Mihatsch, M. J., and Sauter, G. (1998) Patterns of chromosomal imbalances in advanced urinary bladder cancer detected by comparative genomic hybridization. *Am. J. Pathol.* **153**, 1615–1621
9. Bruch, J., Wohr, G., Hautmann, R., Mattfeldt, T., Bruderlein, S., Moller, P., Sauter, S., Hameister, H., Vogel, W., and Paiss, T. (1998) Chromosomal changes during progression of transitional cell carcinoma of the bladder and delineation of the amplified interval on chromosome arm 8q. *Genes Chromosomes Cancer* **23**, 167–174
10. Hovey, R. M., Chu, L., Balazs, M., De Vries, S., Moore, D., Sauter, G., Carroll, P. R., and Waldman, F. M. (1998) Genetic alterations in primary bladder cancers and their metastases. *Cancer Res.* **15**, 3555–3560
11. Simon, R., Burger, H., Brinkschmidt, C., Bocker, W., Hertle, L., and Terpe, H. J. (1998) Chromosomal aberrations associated with invasion in papillary superficial bladder cancer. *J. Pathol.* **185**, 345–351
12. Koo, S. H., Kwon, K. C., Ihm, C. H., Jeon, Y. M., Park, J. W., and Sul, C. K. (1999) Detection of genetic alterations in bladder tumors by comparative genomic hybridization and cytogenetic analysis. *Cancer Genet. Cytogenet.* **110**, 87–93
13. Wodicka, L., Dong, H., Mittmann, M., Ho, M. H., and Lockhart, D. J. (1997) Genome-wide expression monitoring in *Saccharomyces cerevisiae*. *Nat. Biotechnol.* **15**, 1359–1367
14. Christensen, M., Sunde, L., Bolund, L., and Ortoft, T. F. (1999) Comparison of three methods of microsatellite detection. *Scand. J. Clin. Lab. Invest.* **59**, 167–177
15. Celis, J. E., Ostergaard, M., Basse, B., Celis, A., Lauridsen, J. B., Ratz, G. P., Andersen, I., Hein, B., Wolf, H., Orntoft, T. F., and Rasmussen, H. H. (1996) Loss of adipocyte-type fatty acid binding protein and other protein biomarkers is associated with progression of human bladder transitional cell carcinomas. *Cancer Res.* **56**, 4782–4790
16. Celis, J. E., Ratz, G., Basse, B., Lauridsen, J. B., and Celis, A. (1994) in *Cell Biology: A Laboratory Handbook* (Celis, J. E., ed) Vol. 3, pp. 222–230, Academic Press, Orlando, FL
17. Ohlsson, R., Tycko, B., and Sapienza, C. (1998) Monoallelic expression: 'there can only be one'. *Trends Genet.* **14**, 435–438
18. Hollander, G. A., Zuklys, S., Morel, C., Mizoguchi, E., Mobisson, K., Simpson, S., Terhorst, C., Wishart, W., Golan, D. E., Bhan, A. K., and Burakoff, S. J. (1998) Monoallelic expression of the interleukin-2 locus. *Science* **279**, 2118–2121
19. Brannan, C. I., and Bartolomei, M. S. (1999) Mechanisms of genomic imprinting. *Curr. Opin. Genet. Dev.* **9**, 164–170
20. Ohlsson, R., Cui, H., He, L., Pfeifer, S., Malmikumpa, H., Jiang, S., Feinberg, A. P., and Hedborg, F. (1999) Mosaic allelic insulin-like growth factor 2 expression patterns reveal a link between Wilms' tumorigenesis and epigenetic heterogeneity. *Cancer Res.* **59**, 3889–3892
21. Cui, H., Hedborg, F., He, L., Nordenskjold, A., Sandstedt, B., Pfeifer-Ohlsson, S., and Ohlsson, R. (1997) Inactivation of H19, an imprinted and putative tumor repressor gene, is a preneoplastic event during Wilms' tumorigenesis. *Cancer Res.* **57**, 4469–4473
22. Galitski, T., Saldanha, A. J., Styles, C. A., Lander, E. S., and Fink, G. R. (1999) Ploidy regulation of gene expression. *Science* **285**, 251–254
23. Tsao, J., Yatabe, Y., Markl, I. D., Hajyan, K., Jones, P. A., and Shibata, D. (2000) Bladder cancer genotype stability during clinical progression. *Genes Chromosomes Cancer* **29**, 26–32
24. Zong, Q., Schummer, M., Hood, L., and Morris, D. R. (1999) Messenger RNA translation state: the second dimension of high-throughput expression screening. *Proc. Natl. Acad. Sci. U. S. A.* **96**, 10632–10636
25. Anderson, L., and Seilhamer, J. (1997) Comparison of selected mRNA and protein abundances in human liver. *Electrophoresis* **18**, 533–537
26. Ideker, T., Thorsson, V., Ranish, J. A., Christmas, R., Buhler, J., Eng, J. K., Bumgarner, R., Goodlett, D. R., Aebersold, R., and Hood, L. (2001) Integrated genomic and proteomic analyses of a systematically perturbed metabolic network. *Science* **292**, 929–934

research articles Journal of proteome •research

Analysis of Genomic and Proteomic Data Using Advanced Literature Mining

Yanhui Hu, Lisa M. Hines, Haifeng Weng, Dongmei Zuo, Miguel Rivera, Andrea Richardson, and Joshua LaBaer*

Institute of Proteomics, Harvard Medical School–BCMP, 240 Longwood Avenue, Boston, Massachusetts 02115

Received March 13, 2003

High-throughput technologies, such as proteomic screening and DNA micro-arrays, produce vast amounts of data requiring comprehensive analytical methods to decipher the biologically relevant results. One approach would be to manually search the biomedical literature; however, this would be an arduous task. We developed an automated literature-mining tool, termed MedGene, which comprehensively summarizes and estimates the relative strengths of all human gene–disease relationships in Medline. Using MedGene, we analyzed a novel micro-array expression dataset comparing breast cancer and normal breast tissue in the context of existing knowledge. We found no correlation between the strength of the literature association and the magnitude of the difference in expression level when considering changes as high as 5-fold; however, a significant correlation was observed ($r = 0.41$; $p = 0.05$) among genes showing an expression difference of 10-fold or more. Interestingly, this only held true for estrogen receptor (ER) positive tumors, not ER negative. MedGene identified a set of relatively understudied, yet highly expressed genes in ER negative tumors worthy of further examination.

Keywords: bioinformatics • micro-array • text mining • gene-disease association • breast cancer

Introduction

At its current pace, the accumulation of biomedical literature outpaces the ability of most researchers and clinicians to stay abreast of their own immediate fields, let alone cover a broader range of topics. For example, to follow a single disease, e.g., breast cancer, a researcher would have had to scan 130 different journals and read 27 papers per day in 1999.[1] This problem is accentuated with high-throughput technologies such as DNA micro-arrays and proteomics, which require the analysis of large datasets involving thousands of genes, many of which are unfamiliar to a particular researcher. In any microarray experiment, thousands of genes may demonstrate statistically significant expression changes, but only a fraction of these may be relevant to the study. The ability to interpret these datasets would be enhanced if they could be compared to a comprehensive summary of what is known about all genes. Thus, there is a need to summarize existing knowledge in a format that allows for the rapid analysis of associations between genes and diseases or other specific biological concepts.

One solution to this problem is to compile structured digital resources, such as the Breast Cancer Gene Database[1] and the Tumor Gene Database.[2] However, as these resources are hand-curated, the labor-intensive review process becomes a rate-limiting step in the growth of the database. As a result, these databases have a limited scale and the genes are not selected in a systematic fashion.

An alternative approach is automated text mining; a method which involves automated information extraction by searching documents for text strings and analyzing their frequency and context. This approach has been used successfully in several instances for biological applications. In most cases, it has been applied to extract information about the relationships or interactions that proteins or genes have with one another, in the literature or by functional annotation.[3-7] Thus far, few publication have applied text-mining to examine the global relationships between genes and diseases. Perez-Iratxeta et al. automatically examined the GO (Gene Ontology) annotation of genes and their predicted chromosomal locations in order to identify genes linked to inherited disorders.[8]

To obtain a more global understanding of disease development, it would be valuable to incorporate information regarding all possible gene-disease relationships, including biochemical, physiological, pharmacological, epidemiological, as well as genetic. This information would enable comprehensive comparisons between large experimental datasets and existing knowledge in the literature. This would accomplish two things. First, it would serve to validate experiments by demonstrating that known responses occur as predicted. Second, it would rapidly highlight which genes are corroborated by the literature and which genes are novel in a given context. We have utilized a computational approach to literature mining to produce a

* To whom correspondence should be addressed: jlabaer@hms.harvard.edu.

10.1021/pr0340227 CCC: $25.00 © 2003 American Chemical Society

Published on Web 05/13/2003

comprehensive set of gene-disease relationships. In addition, we have developed a novel approach to assess the strength of each association based on the frequency of citation and co-citation. We applied this tool to help interpret the data from a large micro-array gene expression experiment comparing normal and cancerous breast tissue.

Methods

MedGene Database. MedGene is a relational database, storing disease and gene information from NCBI, text mining results, statistical scores, and hyperlinks to the primary literature. MedGene has a web-based user-interface for users to query the database (http://hipseq.med.harvard.edu/MedGene/).

Text Mining Algorithms. MeSH files were downloaded from the MeSH web site at NLM (Nation Library of Medicine) (http://www.nlm.nih.gov/mesh/meshhome.html) and human disease categories were selected. LocusLink files were downloaded from the LocusLink web site at NCBI (http://www.ncbi.nih.gov/LocusLink/). Official/preferred gene symbol, official/preferred gene name, and gene alternative symbols and names, all relevant annotations and URLs for each LocusLink record, were collected. Gene search terms were used for literature searching and included all qualified gene names, gene symbols, and gene family terms. Primary gene keys, predominantly qualified gene family terms and gene official/preferred symbols, were used to index Medline records. If the official/preferred gene symbols did not meet the standards to be an index, then qualified gene official/preferred names were used. A local copy of Medline records (up to July, 2002) was pre-selected.

A JAVA module examined the MeSH terms and then indexed each Medline record with the appropriate disease terms. A separate JAVA module was used to examine the titles and abstracts for gene search terms and then to index the gene-related Medline records with the relevant primary gene key(s).

Statistical Methods. For every gene and disease pair, we counted records that were indexed for both gene and disease (double positive hits), for disease only (disease single hits), for gene only (gene single hits), and for neither gene nor disease (double negative hits) to generate a 2 × 2 contingency table. On the basis of the contingency table-framework, we applied different statistical methods to estimate the strength of gene-disease relationships and evaluated the results. These methods included chi-square analysis, Fisher's exact probabilities, relative risk of gene, and relative risk of disease[8] (http://hipseq.med.harvard.edu/MedGene/). In addition, we computed the "product of frequency", which is the product of the proportion of disease/gene double hits to disease single hits and the proportion of disease/gene double hits to gene single hits. To obtain a normal distribution, we transformed all the statistical scores using the natural logarithm. We selected the log of the product of frequency (LPF) to validate MedGene and to use for the analysis with the micro-array data. Spearman rank-correlation coefficients were used to assess the linear relationship between LPF and micro-array fold change in expression level.

Global Analysis. Diseases with at least 50 related genes were selected for clustering analysis, and the LPF scores were normalized with total score for each disease. Hierarchical clustering was done with the "Cluster" software and the clustering result was visualized using "TreeViewer" (http://rana.lbl.gov/EisenSoftware.htm).

Breast Tissue Micro-Arrays. Eighty-nine breast cancer samples (79% ER-positive) and 7 normal breast tissue samples were selected from the Harvard Breast SPORE frozen tissue repository and were representative of the spectrum of histological types, grades, and hormone receptor immuno-phenotypes of breast cancer. Biotinylated cRNA, generated from the total RNA extracted from the bulk tumor, was hybridized to Affymetrix U95A oligo-nucleotide micro-arrays. These micro-arrays consist of 12 400 probes, which represent approximately 9000 genes. Raw expression values were obtained using GENECHIP software from Affymetrix, and then further analyzed using the DNA-Chip Analyzer (dChip) custom software.

Results

Automated Indexing of Medline Records by Disease and Gene. To study the gene-disease associations in the literature, we first compiled complete lists for human diseases and human genes. To index all Medline records that were relevant to human diseases, the Medical Subject Heading (MeSH) index of Medline records was utilized. MeSH is a controlled medical vocabulary from the National Library of Medicine and consists of a set of terms or subject headings that are arranged in both an alphabetic and an hierarchical structure. Medline records are reviewed manually and MeSH terms are added to each with software assistance.[9,10] Twenty-three human disease category headings along with all of their child terms (see the Supporting Information, Supplemental Table 1, or visit http://hipseq.med.harvard.edu/MedGene/publication/s_Table1.html) were selected from the 2002 MeSH index creating a list of 4033 human diseases.

No index comparable to the MeSH index exists for genes, and thus, it was necessary to apply a string search algorithm for gene names or symbols found in Medline text. A complete list of genes, gene names, gene symbols, and frequently used synonyms were collected from the LocusLink database at NCBI,[11,12] which contains 53 259 independent records keyed by an official gene symbol or name (June 18th, 2002). For the purposes of this study, no distinction was made between genes and their gene products. Authors often use the same name for both, differentiating the two only by the use of italics, if at all. For the intended use of this study, this lack of distinction is unlikely to have a large effect and may in fact be beneficial.

Initial attempts to search the literature using these lists revealed several sources of false positives and false negatives (Table 1). False positives primarily arose when the searched term had other meanings, whereas false negatives arose from syntax discrepancies necessitating the development of filters to reduce these errors. The syntax issues were readily handled by including alternate syntax forms in the search terms. The false positive cases, caused by duplicative and unrelated meanings for the terms, were more difficult to manage. Where possible, case sensitive string mapping reduced inappropriate citations. In many cases, however, this was not sufficient and the terms had to be eliminated entirely, thereby reducing the false positive rate but unavoidably under-representing some genes.

For the purposes of data tracking, a primary gene key was selected to represent all synonyms that correspond to each gene. Medline records were indexed with a primary gene key when any synonym for that key was found in the title or abstract. Case-insensitive string mapping was used for all searches except as noted above. No additional weight was

Table 1. Systematic Sources of False Positives and False Negatives in Unfiltered Data[a]

source of error	error type	example	filter solution
gene symbol/name is not unique	false positive	*MAG*—myelin associated glycoprotein *MAG*—malignancy-associated protein	eliminate this term
gene symbol is unrelated abbreviation	false positive	*PA*—pallid homologue (mouse), pallidin (also abbrev. for Pennsylvania)	eliminate this term
gene symbol/name has language meaning	false positive	*WAS*—Wiskott–Aldrich Syndrome (also the word "was")	case-sensitive string search
nonstandard syntax	false negative	*BAG-1* instead of *BAG1*	add dash term
unofficial gene name/symbol	false negative	*P53* instead of *TP53*	add all gene nicknames
nonspecified gene name	false negative	estrogen receptor instead of Estrogen receptor 1	add family stem term

[a] In preliminary studies, Medline was searched for co-occurrence of genes and diseases and the resulting output was evaluated to identify error sources that were amenable to global filters. Each error source is categorized by the type of error it causes: false positives are suggested relationships that are not real and false negatives are real relationships that are underrepresented. The filter solutions used are indicated. Note that in some cases, the filter solution itself introduces error. In general, error rates maximized sensitivity, even at the expense of specificity if needed.

added for multiple occurrences of a term or the co-occurrence of multiple synonyms for the same gene key.

Medline records were searched with all qualified gene identifiers, such as the official/preferred gene symbol, the official/preferred gene name, all gene nicknames and all syntax variants. In situations where there are several members of a gene family or splice variants, some authors prefer to use a shortened gene family name, e.g., estrogen receptor instead of estrogen receptor 1 (*ESR1*), creating a source of false negatives. For this reason, gene family stem terms were created for all genes that have an alpha or numerical suffix (e.g., *IL2RA*, *TGFβ*, *ESR1*, etc.) and then used to search the literature. The family stem terms were handled separately from the specific gene names so that it would be clear when linkages were made to the gene family versus a specific member in that family.

To improve performance and accuracy, some pre-selection was applied to the records that were scanned. First, review articles were eliminated to avoid redundant treatment of citations. Second, non-English journals were removed because the natural language filters were only relevant to English publications. Finally, journals unlikely to contain primary data about gene-disease relationships were also removed (e.g., *Int. J. Health Educ.*, *Bedside Nurse*, and *J. Health Econ.*). Together, these filters reduced the 12 198 221 Medline publications (July 2002) by 37%.

Ranking the Relative Strengths of Gene-Disease Associations. In total, there were 618 708 gene-disease co-citations, in which 16% (8297) of all studied genes had been associated to a disease and 96% (3875) of all diseases had been associated to at least one gene. To rank the relative strengths of gene disease relationships, we tested several different statistical methods and examined the results. With the exception of the relative risk estimates, the methods provided similar results with respect to the rank order of the gene-disease association strengths. However, after comparing the results to other databases and after consulting disease experts, the log of the product of frequency (LPF) was selected for further analysis because it gave the best results overall.

Validation of MedGene. In developing this tool, it was important to minimize the number of missed genes (false negatives) and miscalled genes (false positives). However, in situations when these goals were in conflict, inclusiveness was prioritized. To determine the false negative rate in MedGene, breast cancer was used as a test case because it was associated with more genes than any other human disease and because

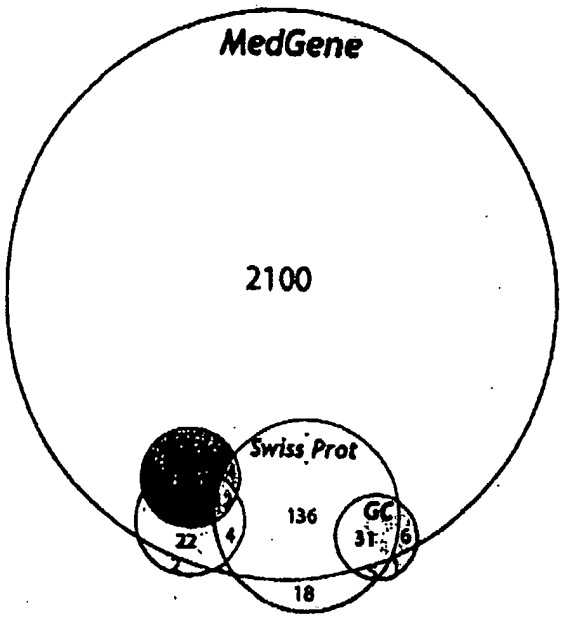

Figure 1. Estimation of the false negative rate by comparison with hand-curated databases. The breast cancer-related genes identified by MedGene were compared with those listed in several other databases including the Tumor Gene Database (TGD),[2] the Breast Cancer Gene Database(BCG),[1] GeneCards (GC)[17] and Swissprot.[18] Genes were considered false negatives if they were represented in at least one of these other databases and not in MedGene and their link to breast cancer was supported by at least one literature reference. All literature references were verified by manual review to confirm their validity. The number of genes in each database or shared by more than one database is indicated. The false negative rate was calculated by genes missed at MedGene (26)/total number of nonoverlapping genes in other databases (285).

there were several public databases that link genes to breast cancer. We compared the list of breast cancer-related genes from MedGene to these databases, illustrated in Figure 1. Among the 285 distinct breast cancer-related genes that were supported by at least one literature citation in these hand-curated databases, 26 were absent from MedGene, suggesting a false negative rate of approximately 9%. To determine why these were missed, all literature references for these genes (80

papers) were reviewed manually (see the Supporting Information, Supplemental Table 2, or visit http://hipseq.med.harvard.edu/MedGene/publication/s_Table 2.html). Among these papers, most false negatives were caused by nonstandard gene terms or gene terms eliminated by our specificity filters. Few genes were missed because they were only mentioned in review papers (0.4%) or they appeared only in the body of the manuscript but not the abstract or title (1.1%). Of note, MedGene identified approximately 2000 additional breast cancer-related genes not listed in any other database.

To assess the false positive error rate, two complementary approaches were used: a detailed analysis of one disease and a global examination of 1000 diseases. The detailed approach examined the false positive error rate and its sources, whereas the global approach tested whether the overall results made biomedical sense.

Using the LPF, 1467 genes related to prostate cancer were assembled in rank order. We then retrieved approximately 300 Medline records each for the highest ranked 100 and the lowest ranked 200 genes and manually reviewed the titles and abstracts to determine the verity of the association. Nearly 80% of the highest ranked 100 genes fell into one of the five categories that reflect meaningful gene-disease relationships (see the Supporting Information, Supplemental Table 3, or visit http://hipseq.med.harvard.edu/MedGene/publication/s_Table 3.html). Among the lowest ranked 200 genes, approximately 70% reflected true relationships. Of the 600 records reviewed, there were only two in which the association between the gene and the disease was described as negative. Both were genes with very low scores. In both cases, the authors did not argue the absence of *any* relationship, but rather that a particular feature of the gene or protein was not shown to be related to human prostate cancer.[13,14]

The coincidence of some gene symbols with medical abbreviations, chemical abbreviations and biological abbreviations resulted in most of the false positives (see the Supporting Information, Supplemental Table 4, or visit http://hipseq.med.harvard.edu/MedGene/publication/s_Table 4.html), emphasizing the importance of the filters that were added in the search algorithm (Table 1). Without the filters, the false positive rate more than doubled, and the false negative rate rose dramatically (data not shown). For example, among the papers about breast cancer, there were only 12 Medline records that referred to *ESR1* and 10 to *ESR2*, whereas almost 2000 papers mentioned estrogen receptor without specifying *ESR1* or *ESR2*; this latter group was detected by the family stem term filter.

To further validate these results, a global analysis of the gene-disease relationships described by MedGene was performed. For this experiment, it was reasoned that the more closely related the diseases are to one another, the more they will be related to the same gene sets. Thus, if the relationships defined by MedGene accurately reflected the literature, then an unsupervised hierarchical clustering of the gene data should group diseases in a manner consistent with common medical thinking. Conversely, if the clustered diseases do not make sense biologically or medically, it may reflect excessive false positives, false negatives, or inappropriate scoring of the data.

To execute this experiment, the gene sets and the corresponding LPF values for 1000 randomly selected diseases (each with at least 50 gene relationships) were used as a dataset for clustering the diseases. A review of the results showed that the resulting disease clusters were indeed logical based upon common medical knowledge (see the Supporting Information, Supplemental Figure 1, or visit http://hipseq.med.harvard.edu/MedGene/publication/s_Figure 1.html). For example, in one such cluster shown in Figure 2, diabetes and its complications grouped together and were also closely linked to diseases associated with starvation states.

The number of genes associated with a given disease can be estimated by adjusting the MedGene number up by the false negative rate (~9%) and down by the false positive rate (~26% on average). Using this, the average disease has 103.7 ± 45.3 (mean ± s.d.) genes associated with it, although the range is quite broad with 2359 genes related to breast cancer, 2122 genes related to lung cancer and no genes related to a number of diseases.

Applying MedGene to the Analysis of Large Datasets. Access to a comprehensive summary of the genes linked to human diseases provided an opportunity to analyze data obtained from a high-throughput experiment. We compared the MedGene breast cancer gene list to a gene expression data set generated from a micro-array analysis comparing breast cancer and normal breast tissue samples. Micro-array analysis identified 2286 genes that had greater than a 1-fold difference in mean expression level between breast cancer samples and normal breast samples. Using MedGene, we sorted the 2286 genes into four classes: 555 genes directly linked to breast cancer in the literature by gene term search (first-degree association by gene name); 328 genes directly linked by family term search (first-degree association by family term); 1021 genes linked to breast cancer only through other breast cancer genes (second-degree association); and 505 genes not previously associated with breast cancer. (See the Supporting Information, Supplemental Figure 2, or visit http://hipseq.med.harvard.edu/MedGene/publication/s_Figure 2.html.) Among the 505 previously unrelated genes, 467 were either newly identified genes or genes that had not previously been associated with any disease. Among the remaining 38 genes, 9 had been related to other cancers, specifically esophageal, colon, uterine, skin, and cervix.

To determine whether the genes highlighted by the micro-array analysis were more likely to have been previously linked to breast cancer in the literature, we created a two-dimensional plot of the fold change of expression level between breast cancer and normal tissue versus the literature score (LPF) (Figure 3A). There was a broad spread of expression changes among the genes directly linked to breast cancer ranging from less than 1-fold change (68%) to over 40-fold (0.3%). Notably, the majority of genes with greater than 10-fold expression changes were linked to breast cancer by first-degree association.

Among all 754 genes directly linked to breast cancer in the literature, there was no correlation between LPF and micro-array fold change ($r = 0.018$, p-value = 0.62). However, when we stratified the analysis based on the magnitude of the fold change, we observed an increasing trend in correlation (Figure 3B) suggesting that genes with a more substantial change in expression level were more likely to have a stronger association in the literature. For genes that had 10-fold change or more in expression level, the correlation increased to 0.41 (p-value = 0.05).

When we evaluated the micro-array data separately for ER positive and ER negative tumors, the trend in correlation between fold change and literature score was highly dependent on estrogen receptor status. Interestingly, there was a similar trend in correlation for ER positive tumors, but no trend in correlation for ER negative tumors.

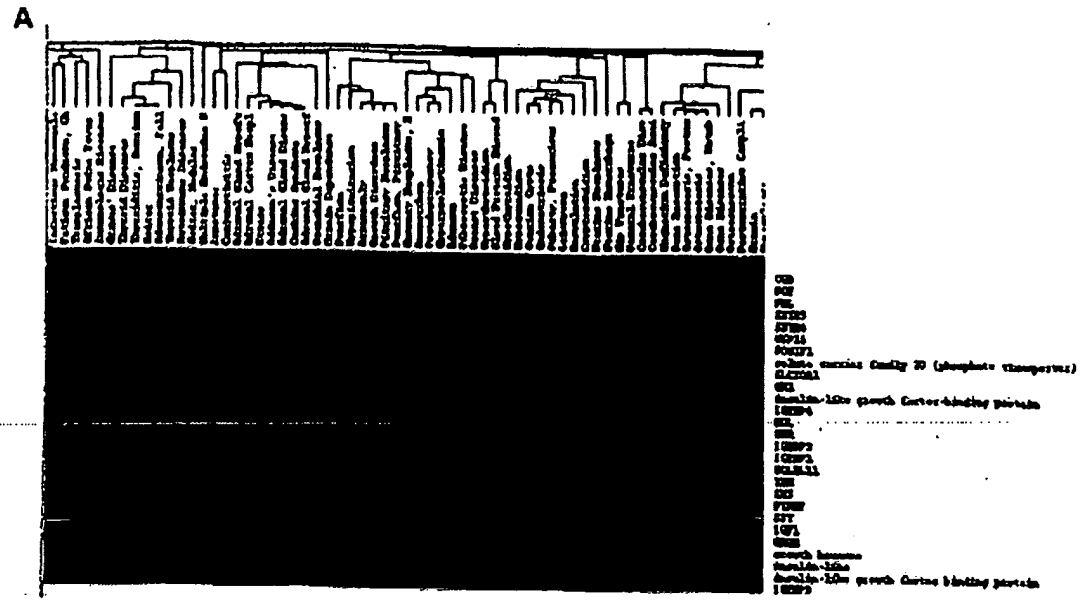

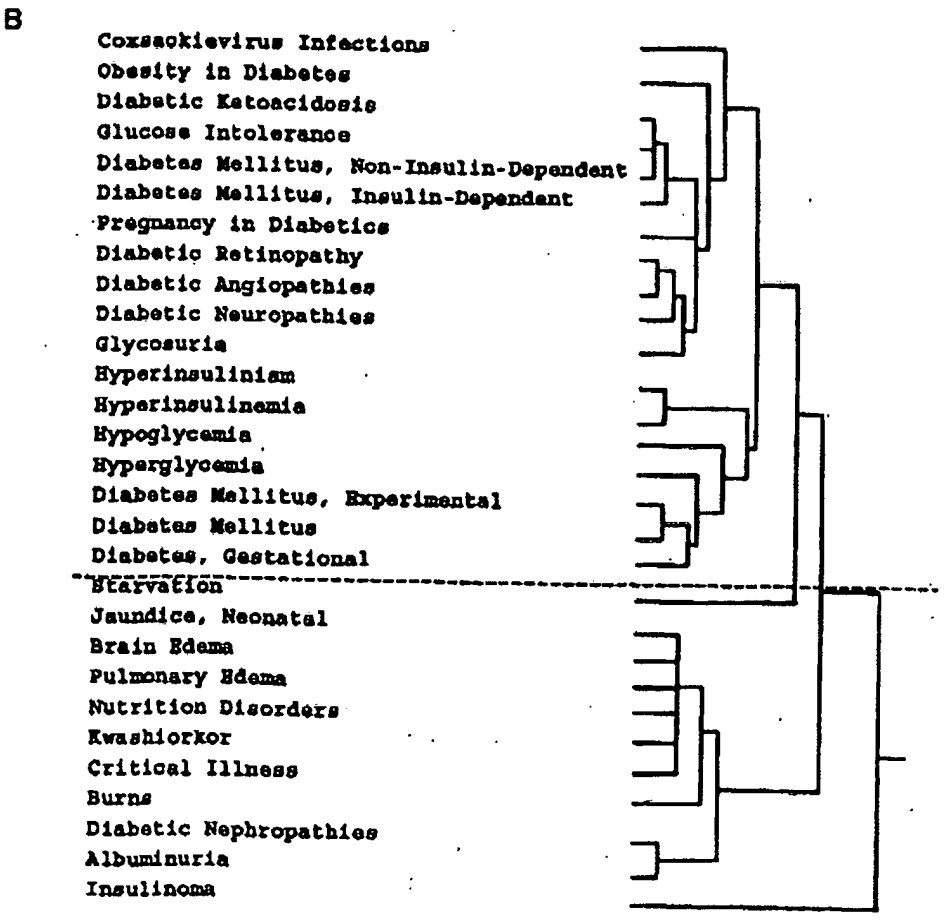

Figure 2. Global validation by clustering analysis. 2(A). The gene sets and the corresponding LPF values for 1000 diseases, each with at least 50 gene relationships, were used in an unsupervised clustering of the diseases based on the gene patterns associated with them. A sample of the data is shown here. 2(B). One of the resulting clusters is shown that corresponds to blood sugar states. Diabetes terms (above the line) and starvation states terms (under the line) clustered together. Within these groups, there is also clustering of diabetic small vessel complications, altered serum chemistries, nutritional disorders, etc.(Supplemental Figure 1: http://hlpseq.med.harvard.edu/MedGene/publication/s_Figure 1.html).

Finally, to validate our findings, we computed similar correlations between the breast cancer expression data and LPF scores generated by MedGene for hypertension, a disease unrelated to breast cancer. As expected, we did not observe an increasing trend in correlation for hypertension.

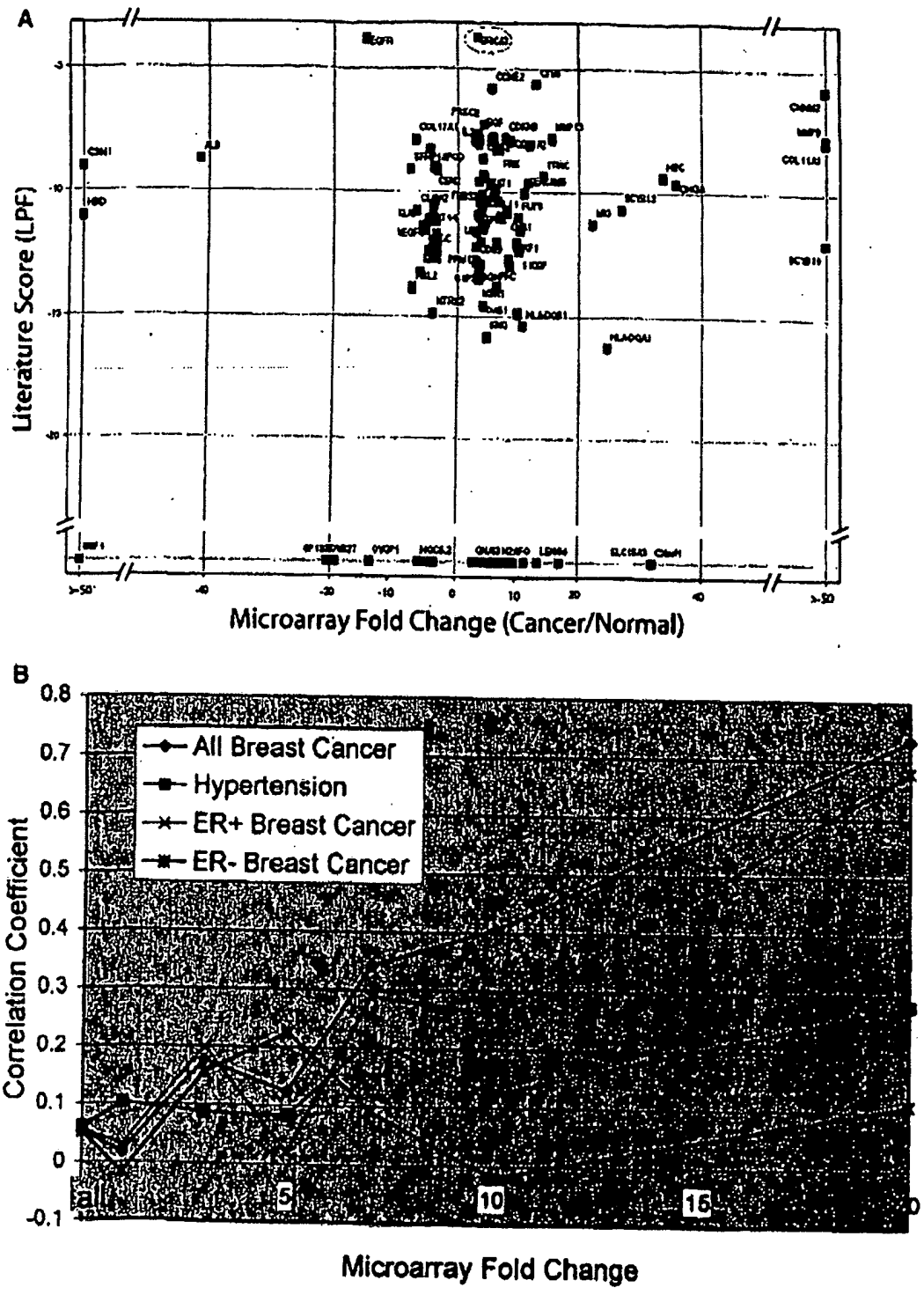

Figure 3. Relationship between literature score and functional data for breast cancer. 3A. The data from an expression analysis of samples for breast tumors and normal breast tissue were analyzed to indicate the fold difference of expression level between breast tumor and normal sample (cutoff ≥ 3-fold change). The fold changes were plotted against the literature score for the same gene set. Green dots represent first-degree association by gene search, blue dots represent first-degree association by family search and red dots represent no-association. Some well-studied genes, such as BRCA2 (pink circle), are not reflected by a substantial difference in expression level. Furthermore, the majority of genes that have no association with breast cancer in the literature had less than 10-fold expression changes (shaded area). 3B. The Spearman rank-correlation coefficients between literature score (LPF) and the fold change of expression level between tumor and normal breast samples (*y*-axis) in relation to the amount of fold change of expression level (*x*-axis). Gene rank lists were generated for breast cancer (blue) and hypertension (pink). Correlations were also computed between the breast cancer gene LPF scores and fold change expression data among estrogen receptor positive tumors only (light blue) and estrogen receptor negative tumors only (purple).

Table 2. Top 25 Genes Related to Selected Human Diseases[a]

breast neoplasms	hypertension	rheumatoid arthritis	bipolar disorder	atherosclerosis
estrogen receptor	*REN*	*RA*	*ERDA1*	apolipoprotein
PGR	*DBP*	*TNFRSF10A*	*SNAP29*	*APOE*
ERBB2	*LEP*	*CRP*	*PFKL*	*LDLR*
BRCA1	*AGT*	*AS*	*DRD2*	*ELN*
BRCA2	*INS*	*ESR1*	*TRH*	*ARG1*
EGFR	kallikrein	*HLA-DRB1*	*IMPA2*	*APOB*
CYP19	*ACE*	*DR1*	*HTR3A*	*APOA1*
TFF1	endothelin	interleukin	*DRD3*	*MSR1*
PSEN2	*S100A6*	*TNF*	*REM*	*LPL*
TP53	*BDK*	*IL6*	*KCNN3*	*PON1*
CES3	*DIANPH*	collagen	*DRD4*	plasminogen activator inhibitor
CEACAM5	*SAR1*	*IL1A*	*HTR2C*	*PLG*
ERBB3	*PIH*	*ACR*	*RELN*	vascular cell adhesion molecule
cyclin	*CD59*	*TNFRSF12*	*DBH*	*ATOH1*
COX5A	*ALB*	*IL2*	*MAOA*	*VWF*
cathepsin	*CYP11B2*	*CHI3L1*	*COMT*	*INS*
ERBB4	*MAT2B*	*IL8*	*HTR2A*	*ARG2*
TRAM	angiotensin receptor	interleukin 1	*SYNJ1*	*ABCA1*
CCND1	*AGTR2*	matrix metalloproteinase	*INPP1*	*OLR1*
EGF	*NPPA*	interferon	*NEDD4L*	collagen
MUC1	*LVM*	*CD68*	*FRA13C*	*MCP*
insulin-like	*DBH*	*IL4*	transducer of *ERBB2*	lipoprotein
BCL2	*NPY*	*IL17*	*BAIAP3*	*APOA2*
mucin	*POMC*	*MMP3*	*ATP1B3*	intercellular adhesion molecule
FGF3	neuropeptide	*SIL*	*DRD5*	*RAB27A*

[a] MedGene results for the top 25 genes associated with breast neoplasms, hypertension, rheumatoid arthritis, bipolar disorder, and atherosclerosis, respectively, ranked by LPF scores. The hyperlink to all the papers co-citing the gene and the disease is available at MedGene website (http://hlpseq.med.harvard.edu/MedGene/).

Discussion

The Human Genome Project heralded a new era in biological research where the emphasis on understanding specific pathways has expanded to global studies of genomic organization and biological systems. High-throughput technologies can provide novel insight into comprehensive biological function but also introduces new challenges. The utility of these technologies is limited to the ability to generate, analyze, and interpret large gene lists. MedGene, a relational database derived by mining the information in Medline, was created to address this need. MedGene users can query for a rank-ordered list of human gene-disease relationships (Table 2) for one or more diseases. Each entry is hyperlinked to the original papers supporting each association and to other relevant databases.

MedGene is an innovative extension of previous text mining approaches. Perez-Iratxeta et al. used the GO annotation and their chromosomal locations to predict genes that may contribute to inherited disorders.[8] MedGene takes a broader view and includes all diseases and all possible gene-disease relationships. Furthermore, MedGene utilizes co-citation to indicate a relationship rather than GO annotation, which is limited to the subset of genes that have GO annotation. Our approach is complementary to that taken by Chaussabel and Sher, who used the frequency of co-cited terms to cluster genes into a hierarchy of gene-gene relationships.[6]

A unique aspect of this tool is the ability to assess the relative strengths of gene-disease relationships based on the frequency of both co-citation and single citation. This presupposes that most co-citations describe a positive association, often referred to as publication bias[15] and is supported by our observations that negative associations are rare (Supplemental Table 3: http://hlpseq.med.harvard.edu/MedGene/publication/s_Table 3.html). Of course, relationships established by frequency of co-citation do not necessarily represent a true biological link; however, it is strong evidence to support a true relationship.

Another important feature of MedGene is the implementation of software filters that substantially reduced the error rate. We estimate that less than 10% of all associations were missed and at least 70% of even the weakest associations were real. For this study, all of the filters that we applied were general ones, e.g., expanding the list of all gene names to address the different syntax forms used by different journals, eliminating gene names that correspond to common English words, etc. The majority of the remaining search term ambiguities were idiosyncratic and difficult to identify systematically without causing a significant rise in false negatives. Alternative approaches, such as the examination of the nearest neighbor terms, need to be considered to further reduce the false positive rate.

It is not uncommon to see expression changes in micro-array experiments as small as 2-fold reported in the literature. Even when these expression changes are statistically significant, it is not always clear if they are biologically meaningful. When comparing expression levels of disease to normal tissue, one expects an enrichment of known disease-related genes to appear in the altered expression group. MedGene provided a unique opportunity to test this notion in the context of existing knowledge on a novel breast cancer micro-array dataset. For genes displaying a 5-fold change or less in tumors compared to normal, there was no evidence of a correlation between altered gene expression and a known role in the disease. This

Table 3. Genes with Large Expression Changes in ER− but Not in ER+ Breast Tumors

gene symbol	fold change (ER+)	fold change (ER−)
KRTHB1	1.0	610.8
BRS3	1.2	89.4
DKK1	1.2	69.8
ZIC1	1.9	59.6
TLR1	1.0	38.5
KIAA0680	2.6	33.2
CDKN3	1.0	30.6
EBI2	4.0	27.9
GZMB	3.8	21.9
STK18	4.7	18.6
GPR49	1.0	14.6
MYO10	1.6	14.4
LAD1	−1.0	13.5
POLE2	4.2	13.0
HMG4	4.4	12.9
BCL2L11	−1.2	12.3
LRP8	2.9	12.2
CCNB2	1.0	11.8
CCNE2	4.0	11.6
FGB	−4.3	11.1
KNSL6	2.9	10.9
H1F5	3.0	10.2
SERPINH2	4.6	10.2
YAP1	1.0	10.0
LPHB	−1.3	−10.4
TCEA2	−1.1	−10.8
TFF1	1.3	−11.4
COL17A1	−4.1	−15.7
POP5	1.1	−16.2
BPAG1	−4.6	−22.3
PDZK1	−1.1	−36.8
VECFC	−2.8	−51.5
MUC6	−1.4	−64.9
SERPINA5	−1.0	−83.1
MEIS1	−1.6	−85.9
CA12	2.4	−150.3

Table 3. MedGene identified a set of relatively understudied, yet highly expressed genes in ER negative, but not ER positive breast tumors. All of these genes have either never been co-cited with breast cancer or have a weak association except those marked with an *.

reflects the many genes whose role in breast cancer may not involve large changes in expression in sporadic tumors (e.g., *BRCA1* and *BRCA2*) and genes whose modest changes in expression may be unrelated to the disease. Strikingly, among genes with a 10-fold change or more in expression level, there was a strong and significant correlation between expression level and a published role in the disease, providing the first global validation of the micro-array approach to identifying disease-specific genes.

The results derived from MedGene have two implications. First, a careful hunt for corroborating evidence of a role in breast cancer should precede any further study of genes with less than 5-fold expression level changes. Second, any genes with 10-fold changes or more are likely to be related to breast cancer and warrant attention. It is likely that this threshold will change depending on the disease as well as the experiment.

Interestingly, the observed correlation was only found among ER-positive tumors, not ER-negative. This may reflect a bias in the literature to study the more prevalent type of tumor in the population. Furthermore, this emphasizes that caution must be taken when interpreting experiments that may contain subpopulations that behave very differently. The MedGene approach identified a set of relatively understudied, yet highly expressed genes in ER-negative tumors that are worthy of further examination (Table 3).

In conclusion, we have developed an automated method of summarizing and organizing the vast biomedical literature. To our knowledge, the resulting database is the most comprehensive and accurate of its kind. By generating a score that reflects the strength of the association, it provides an important tool for the rapid and flexible analysis of large datasets from various high-throughput screening experiments. Furthermore, it can be used for selecting subsets of genes for functional studies, for building disease-specific arrays, for looking at genes common to multiple diseases and various other high-throughput applications. In the future, it will be possible to enhance the utility of the MedGene database by building links between genes and other MeSH terms as well as other biological processes and concepts, such as cell division and responses to small molecules.

Acknowledgment. We would like to thank P. Braun, L. Garraway, J. Pearlberg, and other members of our Institute for helpful discussion. Many thanks to the NLM (National Library of Medicine) for licensing of MEDLINE and the annotation effort of adding MeSH indexes for MEDLINE abstracts. This work was funded by grants from the Breast Cancer Research Foundation and an NHLBI PGA Grant (Vol HL66582-02).

Supporting Information Available: Twenty-three human disease category headings along with all of their child terms selected from the 2002 MeSH Index (Supplemental Table 1); analysis of the causes of false negatives in MedGene (Supplemental Table); meaningful gene-disease relationships found in MedGene (Supplemental Table 3); causes for incorrect assignment of gene indexes (Supplemental Table 4); a review of the results, showing that the resulting disease clusters were indeed logical (Supplemental Figure 1); and a review of the results showing that among the 505 previously unrelated genes, 467 were either newly identified genes or genes that had not previously been associated with any disease (Supplemental Figure 2). This material is available free of charge via the Internet at http://pubs.acs.org and at the web sites mentioned in the text.

References

(1) Baasiri, R. A.; Glasser, S. R.; Steffen, D. L.; Wheeler, D. A. *Oncogene* **1999**, *18*, 7958–7965.
(2) Steffen, D. L.; Levine, A. E.; Yarus, S.; Baasiri, R. A.; Wheeler, D. A. *Bioinformatics* **2000**, *16*, 639–649.
(3) Marcotte, E. M.; Xenarios, I.; Eisenberg, D. *Bioinformatics* **2001**, *17*, 359–363.
(4) Ono, T.; Hishigaki, H.; Tanigami, A.; Takagi, T. *Bioinformatics* **2001**, *17*, 155–161.
(5) Jenssen, T. K.; Laegreid, A.; Komorowski, J.; Hovig, E. *Nat. Genet.* **2001**, *28*, 21–28.
(6) Chaussabel, D.; Sher, A. *Genome Biol.* **2002**, *3*, RESEARCH0055.
(7) Gibbons, F. D.; Roth, F. P. *Genome Res.* **2002**, *12*, 1574–1581.
(8) Perez-Iratxeta, C.; Bork, P.; Andrade, M. A. *Nat. Genet.* **2002**, *31*, 316–319.
(9) Funk, M. E.; Reid, C. A. *Bull. Med. Libr. Assoc.* **1983**, *71*, 176–183.
(10) Humphrey, S. M.; Miller, N. E. *J. Am. Soc. Inf. Sci.* **1987**, *38*, 184–196.
(11) Maglott, D. R.; Katz, K. S.; Sicotte, H.; Pruitt, K. D. *Nucleic Acids Res.* **2000**, *28*, 126–128.
(12) Pruitt, K. D.; Maglott, D. R. *Nucleic Acids Res.* **2001**, *29*, 137–140.
(13) Wadelius, M.; Andersson, A. O.; Johansson, J. E.; Wadelius, C.; Rane, E. *Pharmacogenetics* **1999**, *9*, 333–340.
(14) Adam, R. M.; Borer, J. G.; Williams, J.; Eastham, J. A.; Loughlin, K. R.; Freeman, M. R. *Endocrinology* **1999**, *140*, 5866–5875.
(15) Montori, V. M.; Smieja, M.; Guyatt, G. H. *Mayo Clin. Proc.* **2000**, *75*, 1284–1288.
(16) Denenberg, V. H. *Statistics Experimental Design for Behavioral and Biological Researchers*; Wiley-Liss: New York, 1976.
(17) Rebhan, M.; Chalifa-Caspi, V.; Prilusky, J.; Lancet, D. *Trends Genet.* **1997**, *13*, 163.
(18) Bairoch, A.; Apweiler, R. *Nucleic Acids Res.* **2000**, *28*, 45–48.

PR0340227

Proc. Natl. Acad. Sci. USA
Vol. 95, pp. 14717–14722, December 1998
Cell Biology, Medical Sciences

WISP genes are members of the connective tissue growth factor family that are up-regulated in Wnt-1-transformed cells and aberrantly expressed in human colon tumors

DIANE PENNICA*†, TODD A. SWANSON*, JAMES W. WELSH*, MARGARET A. ROY‡, DAVID A. LAWRENCE*, JAMES LEE‡, JENNIFER BRUSH‡, LISA A. TANEYHILL§, BETHANNE DEUEL‡, MICHAEL LEW¶, COLIN WATANABE‖, ROBERT L. COHEN*, MONA F. MELHEM**, GENE G. FINLEY**, PHIL QUIRKE††, AUDREY D. GODDARD‡, KENNETH J. HILLAN¶, AUSTIN L. GURNEY‡, DAVID BOTSTEIN‡,‡‡, AND ARNOLD J. LEVINE§

Departments of *Molecular Oncology, ‡Molecular Biology, ‖Scientific Computing, and ¶Pathology, Genentech Inc., 1 DNA Way, South San Francisco, CA 94080; **University of Pittsburgh School of Medicine, Veterans Administration Medical Center, Pittsburgh, PA 15240; ††University of Leeds, Leeds, LS29JT United Kingdom; ‡‡Department of Genetics, Stanford University, Palo Alto, CA 94305; and §Department of Molecular Biology, Princeton University, Princeton, NJ 08544

Contributed by David Botstein and Arnold J. Levine, October 21, 1998

ABSTRACT **Wnt family members are critical to many developmental processes, and components of the Wnt signaling pathway have been linked to tumorigenesis in familial and sporadic colon carcinomas. Here we report the identification of two genes, *WISP-1* and *WISP-2*, that are up-regulated in the mouse mammary epithelial cell line C57MG transformed by Wnt-1, but not by Wnt-4. Together with a third related gene, *WISP-3*, these proteins define a subfamily of the connective tissue growth factor family. Two distinct systems demonstrated *WISP* induction to be associated with the expression of Wnt-1. These included (*i*) C57MG cells infected with a Wnt-1 retroviral vector or expressing Wnt-1 under the control of a tetracyline repressible promoter, and (*ii*) Wnt-1 transgenic mice. The *WISP-1* gene was localized to human chromosome 8q24.1–8q24.3. *WISP-1* genomic DNA was amplified in colon cancer cell lines and in human colon tumors and its RNA overexpressed (2- to >30-fold) in 84% of the tumors examined compared with patient-matched normal mucosa. *WISP-3* mapped to chromosome 6q22–6q23 and also was overexpressed (4- to >40-fold) in 63% of the colon tumors analyzed. In contrast, *WISP-2* mapped to human chromosome 20q12–20q13 and its DNA was amplified, but RNA expression was reduced (2- to >30-fold) in 79% of the tumors. These results suggest that the *WISP* genes may be downstream of Wnt-1 signaling and that aberrant levels of *WISP* expression in colon cancer may play a role in colon tumorigenesis.**

Wnt-1 is a member of an expanding family of cysteine-rich, glycosylated signaling proteins that mediate diverse developmental processes such as the control of cell proliferation, adhesion, cell polarity, and the establishment of cell fates (1, 2). Wnt-1 originally was identified as an oncogene activated by the insertion of mouse mammary tumor virus in virus-induced mammary adenocarcinomas (3, 4). Although Wnt-1 is not expressed in the normal mammary gland, expression of Wnt-1 in transgenic mice causes mammary tumors (5).

In mammalian cells, Wnt family members initiate signaling by binding to the seven-transmembrane spanning Frizzled receptors and recruiting the cytoplasmic protein Dishevelled (Dsh) to the cell membrane (1, 2, 6). Dsh then inhibits the kinase activity of the normally constitutively active glycogen synthase kinase-3β (GSK-3β) resulting in an increase in β-catenin levels. Stabilized β-catenin interacts with the transcription factor TCF/Lef1, forming a complex that appears in the nucleus and binds TCF/Lef1 target DNA elements to activate transcription (7, 8). Other experiments suggest that the adenomatous polyposis coli (APC) tumor suppressor gene also plays an important role in Wnt signaling by regulating β-catenin levels (9). APC is phosphorylated by GSK-3β, binds to β-catenin, and facilitates its degradation. Mutations in either APC or β-catenin have been associated with colon carcinomas and melanomas, suggesting these mutations contribute to the development of these types of cancer, implicating the Wnt pathway in tumorigenesis (1).

Although much has been learned about the Wnt signaling pathway over the past several years, only a few of the transcriptionally activated downstream components activated by Wnt have been characterized. Those that have been described cannot account for all of the diverse functions attributed to Wnt signaling. Among the candidate Wnt target genes are those encoding the nodal-related 3 gene, *Xnr3*, a member of the transforming growth factor (TGF)-β superfamily, and the homeobox genes, *engrailed*, *goosecoid*, *twin* (*Xtwn*), and *siamois* (2). A recent report also identifies c-*myc* as a target gene of the Wnt signaling pathway (10).

To identify additional downstream genes in the Wnt signaling pathway that are relevant to the transformed cell phenotype, we used a PCR-based cDNA subtraction strategy, suppression subtractive hybridization (SSH) (11), using RNA isolated from C57MG mouse mammary epithelial cells and C57MG cells stably transformed by a Wnt-1 retrovirus. Overexpression of Wnt-1 in this cell line is sufficient to induce a partially transformed phenotype, characterized by elongated and refractile cells that lose contact inhibition and form a multilayered array (12, 13). We reasoned that genes differentially expressed between these two cell lines might contribute to the transformed phenotype.

In this paper, we describe the cloning and characterization of two genes up-regulated in Wnt-1 transformed cells, *WISP-1* and *WISP-2*, and a third related gene, *WISP-3*. The *WISP* genes are members of the CCN family of growth factors, which includes connective tissue growth factor (CTGF), Cyr61, and *nov*, a family not previously linked to Wnt signaling.

MATERIALS AND METHODS

SSH. SSH was performed by using the PCR-Select cDNA Subtraction Kit (CLONTECH). Tester double-stranded

The publication costs of this article were defrayed in part by page charge payment. This article must therefore be hereby marked "*advertisement*" in accordance with 18 U.S.C. §1734 solely to indicate this fact.

© 1998 by The National Academy of Sciences 0027-8424/98/9514717-6$2.00/0
PNAS is available online at www.pnas.org.

Abbreviations: TGF, transforming growth factor; CTGF, connective tissue growth factor; SSH, suppression subtractive hybridization; VWC, von Willebrand factor type C module.

Data deposition: The sequences reported in this paper have been deposited in the Genbank database (accession nos. AF100777, AF100778, AF100779, AF100780, and AF100781).

†To whom reprint requests should be addressed. e-mail: diane@gene.com.

cDNA was synthesized from 2 μg of poly(A)$^+$ RNA isolated from the C57MG/Wnt-1 cell line and driver cDNA from 2 μg of poly(A)$^+$ RNA from the parent C57MG cells. The subtracted cDNA library was subcloned into a pGEM-T vector for further analysis.

cDNA Library Screening. Clones encoding full-length mouse *WISP-1* were isolated by screening a λgt10 mouse embryo cDNA library (CLONTECH) with a 70-bp probe from the original partial clone 568 sequence corresponding to amino acids 128–169. Clones encoding full-length human *WISP-1* were isolated by screening λgt10 lung and fetal kidney cDNA libraries with the same probe at low stringency. Clones encoding full-length mouse and human *WISP-2* were isolated by screening a C57MG/Wnt-1 or human fetal lung cDNA library with a probe corresponding to nucleotides 1463–1512. Full-length cDNAs encoding *WISP-3* were cloned from human bone marrow and fetal kidney libraries.

Expression of Human *WISP* RNA. PCR amplification of first-strand cDNA was performed with human Multiple Tissue cDNA panels (CLONTECH) and 300 μM of each dNTP at 94°C for 1 sec, 62°C for 30 sec, 72°C for 1 min, for 22–32 cycles. *WISP* and glyceraldehyde-3-phosphate dehydrogenase primer sequences are available on request.

***In Situ* Hybridization.** ^{33}P-labeled sense and antisense riboprobes were transcribed from an 897-bp PCR product corresponding to nucleotides 601–1440 of mouse *WISP-1* or a 294-bp PCR product corresponding to nucleotides 82–375 of mouse *WISP-2*. All tissues were processed as described (40).

Radiation Hybrid Mapping. Genomic DNA from each hybrid in the Stanford G3 and Genebridge4 Radiation Hybrid Panels (Research Genetics, Huntsville, AL) and human and hamster control DNAs were PCR-amplified, and the results were submitted to the Stanford or Massachusetts Institute of Technology web servers.

Cell Lines, Tumors, and Mucosa Specimens. Tissue specimens were obtained from the Department of Pathology (University of Pittsburgh) for patients undergoing colon resection and from the University of Leeds, United Kingdom. Genomic DNA was isolated (Qiagen) from the pooled blood of 10 normal human donors, surgical specimens, and the following ATCC human cell lines: SW480, COLO 320DM, HT-29, WiDr, and SW403 (colon adenocarcinomas), SW620 (lymph node metastasis, colon adenocarcinoma), HCT 116 (colon carcinoma), SK-CO-1 (colon adenocarcinoma, ascites), and HM7 (a variant of ATCC colon adenocarcinoma cell line LS 174T). DNA concentration was determined by using Hoechst dye 33258 intercalation fluorimetry. Total RNA was prepared by homogenization in 7 M GuSCN followed by centrifugation over CsCl cushions or prepared by using RNAzol.

Gene Amplification and RNA Expression Analysis. Relative gene amplification and RNA expression of *WISP*s and c-*myc* in the cell lines, colorectal tumors, and normal mucosa were determined by quantitative PCR. Gene-specific primers and fluorogenic probes (sequences available on request) were designed and used to amplify and quantitate the genes. The relative gene copy number was derived by using the formula $2^{(\Delta ct)}$ where ΔCt represents the difference in amplification cycles required to detect the *WISP* genes in peripheral blood lymphocyte DNA compared with colon tumor DNA or colon tumor RNA compared with normal mucosal RNA. The ∂-method was used for calculation of the SE of the gene copy number or RNA expression level. The *WISP*-specific signal was normalized to that of the glyceraldehyde-3-phosphate dehydrogenase housekeeping gene. All TaqMan assay reagents were obtained from Perkin–Elmer Applied Biosystems.

RESULTS

Isolation of *WISP-1* and *WISP-2* by SSH. To identify Wnt-1-inducible genes, we used the technique of SSH using the mouse mammary epithelial cell line C57MG and C57MG cells that stably express Wnt-1 (11). Candidate differentially expressed cDNAs (1,384 total) were sequenced. Thirty-nine percent of the sequences matched known genes or homologues, 32% matched expressed sequence tags, and 29% had no match. To confirm that the transcript was differentially expressed, semiquantitative reverse transcription–PCR and Northern analysis were performed by using mRNA from the C57MG and C57MG/Wnt-1 cells.

Two of the cDNAs, *WISP-1* and *WISP-2*, were differentially expressed, being induced in the C57MG/Wnt-1 cell line, but not in the parent C57MG cells or C57MG cells overexpressing Wnt-4 (Fig. 1 *A* and *B*). Wnt-4, unlike Wnt-1, does not induce the morphological transformation of C57MG cells and has no effect on β-catenin levels (13, 14). Expression of *WISP-1* was up-regulated approximately 3-fold in the C57MG/Wnt-1 cell line and *WISP-2* by approximately 5-fold by both Northern analysis and reverse transcription–PCR.

An independent, but similar, system was used to examine *WISP* expression after Wnt-1 induction. C57MG cells expressing the *Wnt-1* gene under the control of a tetracycline-repressible promoter produce low amounts of Wnt-1 in the repressed state but show a strong induction of *Wnt-1* mRNA and protein within 24 hr after tetracycline removal (8). The levels of Wnt-1 and *WISP* RNA isolated from these cells at various times after tetracycline removal were assessed by quantitative PCR. Strong induction of Wnt-1 mRNA was seen as early as 10 hr after tetracycline removal. Induction of *WISP* mRNA (2- to 6-fold) was seen at 48 and 72 hr (data not shown). These data support our previous observations that show that *WISP* induction is correlated with Wnt-1 expression. Because the induction is slow, occurring after approximately 48 hr, the induction of *WISP*s may be an indirect response to Wnt-1 signaling.

cDNA clones of human *WISP-1* were isolated and the sequence compared with mouse *WISP-1*. The cDNA sequences of mouse and human *WISP-1* were 1,766 and 2,830 bp in length, respectively, and encode proteins of 367 aa, with predicted relative molecular masses of ≈40,000 (M_r 40 K). Both have hydrophobic N-terminal signal sequences, 38 conserved cysteine residues, and four potential N-linked glycosylation sites and are 84% identical (Fig. 2*A*).

Full-length cDNA clones of mouse and human *WISP-2* were 1,734 and 1,293 bp in length, respectively, and encode proteins of 251 and 250 aa, respectively, with predicted relative molecular masses of ≈27,000 (M_r 27 K) (Fig. 2*B*). Mouse and human *WISP-2* are 73% identical. Human *WISP-2* has no potential N-linked glycosylation sites, and mouse *WISP-2* has one at

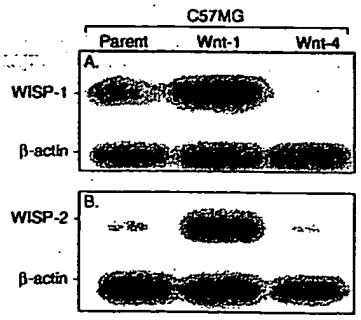

FIG. 1. *WISP-1* and *WISP-2* are induced by Wnt-1, but not Wnt-4, expression in C57MG cells. Northern analysis of *WISP-1* (*A*) and *WISP-2* (*B*) expression in C57MG, C57MG/Wnt-1, and C57MG/Wnt-4 cells. Poly(A)$^+$ RNA (2 μg) was subjected to Northern blot analysis and hybridized with a 70-bp mouse *WISP-1*-specific probe (amino acids 278–300) or a 190-bp *WISP-2*-specific probe (nucleotides 1438–1627) in the 3′ untranslated region. Blots were rehybridized with human β-actin probe.

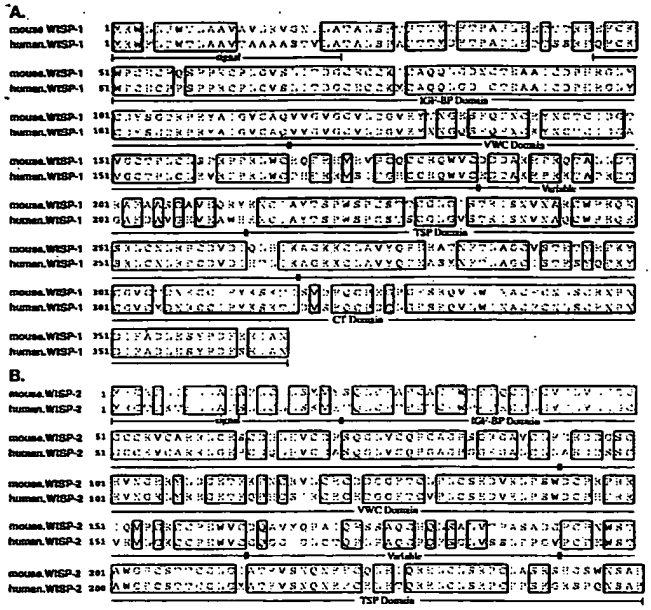

FIG. 2. Encoded amino acid sequence alignment of mouse and human *WISP-1* (*A*) and mouse and human *WISP-2* (*B*). The potential signal sequence, insulin-like growth factor-binding protein (IGF-BP), VWC, thrombospondin (TSP), and C-terminal (CT) domains are underlined.

position 197. *WISP-2* has 28 cysteine residues that are conserved among the 38 cysteines found in *WISP-1*.

Identification of *WISP-3*. To search for related proteins, we screened expressed sequence tag (EST) databases with the WISP-1 protein sequence and identified several ESTs as potentially related sequences. We identified a homologous protein that we have called WISP-3. A full-length human *WISP-3* cDNA of 1,371 bp was isolated corresponding to those ESTs that encode a 354-aa protein with a predicted molecular mass of 39,293. WISP-3 has two potential N-linked glycosylation sites and 36 cysteine residues. An alignment of the three human WISP proteins shows that WISP-1 and WISP-3 are the most similar (42% identity), whereas WISP-2 has 37% identity with WISP-1 and 32% identity with WISP-3 (Fig. 3*A*).

***WISPs* Are Homologous to the CTGF Family of Proteins.** Human *WISP-1*, *WISP-2*, and *WISP-3* are novel sequences; however, mouse *WISP-1* is the same as the recently identified *Elm1* gene. *Elm1* is expressed in low, but not high, metastatic mouse melanoma cells, and suppresses the *in vivo* growth and metastatic potential of K-1735 mouse melanoma cells (15). Human and mouse *WISP-2* are homologous to the recently described rat gene, *rCop-1* (16). Significant homology (36–44%) was seen to the CCN family of growth factors. This family includes three members, CTGF, Cyr61, and the protooncogene *nov*. CTGF is a chemotactic and mitogenic factor for fibroblasts that is implicated in wound healing and fibrotic disorders and is induced by TGF-β (17). Cyr61 is an extracellular matrix signaling molecule that promotes cell adhesion, proliferation, migration, angiogenesis, and tumor growth (18, 19). *nov* (nephroblastoma overexpressed) is an immediate early gene associated with quiescence and found altered in Wilms tumors (20). The proteins of the CCN family share functional, but not sequence, similarity to Wnt-1. All are secreted, cysteine-rich heparin binding glycoproteins that associate with the cell surface and extracellular matrix.

WISP proteins exhibit the modular architecture of the CCN family, characterized by four conserved cysteine-rich domains (Fig. 3*B*) (21). The N-terminal domain, which includes the first 12 cysteine residues, contains a consensus sequence (GCGCCXXC) conserved in most insulin-like growth factor (IGF)-binding proteins (BP). This sequence is conserved in WISP-2 and WISP-3, whereas WISP-1 has a glutamine in the third position instead of a glycine. CTGF recently has been shown to specifically bind IGF (22) and a truncated *nov* protein lacking the IGF-BP domain is oncogenic (23). The von Willebrand factor type C module (VWC), also found in certain collagens and mucins, covers the next 10 cysteine residues, and is thought to participate in protein complex formation and oligomerization (24). The VWC domain of WISP-3 differs from all CCN family members described previously, in that it contains only six of the 10 cysteine residues (Fig. 3 *A* and *B*). A short variable region follows the VWC domain. The third module, the thrombospondin (TSP) domain is involved in binding to sulfated glycoconjugates and contains six cysteine residues and a conserved WSxCSxxCG motif first identified in thrombospondin (25). The C-terminal (CT) module containing the remaining 10 cysteines is thought to be involved in dimerization and receptor binding (26). The CT domain is present in all CCN family members described to date but is absent in WISP-2 (Fig. 3 *A* and *B*). The existence of a putative signal sequence and the absence of a transmembrane domain suggest that WISPs are secreted proteins, an observation supported by an analysis of their expression and secretion from mammalian cell and baculovirus cultures (data not shown).

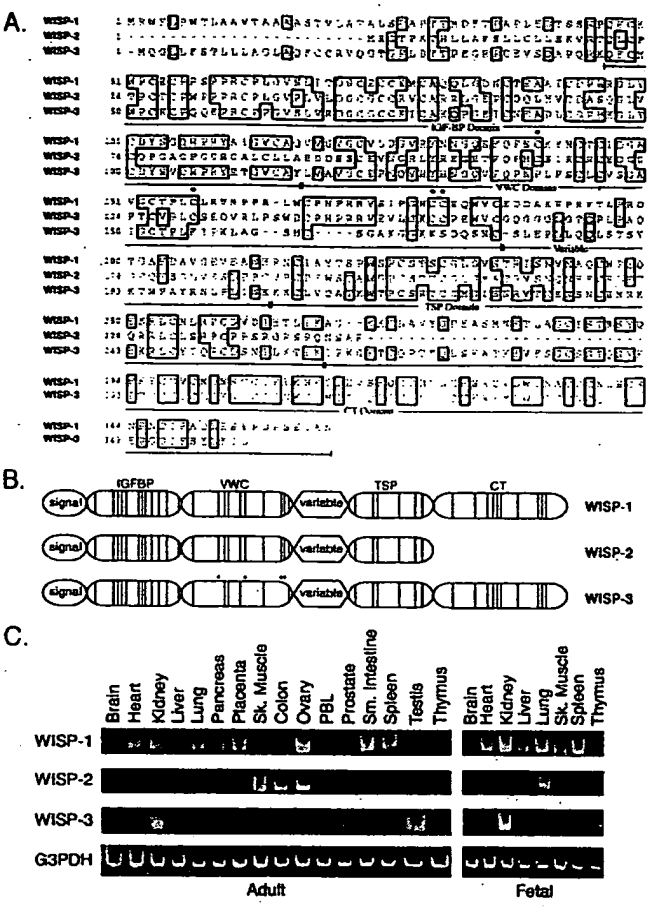

FIG. 3. (*A*) Encoded amino acid sequence alignment of human WISPs. The cysteine residues of WISP-1 and WISP-2 that are not present in WISP-3 are indicated with a dot. (*B*) Schematic representation of the WISP proteins showing the domain structure and cysteine residues (vertical lines). The four cysteine residues in the VWC domain that are absent in WISP-3 are indicated with a dot. (*C*) Expression of *WISP* mRNA in human tissues. PCR was performed on human multiple-tissue cDNA panels (CLONTECH) from the indicated adult and fetal tissues.

Expression of *WISP* mRNA in Human Tissues. Tissue-specific expression of human *WISP*s was characterized by PCR

analysis on adult and fetal multiple tissue cDNA panels. *WISP-1* expression was seen in the adult heart, kidney, lung, pancreas, placenta, ovary, small intestine, and spleen (Fig. 3*C*). Little or no expression was detected in the brain, liver, skeletal muscle, colon, peripheral blood leukocytes, prostate, testis, or thymus. *WISP-2* had a more restricted tissue expression and was detected in adult skeletal muscle, colon, ovary, and fetal lung. Predominant expression of *WISP-3* was seen in adult kidney and testis and fetal kidney. Lower levels of *WISP-3* expression were detected in placenta, ovary, prostate, and small intestine.

***In Situ* Localization of *WISP-1* and *WISP-2*.** Expression of *WISP-1* and *WISP-2* was assessed by *in situ* hybridization in mammary tumors from Wnt-1 transgenic mice. Strong expression of *WISP-1* was observed in stromal fibroblasts lying within the fibrovascular tumor stroma (Fig. 4 *A–D*). However, low-level *WISP-1* expression also was observed focally within tumor cells (data not shown). No expression was observed in normal breast. Like *WISP-1*, *WISP-2* expression also was seen in the tumor stroma in breast tumors from Wnt-1 transgenic animals (Fig. 4 *E–H*). However, *WISP-2* expression in the stroma was in spindle-shaped cells adjacent to capillary vessels, whereas the predominant cell type expressing *WISP-1* was the stromal fibroblasts.

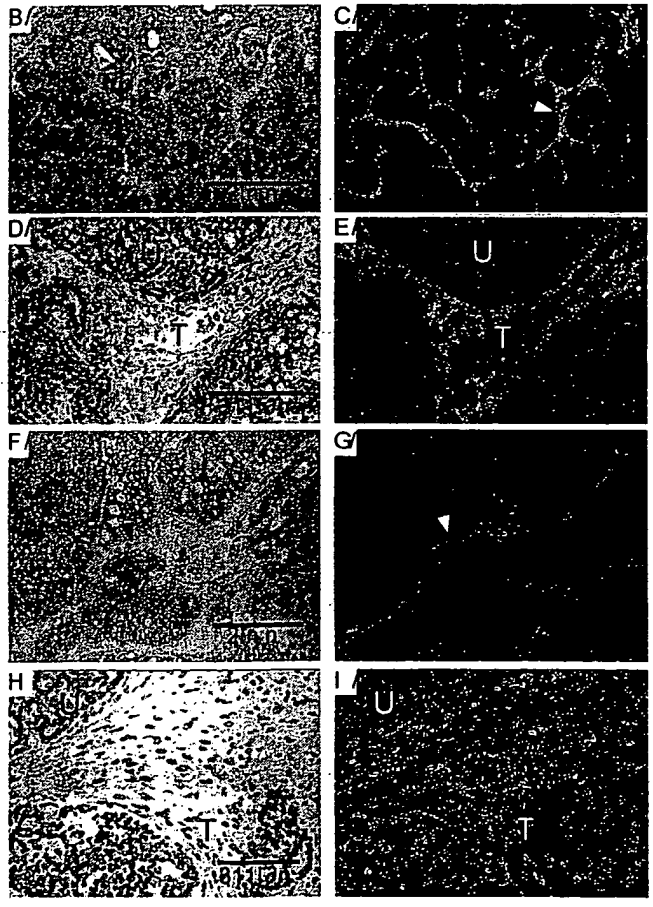

FIG. 4. (*A*, *C*, *E*, and *G*) Representative hematoxylin/eosin-stained images from breast tumors in Wnt-1 transgenic mice. The corresponding dark-field images showing *WISP-1* expression are shown in *B* and *D*. The tumor is a moderately well-differentiated adenocarcinoma showing evidence of adenoid cystic change. At low power (*A* and *B*), expression of *WISP-1* is seen in the delicate branching fibrovascular tumor stroma (arrowhead). At higher magnification, expression is seen in the stromal(s) fibroblasts (*C* and *D*), and tumor cells are negative. Focal expression of *WISP-1*, however, was observed in tumor cells in some areas. Images of *WISP-2* expression are shown in *E–H*. At low power (*E* and *F*), expression of WISP-2 is seen in cells lying within the fibrovascular tumor stroma. At higher magnification, these cells appeared to be adjacent to capillary vessels whereas tumor cells are negative (*G* and *H*).

Chromosome Localization of the *WISP* Genes. The chromosomal location of the human *WISP* genes was determined by radiation hybrid mapping panels. *WISP-1* is approximately 3.48 cR from the meiotic marker AFM259xc5 [logarithm of odds (lod) score 16.31] on chromosome 8q24.1 to 8q24.3, in the same region as the human locus of the *nov*H family member (27) and roughly 4 Mbs distal to c-*myc* (28). Preliminary fine mapping indicates that *WISP-1* is located near D8S1712 STS. *WISP-2* is linked to the marker SHGC-33922 (lod = 1,000) on chromosome 20q12–20q13.1. Human *WISP-3* mapped to chromosome 6q22–6q23 and is linked to the marker AFM211ze5 (lod = 1,000). *WISP-3* is approximately 18 Mbs proximal to CTGF and 23 Mbs proximal to the human cellular oncogene *MYB* (27, 29).

Amplification and Aberrant Expression of *WISPs* in Human Colon Tumors. Amplification of protooncogenes is seen in many human tumors and has etiological and prognostic significance. For example, in a variety of tumor types, c-*myc* amplification has been associated with malignant progression and poor prognosis (30). Because *WISP-1* resides in the same general chromosomal location (8q24) as c-*myc*, we asked whether it was a target of gene amplification, and, if so, whether this amplification was independent of the c-*myc* locus. Genomic DNA from human colon cancer cell lines was assessed by quantitative PCR and Southern blot analysis. (Fig. 5 *A* and *B*). Both methods detected similar degrees of *WISP-1* amplification. Most cell lines showed significant (2- to 4-fold) amplification, with the HT-29 and WiDr cell lines demonstrating an 8-fold increase. Significantly, the pattern of amplification observed did not correlate with that observed for c-*myc*, indicating that the c-*myc* gene is not part of the amplicon that involves the *WISP-1* locus.

We next examined whether the *WISP* genes were amplified in a panel of 25 primary human colon adenocarcinomas. The relative *WISP* gene copy number in each colon tumor DNA was compared with pooled normal DNA from 10 donors by quantitative PCR (Fig. 6). The copy number of *WISP-1* and *WISP-2* was significantly greater than one, approximately 2-fold for *WISP-1* in about 60% of the tumors and 2- to 4-fold for *WISP-2* in 92% of the tumors ($P < 0.001$ for each). The copy number for *WISP-3* was indistinguishable from one ($P = 0.166$). In addition, the copy number of *WISP-2* was significantly higher than that of *WISP-1* ($P < 0.001$).

The levels of *WISP* transcripts in RNA isolated from 19 adenocarcinomas and their matched normal mucosa were

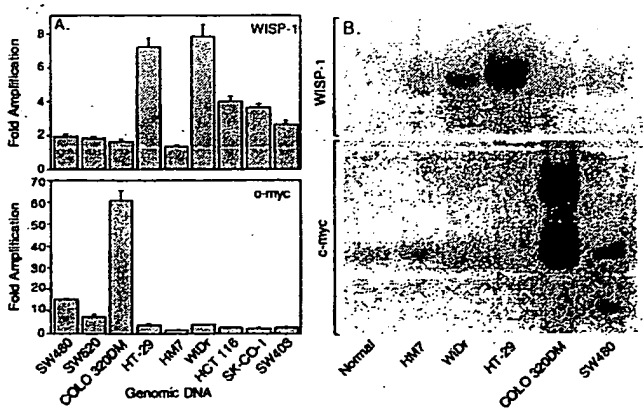

FIG. 5. Amplification of *WISP-1* genomic DNA in colon cancer cell lines. (*A*) Amplification in cell line DNA was determined by quantitative PCR. (*B*) Southern blots containing genomic DNA (10 μg) digested with *Eco*RI (*WISP-1*) or *Xba*I (c-*myc*) were hybridized with a 100-bp human *WISP-1* probe (amino acids 186–219) or a human c-*myc* probe (located at bp 1901–2000). The *WISP* and *myc* genes are detected in normal human genomic DNA after a longer film exposure.

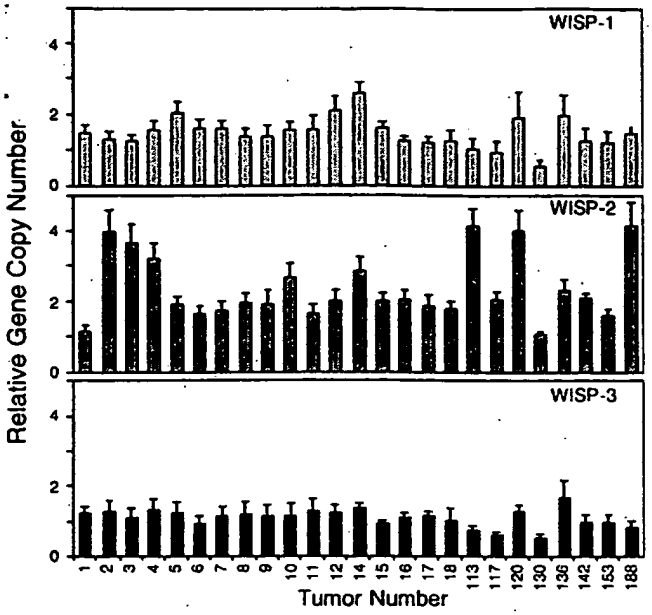

FIG. 6. Genomic amplification of *WISP* genes in human colon tumors. The relative gene copy number of the *WISP* genes in 25 adenocarcinomas was assayed by quantitative PCR, by comparing DNA from primary human tumors with pooled DNA from 10 healthy donors. The data are means ± SEM from one experiment done in triplicate. The experiment was repeated at least three times.

assessed by quantitative PCR (Fig. 7). The level of *WISP-1* RNA present in tumor tissue varied but was significantly increased (2- to >25-fold) in 84% (16/19) of the human colon tumors examined compared with normal adjacent mucosa. Four of 19 tumors showed greater than 10-fold overexpression. In contrast, in 79% (15/19) of the tumors examined, *WISP-2* RNA expression was significantly lower in the tumor than the mucosa. Similar to *WISP-1*, *WISP-3* RNA was overexpressed in 63% (12/19) of the colon tumors compared with the normal mucosa. The amount of overexpression of *WISP-3* ranged from 4- to >40-fold.

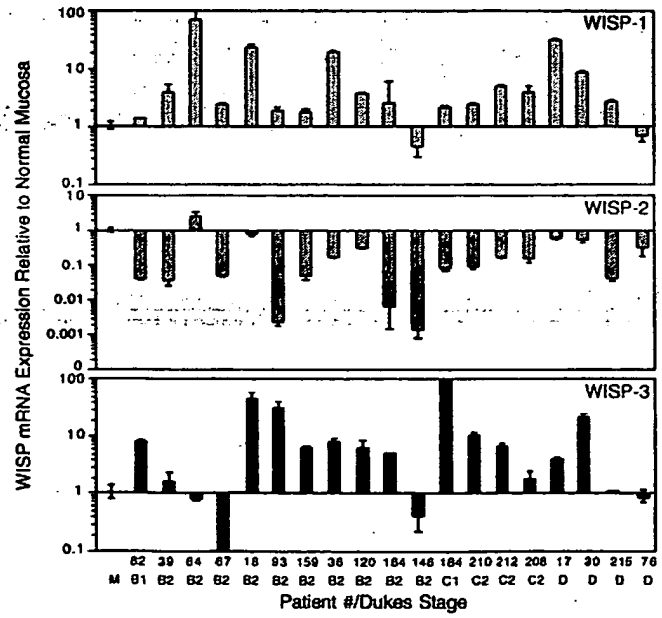

FIG. 7. *WISP* RNA expression in primary human colon tumors relative to expression in normal mucosa from the same patient. Expression of *WISP* mRNA in 19 adenocarcinomas was assayed by quantitative PCR. The Dukes stage of the tumor is listed under the sample number. The data are means ± SEM from one experiment done in triplicate. The experiment was repeated at least twice.

DISCUSSION

One approach to understanding the molecular basis of cancer is to identify differences in gene expression between cancer cells and normal cells. Strategies based on assumptions that steady-state mRNA levels will differ between normal and malignant cells have been used to clone differentially expressed genes (31). We have used a PCR-based selection strategy, SSH, to identify genes selectively expressed in C57MG mouse mammary epithelial cells transformed by Wnt-1.

Three of the genes isolated, *WISP-1*, *WISP-2*, and *WISP-3*, are members of the CCN family of growth factors, which includes CTGF, Cyr61, and *nov*, a family not previously linked to Wnt signaling.

Two independent experimental systems demonstrated that *WISP* induction was associated with the expression of Wnt-1. The first was C57MG cells infected with a Wnt-1 retroviral vector or C57MG cells expressing Wnt-1 under the control of a tetracyline-repressible promoter, and the second was in Wnt-1 transgenic mice, where breast tissue expresses Wnt-1, whereas normal breast tissue does not. No *WISP* RNA expression was detected in mammary tumors induced by polyoma virus middle T antigen (data not shown). These data suggest a link between Wnt-1 and *WISP*s in that in these two situations, *WISP* induction was correlated with Wnt-1 expression.

It is not clear whether the *WISP*s are directly or indirectly induced by the downstream components of the Wnt-1 signaling pathway (i.e., β-catenin-TCF-1/Lef1). The increased levels of *WISP* RNA were measured in Wnt-1-transformed cells, hours or days after Wnt-1 transformation. Thus, *WISP* expression could result from Wnt-1 signaling directly through β-catenin transcription factor regulation or alternatively through Wnt-1 signaling turning on a transcription factor, which in turn regulates *WISP*s.

The *WISP*s define an additional subfamily of the CCN family of growth factors. One striking difference observed in the protein sequence of WISP-2 is the absence of a CT domain, which is present in CTGF, Cyr61, *nov*, WISP-1, and WISP-3. This domain is thought to be involved in receptor binding and dimerization. Growth factors, such as TGF-β, platelet-derived growth factor, and nerve growth factor, which contain a cystine knot motif exist as dimers (32). It is tempting to speculate that WISP-1 and WISP-3 may exist as dimers, whereas WISP-2 exists as a monomer. If the CT domain is also important for receptor binding, WISP-2 may bind its receptor through a different region of the molecule than the other CCN family members. No specific receptors have been identified for CTGF or *nov*. A recent report has shown that integrin $\alpha_v\beta_3$ serves as an adhesion receptor for Cyr61 (33).

The strong expression of *WISP-1* and *WISP-2* in cells lying within the fibrovascular tumor stroma in breast tumors from Wnt-1 transgenic animals is consistent with previous observations that transcripts for the related CTGF gene are primarily expressed in the fibrous stroma of mammary tumors (34). Epithelial cells are thought to control the proliferation of connective tissue stroma in mammary tumors by a cascade of growth factor signals similar to that controlling connective tissue formation during wound repair. It has been proposed that mammary tumor cells or inflammatory cells at the tumor interstitial interface secrete TGF-β1, which is the stimulus for stromal proliferation (34). TGF-β1 is secreted by a large percentage of malignant breast tumors and may be one of the growth factors that stimulates the production of CTGF and WISPs in the stroma.

It was of interest that *WISP-1* and *WISP-2* expression was observed in the stromal cells that surrounded the tumor cells

(epithelial cells) in the Wnt-1 transgenic mouse sections of breast tissue. This finding suggests that paracrine signaling could occur in which the stromal cells could supply WISP-1 and WISP-2 to regulate tumor cell growth on the WISP extracellular matrix. Stromal cell-derived factors in the extracellular matrix have been postulated to play a role in tumor cell migration and proliferation (35). The localization of *WISP-1* and *WISP-2* in the stromal cells of breast tumors supports this paracrine model.

An analysis of *WISP-1* gene amplification and expression in human colon tumors showed a correlation between DNA amplification and overexpression, whereas overexpression of *WISP-3* RNA was seen in the absence of DNA amplification. In contrast, *WISP-2* DNA was amplified in the colon tumors, but its mRNA expression was significantly reduced in the majority of tumors compared with the expression in normal colonic mucosa from the same patient. The gene for human *WISP-2* was localized to chromosome 20q12–20q13, at a region frequently amplified and associated with poor prognosis in node negative breast cancer and many colon cancers, suggesting the existence of one or more oncogenes at this locus (36–38). Because the center of the 20q13 amplicon has not yet been identified, it is possible that the apparent amplification observed for *WISP-2* may be caused by another gene in this amplicon.

A recent manuscript on *rCop-1*, the rat orthologue of *WISP-2*, describes the loss of expression of this gene after cell transformation, suggesting it may be a negative regulator of growth in cell lines (16). Although the mechanism by which *WISP-2* RNA expression is down-regulated during malignant transformation is unknown, the reduced expression of *WISP-2* in colon tumors and cell lines suggests that it may function as a tumor suppressor. These results show that the *WISP* genes are aberrantly expressed in colon cancer and suggest that their altered expression may confer selective growth advantage to the tumor.

Members of the Wnt signaling pathway have been implicated in the pathogenesis of colon cancer, breast cancer, and melanoma, including the tumor suppressor gene adenomatous polyposis coli and β-catenin (39). Mutations in specific regions of either gene can cause the stabilization and accumulation of cytoplasmic β-catenin, which presumably contributes to human carcinogenesis through the activation of target genes such as the *WISP*s. Although the mechanism by which Wnt-1 transforms cells and induces tumorigenesis is unknown, the identification of *WISP*s as genes that may be regulated downstream of Wnt-1 in C57MG cells suggests they could be important mediators of Wnt-1 transformation. The amplification and altered expression patterns of the *WISP*s in human colon tumors may indicate an important role for these genes in tumor development.

We thank the DNA synthesis group for oligonucleotide synthesis, T. Baker for technical assistance, P. Dowd for radiation hybrid mapping, K. Willert and R. Nusse for the tet-repressible C57MG/Wnt-1 cells, V. Dixit for discussions, and D. Wood and A. Bruce for artwork.

1. Cadigan, K. M. & Nusse, R. (1997) *Genes Dev.* **11**, 3286–3305.
2. Dale, T. C. (1998) *Biochem. J.* **329**, 209–223.
3. Nusse, R. & Varmus, H. E. (1982) *Cell* **31**, 99–109.
4. van Ooyen, A. & Nusse, R. (1984) *Cell* **39**, 233–240.
5. Tsukamoto, A. S., Grosschedl, R., Guzman, R. C., Parslow, T. & Varmus, H. E. (1988) *Cell* **55**, 619–625.
6. Brown, J. D. & Moon, R. T. (1998) *Curr. Opin. Cell. Biol.* **10**, 182–187.
7. Molenaar, M., van de Wetering, M., Oosterwegel, M., Peterson-Maduro, J., Godsave, S., Korinek, V., Roose, J., Destree, O. & Clevers, H. (1996) *Cell* **86**, 391–399.
8. Korinek, V., Barker, N., Willert, K., Molenaar, M., Roose, J., Wagenaar, G., Markman, M., Lamers, W., Destree, O. & Clevers, H. (1998) *Mol. Cell. Biol.* **18**, 1248–1256.
9. Munemitsu, S., Albert, I., Souza, B., Rubinfeld, B. & Polakis, P. (1995) *Proc. Natl. Acad. Sci. USA* **92**, 3046–3050.
10. He, T. C., Sparks, A. B., Rago, C., Hermeking, H., Zawel, L., da Costa, L. T., Morin, P. J., Vogelstein, B. & Kinzler, K. W. (1998) *Science* **281**, 1509–1512.
11. Diatchenko, L., Lau, Y. F., Campbell, A. P., Chenchik, A., Moqadam, F., Huang, B., Lukyanov, S., Lukyanov, K., Gurskaya, N., Sverdlov, E. D. & Siebert, P. D. (1996) *Proc. Natl. Acad. Sci. USA* **93**, 6025–6030.
12. Brown, A. M., Wildin, R. S., Prendergast, T. J. & Varmus, H. E. (1986) *Cell* **46**, 1001–1009.
13. Wong, G. T., Gavin, B. J. & McMahon, A. P. (1994) *Mol. Cell. Biol.* **14**, 6278–6286.
14. Shimizu, H., Julius, M. A., Giarre, M., Zheng, Z., Brown, A. M. & Kitajewski, J. (1997) *Cell Growth Differ.* **8**, 1349–1358.
15. Hashimoto, Y., Shindo-Okada, N., Tani, M., Nagamachi, Y., Takeuchi, K., Shiroishi, T., Toma, H. & Yokota, J. (1998) *J. Exp. Med.* **187**, 289–296.
16. Zhang, R., Averboukh, L., Zhu, W., Zhang, H., Jo, H., Dempsey, P. J., Coffey, R. J., Pardee, A. B. & Liang, P. (1998) *Mol. Cell. Biol.* **18**, 6131–6141.
17. Grotendorst, G. R. (1997) *Cytokine Growth Factor Rev.* **8**, 171–179.
18. Kireeva, M. L., Mo, F. E., Yang, G. P. & Lau, L. F. (1996) *Mol. Cell. Biol.* **16**, 1326–1334.
19. Babic, A. M., Kireeva, M. L., Kolesnikova, T. V. & Lau, L. F. (1998) *Proc. Natl. Acad. Sci. USA* **95**, 6355–6360.
20. Martinerie, C., Huff, V., Joubert, I., Badzioch, M., Saunders, G., Strong, L. & Perbal, B. (1994) *Oncogene* **9**, 2729–2732.
21. Bork, P. (1993) *FEBS Lett.* **327**, 125–130.
22. Kim, H. S., Nagalla, S. R., Oh, Y., Wilson, E., Roberts, C. T., Jr. & Rosenfeld, R. G. (1997) *Proc. Natl. Acad. Sci. USA* **94**, 12981–12986.
23. Joliot, V., Martinerie, C., Dambrine, G., Plassiart, G., Brisac, M., Crochet, J. & Perbal, B. (1992) *Mol. Cell. Biol.* **12**, 10–21.
24. Mancuso, D. J., Tuley, E. A., Westfield, L. A., Worrall, N. K., Shelton-Inloes, B. B., Sorace, J. M., Alevy, Y. G. & Sadler, J. E. (1989) *J. Biol. Chem.* **264**, 19514–19527.
25. Holt, G. D., Pangburn, M. K. & Ginsburg, V. (1990) *J. Biol. Chem.* **265**, 2852–2855.
26. Voorberg, J., Fontijn, R., Calafat, J., Janssen, H., van Mourik, J. A. & Pannekoek, H. (1991) *J. Cell. Biol.* **113**, 195–205.
27. Martinerie, C., Viegas-Pequignot, E., Guenard, I., Dutrillaux, B., Nguyen, V. C., Bernheim, A. & Perbal, B. (1992) *Oncogene* **7**, 2529–2534.
28. Takahashi, E., Hori, T., O'Connell, P., Leppert, M. & White, R. (1991) *Cytogenet. Cell Genet.* **57**, 109–111.
29. Meese, E., Meltzer, P. S., Witkowski, C. M. & Trent, J. M. (1989) *Genes Chromosomes Cancer* **1**, 88–94.
30. Garte, S. J. (1993) *Crit. Rev. Oncog.* **4**, 435–449.
31. Zhang, L., Zhou, W., Velculescu, V. E., Kern, S. E., Hruban, R. H., Hamilton, S. R., Vogelstein, B. & Kinzler, K. W. (1997) *Science* **276**, 1268–1272.
32. Sun, P. D. & Davies, D. R. (1995) *Annu. Rev. Biophys. Biomol. Struct.* **24**, 269–291.
33. Kireeva, M. L., Lam, S. C. T. & Lau, L. F. (1998) *J. Biol. Chem.* **273**, 3090–3096.
34. Frazier, K. S. & Grotendorst, G. R. (1997) *Int. J. Biochem. Cell. Biol.* **29**, 153–161.
35. Wernert, N. (1997) *Virchows Arch.* **430**, 433–443.
36. Tanner, M. M., Tirkkonen, M., Kallioniemi, A., Collins, C., Stokke, T., Karhu, R., Kowbel, D., Shadravan, F., Hintz, M., Kuo, W. L., *et al.* (1994) *Cancer Res.* **54**, 4257–4260.
37. Brinkmann, U., Gallo, M., Polymeropoulos, M. H. & Pastan, I. (1996) *Genome Res.* **6**, 187–194.
38. Bischoff, J. R., Anderson, L., Zhu, Y., Mossie, K., Ng, L., Souza, B., Schryver, B., Flanagan, P., Clairvoyant, F., Ginther, C., *et al.* (1998) *EMBO J.* **17**, 3052–3065.
39. Morin, P. J., Sparks, A. B., Korinek, V., Barker, N., Clevers, H., Vogelstein, B. & Kinzler, K. W. (1997) *Science* **275**, 1787–1790.
40. Lu, L. H. & Gillett, N. (1994) *Cell Vision* **1**, 169–176.

Proc. Natl. Acad. Sci. USA
Vol. 83, pp. 4049–4052, June 1986
Medical Sciences

Variable expression of the translocated c-*abl* oncogene in Philadelphia-chromosome-positive B-lymphoid cell lines from chronic myelogenous leukemia patients

JAMES B. KONOPKA*‡, STEVEN CLARK*, JAMI MCLAUGHLIN*, MASAKUZU NITTA†, YOSHIRO KATO†, ANNABEL STRIFE†, BAYARD CLARKSON†, AND OWEN N. WITTE*§

*Department of Microbiology and Molecular Biology Institute, University of California, Los Angeles, 405 Hilgard Avenue, Los Angeles, CA 90024; and †The Laboratory of Hematopoietic Cell Kinetics and The Laboratory of Cancer Genetics and Cytogenetics, Memorial Sloan-Kettering Cancer Center, 1275 York Avenue, New York, NY 10021

Communicated by Michael Potter, February 10, 1986

ABSTRACT **The consistent cytogenetic translocation of chronic myelogenous leukemia (the Philadelphia chromosome, Ph^1) has been observed in cells of multiple hematopoietic lineages. This translocation creates a chimeric gene composed of breakpoint-cluster-region (*bcr*) sequences from chromosome 22 fused to a portion of the *abl* oncogene on chromosome 9. The resulting gene product ($P210^{c\text{-}abl}$) resembles the transforming protein of the Abelson murine leukemia virus in its structure and tyrosine kinase activity. $P210^{c\text{-}abl}$ is expressed in Ph^1-positive cell lines of myeloid lineage and in clinical specimens with myeloid predominance. We show here that Epstein–Barr virus-transformed B-lymphocyte lines that retain Ph^1 can express $P210^{c\text{-}abl}$. The level of expression in these B-cell lines is generally lower and more variable than that observed for myeloid lines. Protein expression is not related to amplification of the *abl* gene but to variation in the level of *bcr-abl* mRNA produced from a single Ph^1 template.**

Chronic myelogenous leukemia (CML) is a disease of the pluripotent stem cell (1). In greater than 95% of patients, the leukemic cells contain the cytogenetic marker known as the Philadelphia chromosome, or Ph^1 (2). This reciprocal translocation event between the long arms of chromosomes 9 and 22 has been used as a disease-specific marker for diagnosis and evaluation of therapy. Multiple hematopoietic lineages, including myeloid and B-lymphoid, contain Ph^1 in early or chronic phase, as well as in the more acute accelerated and blast crisis phases of the disease.

One molecular consequence of Ph^1 is the translocation of the chromosomal arm containing the c-*abl* gene on chromosome 9 into the middle of the breakpoint-cluster region (*bcr*) gene on chromosome 22 (3–6). Although the precise translocation breakpoints are variable, an RNA-splicing mechanism generates a very similar 8-kilobase (kb) mRNA in each case (5–9). The hybrid *bcr-abl* message encodes a structurally altered form of the *abl* oncogene product, called $P210^{c\text{-}abl}$ (10–13), with an amino-terminal segment derived from a portion of the exons of *bcr* on chromosome 22 and a carboxyl-terminal segment derived from a major portion of the exons of the c-*abl* gene on chromosome 9. The chimeric structure of *bcr-abl* and the resulting $P210^{c\text{-}abl}$ is similar to the structure of the Abelson murine leukemia virus *gag-abl* genome and resulting $P160^{v\text{-}abl}$ transforming gene product. Both proteins have very similar tyrosine kinase activities (10, 11, 14) which can be distinguished by their relative stability to denaturing detergents and by their ATP requirements from the recently described tyrosine kinase activity of the c-*abl* gene product (15).

In concert with structural modification of the amino-terminal portion of the *abl* gene, increased level of expression has been implicated in activation of c-*abl* oncogenic potential. Myeloid and erythroid cell lines and clinical samples derived from acute-phase CML patients contain about 10-fold higher levels of the 8-kb *bcr-abl* mRNA and $P210^{c\text{-}abl}$ than the c-*abl* mRNA forms (6 and 7 kb) and $P145^{c\text{-}abl}$ gene product (5, 8, 9, 11). The higher level of expression of the chimeric *bcr-abl* message in acute-phase cells is not likely to be solely due to the presence of the *bcr* promoter sequences at the 5′ end of the gene, since the normal 4.5-kb and 6.7-kb *bcr*-encoded mRNA species are expressed at an even lower level than the normal c-*abl* messages (5, 6).

We have analyzed a series of Epstein–Barr virus-immortalized B-lymphoid cell lines derived from CML patients (16). With such *in vitro* clonal cell lines, we can evaluate whether the presence of Ph^1 always results in synthesis of the chimeric *bcr-abl* message and protein, and whether the quantitative expression varies for cells of B-lymphoid lineage as compared to previously examined myeloid cell lines. Our results show that cell lines that retain Ph^1 do express *bcr-abl* message and protein, but that the level is generally lower and more variable than previously seen for myeloid cell lines. The demonstration that the Ph^1 chromosomal template can vary in its level of expression of $P210^{c\text{-}abl}$ suggests that secondary mechanisms, beyond the translocation itself, contribute to the regulation of the *bcr-abl* gene in different cell types or subclones that derive from the affected stem cell.

MATERIALS AND METHODS

Cells and Cell Labelings. Epstein–Barr virus-transformed B-lymphoid cell lines were established from peripheral blood samples of chronic- and acute-phase CML patients as reported (16). The cell lines are designated according to patient number, karyotype, and lineage. For example, SK-CML7Bt(9,22)-33 refers to CML patient 7, B-lymphoid cell line, 9;22 translocation (Ph^1), cell line 33; and SK-CML7BN-2 refers to B-cell line 2 with a normal karyotype derived from the same patient. Repeat karyotype analysis was performed to verify the retention of Ph^1 just prior to analysis for *abl* protein and RNA. Cells were maintained in RPMI 1640 medium with 20% fetal bovine serum. We have not observed any consistent pattern of *in vitro* growth rate that correlates to the stage of disease at the time of transformation with Epstein–Barr virus. Cells (1.5×10^7) were washed twice with Dulbecco's modified Eagle's medium lacking phosphate and

The publication costs of this article were defrayed in part by page charge payment. This article must therefore be hereby marked "*advertisement*" in accordance with 18 U.S.C. §1734 solely to indicate this fact.

Abbreviations: *bcr*, breakpoint-cluster region; CML, chronic myelogenous leukemia; kb, kilobase(s).

‡Present address: Department of Genetics, University of Washington, Seattle, WA 98195.
§To whom correspondence should be addressed.

supplemented with 5% dialyzed fetal bovine serum. Cells were then resuspended in 2 ml of the minimal medium. Labeling was started with the addition of [^{32}P]orthophosphate (1 mCi/ml; ICN; 1 Ci = 37 GBq) and continued at 37°C for 3–4 hr.

Immunoprecipitation and Immunoblotting. Immunoprecipitations were carried out as described (10). Cells (1.5×10^7) were washed with phosphate-buffered saline and extracted with 3–5 ml of phosphate lysis buffer (1% Triton X-100/0.1 $NaDodSO_4$/0.5% deoxycholate/10 mM Na_2HPO_4, pH 7.5/100 mM NaCl) with 5 mM EDTA and 5 mM phenylmethylsulfonyl fluoride. Extracts were clarified by centrifugation and precipitated with normal or rabbit anti-abl sera (anti-pEX-2 or anti-pEX-5) (17). The precipitated proteins were electrophoresed in a $NaDodSO_4$/8% polyacrylamide gel. ^{32}P-labeled proteins were detected by autoradiography. Alternatively, *abl* proteins were detected by immunoblotting. Extracts from unlabeled cells were clarified, and proteins were concentrated by immunoprecipitation with rabbit antisera against *abl*-encoded proteins [anti-pEX-2 and anti-pEX-5 combined (17)] and then fractionated in 8% acrylamide gels. The proteins were transferred from the gel to nitrocellulose filters, using protease-facilitated transfer (18). The *abl*-encoded proteins were detected using murine monoclonal antibodies as a probe and peroxidase-conjugated goat anti-mouse second stage antibody (Bio-Rad) for development. Rabbit antisera and mouse monoclonal antibodies to *abl* proteins were prepared using bacterially expressed regions of the v-*abl* protein as immunogens (17, 19). Anti-pEX-2 antibodies react with the internal tyrosine kinase domain and anti-pEX-5 antibodies react with the carboxyl-terminal segment of the *abl* proteins.

RNA Analysis. RNA was extracted from 10^8 cells by the $NaDodSO_4$/urea/phenol method (20). Polyadenylylated RNA was purified by oligo(dT) affinity chromatography. Samples were electrophoresed in a 1% agarose/formaldehyde gel and transferred to nitrocellulose. *abl* RNA species were detected by hybridization with a nick-translated v-*abl* fragment probe (21).

DNA Analysis. DNA was prepared from 5×10^7 cells of each cell line and processed for Southern blots with a v-*abl* probe as described (21).

RESULTS

Variable Levels of P210$^{c\text{-}abl}$ Are Detected in Ph^1-Positive Cell Lines. Ph^1-positive and Ph^1-negative, Epstein–Barr virus-transformed B-lymphocyte cell lines derived from the same patient were examined for P210$^{c\text{-}abl}$ synthesis by immunoprecipitation of [^{32}P]orthophosphate-labeled cell extracts with anti-abl sera (Fig. 1). The normal c-*abl* protein P145$^{c\text{-}abl}$ was detected at a similar level in multiple Ph^1-positive and Ph^1-negative cell lines. P210$^{c\text{-}abl}$ was only detected in the Ph^1-positive cell lines because the *bcr-abl* chimeric gene which encodes P210$^{c\text{-}abl}$ resides on the Ph^1 (4, 5, 11, 13). The level of P210$^{c\text{-}abl}$ was about 4- to 5-fold higher than the level of P145$^{c\text{-}abl}$ in the SK-CML7Bt-33 cell line (Fig. 1*A*, +). The Ph^1-positive erythroid-progenitor cell line K562 (*C*) showed a level of P210$^{c\text{-}abl}$ about 10-fold higher than P145$^{c\text{-}abl}$. However, the level of P210$^{c\text{-}abl}$ was about one-fifth that of P145$^{c\text{-}abl}$ in the Ph^1-positive SK-CML16Bt-1 cell line (Fig. 1*B*, +). Comparison of different autoradiographic exposures roughly indicated that the level of P210$^{c\text{-}abl}$ varies over a 20-fold range between these Ph^1-positive B-cell lines. Analysis of four additional Ph^1-positive B-cell lines demonstrated that the level of P210$^{c\text{-}abl}$ fell into two general classes; some cell lines had a level of P210$^{c\text{-}abl}$ similar to SK-CML7Bt-33 and others had the low level similar to SK-CML16Bt-1 (Table 1). This differs from previous studies with Ph^1-positive myeloid cell lines and patient samples derived from acute-phase CML patients, in which P210$^{c\text{-}abl}$ was detected at a 10-fold higher level than P145$^{c\text{-}abl}$ (refs. 10 and 11; Table 1). There was no large difference in level of chimeric mRNA and P210$^{c\text{-}abl}$ expressed in four myeloid/erythroid-lineage Ph^1-positive cell lines (K562, EM2, EM3, CML22, and BV173; refs. 9 and 11), despite a 4- to 5-fold amplification of *abl*-related sequences in the K562 cell line.

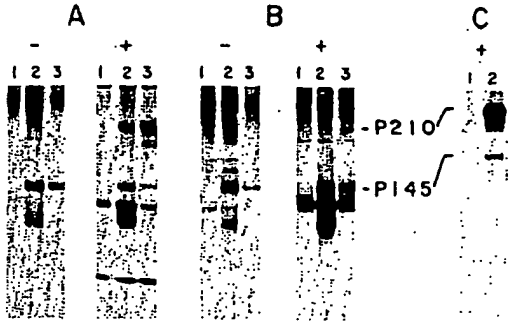

FIG. 1. Detection of variable levels of P210$^{c\text{-}abl}$ in Ph^1-positive B-cell lines. Production of P145$^{c\text{-}abl}$ and P210$^{c\text{-}abl}$ in Epstein–Barr virus-transformed B-cell lines derived from a blast-crisis (*A*) and a chronic-phase (*B*) CML patient was examined by metabolic labeling with [^{32}P]orthophosphate and immunoprecipitation. Ph^1-negative (−) and Ph^1-positive (+) cell lines derived from each patient were analyzed. The Ph^1-negative cell line in *A*,− is SK-CML7BN-2 and in *B*,− is SK-CML16BN-1. The Ph^1-positive cell line in *A*,+ is SK-CML7Bt-33 and in *B*,+ is SK-CML16Bt-1. The K562 cell line, a Ph^1-positive erythroid progenitor cell line spontaneously derived from a blast-crisis patient (33), is represented in *C*. Cells (1.5×10^7) were metabolically labeled with 2 mCi of [^{32}P]orthophosphate for 3–4 hr and then were extracted and clarified by centrifugation. Samples were immunoprecipitated with control normal serum (lanes 1), anti-pEX-2 (lanes 2), or anti-pEX-5 (lanes 3) and analyzed by $NaDodSO_4$/8% PAGE followed by autoradiography with an intensifying screen (3 days for *A* and *C*, 10 days for *B*).

Detection of different levels of P210$^{c\text{-}abl}$ in Fig. 1 could be due to decreased phosphorylation of P210$^{c\text{-}abl}$, a lower level of P210$^{c\text{-}abl}$ synthesis, or altered stability of the protein. To help distinguish among these possibilities, the steady-state level of P210$^{c\text{-}abl}$ in the cell lines was assayed by immunoblotting. The results show that SK-CML7Bt-33 (Fig. 2*A*, +) had a higher level of P210$^{c\text{-}abl}$ than P145, similar to the results with metabolic labeling (Fig. 1). We did not detect P210$^{c\text{-}abl}$ by immunoblotting with 2×10^7 cells of line SK-CML8Bt-3 (Fig. 2*B*, +). Reconstruction experiments using dilutions of cell extracts showed that we could detect about 5–10% the level of P210$^{c\text{-}abl}$ expressed in the K562 cell line (data not shown). We infer that the steady-state level of P210$^{c\text{-}abl}$ in SK-CML8Bt-3 is lower than the level in SK-CML7Bt-33 by a factor of at least 10. The level of P210$^{c\text{-}abl}$ detected in these assays correlated with the amount of P210$^{c\text{-}abl}$ tyrosine kinase activity that could be detected *in vitro* (data not shown).

Different Levels of P210$^{c\text{-}abl}$ Are Reflected in the Amount of Stable *bcr-abl* mRNA. To identify the basis for detection of variable levels of P210$^{c\text{-}abl}$, we examined the production of the *abl* RNA. RNA blot hybridization analysis using a v-*abl* probe (Fig. 3) showed that the normal 6- and 7-kb c-*abl* mRNAs were present at a similar level in Ph^1-positive and -negative cell lines derived from different patients. However, the 8-kb mRNA that encodes P210$^{c\text{-}abl}$ was detected at a 10-fold higher level in SK-CML7Bt-33 (Fig. 3*A*, +) than in SK-CML16Bt-1 (*B*, +), which correlated with the relative level of P210$^{c\text{-}abl}$ detected in each cell line. Analysis of additional cell lines demonstrated that the level of 8-kb RNA directly correlated with the level of P210$^{c\text{-}abl}$ (Table 1). The variation in level of 8-kb RNA detected in these cell lines was not due to loss or gain of Ph^1, because cytogenetic analysis confirmed the presence of Ph^1 in these cell lines (ref. 16 and

Table 1. Relative levels of *bcr-abl* expression in Epstein–Barr virus-immortalized B-cell lines and myeloid CML lines

Cell line*	CML phase†	Ph¹‡	P210§	8-kb mRNA¶
SK-CML7BN-2	BC	−	−	−
SK-CML8BN-10	Chronic	−	−	−
SK-CML8BN-12	Chronic	−	−	−
SK-CML16BN-1	Chronic	−	−	−
SK-CML35BN-1	Chronic	−	−	−
SK-CML7B5-33	BC	+	+++	+++
SK-CML21Bt-1	Acc	+	+++	+++
SK-CML21Bt-6	Acc	+	+++	+++
SK-CML8Bt-3	Chronic	+	+	±
SK-CML16Bt-1	Chronic	+	+	+
SK-CML35Bt-2	Chronic	+	+	+
K562	BC	+	+++++	+++++
BV173	BC	+	+++++	+++++
EM2	BC	+	+++++	+++++

*Cell lines derived from CML patients by transformation with Epstein–Barr virus as described (16). Names of cell lines indicate patient number and Ph¹ status: SK-CML7Bt indicates a cell line derived from patient 7 that carries the 9;22 Ph¹ translocation; N indicates a normal karyotype. Myeloid-erythroid cell lines (K562, EM2, and BV173) are described in previous publications (9, 11, 22, 33).

†Status of patient at the time cell line was derived. BC, blast crisis; Acc, accelerated phase.

‡Presence (+) or absence (−) of Ph¹ as demonstrated by karyotypic or Southern blot analysis.

§$P210^{c\text{-}abl}$ detected as described in legend to Fig. 1. B-cell lines derived from blast-crisis and accelerated-phase patients had levels of P210 3- to 5-fold higher (+++) than levels of P145. Chronic-phase-derived cell lines had P210 levels lower than or just equivalent (+) to the level of P145. Myeloid and erythroid lines had levels of P210 5- to 10-fold higher than P145 (+++++).

¶Eight-kilobase *bcr-abl* mRNA detected as described in legend to Fig. 2. Symbols: ±, borderline detectable; +++++, level of 8-kb mRNA 5- to 10-fold higher than that of the 6- and 7-kb c-*abl* mRNA species; +++, level of 8-kb mRNA 3- to 5-fold higher than that of the 6- and 7-kb species; +, a level approximately equivalent to that of the 6- and 7-kb messages.

data not shown). There was no difference in the copy number of *abl*-related sequences as judged by Southern blot analysis (Fig. 4). Only the K562 cell line control showed an amplification of *abl* sequences, as previously reported (22, 23). These combined data suggest that differential *bcr-abl* mRNA expression from a single gene template is responsible for the variable levels of $P210^{c\text{-}abl}$ detected. This could be mediated

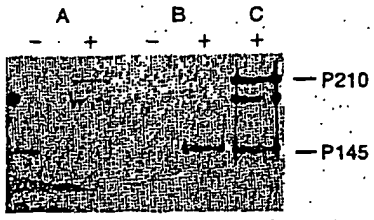

FIG. 2. Analysis of steady-state *abl* protein levels by immunoblotting. Cell extracts prepared from 2×10^7 cells of lines SK-CML7BN-2 (*A*,−), SK-CML7Bt-33 (*A*,+), SK-CML8BN-10 (*B*,−), and SK-CML8Bt-3 (*B*,+) were concentrated by immunoprecipitation with anti-pEX-2 plus anti-pEX-5. Samples were then electrophoresed in a NaDodSO₄/8% polyacrylamide gel and transferred to nitrocellulose, using protease-facilitated transfer (18). *abl* proteins were detected using a mixture of two monoclonal antibodies directed against the pEX-2 and pEX-5 *abl*-protein fragments produced in bacteria (19) as a probe and a peroxidase-conjugated goat anti-mouse second-stage antibody (Bio-Rad) for development.

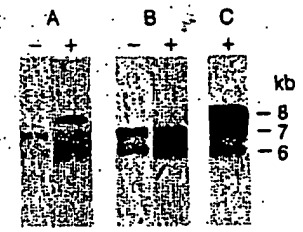

FIG. 3. Comparison of *abl* RNA levels in Ph¹-positive and -negative B-cell lines. The levels of the normal 6- and 7-kb c-*abl* RNAs and the 8-kb *bcr-abl* RNA were analyzed by blot hybridization using a v-*abl* probe. RNA was extracted from Ph¹-negative lines SK-CML7BN-2 (*A*,−) and SK-CML16BN-1 (*B*,−), from Ph¹-positive lines SK-CML6Bt-33 (*A*,+) and SK-CML16Bt-3 (*B*,+), and from line K562 (*C*,+) by the NaDodSO₄/urea/phenol method (20). Polyadenylylated RNA was purified by oligo(dT) affinity chromatography, and 15 μg of each sample was electrophoresed in a 1% agarose/formaldehyde gel and then transferred to nitrocellulose. The blotted RNAs were hybridized with a nick-translated v-*abl* fragment probe (21) and then autoradiographed for 4 days.

by factors influencing the transcription rate of the *bcr-abl* gene or the stability of the mRNA.

DISCUSSION

Several lines of evidence suggest that formation of Ph¹ is not the primary event that affects the stem cell in CML. Patients have been identified that present with the clinical picture of CML but only later develop Ph¹ (1). This observation, coupled with studies of *G6PD* (glucose-6-phosphate dehydrogenase)-heterozygous females with CML that demonstrate stem-cell clonality by isozyme analysis among cell

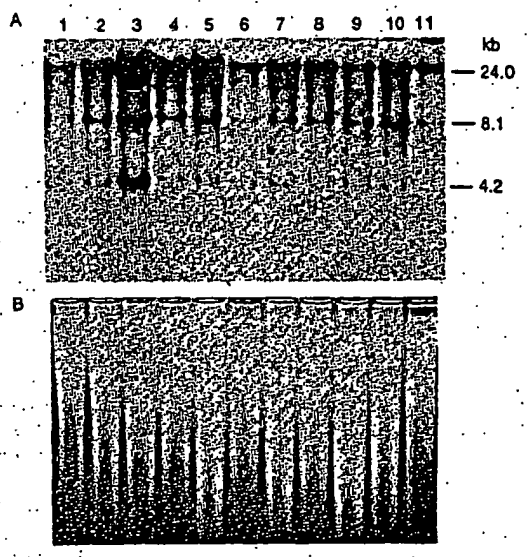

FIG. 4. Southern blot analysis of *abl* sequences in Ph¹-positive and -negative B-cell lines. High molecular weight DNA (15 μg) was digested with restriction endonuclease *Bam*HI, separated in a 0.8% agarose gel, and then transferred to nitrocellulose. The blotted DNA fragments were hybridized with a nick-translated, 2.4-kb *Bgl* II v-*abl* fragment (1.5×10^8 cpm/μg; ref. 21) and exposed for 4 days. (*A*) Autoradiogram of *abl*-specific fragments in cell lines HL-60 (lane 1), EM2 (lane 2), K562 (lane 3), SK-CML7Bt-33 (lane 4), SK-CML8Bt-3 (lane 5), SK-CML16Bt-1 (lane 6), SK-CML21Bt-6 (lane 7), SK-CML35Bt-2 (lane 8), SK-CML7BN-2 (lane 9), SK-CML8BN-2 (lane 10), and SK-CML35BN-1 (lane 11). (*B*) Ethidium bromide staining of agarose gel prior to transfer to nitrocellulose, showing the level of variation in amount of DNA loaded per lane.

populations that lack the Ph^1 marker, supports a secondary or complementary role for Ph^1 in the progression of the disease (24, 25). This chromosome marker is found in chronic, accelerated, and blast-crisis phases of the disease. It is likely that Ph^1 confers some growth advantage, since cells with the marker chromosome eventually predominate the marrow and peripheral blood even in chronic phase. During the phase of blast crisis, many patients develop additional chromosome abnormalities, including duplication of Ph^1, a variety of trisomies, and complex translocations (26). This is suggestive evidence for Ph^1 being a necessary but not sufficient genetic change for the full evolution of the disease.

The realization that one molecular result of Ph^1 is the generation of a chimeric *bcr-abl* protein with functional characteristics and structure analogous to the *gag-abl* transforming protein of the Abelson murine leukemia virus strengthens the argument for an important role of Ph^1 in the pathogenesis of CML. Although the Abelson virus is generally considered a rapidly transforming retrovirus, its effects can range from overcoming growth factor requirements, to cellular lethality, to induction of highly oncogenic tumors in a number of hematopoietic cell lineages (27, 28). Even in the transformation of murine cell targets, there are several lines of evidence that suggest that the growth-promoting activity of the v-*abl* gene product is complemented by further cellular changes in the production of the malignant-cell phenotype (29–31).

The regulation of *bcr-abl* gene expression is complex because the 5′ end of the gene is derived from the non-*abl* sequences, *bcr*, normally found on chromosome 22 (6). The level of stable message for the normal *bcr* gene and the normal *abl* gene are both much lower than the level of the *bcr-abl* message and protein from cell lines and clinical specimens derived from myeloid blast-crisis patients (5, 6, 11). Therefore, the high level of *bcr-abl* expression cannot simply be attributed to the regulatory sequences associated with *bcr*. Possibly, creation of the chimeric gene disrupts the normal regulatory sequences and results in a higher level of expression. Variation in *bcr-abl* expression may result from secondary changes in the structure of the chimeric gene or function of *trans*-acting factors that occur during evolution of the disease. Our analysis of $P210^{c\text{-}abl}$ and the 8-kb mRNA in Epstein–Barr virus-transformed Ph^1-positive B-cell lines demonstrates that stable message and protein levels from the *bcr-abl* gene can vary over a wide range. This variation does not result from a change in the number of *bcr-abl* templates secondary to gene amplification but more likely from changes in either transcription rate or mRNA stability. We suspect this range of *bcr-abl* expression is not limited to lymphoid cells. Analysis of peripheral blood leukocytes derived from an unusual CML patient who has been in chronic phase with myeloid predominance for 16 years showed a level of $P210^{c\text{-}abl}$ one-fifth that of $P145^{c\text{-}abl}$, as detected by metabolic labeling with [^{32}P]orthophosphate and immunoprecipitation (S.C., O.N.W., and P. Greenberg, unpublished observations). Lower levels of expression of the chimeric mRNA have been demonstrated in clinical samples from chronic-phase CML patients compared to acute-phase CML patients (9). Others have reported chronic-phase patients with variable but, in some cases, relatively high levels of the *bcr-abl* mRNA (32). The sampling variation and the heterogenous mixture of cell types in clinical samples complicate such analyses. Further work is needed to evaluate whether there is a defined change in $P210^{c\text{-}abl}$ expression during the progression of CML. It is interesting to note that among the limited sample of Ph^1-positive B-cell lines we have examined (Table 1), we have seen higher levels of $P210^{c\text{-}abl}$ in those derived from patients at more advanced stages of the disease. It will be important to search for cell-type-specific mechanisms that might regulate expression of *bcr-abl* from Ph^1.

We thank Bonnie Hechinger and Carol Crookshank for excellent secretarial assistance and Margaret Newman for excellent technical assistance. This work was supported by grants from the National Institutes of Health (to O.N.W. and B.C.). J.B.K. was supported as a predoctoral fellow on the Public Health Service Cellular and Molecular Biology Training Grant GM07185. S.C. is a postdoctoral fellow of the Leukemia Society of America.

1. Champlin, R. E. & Golde, D. W. (1985) *Blood* 65, 1039–1047.
2. Rowley, J. D. (1973) *Nature (London)* 243, 290–291.
3. Heisterkamp, N., Stephenson, J. R., Groffen, J., Hansen, P. F., de Klein, A., Bartram, C. R. & Grosveld, G. (1983) *Nature (London)* 306, 239–242.
4. Bartram, C. R., de Klein, A., Hagemeijer, A., van Agthoven, T., van Kessel, A. G., Bootsma, D., Grosveld, G., Ferguson-Smith, M. A., Davies, T., Stone, M., Heisterkamp, N., Stephenson, J. R. & Groffen, J. (1983) *Nature (London)* 306, 277–280.
5. Shtivelman, E., Lifshitz, B., Gale, R. P. & Canaani, D. (1985) *Nature (London)* 315, 550–554.
6. Heisterkamp, N., Stam, K. & Groffen, J. (1985) *Nature (London)* 315, 758–761.
7. Groffen, J., Stephenson, J. R., Heisterkamp, N., de Klein, A., Bartram, C. R. & Grosveld, G. (1984) *Cell* 36, 93–99.
8. Gale, R. P. & Canaani, E. (1984) *Proc. Natl. Acad. Sci. USA* 81, 5648–5652.
9. Collins, S., Kubonishi, L., Miyoshi, I. & Groudine, M. T. (1984) *Science* 225, 72–74.
10. Konopka, J. B., Watanabe, S. M. & Witte, O. N. (1984) *Cell* 7, 1035–1042.
11. Konopka, J. B., Watanabe, S. M., Singer, J., Collins, S. & Witte, O. N. (1985) *Proc. Natl. Acad. Sci. USA* 82, 1810–1814.
12. Kloetzer, W., Kurzrock, R., Smith, L., Talpaz, M., Spiller, M., Gutterman, J. & Arlinghaus, R. (1985) *Virology* 140, 230–238.
13. Kozbor, D., Giallongo, A., Sierzega, M. E., Konopka, J. B., Witte, O. N., Showe, L. C. & Croce, C. M. (1985) *Nature (London)*, in press.
14. Davis, R. L., Konopka, J. B. & Witte, O. N. (1985) *Mol. Cell Biol.* 5, 204–213.
15. Konopka, J. B. & Witte, O. N. (1985) *Mol. Cell. Biol.* 5, 3116–3123.
16. Nitta, M., Kato, Y., Strife, A., Wachter, M., Fried, J., Perez, A., Jhanwar, S., Duigou, R., Chaganti, R. S. K. & Clarkson, B. (1985) *Blood* 66, 1053–1061.
17. Konopka, J. B., Davis, J. L., Watanabe, S. M., Ponticelli, A. S., Schiff-Maker, L., Rosenberg, N. & Witte, O. N. (1984) *Virology* 51, 223–232.
18. Gibson, W. (1981) *Anal. Biochem.* 118, 1–3.
19. Schiff-Maker, L., Konopka, J. B., Clark, S., Witte, O. N. & Rosenberg, N. (1986) *J. Virol.* 57, 1182–1186.
20. Schwartz, R. C., Sonenshein, G. E., Bothwell, A. & Gefter, M. L. (1981) *J. Immunol.* 126, 2104–2108.
21. Goff, S. P., Gilboa, E., Witte, O. N. & Baltimore, D. (1980) *Cell* 22, 777–785.
22. Collins, S. J. & Groudine, M. T. (1983) *Proc. Natl. Acad. Sci. USA* 80, 4813–4817.
23. Selden, J. R., Emanuel, B. S., Wang, E., Cannizzaro, L., Palumbo, A., Erikson, J., Nowell, P. C., Rovera, G. & Croce, C. M. (1983) *Proc. Natl. Acad. Sci. USA* 80, 7289–7292.
24. Fialkow, P. J., Martin, P. J., Najfeld, V., Penfold, G. K., Jacobson, R. J. & Hansen, J. A. (1981) *Blood* 58, 158–163.
25. Martin, P. J., Najfeld, V. & Fialkow, P. J. (1982) *Can. Gen. Cytogenet.* 6, 359–368.
26. Rowley, J. D. (1980) *Annu. Rev. Genet.* 14, 17–40.
27. Whitlock, C. A. & Witte, O. N. (1984) *Adv. Immunol.* 37, 74–98.
28. Pierce, J. H., Di Fiore, P. P., Aaronson, S. A., Potter, M., Pumphrey, J., Scott, A. & Ihle, J. N. (1985) *Cell* 41, 685–693.
29. Whitlock, C. A., Ziegler, S. & Witte, O. N. (1983) *Mol. Cell. Biol.* 3, 596–604.
30. Wolf, D., Harris, N. & Rotter, V. (1984) *Cell* 38, 119–126.
31. Klein, G. & Klein, E. (1985) *Nature (London)* 315, 190–195.
32. Stam, K., Jr., Heisterkamp, N., Grosveld, G., de Klein, A., Verma, R., Colemen, M., Dosik, H. & Groffen, J. (1985) *N. Engl. J. Med.* 313, 1429–1433.
33. Lozzio, C. B. & Lozzio, B. B. (1975) *Blood* 45, 321–334.

GENES VII

Benjamin Lewin

Oxford New York Tokyo
Oxford University Press
1997

CHAPTER 29
Regulation of transcription

The phenotypic differences that distinguish the various kinds of cells in a higher eukaryote are largely due to differences in the expression of genes that code for proteins, that is, those transcribed by RNA polymerase II. In principle, the expression of these genes might be regulated at any one of several stages. The concept of the "level of control" implies that gene expression is not necessarily an automatic process once it has begun. It could be regulated in a gene-specific way at any one of several sequential steps. We can distinguish (at least) five potential control points, forming the series:

Activation of gene structure
↓
Initiation of transcription
↓
Processing the transcript
↓
Transport to cytoplasm
↓
Translation of mRNA

The existence of the first step is implied by the discovery that genes may exist in either of two structural conditions. Relative to the state of most of the genome, genes are found in an "active" state in the cells in which they are expressed (see Chapter 27). The change of structure is distinct from the act of transcription, and indicates that the gene is "transcribable." This suggests that acquisition of the "active" structure must be the first step in gene expression.

Transcription of a gene in the active state is controlled at the stage of initiation, that is, by the interaction of RNA polymerase with its promoter. This is now becoming susceptible to analysis in the *in vitro* systems (see Chapter 28). For most genes, this is a major control point; probably it is the most common level of regulation.

There is at present no evidence for control at subsequent stages of transcription in eukaryotic cells, for example, via antitermination mechanisms.

The primary transcript is modified by capping at the 5′ end, and usually also by polyadenylation at the 3′ end. Introns must be spliced out from the transcripts of interrupted genes. The mature RNA must be exported from the nucleus to the cytoplasm. Regulation of gene expression by selection of sequences at the level of nuclear RNA might involve any or all of these stages, but the one for which we have most evidence concerns changes in splicing; some genes are expressed by means of alternative splicing patterns whose regulation controls the type of protein product (see Chapter 30).

Finally, the translation of an mRNA in the cytoplasm can be specifically controlled. There is little evidence for the employment of this mechanism in adult somatic cells, but it does occur in some embryonic situations, as described in Chapter 7. The mechanism is presumed to involve the blocking of initiation of translation of some mRNAs by specific protein factors.

But having acknowledged that control of gene expression can occur at multiple stages, and that production of RNA cannot inevitably be equated with production of protein, it is clear

that the overwhelming majority of regulatory events occur at the initiation of transcription. Regulation of tissue-specific gene transcription lies at the heart of eukaryotic differentiation; indeed, we see examples in Chapter 38 in which proteins that regulate embryonic development prove to be transcription factors. A regulatory transcription factor serves to provide common control of a large number of target genes, and we seek to answer two questions about this mode of regulation: what identifies the common target genes to the transcription factor; and how is the activity of the transcription factor itself regulated in response to intrinsic or extrinsic signals?

Response elements identify genes under common regulation

The principle that emerges from characterizing groups of genes under common control is that *they share a promoter element that is recognized by a regulatory transcription factor.* An element that causes a gene to respond to such a factor is called a response element; examples are the HSE (heat shock response element), GRE (glucocorticoid response element), SRE (serum response element).

The properties of some inducible transcription factors and the elements that they recognize are summarized in Table 29.1. Response elements have the same general characteristics as upstream elements of promoters or enhancers. They contain short consensus sequences, and copies of the response elements found in different genes are closely related, but not necessarily identical. The region bound by the factor extends for a short distance on either side of the consensus sequence. In promoters, the elements are not present at fixed distances from the startpoint, but are usually <200 bp upstream of it. The presence of a single element usually is sufficient to confer the regulatory response, but sometimes there are multiple copies.

Table 29.1 Inducible transcription factors bind to response elements that identify groups of promoters or enhancers subject to coordinate control.

Regulatory Agent	Module	Consensus	Factor
Heat shock	HSE	CNNGAANNTCCNNG	HSTF
Glucocorticoid	GRE	TGGTACAAATGTTCT	Receptor
Phorbol ester	TRE	TGACTCA	AP1
Serum	SRE	CCATATTAGG	SRF

Response elements may be located in promoters or in enhancers. Some types of elements are typically found in one rather than the other: usually an HSE is found in a promoter, while a GRE is found in an enhancer. We assume that all response elements function by the same general principle. *A gene is regulated by a sequence at the promoter or enhancer that is recognized by a specific protein. The protein functions as a transcription factor needed for RNA polymerase to initiate. Active protein is available only under conditions when the gene is to be expressed; its absence means that the promoter is not activated by this particular circuit.*

An example of a situation in which many genes are controlled by a single factor is provided by the heat shock response. This is common to a wide range of prokaryotes and eukaryotes and involves multiple controls of gene expression: an increase in temperature turns off transcription of some genes, turns on transcription of the heat shock genes, and causes changes in the translation of mRNAs. The control of the heat shock genes illustrates the differences between prokaryotic and eukaryotic modes of control. In bacteria, a new sigma factor is synthesized that directs RNA polymerase holoenzyme to recognize an alter-

Discordant Protein and mRNA Expression in Lung Adenocarcinomas*

Guoan Chen‡, Tarek G. Gharib‡, Chiang-Ching Huang§, Jeremy M. G. Taylor§, David E. Misek¶, Sharon L. R. Kardia‖, Thomas J. Giordano**, Mark D. Iannettoni‡, Mark B. Orringer‡, Samir M. Hanash¶, and David G. Beer‡ ‡‡

The relationship between gene expression measured at the mRNA level and the corresponding protein level is not well characterized in human cancer. In this study, we compared mRNA and protein expression for a cohort of genes in the same lung adenocarcinomas. The abundance of 165 protein spots representing 98 individual genes was analyzed in 76 lung adenocarcinomas and nine non-neoplastic lung tissues using two-dimensional polyacrylamide gel electrophoresis. Specific polypeptides were identified using matrix-assisted laser desorption/ionization mass spectrometry. For the same 85 samples, mRNA levels were determined using oligonucleotide microarrays, allowing a comparative analysis of mRNA and protein expression among the 165 protein spots. Twenty-eight of the 165 protein spots (17%) or 21 of 98 genes (21.4%) had a statistically significant correlation between protein and mRNA expression ($r > 0.2445$; $p < 0.05$); however, among all 165 proteins the correlation coefficient values (r) ranged from −0.467 to 0.442. Correlation coefficient values were not related to protein abundance. Further, no significant correlation between mRNA and protein expression was found ($r = -0.025$) if the average levels of mRNA or protein among all samples were applied across the 165 protein spots (98 genes). The mRNA/protein correlation coefficient also varied among proteins with multiple isoforms, indicating potentially separate isoform-specific mechanisms for the regulation of protein abundance. Among the 21 genes with a significant correlation between mRNA and protein, five genes differed significantly between stage I and stage III lung adenocarcinomas. Using a quantitative analysis of mRNA and protein expression within the same lung adenocarcinomas, we showed that only a subset of the proteins exhibited a significant correlation with mRNA abundance.
Molecular & Cellular Proteomics 1:304–313, 2002.

Lung cancer is the leading cause of cancer death for both men and women in the United States. Adenocarcinomas of the lung comprise ~40% of all new cases of non-small cell lung cancer and are now the most common histologic type. Functional genomics, broadly defined as the comprehensive analysis of genes and their products, have become a recent focus of the life sciences (1). Application of these approaches to lung adenocarcinomas has the potential to aid in the identification of high risk patients with resectable early stage lung cancer that may benefit from adjuvant therapy, as well as to identify new therapeutic targets. In human lung cancer, however, little is currently understood regarding the relationship between gene expression as determined by measuring mRNA levels and the corresponding abundance of the protein products.

A number of powerful techniques for analysis of gene expression have been used including differential display (2), serial analysis of gene expression (3), DNA microarrays (4), and proteomics via two-dimensional polyacrylamide gel electrophoresis and mass spectrometry (5). Bioinformatics tools have also been developed to help determine quantitative mRNA/protein expression profiles of all types of cells and tissues (6) and now can be applied to benign and malignant tumors. DNA microarrays (cDNA and oligonucleotide) permit the parallel assessment of thousands of genes and have been utilized in gene expression monitoring (7), polymorphism analysis (8), and DNA sequencing (9). Recent studies have focused on classification or identification of subgroups of lung tumors using DNA microarrays (10, 11). The use of mRNA expression patterns by themselves, however, is insufficient for understanding the expression of protein products, as additional post-transcriptional mechanisms, including protein translation, post-translational modification, and degradation, may influence the level of a protein present in a given cell or tissue. Proteomic analyses, a complementary technology to DNA microarrays for monitoring gene expression, involves protein separation and quantitative assessment of protein spots using 2D[1]-PAGE and protein identification using mass spectrometry. By combining proteomic and transcriptional analyses of the same samples, however, it may be possible to understand the complex mechanisms influencing protein expression in human cancer.

In this study, we determined mRNA and protein levels for 165 proteins (98 genes) in 76 lung adenocarcinomas and nine

From the Departments of ‡Surgery, §Biostatistics, ‖Epidemiology, **Pathology, and ¶Pediatrics, University of Michigan, Ann Arbor, Michigan 48109

Received, January 21, 2002, and in revised form, March 4, 2002
Published, MCP Papers in Press, March 12, 2001, DOI 10.1074/mcp.M200008-MCP200

[1] The abbreviations used are: 2D, two-dimensional; MALDI-MS, matrix-assisted laser desorption/ionization mass spectrometry.

© 2002 by The American Society for Biochemistry and Molecular Biology, Inc.
This paper is available on line at http://www.mcponline.org

TABLE I

Correlation coefficients of protein and mRNA where only one spot was present on 2D gels

r^*, correlation coefficient value > 0.2445; $p < 0.05$. Values in boldface are significant at $p < 0.05$.

Spot	Unigene	Gene name	r^*	Protein name
1104	Hs.184510	SFN	**0.4337**	14-3-3 σ
0994	Hs.77840	ANXA4	**0.4219**	Annexin IV
1314	Hs.10958	DJ-1	**0.3982**	DJ-1 protein/MER5
1454	Hs.75428	SOD1	**0.3863**	Superoxide dismutase (Cu-Zn)
1638	Hs.227751	LGALS1	**0.3318**	Galectin 1
0264	Hs.129548	HNRPK	**0.3034**	Transformation up-regulated nuclear protein
1405	Hs.111334	FTL	**0.2849**	Ferritin light chain
0963	Hs.300711	ANXA5	**0.2468**	Annexin V
1252	Hs.4745	PSMC	**0.2445**	26 S proteasome p28
0906	Hs.234489	LDHB	0.4420	L-lactate dehydrogenase H chain (LDH-B)
1171	Hs.241515	COX11	0.2310	COX 11
1160	Hs.181013	PGAM1	0.2023	Phosphoglycerate mutase
0759	Hs.74635	DLD	0.1965	Dihydrolipoamide dehydrogenase precursor
1193	Hs.83383	AOE372	0.1932	Antioxidant enzyme AOE372
0172	Hs.3069	HSPA9B	0.1872	GRP75
0777	Hs.979	PDHB	0.1855	Pyruvate dehydrogenase E1-β subunit precursor
1249	Hs.226795	GSTP1	0.1773	Glutathione *S*-transferase pi (GST-pi)
1685	Hs.76136	TXN	0.1732	Thioredoxin
1205	Hs.82314	HPRT1	0.1588	HG phosphoribosyltransferase
1230	Hs.279860	TPT1	0.1466	Translationally controlled tumor protein (TCTP)
0603	Hs.181357	LAMR1	0.1463	LAMR
1358	Hs.28914	APRT	0.1399	Adenine phosphoribosyl transferase
1410	Hs.82113	DUT	0.1213	dUTP pyrophosphatase (dUTPase)
1825	Hs.112378	LIMS1	0.1213	Pinch-2 protein
0871	Hs.250502	CA8	0.1122	Carbonic anhydrase-related protein; Syntaxin
0289	Hs.82916	CCT6A	0.1106	Chaperonin-like protein
1143	Hs.11465	GSTTLp28	0.0997	Glutathione *S*-transferase homolog (GST homolog)
1456	Hs.118638	NME1	0.0932	Nm23 (NDPKA)
1598	Hs.278503	RIG	0.0905	RIIG (U32331)
1354	Hs.89761	ATP5D	0.0904	FIFO-type ATP synthase subunit d
1445	Hs.155485	HIP2	0.0843	Huntingtin interacting protein 2 (HIP2)
1479	Hs.177486	APP	0.0746	Amyloid B4A
0608	Hs.182265	KRT19	0.0439	Cytokeratin 19
1071	Hs.10842	RAN	0.0277	GTP-binding nuclear protein RAN(TC4)
0991	Hs.297939	CTSB	0.0254	Cathepsin B
0842	Hs.77274	PLAU	0.0248	Urokinase plasminogen activator
0823	Hs.198248	B4GALT1	0.0183	β 1,4-galactosyl transferase
0613	Hs.1247	APOA4	0.0176	Apolipoprotein A4 (ApoA4)
1338	Hs.104143	CLTA	0.0123	Clathrin light chain A
0902	Hs.5123	SID6-306	0.0117	Cytosolic inorganic pyrophosphatase
1688	Hs.1473	GRP	−0.0040	Preprogastrin-releasing peptide
0265	Hs.274402	HSPA1B	−0.0071	Heat shock-induced protein
1414	Hs.77541	ARF5	−0.0096	ADP-ribosylation factor 1
0710	Hs.97206	HIP1	−0.0114	Huntingtin interacting protein 1 (HIP1)
0532	Hs.170328	MSN	−0.0132	Moesin/E
0525	Hs.284255	ALPP	−0.0148	Alkaline phosphate, placental
0513	Hs.76901	PDIR	−0.0289	Protein disulfide isomerase-related protein 5
1659	Hs.256697	HINT	−0.0312	Protein kinase C inhibitor
1262	Hs.7016	RAB7	−0.0362	Rab 7 protein
0190	Hs.184411	ALB	−0.0470	Albumin
0948	Hs.2795	LDHA	−0.0549	Lactate dehydrogenase-A (LDHA)
0502	Hs.180532	GPI	−0.0575	Hsp89
0152	Hs.75410	HSPA5	−0.0840	GRP78
1054	Hs.74276	CLIC1	−0.0686	Nuclear chloride channel (RNCC protein)
0709	Hs.253495	SFTPD	−0.0936	Pulmonary surfactant protein D
0867	Hs.78998	PCNA	−0.0982	PCNA
0165	Hs.180414	HSPA8	−0.1014	Heat shock cognate protein, 71 kDa
1109	Hs.75103	YWHAZ	−0.1018	14-3-3 ζ/Δ
0137	Hs.554	SSA2	−0.1032	Ro/ss-A antigen

TABLE I—*continued*

Spot	Unigene	Gene name	r	Protein name
0278	Hs.4112	TCP1	−0.1237	T-complex protein I, α subunit
1769	Hs.9614	NPM1	−0.1738	B23/numatrin
0089	Hs.74335	HSPCB	−0.2049	Hsp90
2511	Hs.153179	FABP5	−0.2109	E-FABP/FABP5
1739	Hs.16488	CALR	−0.2344	Calreticulin S2
1138	Hs.301961	GSTM4	−0.2438	Glutathione S-transferase M4 (GST m4)
2533	Hs.77060	PSMB6	−0.2512	Macropain subunit Δ

non-neoplastic lung tissues. Protein levels were determined using quantitative 2D-PAGE analysis, and the separated protein polypeptides were identified using matrix-assisted laser desorption/ionization mass spectrometry (MALDI-MS). The corresponding mRNA levels for the identified proteins within the same samples were determined using oligonucleotide microarrays. Correlation analyses showed that protein abundance is likely a reflection of the transcription for a subset of proteins, but translation and post-translational modifications also appear to influence the expression levels of many individual proteins in lung adenocarcinomas.

EXPERIMENTAL PROCEDURES

Tissues—Fifty-seven stage I and 19 stage III lung adenocarcinomas, as well as nine non-neoplastic lung tissue samples, were used for protein and mRNA analyses. Patient consent was obtained, and the project was approved by the Institutional Review Board. All tissues were obtained after resection at the University of Michigan Health System between May 1991 and July 1998. Tissues were all snap-frozen in liquid nitrogen and then stored at −80 °C. The patients included 46 females and 30 males ranging in age from 40.9 to 84.6 (average 63.8) years. Most patients (66/76) demonstrated a positive smoking history. Sixty-one tumor samples were classified as bronchial-derived, 14 were classified as bronchoalveolar, and one had both features. Eighteen tumor samples were classified as well differentiated, 38 were classified as moderate, and 19 were classified as poorly differentiated adenocarcinomas. Hematoxylin-stained cryostat sections (5 μm), prepared from the same tumor pieces to be utilized for protein and mRNA isolation, were evaluated by a pathologist and compared with hematoxylin- and eosin-stained sections made from paraffin blocks of the same tumors. Specimens were excluded from analysis if they showed unclear or mixed histology (*e.g.* adenosquamous), tumor cellularity less than 70%, potential metastatic origin as indicated by previous tumor history, extensive lymphocytic infiltration, or fibrosis or if the patient had received prior chemotherapy or radiotherapy.

Oligonucleotide Array Hybridization—The HuGeneFL oligonucleotide arrays (Affymetrix, Santa Clara, CA) containing 6800 genes were used in this study. Total RNA was isolated from all samples using Trizol reagent (Invitrogen). The resulting RNA was then subjected to further purification using RNeasy spin columns (Qiagen). Preparation of cRNA, hybridization, and scanning of the HuGeneFL arrays were performed according to the manufacturer's protocol (Affymetrix, Santa Clara, CA). Data analysis was performed using GeneChip 4.0 software. The gene expression profile of each tumor was normalized to the median gene expression profile for the entire sample. Details of data trimming and normalization are described elsewhere (11).

2D-PAGE and Quantitative Protein Analysis—Tissue for both protein and mRNA isolation came from contiguous areas of each sample. Protein separation using 2D-PAGE, silver staining, and digitization were performed as described previously (12, 13). Our 2D-PAGE system allows us to run 20 gels at one time (one batch). Spot detection and quantification were accomplished utilizing Bio Image Visage System software (Bioimage Corp., Ann Arbor, MI). The integrated intensity of each spot was calculated as the measured optical density units × mm^2. Of the total possible 2000 spots detectable on each gel, 820 spots on the gel of each sample were matched using a Gel-ed match program with the same spots on a chosen "master" gel. In each sample, 250 ubiquitously expressed reference spots were used to adjust for variations between gels, such as that created by subtle differences in protein loading or gel staining. Slight differences because of batch were corrected after spot-size quantification.

Mass Spectrometry and 2D Western Blotting—Preparative 2D gels were run using extracts from A549 lung adenocarcinoma cells (obtained from ATCC) and using the identical experimental conditions as the analytical 2D gels, except 30% more protein was loaded. The resolved protein gels were silver-stained using successive incubations in 0.02% sodium thiosulfate for 2 min, 0.1% silver nitrate for 40 min, and 0.014% formaldehyde plus 2% sodium carbonate for 10 min. For protein identification, protein polypeptides underwent trypsin digestion followed by MALDI-MS using a MALDI-TOF Voyager-DE mass spectrometer (Perseptive Biosystems, Framingham, MA). The masses were compared with known trypsin digest databases using the MS-FIT database (University of California, San Francisco; prospector.ucsf.edu/ucsfhtml3.2/msfit.htm). Some of the polypeptides included in the analysis had been identified prior to this study on the basis of sequencing (14). The identified protein spots used in this paper are shown in Fig. 1*A*. The method for 2D-PAGE Western blot verification was as described previously (15). The 2D Western blots of GRP58 and Op18 are shown in Fig. 1, *C* and *E*; the others, such as GRP78, GRP75, HSP70, HSC70, KRT8, KRT18, KRT19, Vimentin, ApoJ, 14–3-3, Annexin I, Annexin II, PGP9.5, DJ-1, GST-pi, and PGAM, are described elsewhere.[2]

Statistical Analysis—Missing values were replaced with the mean value of the protein spot. The transform $x \rightarrow \log(1 + x)$ was applied to normalize all protein expression values. The relationship between protein and mRNA expression levels within the same samples was examined using the Spearman correlation coefficient analysis (16). To identify potentially significant correlations between gene and protein expression, we used an analytical strategy similar to SAM (significance analysis of microarrays) (17), which uses a permutation technique to determine the significance of changes in gene expression between different biological states. To obtain permuted correlation coefficients between gene and protein expression, genes were exchanged first in such a way that permutated correlation coefficient were calculated based on pseudo pairs of genes and proteins. The distribution of permutated correlation coefficients became stable after 60 permutations. This procedure was then repeated 60 times to obtain 60 sets of permutated correlation coefficients. For each of the 60 permutations, the correlations of genes and proteins were ranked

[2] Chen *et al.*, submitted for publication.

TABLE II

Correlation coefficients of protein and mRNA where multiple isoforms were present on 2D gels

r^*, correlation coefficient value > 0.2445; $p < 0.05$. Values in boldface are significant at $p < 0.05$.

Spot	Unigene	Gene name	r^*	Protein name
1494	Hs.81915	LAP18	0.4003	OP18 (Stathmin)
0957	Hs.77899	TPM1	0.3930	Tropomyosins 1–5
0353	Hs.289101	GRP58	0.3802	Protease disulfide isomerase (GRP58)
0855	Hs.169476	GAPD	0.3693	Glyceraldehyde-3-phosphate dehydrogenase
1198	Hs.41707	HSPB3	0.3668	Hsp27
1203	Hs.83848	TPI1	0.3395	Triose phosphate isomerase (TPI)
0523	Hs.65114	KRT18	0.3335	Cytokeratin 18
1492	Hs.81915	LAP18	0.3234	OP18 (Stathmin)
1493	Hs.81915	LAP18	0.3154	OP18 (Stathmin)
1181	Hs.78225	ANXA1	0.3102	Annexin variant I
0439	Hs.242463	KRT8	0.3049	Cytokeratin 8
0505	Hs.297753	VIM	0.2939	Vimentin
0593	Hs.297753	VIM	0.2809	Vimentin
1874	Hs.75313	AKR1B1	0.2790	Aldose reductase
0935	Hs.75544	YWHAH	0.2775	14-3-3 η
2524	Hs.78225	ANXA1	0.2612	Annexin I
2324	Hs.65114	KRT18	0.2601	Cytokeratin 18
1192	Hs.41707	HSPB3	0.2558	Hsp27
0350	Hs.289101	GRP58	0.2516	Phospholipase C (GRP58)
0992	Hs.75313	AKR1B1	−0.2460	Aldose reductase
0861	Hs.75313	AKR1B1	0.0761	Aldose reductase
0853	Hs.75313	AKR1B1	−0.0675	Aldose reductase
2503	Hs.76392	ALDH1	−0.0565	Aldehyde dehydrogenase
0381	Hs.76392	ALDH1	−0.0371	Aldehyde dehydrogenase
0371	Hs.76392	ALDH1	−0.0680	Aldehyde dehydrogenase
1179	Hs.78225	ANXA1	0.2052	Annexin variant I
0762	Hs.78225	ANXA1	−0.0739	Annexin I
0760	Hs.78225	ANXA1	−0.0228	Annexin I
2506	Hs.217493	ANXA2	0.2223	Lipocotin (annexin II)
0772	Hs.217493	ANXA2	0.2080	Lipocotin (annexin II)
0723	Hs.217493	ANXA2	0.0701	Lipocotin
1239	Hs.93194	APOA1	0.1133	Apolipoprotein A1 (ApoA1)
1237	Hs.93194	APOA1	−0.0373	Apolipoprotein A1 (ApoA1)
1234	Hs.93194	APOA1	−0.0894	Apolipoprotein A1 (ApoA1)
0428	Hs.25	ATP5B	0.0080	ATP synthase β subunit precursor
0427	Hs.25	ATP5B	0.0122	ATP synthase β subunit precursor
0424	Hs.25	ATP5B	−0.0992	ATP synthase β subunit precursor
0863	Hs.75106	CLU	−0.0483	Apolipoprotein J (ApoJ)
0780	Hs.75106	CLU	−0.0443	Apolipoprotein J (ApoJ)
1527	Hs.119140	EIF5A	−0.0726	eIF-5A
1484	Hs.119140	EIF5A	−0.0378	eIF-5A
1728	Hs.5241	FABP1	−0.1916	L-FABP
1712	Hs.5241	FABP1	−0.0473	L-FABP
0947	Hs.169476	GAPD	0.1745	Glyceraldehyde-3-phosphate dehydrogenase
1232	Hs.75207	GLO1	0.2249	Glyoxalase-I
1229	Hs.75207	GLO1	0.0450	Glyoxalase-1
1595	Hs.158300	HAP1	−0.0137	Huntingtin-associated protein 1 (neuroan 1)
1810	Hs.75990	HP	−0.4672	α-Haptoglobin
1459	Hs.75990	HP	0.0802	α-Haptoglobin
1458	Hs.75990	HP	−0.0305	α-Haptoglobin
0619	Hs.75990	HP	0.0461	B-haptoglobin
0615	Hs.75990	HP	−0.0034	B-haptoglobin
1250	Hs.41707	HSPB3	−0.1024	Hsp27
0549	Hs.79037	HSPD1	0.1074	Hsp60
0338	Hs.79037	HSPD1	0.2265	Hsp60
0333	Hs.79037	HSPD1	0.1383	Hsp60
0331	Hs.79037	HSPD1	0.1603	Hsp60
2381	Hs.65114	KRT18	0.2016	Cytokeratin 18
0535	Hs.65114	KRT18	0.1106	Cytokeratin 18

TABLE II—*continued*

Correlation coefficients of protein and mRNA where multiple isoforms were present on 2D gels

r^*, correlation coefficient value > 0.2445; $p < 0.05$. Values in boldface are significant at $p < 0.05$.

Spot	Unigene	Gene name	r^*	Protein name
0529	Hs.65114	KRT18	0.1279	Cytokeratin 18
0528	Hs.65114	KRT18	0.0414	Cytokeratin 18
0527	Hs.65114	KRT18	0.0436	Cytokeratin 18
0514	Hs.65114	KRT18	0.0733	Cytokeratin 18
0451	Hs.242463	KRT8	−0.0111	Cytokeratin 8
0446	Hs.242463	KRT8	0.0347	Cytokeratin 8
0444	Hs.242463	KRT8	−0.1311	Cytokeratin 8
0443	Hs.242463	KRT8	0.0942	Cytokeratin 8
1488	Hs.81915	LAP18	0.0495	OP18 (Stathmin)
0321	Hs.75655	P4HB	−0.0548	PDI (prolyl-4-OH-B)
0320	Hs.75655	P4HB	−0.0041	PDI (prolyl-4-OH-B)
1063	Hs.75323	PHB	0.0441	Prohibitin
0837	Hs.75323	PHB	0.1402	Prohibitin
0326	Hs.297681	SERPINA1	−0.0227	α-1-Antitrypsin
0322	Hs.297681	SERPINA1	−0.0277	α-1-Antitrypsin
0241	Hs.297681	SERPINA1	−0.0148	α-1-Antitrypsin
1280	Hs.301254	SFTPA1	−0.1488	Pulmonary surfactant-associated protein
1278	Hs.301254	SFTPA1	−0.2040	Pulmonary surfactant-associated protein
0866	Hs.73980	TNNT1	0.1162	Troponin T
0778	Hs.73980	TNNT1	0.0740	Troponin T
1213	Hs.83848	TPI1	0.0024	Triose phosphate isomerase (TPI)
1210	Hs.83848	TPI1	0.0490	Triose phosphate isomerase (TPI)
1207	Hs.83848	TPI1	−0.1615	Triose phosphate isomerase (TPI)
1204	Hs.83848	TPI1	0.0209	Triose phosphate isomerase (TPI)
1202	Hs.83848	TPI1	0.0721	Triose phosphate isomerase (TPI)
1161	Hs.83848	TPI1	0.2265	Triose phosphate isomerase (TPI)
1052	Hs.77899	TPM1	−0.1040	Tropomysin clean-product
1039	Hs.77899	TPM1	−0.2999	Cytoskeletal tropomyosin
1035	Hs.77899	TPM1	−0.3821	Tropomyosin
0783	Hs.77899	TPM1	0.0757	Tropomyosins 1–6
1574	Hs.194366	TTR	−0.0065	Transthyretin
0809	Hs.194366	TTR	0.0399	Transthyretin multimere
2202	Hs.76118	UCHL1	−0.0220	Ubiquitin carboxyl-terminal hydrolase isozyme L1
1246	Hs.76118	UCHL1	−0.1261	Ubiquitin carboxyl-terminal hydrolase isozyme L1
1242	Hs.76118	UCHL1	0.1473	Ubiquitin carboxyl-terminal hydrolase isozyme L1
0606	Hs.297753	VIM	0.0951	Vimentin
0594	Hs.297753	VIM	−0.2664	Vimentin-derived protein (vid4)
0508	Hs.297753	VIM	0.1008	Vimentin-derived protein (vid2)
0419	Hs.297753	VIM	0.0032	Vimentin-derived protein (vid1)
1279	Hs.75544	YWHAH	0.0059	14-3-3 η

such that $\rho_p(i)$ denotes the ith largest correlation coefficient for pth permutation. Hence, the expected correlation coefficient, $\rho_E(i)$, was the average over the 60 permutations, $\rho_E(i) = \sum_{p=1}^{60} \rho_p(i)/60$. A scatter plot of observed correlations ($\rho(i)$) *versus* the expected correlations is shown in Fig. 2*D*. For this study, we chose threshold $\Delta = 0.115$ so that correlation would be considered significant if absolute value of difference between $\rho(i)$ and $\rho_E(i)$ was greater than the threshold. Twenty-nine (including one with observed correlation coefficient −0.4672) of 165 pairs of gene and protein expression were called significant in such criteria, and the permuted data generated an average of 5.1 falsely significant pairs of gene and protein expression. This provided an estimated false discovery rate (the percentage of pairs of gene and protein expression identified by chance) for our data set.

RESULTS

Correlation of Individual Proteins and mRNA Expression within Each Tumor—We have examined quantitatively 165 protein spots on 2D gels representing 98 genes and compared protein levels with mRNA levels for a cohort of 85 lung adenocarcinomas and normal lung samples. Of the 165 protein spots, 69 proteins were represented by only one known spot on 2D gels for an individual gene, whereas 96 protein spots showed multiple protein products from 29 different genes. 2D Western blotting verified the proteins identified by mass spectrometry when specific antibodies were available. Spearman correlation coefficients of the proteins and their associated mRNA for each protein spot were generated using all 76 lung adenocarcinomas and nine non-neoplastic lung tissues (see Tables I and II, and see Figs. 1 and 2). The correlation coefficients (r) ranged from −0.467 to 0.442 (Fig. 2*D*). A total of 28 protein spots (21 genes) were found to have a statistically significant correlation between expression of

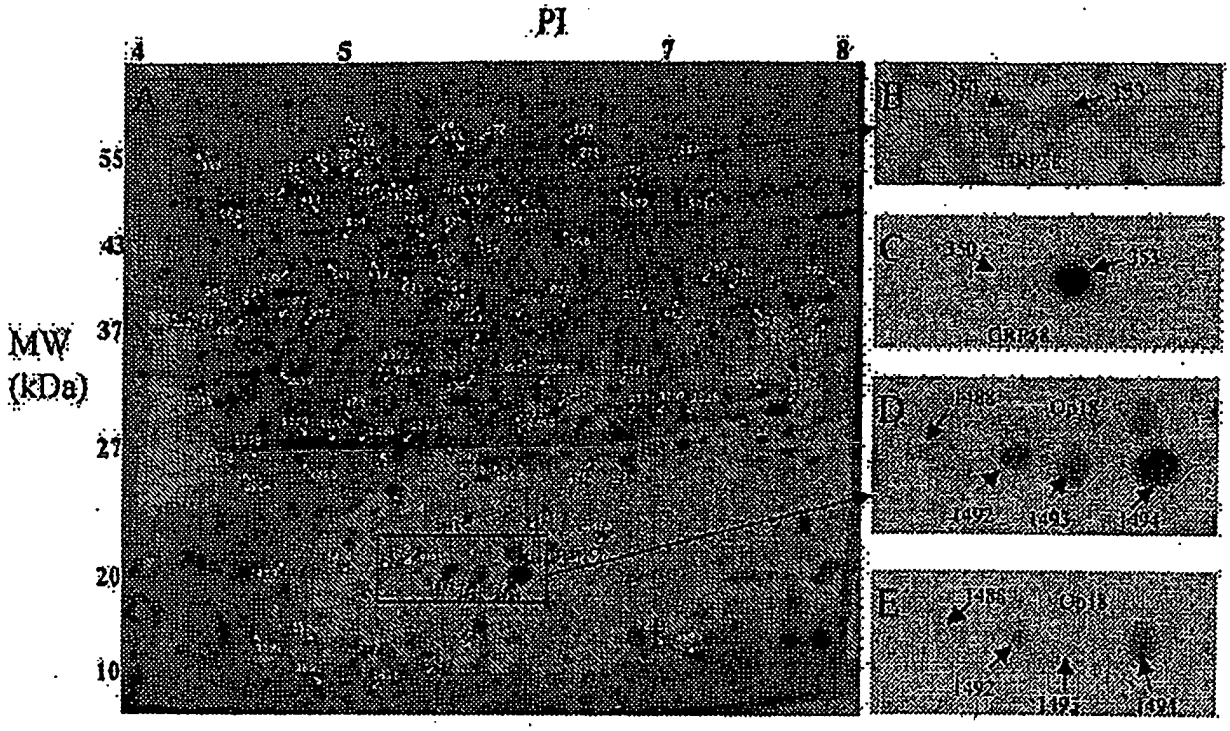

FIG. 1. *A*, digital image of a silver-stained 2D-PAGE separation of a stage I lung adenocarcinoma showing protein spots separated by molecular mass (*MW*) and isoelectric point (*PI*). Twenty-eight protein spots whose expression levels are correlated with mRNA abundance are indicated by the *black arrows*. *B*, the outlined areas of *A* showing protein GRP58. *C*, 2D Western blot of GRP58 from the A549 lung adenocarcinoma cell line. *D*, the outlined areas of *A* showing the protein isoforms of Op18. *E*, 2D Western blot of Op18 from A549 cells.

their protein and mRNA ($r > 0.2445$; $p < 0.05$). This accounts for 17% (28/165) of the 165 protein spots. Among the 69 genes for which only a single protein spot was known (Table I), nine genes (9/69, 13%) were observed to show a statistically significant relationship between protein and mRNA abundance ($r > 0.2445$; $p < 0.05$). The proteins whose expression levels were correlated with their mRNA abundance included those involved in signal transduction, carbohydrate metabolism, apoptosis, protein post-translational modification, structural proteins, and heat shock proteins (Table III).

Individual Isoforms of the Same Protein Have Different Protein/mRNA Correlation Coefficients—Of the 165 protein spots, 98 represent protein products of 29 genes with at least two isoforms. Among these 98 protein spots, 19 (19/98 protein spots, 20%) showed a statistically significant correlation between their protein and mRNA expression ($r > 0.2445$; $p < 0.05$) (Table II) and represented 12 genes (12/29, 41%). Individual isoforms of the same protein demonstrated different protein/mRNA correlation coefficients. For example, 2D-PAGE/Western analysis revealed four isoforms of OP18 differing in regards to isoelectric point but similar in molecular weight. Three of the four isoforms (spots 1492, 1493, and 1494) showed a statistically significant correlation between their protein and mRNA abundance ($r = 0.3234$, 0.3154, and 0.4003, respectively). The forth isoform (spot 1488) showed no correlation between protein and mRNA expression ($r = 0.0495$). Similarly, just one of five quantified isoforms of cytokeratin 8 (spot 439) demonstrated a statistically significant correlation between protein and mRNA abundance ($r = 0.3049$; $p < 0.05$) (Table II).

In addition to differences in the relationship between mRNA levels and protein expression among separate isoforms, some genes with very comparable mRNA levels showed a 24-fold difference in their protein expression. Genes with comparable protein expression levels also showed up to a 28-fold variance in their mRNA levels.

Lack of Correlation for mRNA and Protein Expression when Using Average Tumor Values across All 165 Protein Spots (98 Genes)—The relationship between mRNA and protein expression was also examined by using the average expression values for all samples. To analyze this relationship using this approach, the average value for each protein or mRNA was generated using all 85 lung tissue samples. The range of normalized average protein values ranged from −0.0846 to 0.0979 (raw value 0.0036 to 4.1947), and the range for mRNA was from 0 to 15260.5 for all 165 individual protein spots. The Spearman correlation coefficient for the whole data set (165 protein spots/98 genes) was −0.025 (Fig. 3*A*). Even for the 28 protein spots (Fig. 2*D*) that were found to have a statistically significant correlation between their mRNA and protein, use of

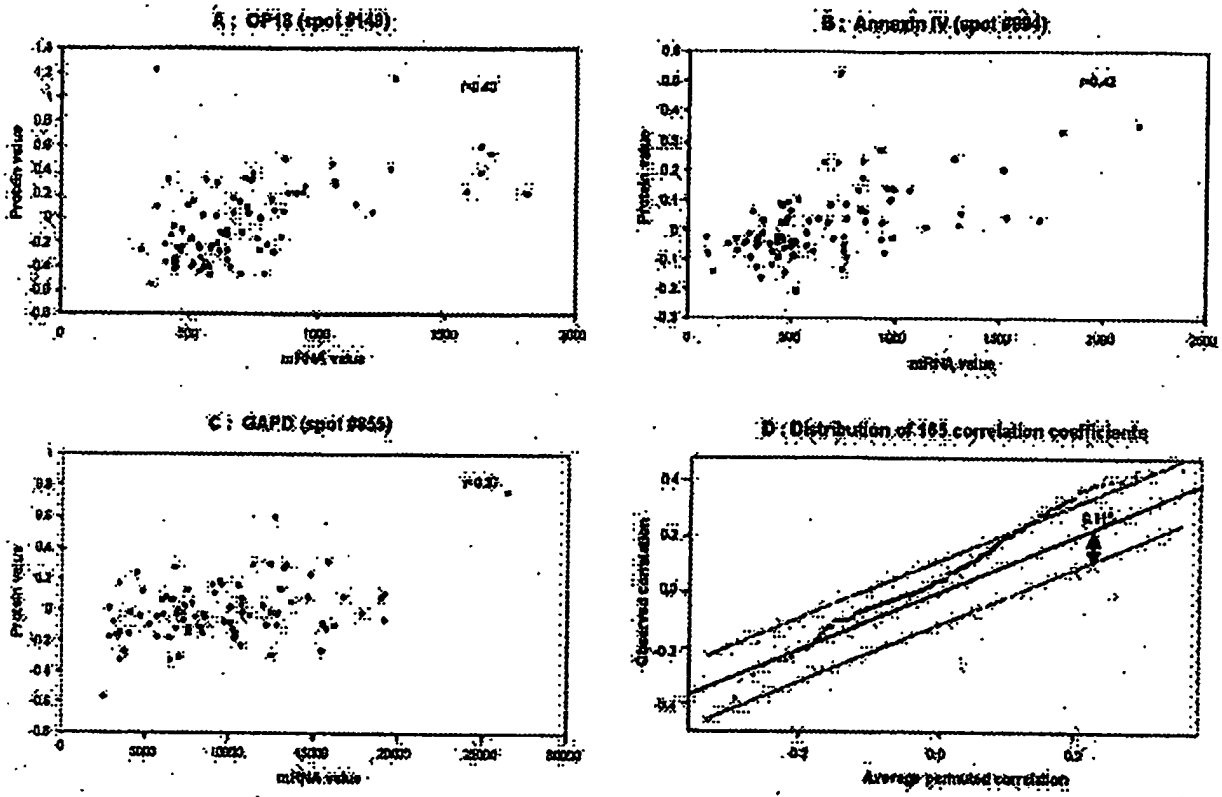

FIG. 2. *A–C*, plots showing the correlation between mRNA and protein for the three selected genes Op18, Annexin IV, and GAPD for all 76 lung adenocarcinomas and nine non-neoplastic lung samples ($p < 0.05$). *D*, distribution of all 165 Spearman correlation coefficients (r) and verification analysis using SAM. A more detailed description of the method is provided under "Experimental Procedures." Approximately 17% of the 165 proteins demonstrate a significant correlation between mRNA and protein levels as demonstrated by the values shown beyond the outer range of threshold $\Delta = 0.115$. Normalized protein values were used, thus negative values for some proteins are observed.

the average value resulted in a correlation coefficient value of −0.035, which was not significant (Fig. 3*B*).

Lack of a Relationship between Protein/mRNA Correlation Coefficients and Average Protein Abundance—To determine whether an absolute protein level might influence the correlation with mRNA, the mean value of each protein (relative abundance) and the Spearman protein/mRNA correlation coefficients among all 85 samples were examined. No relationship between the protein abundance and the correlation coefficients was observed ($r = 0.039$; $p > 0.05$). A detailed analysis of separate subsets of proteins with differing levels of abundance (less than −0.0014, larger than −0.0014, or larger than 0.0077) also showed a lack of correlation between mRNA and protein expression among the 83 (50%), 82 (50%), and 41 (25%) of 165 total protein spots, respectively ($r = 0.016$, 0.08, and 0.172, respectively).

Stage-related Changes in the Protein/mRNA Correlation Coefficients—To determine whether the 21 genes (28 protein spots) showing a significant correlation between the protein and mRNA expression among all samples demonstrate changes in this relationship during tumor progression, the correlations were examined separately for stage I ($n = 57$) and stage III ($n = 19$) lung adenocarcinomas (Table III). The number of non-neoplastic lung samples ($n = 9$) was insufficient for a separate correlation analysis of this group. Many of the protein spots represent one of several known protein isoforms for a given gene. The majority of genes (16/21) did not differ in the protein/mRNA correlation between stage I and stage III tumors indicating a similar regulatory relationship between the mRNA and protein spot. GRP-58, PSMC, SOD1, TPI1, and VIM, however, were found to demonstrate significant differences in the correlation coefficients between stage I and stage III lung adenocarcinomas. For GRP-58, PSMC, and VIM the change in the correlation coefficient was because of a relative increase in protein expression in stage III tumors. For SOD and TPI the change resulted from a relative decrease in expression of this specific protein in stage III tumors.

DISCUSSION

Relatively little is known about the regulatory mechanisms controlling the complex patterns of protein abundance and post-translational modification in tumors. Most reports concerning the regulation of protein translation have focused on

TABLE III
Stage-dependent analysis of protein-mRNA correlation coefficients
r, correlation coefficient. Values in boldface indicate a significant difference between stage I and stage III.

Spot	Gene name	r (Stage I)	r (Stage III)	Function
1874	AKR1B1	0.269	0.106	Carbohydrate metabolism; electron transporter
2524	ANXA1	0.184	0.572	Phospholipase inhibitor; signal transduction
0994	ANXA4	0.660	0.382	Phospholipase inhibitor
0963	ANXA5	0.241	0.390	Phospholipase inhibitor; calcium binding; phospholipid binding
1314	DJ-1	0.363	0.354	Signal transduction
1405	FTL	0.126	0.358	Iron storage protein
0855	GAPD	0.243	0.581	Carbohydrate metabolism (glycolysis regulation)
0350	GRP58	0.327	−0.087	Signal transduction; protein disulfide isomerase
0264	HNRPK	0.360	0.243	RNA-binding protein (RNA processing/modification)
1192	HSPB3	0.457	0.633	Heat shock protein
0523	KRT18	0.115	0.371	Structural protein
0439	KRT8	0.323	0.436	Structural protein
1492	LAP18	0.483	0.663	Signal transduction; cell growth and maintenance
1638	LGALS1	0.200	0.528	Apoptosis; cell adhesion; cell size control
1252	PSMC	0.253	0.060	Protein degradation
1104	SFN	0.465	0.475	Signal transduction (protein kinase C inhibitor)
1454	SOD1	0.352	0.079	Oxidoreductase
1203	TPI1	0.378	0.009	Carbohydrate metabolism
0957	TPM1	0.475	0.226	Structural protein (muscle); control of heart
0593	VIM	−0.054	0.556	Structural protein
0935	YWHAH	0.283	0.210	Signal transduction

one or several protein products (18). Celis *et al.* (19) found a good correlation between transcript and protein levels among 40 well resolved, abundant proteins using a proteomic and microarray study of bladder cancer. By comparing the mRNA and protein expression levels within the same tumor samples, we found that 17% (28/165) of the protein spots (21/98 genes) show a statistically significant correlation between mRNA and protein. These proteins appear to represent a diverse group of gene products and include those involved in signal transduction, carbohydrate metabolism, protein modification, cell structure, heat shock, and apoptosis. These results suggest that expression of this subset of 165 proteins is likely to be regulated at the transcriptional level in these tissues. The majority of the protein isoforms, however, did not correlate with mRNA levels, and thus their expression is regulated by other mechanisms. We also observed a subset of proteins that demonstrated a negative correlation with the mRNA expression values; for example α-haptoglobin demonstrated a strong negative correlation with its mRNA expression values. This may reflect negative feedback on the mRNA or the protein or the presence of other regulatory influences that are not understood currently.

Post-translational modification or processing will result in individual protein products of the same gene migrating to different locations on 2D-PAGE gels (20). Because the identity of all possible isoforms for each protein examined has not been characterized completely, this may influence the correlation analyses performed in this study. This is partly because of limitations of the 2D-PAGE and mass spectrometry technologies (21, 22). Potential inconsistencies between mRNA and protein correlations that have been reported may also be because of differences, even in the same gene, in the mechanisms of protein translation among different cells or as measured in different laboratories (23).

In this study, we examined 165 protein spots identified in lung adenocarcinomas. Ninety-six protein spots, representing the products of 29 genes, contained at least two protein isoforms. Nineteen of 96 protein spots, representing 12 genes, were shown to have a statistically significant correlation between their protein and mRNA expression, suggesting that the levels of these proteins reflects the transcription of the corresponding genes. Differences in protein/mRNA correlations were found among the individual isoforms of a given protein. For example, of the four OP18 isoforms, three showed a statistically significant correlation between the protein and mRNA expression levels. The lack of relationship for the one isoform, however, indicates that individual protein isoforms of the same gene product can be regulated differentially. This is not unexpected and likely reflects other post-translational mechanisms that can influence isoform abundance in tissues and cancer.

In addition to the analyses of the correlation of mRNA/protein within the same tumor samples, we also tested the global relationship between mRNA and the corresponding protein abundance across all 165 protein spots in the lung samples. A protein and mRNA average value for each gene was generated using all 85 lung tissues samples. We observed a very wide range of normalized average protein and mRNA values. The correlation coefficient generated using this average value data set was −0.025, and even for the 28 protein spots that showed a statistically significant correlation between individual mRNA and proteins, the correlation value was only −0.035. This suggests that it is not possible to predict overall protein expression levels based on average

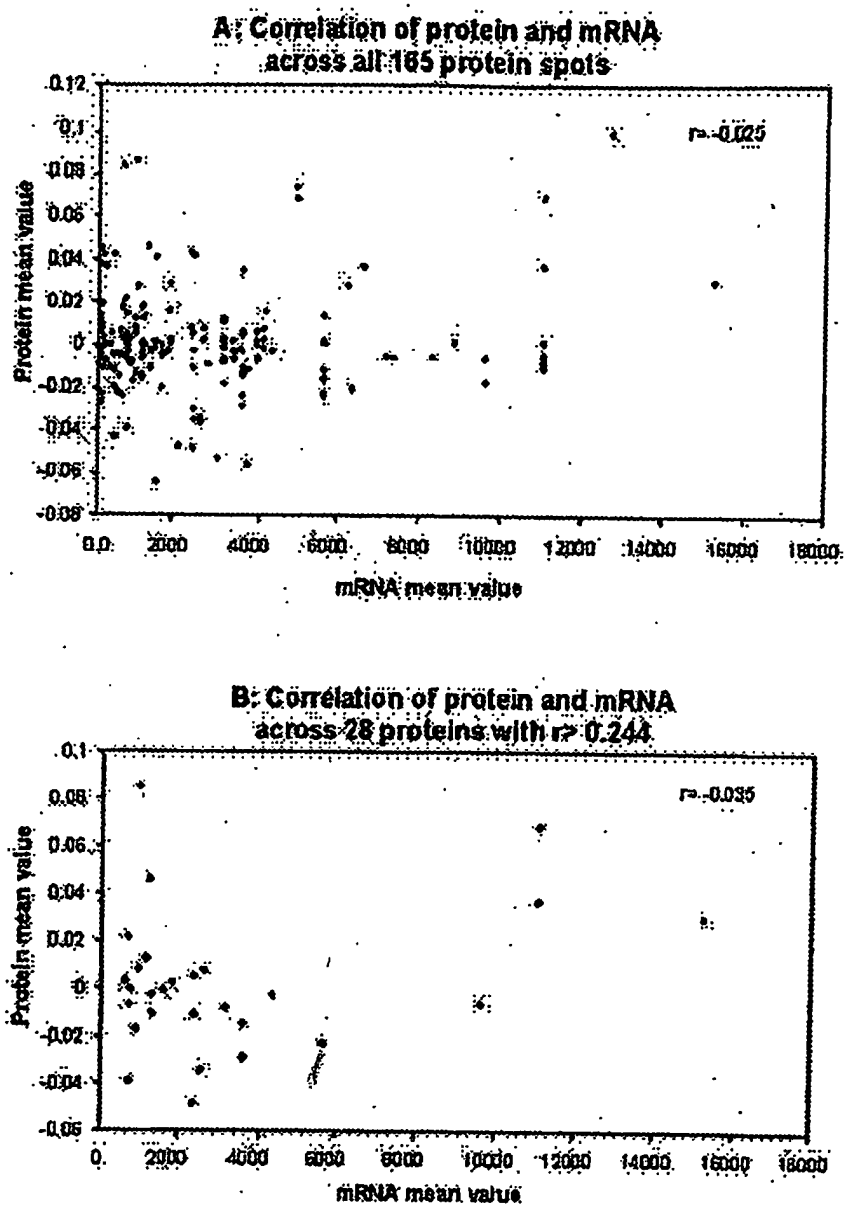

FIG. 3. The overall correlation of mRNA and protein levels across all 165 protein spots (*A*) and across 28 protein spots that contained individual *r* values larger than 0.244 (*B*) are shown. Each protein or mRNA mean value was calculated based on all 76 lung adenocarcinomas and nine non-neoplastic lung samples using quantitative 2D-PAGE and Affymetrix oligonucleotide microarrays. The Spearman correlation coefficients for the two data sets (*A* and *B*) were −0.025 and −0.035, respectively, indicating a lack of correlation if mean values for mRNA and protein for all samples is used.

mRNA abundance in lung cancer samples. This conclusion is also supported by previous results from Anderson and Seilhamer (24), who examined 19 genes in human liver cells, and by Gygi *et al.* (25), who examined 106 genes in yeast. Both studies found a lack of correlation between mRNA and protein expression when average or overall levels were used.

A good correlation was reported when the 11 most abundant proteins were examined in yeast (25), suggesting that the level of protein abundance may be a factor that may influence the correlation between mRNA and protein. In the present study, a fairly wide range of mean protein values among 165 protein spots in lung adenocarcinomas was observed, and the correlation coefficients also varied from −0.467 to 0.442. A comparison between the mean value of each protein and the correlation coefficient generated using all 85 tissue samples did not reveal a strong relationship between the overall protein abundance and the correlation coefficients ($r = 0.039$; $p > 0.05$). Detailed analysis of different subsets of protein abundance also failed to show a correlation between mRNA and protein expression. Thus in contrast to yeast, a relationship between mRNA/protein correlation coefficient and protein abundance in human lung adenocarcinomas was not observed.

The results of this study indicate that the level of protein abundance in lung adenocarcinomas is associated with the corresponding levels of mRNA in 17% (28 proteins) of the total 165 protein spots examined. This was substantially

higher than the amount predicted to result by chance alone (which was 5.1) and suggests that a transcriptional mechanism likely underlies the abundance of these proteins in lung adenocarcinomas. We also demonstrate that the expression of individual isoforms of the same protein may or may not correlate with the mRNA, indicating that separate and likely post-translational mechanisms account for the regulation of isoform abundance. These mechanisms may also account for the differences in the correlation coefficients observed between stage I and stage III tumors, indicating that specific protein isoforms show regulatory changes during tumor progression. Further studies in lung adenocarcinomas will examine the relationship between the expression of individual protein isoforms and specific clinical-pathological features of these tumors, such as the presence of angiolymphatic invasion, and nodal or pleural surface involvement. The potential to identify specific protein isoforms associated with biological behavior in lung adenocarcinomas would be of considerable interest and will add to our understanding of the regulation of gene products by transcriptional, translational, and post-translational mechanisms.

Acknowledgments—We thank Kerby A. Shedden, Rork D. Kuick, Eric Puravs, Robert Hinderer, Melissa C. Krause, and Christopher Wood for assistance in this study.

* This work was supported by NCI, National Institutes of Health Grant U19 CA-85953. The costs of publication of this article were defrayed in part by the payment of page charges. This article must therefore be hereby marked "*advertisement*" in accordance with 18 U.S.C. Section 1734 solely to indicate this fact.

‡‡ To whom correspondence should be addressed: General Thoracic Surgery, SRB II, B560, Box 0686, University of Michigan Medical School, Ann Arbor, MI 48109-086; E-mail: dgbeer@umich.edu.

REFERENCES

1. Ideker, T., Thorsson, V., Ranish, J. A., Christmas, R., Buhler, J., Eng, J. K., Bumgarner, R., Goodlett, D. R., Aebersold, R., Hood, L. (2001) Integrated genomic and proteomic analyses of a systematically perturbed metabolic network. *Science* 292, 929–934
2. Liang, P., Pardee, A. B. (1998) Differential display. A general protocol. *Mol. Biotechnol.* 10, 261–267
3. Porter, D. A., Krop, I. E., Nasser, S., Sgroi, D., Kaelin, C. M., Marks, J. R., Riggins, G., Polyak, K. (2001) A sage (serial analysis of gene expression) view of breast tumor progression. *Cancer Res.* 61, 5697–5702
4. Bittner, M., Meltzer, P., Chen, Y., Jiang, Y., Seftor, E., Hendrix, M., Radmacher, M., Simon, R., Yakhini, Z., Ben-Dor, A., Sampas, N., Dougherty, E., Wang, E., Marincola, F., Gooden, C., Lueders, J., Glatfelter, A., Pollock, P., Carpten, J., Gillanders, E., Leja, D., Dietrich, K., Beaudry, C., Berens, M., Alberts, D., Sondak, V. (2000) Molecular classification of cutaneous malignant melanoma by gene expression profiling. *Nature* 406, 536–540
5. Fung, E. T., Wright, G. L., Jr., Dalmasso, E. A. (2000) Proteomic strategies for biomarker identification: progress and challenges. *Curr. Opin. Mol. Ther.* 2, 643–650
6. Davidson, D., Baldock, R. (2001) Bioinformatics beyond sequence: mapping gene function in the embryo. *Nat. Rev. Genet.* 2, 409–417
7. Chee, M., Yang, R., Hubbell, E., Berno, A., Huang, X. C., Stern, D., Winkler, J., Lockhart, D. J., Morris, M. S., Fodor, S. P. (1996) Accessing genetic information with high-density DNA arrays. *Science* 274, 610–614
8. Wang, D. G., Fan, J. B., Siao, C. J., Berno, A., Young, P., Sapolsky, R., Ghandour, G., Perkins, N., Winchester, E., Spencer, J., Kruglyak, L., Stein, L., Hsie, L., Topaloglou, T., Hubbell, E., Robinson, E., Mittmann, M., Morris, M. S., Shen, N., Kilburn, D., Rioux, J., Nusbaum, C., Rozen, S., Hudson, T. J., Lander, E. S. (1998) Large-scale identification, mapping, and genotyping of single-nucleotide polymorphisms in the human genome. *Science* 280, 1077–1082
9. Pease, A. C., Solas, D., Sullivan, E. J., Cronin, M. T., Holmes, C. P., Fodor, S. P. (1994) Light-generated oligonucleotide arrays for rapid DNA sequence analysis. *Proc. Natl. Acad. Sci. U. S. A.* 91, 5022–5026
10. Bhattacharjee, A., Richards, W. G., Staunton, J., Li, C., Monti, S., Vasa, P., Ladd, C., Beheshti, J., Bueno, R., Gillette, M., Loda, M., Weber, G., Mark, E. J., Lander, E. S., Wong, W., Johnson, B. E., Golub, T. R., Sugarbaker, D. J., Meyerson, M. (2001) Classification of human lung carcinomas by mRNA expression profiling reveals distinct adenocarcinoma subclasses. *Proc. Natl. Acad. Sci. U. S. A.* 98, 13790–13795
11. Giordano, T. J., Shedden, K. A., Schwartz, D. R., Kuick, R., Taylor, J. M. G., Lee, N., Misek, D. E., Greenson, J. K., Kardia, S. L. R., Beer, D. G., Rennert, G., Cho, K. R., Gruber, S. B., Fearon, E. R., Hanash, S. (2001) Organ-specific molecular classification of lung, colon and ovarian adenocarcinomas using gene expression profiles. *Am. J. Pathol.* 159, 1231–1238
12. Strahler, J. R., Kuick, R., Hanash, S. M. (1989) In *Protein Structure: A Practical Approach* (Creighton, T., ed) pp. 65–92, IRL Press, Oxford
13. Merril, C. R., Dunau, M. L., Goldman, D. (1981) A rapid sensitive silver stain for polypeptides in polyacrylamide gels. *Anal. Biochem.* 101, 201–207
14. Hanash, S. M., Strahler, J. R., Chan, Y., Kuick, R., Teichroew, D., Neel, J. V., Hallat, N., Keim, D. R., Gratiot-Deans, J., Ungar, D., Richardson, B. C. (1993) Data base analysis of protein expression patterns during T-cell ontogeny and activation. *Proc. Natl. Acad. Sci. U. S. A.* 90, 3314–3318
15. Brichory, F. M., Misek, D. E., Yim, A. M., Krause, M. C., Giordano, T. J., Beer, D. G., Hanash, S. M. (2001) An immune response manifested by the common occurrence of annexins I and II autoantibodies and high circulating levels of IL-6 in lung cancer. *Proc. Natl. Acad. Sci. U. S. A.* 98, 9824–9829
16. Lavens-Phillips, S. E., MacGlashan, D. W., Jr. (2000) The tyrosine kinases p53/56lyn and p72syk are differentially expressed at the protein level but not at the messenger RNA level in nonreleasing human basophils. *Am. J. Respir. Cell Mol. Biol.* 23, 566–571
17. Tusher, V. G., Tibshirani, R., Chu, G. (2001) Significance analysis of microarrays applied to the ionizing radiation response. *Proc. Natl. Acad. Sci. U. S. A.* 98, 5116–5121
18. Tew, K. D., Monks, A., Barone, L., Rosser, D., Akerman, G., Montali, J. A., Wheatley, J. B., Schmidt, D. E., Jr. (1996) Glutathione-associated enzymes in the human cell lines of the National Cancer Institute Drug Screening Program. *Mol. Pharmacol.* 50, 149–159
19. Celis, J. E., Kruhoffer, M., Gromova, I., Frederiksen, C., Ostergaard, M., Thykjaer, T., Gromov, P., Yu, J., Palsdottir, H., Magnusson, N., Orntoft, T. F. (2000) Gene expression profiling: monitoring transcription and translation products using DNA microarrays and proteomics. *FEBS Lett.* 480, 2–16
20. Anderson, N. L., Anderson, N. G. (1998) Proteome and proteomics: new technologies, new concepts, and new words. *Electrophoresis* 19, 1853–1861
21. Gygi, S. P., Corthals, G. L., Zhang, Y., Rochon, Y., Aebersold, R. (2000) Evaluation of two-dimensional gel electrophoresis-based proteome analysis technology. *Proc. Natl. Acad. Sci. U. S. A.* 97, 9390–9395
22. Fey, S. J., Larsen, P. M. (2001) 2D or not 2D. Two-dimensional gel electrophoresis. *Curr. Opin. Chem. Biol.* 5, 26–33
23. McBride, S., Walsh, D., Malsady, P., Daly, N., Clynes, M. (1999) Bromodeoxyuridine induces keratin protein synthesis at a posttranscriptional level in human lung tumor cell lines. *Differentiation* 64, 185–193
24. Anderson, L., Seilhamer, J. (1997) A comparison of selected mRNA and protein abundances in human liver. *Electrophoresis* 18, 533–537
25. Gygi, S. P., Rochon, Y., Franza, B. R., Aebersold, R. (1999) Correlation between protein and mRNA abundance in yeast. *Mol. Cell. Biol.* 19, 1720–1730

MOLECULAR AND CELLULAR BIOLOGY, Nov. 1999, p. 7357–7368 Vol. 19, No. 11
0270-7306/99/$04.00+0
Copyright © 1999, American Society for Microbiology. All Rights Reserved.

A Sampling of the Yeast Proteome

B. FUTCHER,[1]* G. I. LATTER,[1] P. MONARDO,[1] C. S. MCLAUGHLIN,[2] AND J. I. GARRELS[3]

Cold Spring Harbor Laboratory, Cold Spring Harbor, New York 11724[1]; Department of Biological Chemistry, University of California, Irvine, California 92717[2]; and Proteome, Inc., Beverly, Massachusetts 01915[3]

Received 15 June 1999/Returned for modification 16 July 1999/Accepted 28 July 1999

In this study, we examined yeast proteins by two-dimensional (2D) gel electrophoresis and gathered quantitative information from about 1,400 spots. We found that there is an enormous range of protein abundance and, for identified spots, a good correlation between protein abundance, mRNA abundance, and codon bias. For each molecule of well-translated mRNA, there were about 4,000 molecules of protein. The relative abundance of proteins was measured in glucose and ethanol media. Protein turnover was examined and found to be insignificant for abundant proteins. Some phosphoproteins were identified. The behavior of proteins in differential centrifugation experiments was examined. Such experiments with 2D gels can give a global view of the yeast proteome.

The sequence of the yeast genome has been determined (9). More recently, the number of mRNA molecules for each expressed gene has been measured (27, 30). The next logical level of analysis is that of the expressed set of proteins. We have begun to analyze the yeast proteome by using two-dimensional (2D) gels.

2D gel electrophoresis separates proteins according to isoelectric point in one dimension and molecular weight in the other dimension (21), allowing resolution of thousands of proteins on a single gel. Although modern imaging and computing techniques can extract quantitative data for each of the spots in a 2D gel, there are only a few cases in which quantitative data have been gathered from 2D gels. 2D gel electrophoresis is almost unique in its ability to examine biological responses over thousands of proteins simultaneously and should therefore allow us a relatively comprehensive view of cellular metabolism.

We and others have worked toward assembling a yeast protein database consisting of a collection of identified spots in 2D gels and of data on each of these spots under various conditions (2, 7, 8, 10, 23, 25). These data could then be used in analyzing a protein or a metabolic process. *Saccharomyces cerevisiae* is a good organism for this approach since it has a well-understood physiology as well as a large number of mutants, and its genome has been sequenced. Given the sequence and the relative lack of introns in *S. cerevisiae*, it is easy to predict the sequence of the primary protein product of most genes. This aids tremendously in identifying these proteins on 2D gels.

There are three pillars on which such a database rests: (i) visualization of many protein spots simultaneously, (ii) quantification of the protein in each spot, and (iii) identification of the gene product for each spot. Our first efforts at visualization and identification for *S. cerevisiae* have been described elsewhere (7, 8). Here we describe quantitative data for these proteins under a variety of experimental conditions.

MATERIALS AND METHODS

Strains and media. *S. cerevisiae* W303 (*MATa ade2-1 his3-11,15 leu2-3, 112 trp1-1 ura3-1 can1-100*) was used (26). −Met YNB (yeast nitrogen base) medium was 1.7 g of YNB (Difco) per liter, 5 g of ammonium sulfate per liter, and adenine, uracil, and all amino acids except methionine; −Met −Cys YNB medium was the same but without methionine or cysteine. Medium was supplemented with 2% glucose (for most experiments) or with 2% ethanol (for ethanol experiments). Low-phosphate YEPD was described by Warner (28).

Isotopic labeling of yeast and preparation of cell extracts. Yeast strains were labeled and proteins were extracted as described by Garrels et al. (7, 8). Briefly, cells were grown to 5×10^6 cells per ml at 30°C; 1 ml of culture was transferred to a fresh tube, and 0.3 mCi of [^{35}S]methionine (e.g., Express protein labeling mix; New England Nuclear) was added to this 1-ml culture. The cells were incubated for a further 10 to 15 min and then transferred to a 1.5-ml microcentrifuge tube, chilled on ice, and harvested by centrifugation. The supernatant was removed, and the cell pellet was resuspended in 100 μl of lysis buffer (20 mM Tris-HCl [pH 7.6], 10 mM NaF, 10 mM sodium pyrophosphate, 0.5 mM EDTA, 0.1% deoxycholate; just before use, phenylmethylsulfonyl fluoride was added to 1 mM, leupeptin was added to 1 μg/ml, pepstatin was added to 1 μg/ml, tosylsulfonyl phenylalanyl chloromethyl ketone was added to 10 μg/ml, and soybean trypsin inhibitor was added to 10 μg/ml).

The resuspended cells were transferred to a screw-cap 1.5-ml polypropylene tube containing 0.28 g of glass beads (0.5-mm diameter; Biospec Products) or 0.40 g of zirconia beads (0.5-mm diameter; Biospec Products). After the cap was secured, the tube was inserted into a MiniBeadbeater 8 (Biospec Products) and shaken at medium high speed at 4°C for 1 min. Breakage was typically 75%. Tubes were then spun in a microcentrifuge for 10 s at 5,000 × *g* at 4°C.

With a very fine pipette tip, liquid was withdrawn from the beads and transferred to a prechilled 1.5-ml tube containing 7 μl of DNase I (0.5 mg/ml; Cooper product no. 6330)–RNase A (0.25 mg/ml; Cooper product no. 5679)–Mg (50 mM $MgCl_2$) mix. Typically 70 μl of liquid was recovered. The mixture was incubated on ice for 10 min to allow the RNase and DNase to work.

Next, 75 μl of 2× dSDS (2× dSDS is 0.6% sodium dodecyl sulfate [SDS], 2% mercaptoethanol, and 0.1 M Tris-HCl [pH 8]) was added. The tube was plunged into boiling water, incubated for 1 min, and then plunged into ice. After cooling, the tube was centrifuged at 4°C for 3 min at 14,000 × *g*. The supernatant was transferred to a fresh tube and frozen at −70°C. About 5 μl of this supernatant was used for each 2D gel.

2D polyacrylamide gels. 2D gels were made and run as described elsewhere (6–8).

Image analysis of the gels. The Quest II software system was used for quantitative image analysis (20, 22). Two techniques were used to collect quantitative data for analysis by Quest II software. First, before the advent of phosphorimagers, gels were dried and fluorographed. Each gel was exposed to film for three different times (typically 1 day, 2 weeks, and 6 weeks) to increase the dynamic range of the data. The films were scanned along with calibration strips to relate film optical density to disintegrations per minute in the gels and analyzed by the software to obtain a linear relationship between disintegrations per minute in the spots and optical densities of the film images. The quantitative data are expressed as parts per million of the total cellular protein. This value is calculated from the disintegrations per minute of the sample loaded onto the gel and by comparing the film density of each data spot with density of the film over the calibration strips of known radioactivity exposed to the same film. This yields the disintegrations per minute per millimeter for each spot on the gel and thence its parts-per-minute value.

After the advent of phosphorimaging, gels bearing ^{35}S-labeled proteins were exposed to phosphorimager screens and scanned by a Fuji phosphorimager, typically for two exposures per gel. Calibration strips of known radioactivity were exposed simultaneously. Scan data from the phosphorimager was assimilated by Quest II software, and quantitative data were recorded for the spots on the gels.

* Corresponding author. Mailing address: Cold Spring Harbor Laboratory, Cold Spring Harbor, NY 11724. Phone: (516) 367-8828. Fax: (516) 367-8369. E-mail: futcher@cshl.org.

Downloaded from mcb.asm.org by on December 5, 2008

Measurements of protein turnover. Cells in exponential phase were pulse-labeled with [^{35}S]methionine, excess cold Met and Cys were added, and samples of equal volume were taken from the culture at intervals up to 90 min (in one experiment) or up to 160 min (in a second experiment). Incorporation of ^{35}S into protein was essentially 100% by the first sample (10 min). Extracts were made, and equal fractions of the samples were loaded on 2D gels (i.e., the different samples had different amounts of protein but equal amounts of ^{35}S). Spots were quantitated with a phosphorimaging and Quest software.

The software was queried for spots whose radioactivity decreased through the time course. The algorithm examined all data points for all spots, drew a best-fit line through the data points, and looked for spots where this line had a statistically significant negative slope. In one of the experiments, there was one such spot. To the eye, this was a minor, unidentified spot seen only in the first two samples (10 and 20 min). In the other experiment, the Quest software found no spots meeting the criteria. Therefore, we concluded that none of the identified spots (and all but one of the visible spots) represented proteins with long half-lives.

Centrifugal fractionation. Cells were labeled, harvested, and broken with glass beads by the standard method described above except that no detergent (i.e., no deoxycholate) was present in the lysis buffer. The crude lysate was cleared of unbroken cells and large debris by centrifugation at 300 × *g* for 30 s. The supernatant of this centrifugation was then spun at 16,000 × *g* for 10 min to give the pellet used for Fig. 6B. The supernatant of the 16,000 × *g*, 10-min spin was then spun at 100,000 × *g* for 30 min to give the supernatant used for Fig. 6A.

Protein abundance calculations. A haploid yeast cell contains about 4×10^{-12} g of protein (1, 15). Assuming a mean protein mass of 50 kDa, there are about 50×10^6 molecules of protein per cell. There are about 1.8 methionines per 10 kDa of protein mass, which implies 4.5×10^8 molecules of methionine per cell (neglecting the small pool of free Met). We measured (i) the counts per minute in each spot on the 2D gels, (ii) the total number of counts on each gel (by integrating counts over the entire gel), and (iii) the total number of counts loaded on the gel (by scintillation counting of the original sample). Thus, we know what fraction of the total incorporated radioactivity is present in each spot. After correcting for the methionine (and cysteine [see below]) content of each protein, we calculated an absolute number of protein molecules based on the fraction of radioactivity in each spot and on 50×10^6 total molecules per cell.

The labeling mixture used contained about one-fifth as much radioactive cysteine as radioactive methionine. Therefore, the number of cysteine molecules per protein was also taken into account in calculating the number of molecules of protein, but Cys molecules were weighted one-fifth as heavily as Met molecules.

mRNA abundance calculations. For estimation of mRNA abundance, we used SAGE (serial analysis of gene expression) data (27) and Affymetrix chip hybridization data (29a, 30). The mRNA column in Table 1 shows mRNA abundance calculated from SAGE data alone. However, the SAGE data came from cells growing in YEPD medium, whereas our protein measurements were from cells growing in YNB medium. In addition, SAGE data for low-abundance mRNAs suffers from statistical variation. Therefore, we also used chip hybridization data (29a, 30) for mRNA from cells grown in YNB. These hybridization data also had disadvantages. First, the amounts of high-abundance mRNAs were systematically underestimated, probably because of saturation in the hybridizations, which used 10 μg of cRNA. For example, the abundance of *ADH1* mRNA was 197 copies per cell by SAGE but only 32 copies per cell by hybridization, and the abundance of *ENO2* mRNA was 248 copies per cell by SAGE but only 41 by hybridization. When the amount of cRNA used in the hybridization was reduced to 1 μg, the apparent amounts of mRNA were similar to the amounts determined by SAGE (29a, 29b). However, experiments using 1 μg of cRNA have been done for only some genes (29a). Because amounts of mRNA were normalized to 15,000 per cell, and because the amounts of abundant mRNAs were underestimated, there is a 2.2-fold overestimate of the abundance of nonabundant mRNAs. We calculated this factor of 2.2 by adding together the number of mRNA molecules from a large number of genes expressed at a low level for both SAGE data and hybridization data. The sum for the same genes from hybridization data is 2.2-fold greater than that from SAGE data.

To take into account these difficulties, we compiled a list of "adjusted" mRNA abundance as follows. For all high-abundance mRNAs of our identified proteins, we used SAGE data. For all of these particular mRNAs, chip hybridization suggested that mRNA abundance was the same in YEPD and YNB media. For medium-abundance mRNAs, SAGE data were used, but when hybridization data showed a significant difference between YEPD and YNB, then the SAGE data were adjusted by the appropriate factor. Finally, for low-abundance mRNAs, we used data from chip hybridizations from YNB medium but divided by 2.2 to normalize to the SAGE results. These calculations were completed without reference to protein abundance.

CAI. The codon adaptation index (CAI) was taken from the yeast proteome database (YPD) (13), for which calculations were made according to Sharp and Li (24). Briefly, the index uses a reference set of highly expressed genes to assign a value to each codon, and then a score for a gene is calculated from the frequency of use of the various codons in that gene (24).

Statistical analysis. The JMP program was used with the aid of T. Tully. The JMP program showed that neither mRNA nor protein abundances were normally distributed; therefore, Spearman rank correlation coefficients (r_s) were calculated. The mRNA (adjusted and unadjusted) and protein data were also transformed so that Pearson product-moment correlation coefficients (r_p) could be calculated. First, this was done by a Box-Cox transformation of log-transformed data. This transformation produced normal distributions, and an r_p of 0.76 was achieved. However, because the Box-Cox transformation is complex, we also did a simpler logarithmic transformation. This produced a normal distribution for the protein data. However, the distribution for the mRNA and adjusted mRNA data was close to, but not quite, normal. Nevertheless, we calculated the r_p and found that it was 0.76, identical to the coefficient from the Box-Cox transformed data. We therefore believe that this correlation coefficient is not misleading, despite the fact that the log(mRNA) distribution is not quite normal.

RESULTS

Visualization of 1,400 spots on three gel systems. Yeast proteins have isoelectric points ranging from 3.1 to 12.8, and masses ranging from less than 10 kDa to 470 kDa. It is difficult to examine all proteins on a single kind of gel, because a gel with the needed range in pI and mass would give poor resolution of the thousands of spots in the central region of the gel. Therefore, we have used three gel systems: (i) pH "4 to 8" with 10% polyacrylamide; (ii) pH "3 to 10" with 10% polyacrylamide; and (iii) nonequilibrium with 15% polyacrylamide (7, 8). Each gel system allows good resolution of a subset of yeast proteins.

Figure 1 shows a pH 4–8, 10% polyacrylamide gel. The pH at the basic end of the isoelectric focusing gel cannot be maintained throughout focusing, and so the proteins resolved on such gels have isoelectric points between pH 4 and pH 6.7. For these pH 4–8 gels, we see 600 to 900 spots on the best gels after multiple exposures.

The pH 3–10 gels (not shown) extend the pI range somewhat beyond pH 7.5, allowing detection of several hundred additional spots. Finally, we use nonequilibrium gels with 15% acrylamide in the second dimension. These allow visualization of about 100 very basic proteins and about 170 small proteins (less than 20 kDa). In total, using all three gel systems, about 1,400 spots can be seen. These represent about 1,200 different proteins, which is about one-quarter to one-third of the proteins expressed under these conditions (27, 30). Here, we focus on the proteins seen on the pH 4–8 gels.

Although nearly all expressed proteins are present on these gels, the number seen is limited by a problem we call coverage. Since there are thousands of proteins on each gel, many proteins comigrate or nearly comigrate. When two proteins are resolved, but are close together, and one protein spot is much more intense than the other, a problem arises in visualizing the weaker spot: at long exposures when the weak signal is strong enough for detection, the signal from the strong spot spreads and covers the signal from the weaker spot. Thus, weak spots can be seen only when they are well separated from strong spots.

For a given gel, the number of detectable spots initially rises with exposure time. However, beyond an optimal exposure, the number of distinguishable spots begins to decrease, because signals from strong spots cover signals from nearby weak spots. At long exposures, the whole autoradiogram turns black. Thus, there is an optimum exposure yielding the maximum number of spots, and at this exposure the weakest spots are not seen.

Largely because of the problem of coverage, the proteins seen are strongly biased toward abundant proteins. All identified proteins have a CAI of 0.18 or more, and we have identified no transcription factors or protein kinases, which are nonabundant proteins. Thus, this technology is useful for examining protein synthesis, amino acid metabolism, and glycolysis but not for examining transcription, DNA replication, or the cell cycle.

Downloaded from mcb.asm.org by on December 5, 2008

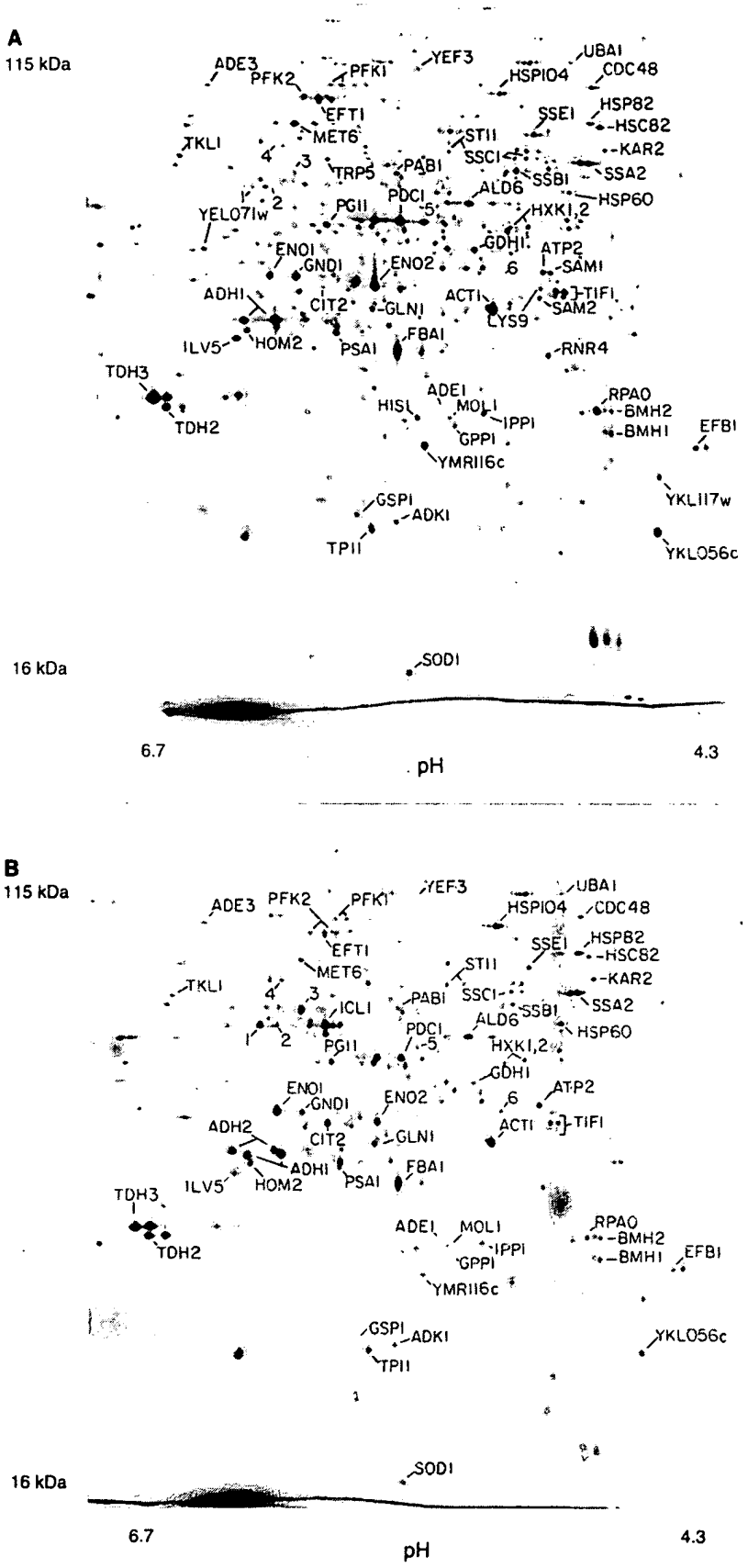

FIG. 1. 2D gels. The horizontal axis is the isoelectric focusing dimension, which stretches from pH 6.7 (left) to pH 4.3 (right). The vertical axis is the polyacrylamide gel dimension, which stretches from about 15 kDa (bottom) to at least 130 kDa (top). For panel A, extract was made from cells in log phase in glucose; for panel B, cells were grown in ethanol. The spots labeled 1 through 6 are unidentified proteins highly induced in ethanol.

Downloaded from mcb.asm.org by on December 5, 2008

Spot identification. The identification of various spots has been described elsewhere (7, 8). At present, 169 different spots representing 148 proteins have been identified. Many of these spots have been independently identified (2, 10, 23, 25). The main methods used in spot identification have been analysis of amino acid composition, gene overexpression, peptide sequencing, and mass spectrometry.

Pulse-chase experiments and protein turnover. Pulse-chase experiments were done to measure protein half-lives (Materials and Methods). Cells were labeled with [^{35}S]methionine for 10 min, and then an excess of unlabeled methionine was added. Samples were taken at 0, 10, 20, 30, 60, and 90 min after the beginning of the chase. Equal amounts of ^{35}S were loaded from each sample; 2D gels were run, and spots were quantitated. Surprisingly, almost every spot was nearly constant in amount of radioactivity over the entire time course (not shown). A few spots shifted from one position to another because of post-translational modifications (e.g., phosphorylation of Rpa0 and Efb1). Thus, the proteins being visualized are all or nearly all very stable proteins, with half-lives of more than 90 min. Gygi et al. (10) have come to a similar conclusion by using the N-end rule to predict protein half-lives. This result does not imply that all yeast proteins are stable. The proteins being visualized are abundant proteins; this is partly because they are stable proteins.

Protein quantitation. Because all of the proteins seen had effectively the same half-life, the abundance of each protein was directly proportional to the amount of radioactivity incorporated during labeling. Thus, after taking into account the total number of protein molecules per cell, the average content of methionine and cysteine, and the methionine and cysteine content of each identified protein, we could calculate the abundance of each identified protein (Tables 1 and 2; Materials and Methods). About 1,000 unidentified proteins were also quantified, assuming an average content of Met and Cys.

Many proteins give multiple spots (7, 8). The contribution from each spot was summed to give the total protein amount. However, many proteins probably have minor spots that we are not aware of, causing the amount of protein to be underestimated.

When the proteins on a pH 4–8 gel were ordered by abundance, the most abundant protein had 8,904 ppm, the 10th most abundant had 2,842 ppm, the 100th most abundant had 314 ppm, the 500th most abundant had 57 ppm, and the 1,000th most abundant (visualized at greater than optimum exposure) had 23 ppm. Thus, there is more than a 300-fold range in abundance among the visualized proteins. The most abundant 10 proteins account for about 25% of the total protein on the pH 4–8 gel, the most abundant 60 proteins account for 50%, and the most abundant 500 proteins account for 80%. Since it seems likely that the pH 4–8 gels give a representative sampling of all proteins, we estimate that half of the total cellular protein is accounted for by fewer than 100 different gene products, principally glycolytic enzymes and proteins involved in protein synthesis.

Correlation of protein abundance with mRNA abundance. Estimates of mRNA abundance for each gene have been made by SAGE (27) and by hybridization of cRNA to oligonucleotide arrays (30). These two methods give broadly similar results, yet each method has strengths and weaknesses (Materials and Methods). Table 1 lists the number of molecules of mRNA per cell for each gene studied. One measurement (mRNA) uses data from SAGE analysis alone (27); a second incorporates data from both SAGE and hybridization (30) (adjusted mRNA) (Table 1; Materials and Methods). We correlated protein abundance with mRNA abundance (Fig. 2). For adjusted mRNA versus protein, the Spearman rank correlation coefficient, r_s, was 0.74 ($P < 0.0001$), and the Pearson correlation coefficient, r_p, on log transformed data (Materials and Methods) was 0.76 ($P < 0.00001$). We obtained similar correlations for mRNA versus protein and also for other data transformations (Materials and Methods). Thus, several statistical methods show a strong and significant correlation between mRNA abundance and protein abundance. Of course, the correlation is far from perfect; for mRNAs of a given abundance, there is at least a 10-fold range of protein abundance (Fig. 2). Some of this scatter is probably due to posttranscriptional regulation, and some is due to errors in the mRNA or protein data. For example, the protein Yef3 runs poorly on our gels, giving multiple smeared spots. Its abundance has probably been underestimated, partly explaining the low protein/mRNA ratio of Yef3. It is the most extreme outlier in Fig. 2.

These data on mRNA (27, 30) and protein abundance (Table 1) suggest that for each mRNA molecule, there are on average 4,000 molecules of the cognate protein. For instance, for Act1 (actin) there are about 54 molecules of mRNA per cell and about 205,000 molecules of protein. Assuming an mRNA half-life of 30 min (12) and a cell doubling time of 120 min, this suggests that an individual molecule of mRNA might be translated roughly 1,000 times. These calculations are limited to mRNAs for abundant proteins, which are likely to be the mRNAs that are translated best.

A full complement of cell protein is synthesized in about 120 min under these conditions. Thus, 4,000 molecules of protein per molecule of mRNA implies that translation initiates on an mRNA about once every 2 s. This is a remarkably high rate; it implies that if an average mRNA bears 10 ribosomes engaged in translation, then each ribosome completes translation in 20 s; if an average protein has 450 residues; this in turn implies translation of over 20 amino acids per s, a rate considerably higher than estimated for mammalians (3 to 8 amino acids per s) (18). These estimates depend on the amount of mRNA per cell (11, 27).

The large number of protein molecules that can be made from a single mRNA raises the issue of how abundance is controlled for less abundant proteins. Many nonabundant proteins may be unstable, and this would reduce the protein/mRNA ratio. In addition, many nonabundant proteins may be translated at suboptimal rates. We have found that mRNAs for nonabundant proteins usually have suboptimal contexts for translational initiation. For example, there are over 600 yeast genes which probably have short open reading frames in the mRNA upstream of the main open reading frame (17a). These may be devices for reducing the amount of protein made from a molecule of mRNA.

Correlation of codon bias with protein abundance. The mRNAs for highly expressed proteins preferentially use some codons rather than others specifying the same amino acid (14). This preference is called codon bias. The codons preferred are those for which the tRNAs are present in the greatest amounts. Use of these codons may make translation faster or more efficient and may decrease misincorporation. These effects are most important for the cell for abundant proteins, and so codon bias is most extreme for abundant proteins. The effect can be dramatic—highly biased mRNAs may use only 25 of the 61 codons.

We asked whether the correlation of codon bias with abundance continues for medium-abundance proteins. There are various mathematical expressions quantifying codon bias; here, we have used the CAI (24) (Materials and Methods) because it gives a result between 0 and 1. The r_s for CAI versus protein abundance is 0.80 ($P < 0.0001$), similar to the mRNA-protein

Downloaded from mcb.asm.org by on December 5, 2008

TABLE 1. Quantitative data[a]

Function	Name	CAI	mRNA	Adjusted mRNA	Protein (Glu) (10^3)	Protein (Eth) (10^3)	E/G ratio
Carbohydrate metabolism	Adh1	0.810	197	197	1,230	972	0.79
	Adh2	0.504	0		0	963	>20
	Cit2	0.185	1	2.8	23	288	12
	Eno1	0.870	No *Nla*		410	974	2.4
	Eno2	0.892	248	248	650	215	0.33
	Fba1	0.868	179	179	640	608	0.95
	Hxk1,2	0.500	13	10.5	62	46	
	Icl1	0.251	0		0	671	>20
	Pdb1	0.342	5	5	41	33	
	Pdc1	0.903	226	226	280	205	0.73
	Pfk1	0.465	5	5	75	53	0.71
	Pgi1	0.681	14	14	160	120	0.75
	Pyc1	0.260	1	0.7	37	34	
	Tal1	0.579	5	5	110	35	
	Tdh2	0.904	63	63	430	876	NR
	Tdh3	0.924	460	460	1,670	1,927	NR
	Tpi1	0.817	No *Nla*		No Met	No Met	
Protein synthesis	Efb1	0.762	33	16.5	358	362	
	Eft1,2	0.801	26	26	99	54	0.55
	Prt1	0.303	4	0.7	12	6	
	Rpa0	0.793	246	246	277	100	0.36
	Tif1,2	0.752	29	29	233	106	0.46
	Yef3	0.777	36	36	14	ND	
Heat shock	Hsc82	0.581	2	2.9	112	75	0.67
	Hsp60	0.381	9	2.3	35	82	2.3
	Hsp82	0.517	2	1.3	52	135	2.6
	Hsp104	0.304	7	7	70	161	2.3
	Kar2	0.439	5	10.1	43	102	2.4
	Ssa1	0.709	2	4.3	303	421	1.4
	Ssa2	0.802	10	5	213	324	1.5
	Ssb1,2	0.850	50	50	270	85	
	Ssc1	0.521	2	2.6	68	80	1.2
	Sse1	0.521	8	8	96	48	
	Sti1	0.247	1	1.1	25	44	1.7
Amino acid synthesis	Ade1	0.229	4	4	14	27	
	Ade3	0.276	2	1.7	12	9	
	Ade5,7	0.257	2	1.4	14	4	
	Arg4	0.229	1	8.1	41	41	
	Gdh1	0.585	10	27	148	55	
	Gln1	0.524	11	11	77	104	1.3
	His4	0.267	3	3	15	23	1.5
	Ilv5	0.801	6	6	152	109	0.7
	Lys9	0.332	4	4	32	17	0.52
	Met6	0.657	No *Nla*	22	190	80	0.42
	Pro2	0.248	3	3	30	12	
	Ser1	0.258	2	1.2	15	8	
	Trp5	0.319	5	5	28	12	
Miscellaneous	Act1	0.710	54	54	205	164	0.78
	Adk1	0.531	No *Nla*		47	43	
	Ald6	0.520	3	3	181	159	
	Atp2	0.424	1	4.1	76	109	1.4
	Bmh1	0.322	46	46	191	137	0.72
	Bmh2	0.384	1	1.4	134	147	
	Cdc48	0.306	2	2.4	32	26	
	Cdc60	0.299	2	0.86	6	2	
	Erg20	0.373	5	5	92	39	
	Gpp1	0.603	16	5	234	158	
	Gsp1	0.621	3	3	115	39	0.34
	Ipp1	0.620	4	4	254	147	0.58
	Lcb1	0.173	0.3	0.8	19	40	
	Mol1	0.423	0	0.45	20	16	
	Pab1	0.488	3	3	41	19	0.47
	Psa1	0.600	15	15	148	56	
	Rnr4	0.497	6	6	44	37	
	Sam1	0.494	5	5	59	21	
	Sam2	0.497	3	15	63	20	
	Sod1	0.376	36	36	631	618	
	Uba1	0.212	2	2	14	20	
	YKL056	0.731	62	62	253	112	0.44
	YLR109	0.549	21	21	930		
	YMR116	0.777	41	41	184	40	0.20

[a] CAI, a measure of codon bias, is taken from the YPD. mRNA, number of mRNA molecules per cell from SAGE data (27); adjusted mRNA, number of mRNA molecules per cell based on both SAGE and chip hybridization (30) (see Materials and Methods); Protein (Glu), number of molecules of protein per cell in YNB-glucose; Protein (Eth), number of molecules of protein per cell in YNB-ethanol; E/G ratio, ratio of protein abundance in ethanol to glucose. The E/G ratio is not given if it was close to 1 or if it was not repeatable (NR) in multiple gels. Some gene products (e.g., Tif1 and Tif2 [Tif1,2]) were difficult to distinguish on either a protein or an mRNA basis; these are pooled. No *Nla*, there was no suitable *Nla*III site in the 3′ region of the gene, and so there are no SAGE mRNA data; No Met, the mature gene product contains no methionines, and so there are no reliable protein data.

Downloaded from mcb.asm.org by on December 5, 2008

TABLE 2. Functions of proteins listed in Table 1

Name[a]	YPD title lines[b]
Adh1	Alcohol dehydrogenase I; cytoplasmic isozyme reducing acetaldehyde to ethanol, regenerating NAD^+
Adh2	Alcohol dehydrogenase II; oxidizes ethanol to acetaldehyde, glucose repressed
Cit2	Citrate synthase, peroxisomal (nonmitochondrial); converts acetyl-CoA and oxaloacetate to citrate plus CoA
Eno1	Enolase 1 (2-phosphoglycerate dehydratase); converts 2-phospho-D-glycerate to phosphoenolpyruvate in glycolysis
Eno2	Enolase 2 (2-phosphoglycerate dehydratase); converts 2-phospho-D-glycerate to phosphoenolpyruvate in glycolysis
Fba1	Fructose bisphosphate aldolase II; sixth step in glycolysis
Hxk1	Hexokinase I; converts hexoses to hexose phosphates in glycolysis; repressed by glucose
Hxk2	Hexokinase II; converts hexoses to hexose phosphates in glycolysis and plays a regulatory role in glucose repression
Icl1	Isocitrate lyase, peroxisomal; carries out part of the glyoxylate cycle; required for gluconeogenesis
Pdb1	Pyruvate dehydrogenase complex, E1 beta subunit
Pdc1	Pyruvate decarboxylase isozyme 1
Pfk1	Phosphofructokinase alpha subunit, part of a complex with Pfk2p which carries out a key regulatory step in glycolysis
Pgi1	Glucose-6-phosphate isomerase, converts glucose-6-phosphate to fructose-6-phosphate
Pyc1	Pyruvate carboxylase 1; converts pyruvate to oxaloacetate for gluconeogenesis
Tal1	Transaldolase; component of nonoxidative part of pentose phosphate pathway
Tdh2	Glyceraldehyde-3-phosphate dehydrogenase 2; converts D-glyceraldehyde 3-phosphate to 1,3-dephosphoglycerate
Tdh3	Glyceraldehyde-3-phosphate dehydrogenase 3; converts D-glyceraldehyde 3-phosphate to 1,3-dephosphoglycerate
Tpi1	Triosephosphate isomerase; interconverts glyceraldehyde-3-phosphate and dihydroxyacetone phosphate
Efb1	Translation elongation factor EF-1β; GDP/GTP exchange factor for Tef1p/Tef2p
Eft1	Translation elongation factor EF-2; contains diphthamide which is not essential for activity; identical to Eft2p
Eft2	Translation elongation factor EF-2; contains diphthamide which is not essential for activity; identical to Eft1p
Prt1	Translation initiation factor eIF3 beta subunit (p90); has an RNA recognition domain
Rpa0 (RPP0)	Acidic ribosomal protein A0
Tif1	Translation initiation factor 4A (eIF4A) of the DEAD box family
Tif2	Translation initiation factor 4A (eIF4A) of the DEAD box family
Yef3	Translation elongation factor EF-3A; member of ATP-binding cassette superfamily
Hsc82	Chaperonin homologous to *E. coli* HtpG and mammalian HSP90
Hsp60	Mitochondrial chaperonin that cooperates with Hsp10p; homolog of *E. coli* GroEL
Hsp82	Heat-inducible chaperonin homologous to *E. coli* HtpG and mammalian HSP90
Hsp104	Heat shock protein required for induced thermotolerance and for resolubilizing aggregates of denatured proteins; important for [psi$^-$]-to-[PSI$^+$] prion conversion
Kar2	Heat shock protein of the endoplasmic reticulum lumen required for protein translocation across the endoplasmic reticulum membrane and for nuclear fusion; member of the HSP70 family
Ssa1	Cytoplasmic chaperone; heat shock protein of the HSP70 family
Ssa2	Cytoplasmic chaperone; member of the HSP70 family
Ssb1	Heat shock protein of HSP70 family involved in the translational apparatus
Ssb2	Heat shock protein of HSP70 family, cytoplasmic
Ssc1	Mitochondrial protein that acts as an import motor with Tim44p and plays a chaperonin role in receiving and folding of protein chains during import; heat shock protein of HSP70 family
Sse1	Heat shock protein of the HSP70 family; multicopy suppressor of mutants with hyperactivated Ras/cyclic AMP pathway
Sti1	Stress-induced protein required for optimal growth at high and low temperature; has tetratricopeptide repeats
Ade1	Phosphoribosylamidoimidazole-succinocarboxamide synthase; catalyzes the seventh step in de novo purine biosynthesis pathway
Ade3	C_1 tetrahydrofolate synthase (trifunctional enzyme), cytoplasmic
Ade5,7	Phosphoribosylamine-glycine ligase plus phosphoribosylformylglycinamidine cyclo-ligase; bifunctional protein
Arg4	Argininosuccinate lyase; catalyzes the final step in arginine biosynthesis
Gdh1	Glutamate dehydrogenase ($NADP^+$); combines ammonia and α-ketoglutarate to form glutamate
Gln1	Glutamine synthetase; combines ammonia to glutamate in ATP-driven reaction
His4	Phosphoribosyl-AMP cyclohydrolase/phosphoribosyl-ATP pyrophosphohydrolase/histidinol dehydrogenase; 2nd, 3rd, and 10th steps of his biosynthesis pathway
Ilv5	Ketol-acid reductoisomerase (acetohydroxy, acid reductoisomerase) (alpha-keto-β-hydroxylacyl) reductoisomerase); second step in Val and Ilv biosynthesis pathway
Lys9	Saccharopine dehydrogenase ($NADP^+$, L-glutamate forming) (saccharopine reductase), seventh step in lysine biosynthesis pathway
Met6	Homocysteine methyltransferase; (5-methyltetrahydropteroyl triglutamate-homocysteine methyltransferase), methionine synthase, cobalamin independent
Pro2	γ-Glutamyl phosphate reductase (phosphoglutamate dehydrogenase), proline biosynthetic enzyme
Ser1	Phosphoserine transaminase; involved in synthesis of serine from 3-phosphoglycerate
Trp5	Tryptophan synthase, last (5th) step in tryptophan biosynthesis pathway
Act1	Actin; involved in cell polarization, endocytosis, and other cytoskeletal functions
Adk1	Adenylate kinase (GTP:AMP phosphotransferase), cytoplasmic
Ald6	Cytosolic acetaldehyde dehydrogenase
Atp2	Beta subunit of F1-ATP synthase; 3 copies are found in each F1 oligomer
Bmh1	Homolog of mammalian 14-3-3 protein; has strong similarity to Bmh2p
Bmh2	Homolog of mammalian 14-3-3 protein; has strong similarity to Bmh1p
Cdc48	Protein of the AAA family of ATPases; required for cell division and homotypic membrane fusion
Cdc60	Leucyl-tRNA synthetase, cytoplasmic
Erg20	Farnesyl pyrophosphate synthetase; may be rate-limiting step in sterol biosynthesis pathway
Gpp1 (Rhr2)	DL-Glycerol phosphate phosphatase
Gsp1	Ran, a GTP-binding protein of the Ras superfamily involved in trafficking through nuclear pores
Ipp1	Inorganic pyrophosphatase, cytoplasmic
Lcb1	Component of serine C-palmitoyltransferase; first step in biosynthesis of long-chain base component of sphingolipids
Mol1 (Thi4)	Thiamine-repressed protein essential for growth in the absence of thiamine
Pab1	Poly(A)-binding protein of cytoplasm and nucleus; part of the 3′-end RNA-processing complex (cleavage factor I); has 4 RNA recognition domains
Psa1	Mannose-1-phosphate guanyltransferase; GDP-mannose pyrophosphorylase
Rnr4	Ribonucleotide reductase small subunit
Sam1	*S*-Adenosylmethionine synthetase 1
Sam2	*S*-Adenosylmethionine synthetase 2
Sod1	Copper-zinc superoxide dismutase
Uba1	Ubiquitin-activating (E1) enzyme
YKL056	Resembles translationally controlled tumor protein of animal cells and higher plants
YLR109 (Ahp1)	Alkyl hydroperoxide reductase
YMR116 (Asc1)	Abundant protein with effects on translational efficiency and cell size, has two WD (WD-40) repeats

[a] Accepted name from the *Saccharomyces* genome database and YPD. Names in parentheses represent recent changes.
[b] Courtesy of Proteome, Inc., reprinted with permission.

Downloaded from mcb.asm.org by on December 5, 2008

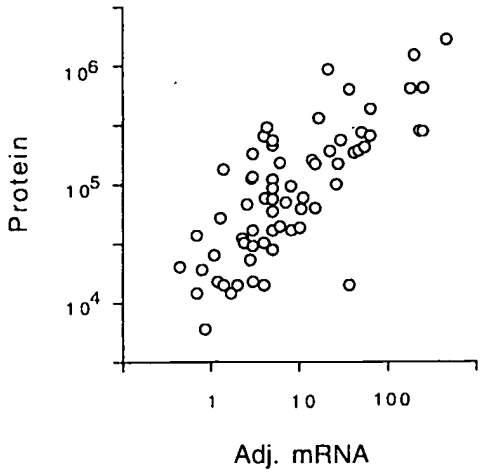

FIG. 2. Correlation of protein abundance with adjusted mRNA abundance. The number of molecules per cell of each protein is plotted against the number of molecules per cell of the cognate mRNA, with an r_p of 0.76. Note the logarithmic axes. Data for mRNA were taken from references 27 and 30 and combined as described in Materials and Methods.

correlation, confirming a strong correlation between CAI and protein abundance (Fig. 3). The relationship between CAI and protein abundance is log linear from about 1,000,000 to about 10,000 molecules per cell. We have no data for rarer proteins.

It is not clear whether CAI reflects maximum or average levels of protein expression. The proteins used for the CAI-protein correlation included some proteins which were not expressed at maximum levels under the condition of the experiment (Hsc82, Hsp104, Ssa1, Ade1, Arg4, His4, and others). When these proteins were removed from consideration and the correlation between CAI and the remaining (presumably constitutive) proteins was recalculated, the r_s was essentially unchanged (not shown).

The equation describing the graph in Fig. 3 is log (protein molecules/cell) = (2.3 × CAI) + 3.7. Thus, under certain conditions (a CAI of 0.3 or greater; a constitutively expressed gene), a very rough estimate of protein abundance can be made by raising 10 to the power of [(2.3 × CAI) + 3.7].

The distribution of CAI over the genome (Fig. 4) consists of a lower, bell-shaped distribution, possibly indicating a region where there is no selection for codon bias, and an upper, flat distribution, starting at a CAI of about 0.3, possibly indicating a region where there is selection for codon bias. Almost all of the proteins whose abundance we have measured are in the upper, flat portion of the distribution. In the lower, bell-shaped region, we do not know whether there is a correlation between CAI and protein abundance.

Changes in protein abundance in glucose and ethanol. A comparison of cells grown in glucose (Fig. 1A) with cells grown in ethanol (Fig. 1B) is shown in Table 1. As is well known, some proteins are induced tremendously during growth on ethanol. Two striking examples are the peroxisomal enzymes Icl1 (isocitrate lyase) and Cit2 (citrate synthase), which are induced in ethanol by more than 100- and 12-fold, respectively (Fig. 1; Table 1). These enzymes are key components of the glyoxylate shunt, which diverts some acetyl coenzyme A (acetyl-CoA) from the tricarboxylic acid cycle to gluconeogenesis. *S. cerevisiae* requires large amounts of carbohydrate for its cell wall; in ethanol medium, this carbohydrate comes from gluconeogenesis, which depends on the glyoxylate shunt and on the glycolytic pathway running in reverse. The need for gluconeogenesis also explains why glycolytic enzymes are abundant even in ethanol medium. Thus, 2D gel analysis shows the prominence of the glycolytic and glyoxylate shunt enzymes in cells grown on ethanol, emphasizing that gluconeogenesis, presumably largely for production of the cell wall, is a major metabolic activity under these conditions.

During gluconeogenesis, substrate-product relationships are reversed for the glycolytic enzymes. One might expect that not all glycolytic enzymes would be well adapted to the reverse reaction. Indeed, 2D gels show that in ethanol, Adh2 (alcohol dehydrogenase 2) is strongly induced (16), while its isozyme Adh1 is not greatly affected. Adh1 and Adh2 each interconvert acetaldehyde and ethanol. Adh1 has a relatively high K_m for ethanol (17 mM), while Adh2 has a lower K_m (0.8 mM) (5). Thus, it is thought that Adh1 is specialized for glycolysis (acetaldehyde to ethanol), while Adh2 is specialized for respiration (ethanol to acetaldehyde) (5, 29). Similarly, Eno1 (enolase 1) is induced in ethanol, while its isozyme Eno2 (enolase 2) decreases in abundance (Table 1) (4, 19). Eno1 is inhibited by 2-phosphoglycerate (the glycolytic substrate), while Eno2 is inhibited by phosphoenolpyruvate (the gluconeogenic substrate) (4). Perhaps Eno1 has a lower K_m for phosphoenolpyruvate than does Eno2, though to our knowledge this has not been tested. Thus, the 2D gels distinguish isozymes specialized for growth on glucose (Adh1 and Eno2) from isozymes specialized for ethanol (Adh2 and Eno1).

Many heat shock proteins (e.g., Hsp60, Hsp82, Hsp104, and Kar2) were about twofold more abundant in ethanol medium than in glucose medium. This is consistent with the increased heat resistance of cells grown in ethanol (3).

Enzymes involved in protein synthesis (Eft1, Rpa0, and Tif1) were about twice as abundant in glucose medium as in ethanol medium. This may reflect the higher growth rate of the cells in glucose.

Phosphorylation of proteins. To examine protein phosphorylation, we labeled cells with ^{32}P and ran 2D gels to examine phosphoproteins. About 300 distinct spots, probably representing 150 to 200 proteins, could be seen on pH 4–8 gels (Fig. 5B). We then aligned autoradiograms of three gels, each with a different kind of labeled protein (^{32}P only [Fig. 5B], ^{32}P plus ^{35}S [Fig. 5A], and ^{35}S only [not shown, but see Fig. 1 for example]). In this way, we made provisional identification of

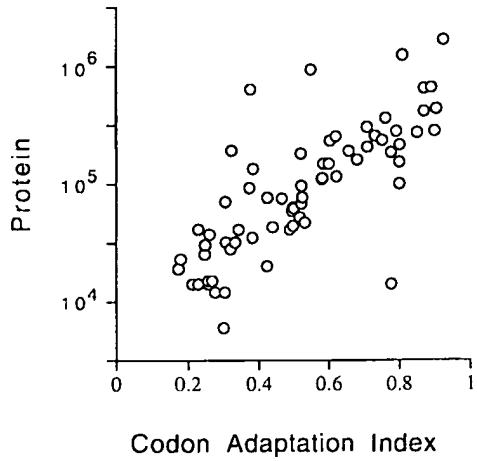

FIG. 3. Correlation of protein abundance with CAI. The number of molecules per cell of each protein is plotted against the CAI for that protein. Note the logarithmic scale on the protein axis. Data for the CAI are from the YPD database (13).

Downloaded from mcb.asm.org by on December 5, 2008

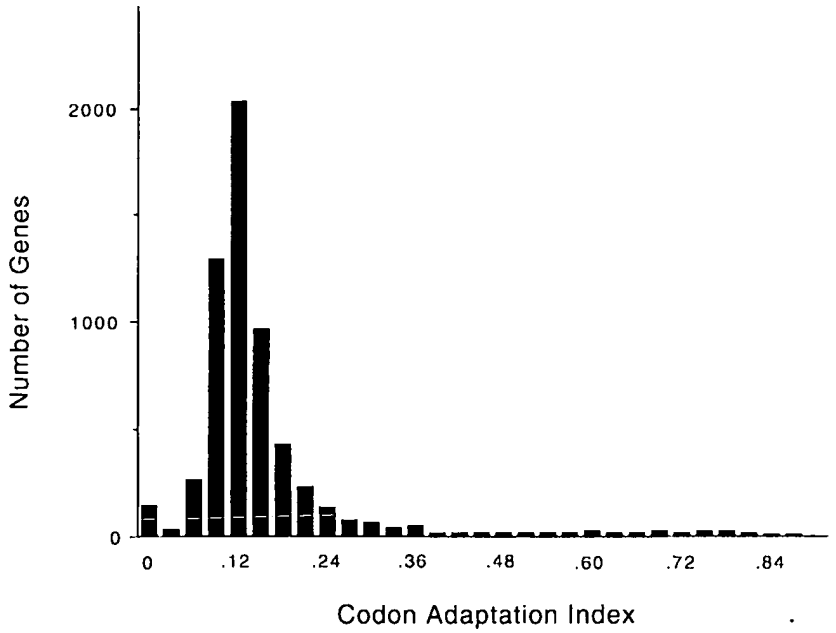

FIG. 4. Distribution of CAI over the whole genome, shown in intervals of 0.030 (i.e., there are 150 genes with a CAI between 0.000 and 0.030, inclusive; 31 genes with a CAI between 0.031 and 0.060; 269 genes with a CAI between 0.061 and 0.090; 1,296 genes with a CAI between 0.091 and 0.120; etc.). The distribution peaks with 2,028 genes with a CAI between 0.121 and 0.150.

some of the ^{32}P-labeled spots as particular ^{35}S-labeled spots. All such identifications are somewhat uncertain, since precise alignments are difficult, and of course multiple spots may exactly comigrate. Nevertheless, we believe that most of the provisional identifications are probably correct. Among the major ^{32}P-labeled proteins are the hexokinases Hxk1 and Hxk2, the acidic ribosome-associated protein Rpa0, the translation factors Yef3 and Efb1, and probably Hsp70 heat shock proteins of the Ssa and Ssb families. Rpa0 and Efb1 are quantitatively monophosphorylated.

Many yeast proteins resolve into multiple spots on these 2D gels (7). Yef3 has five or more spots, at least four of which comigrate with ^{32}P. Tpi1 has a major spot showing no ^{32}P labeling and a minor, more acidic spot which overlaps with some ^{32}P label. Tif1 has at least seven spots (7); two of these overlap with some ^{32}P label, but five do not (Fig. 5). Eft1 has at least three spots (7), and none of these overlap with ^{32}P, although there are three nearby, unidentified ^{32}P-labeled spots (a, c, and d in Fig. 5). Spots that seem to be extra forms of Met6, Pdc1, Eno2, and Fba1 can be seen in Fig. 6A, but there is little ^{32}P at these positions in Fig. 5. Thus, phosphorylation explains some but not all of the different protein isoforms seen.

The cell cycle is regulated in part by phosphorylation. We compared ^{32}P-labeled proteins from cells synchronized in G_1 with α-factor, in cells synchronized in G_1 by depletion of G_1 cyclins, and in cells synchronized in M phase with nocodazole. Only very minor differences were seen, and these were difficult to reproduce. The cell cycle proteins regulated by phosphorylation may not be abundant enough for this technique to be applied easily.

Centrifugal fractionation. We fractionated ^{35}S-labeled extracts by centrifugation (Materials and Methods). Figure 6A shows the proteins in the supernatant of a high-speed (100,000 × *g*, 30 min) centrifugation, while Fig. 6B shows the proteins in the pellet of a low-speed (16,000 × *g*, 10 min) centrifugation. Many proteins are tremendously enriched in one fraction or the other, while others are present in both. Most glycolytic enzymes (e.g., Tdh2, Tdh3, Eno2, Pdc1, Adh1, and Fba1) are enriched in the supernatant fraction. The only exception is Pfk1 (not indicated), which is found in both pellet and supernatant fractions. Many proteins involved in protein synthesis (Eft1, Yef3, Prt1, Tif1, and Rpa0) are in the pellet, possibly because of the association of ribosomes with the endoplasmic reticulum. However, Efb1 is in the supernatant, as is a substantial portion of the Eft1. Perhaps surprisingly, several mitochondrial proteins (Atp2 [not shown] and Ilv5) are largely in the supernatant. Perhaps glass bead breakage of cells releases mitochondrial proteins. The nuclear protein Gsp1 is in the pellet fraction. The enrichment produced by centrifugation makes it possible to see minor spots which are otherwise poorly resolved from surrounding proteins. Figure 6B shows that the previously identified Tif1 spot is surrounded by as many as six other spots that cofractionate. We observed six identical or very similar additional spots when we overexpressed Tif1 from a high-copy-number plasmid (not shown). Signal overlaps only one or two of these spots in ^{32}P-labeling experiments (Fig. 5), and so the different forms are not mainly due to different phosphorylation states.

DISCUSSION

Our experience with developing a 2D gel protein database for *S. cerevisiae* is summarized here. With current technology, we can see the most abundant 1,200 proteins, which is about one-third to one-quarter of the proteins expressed. The remaining proteins will be difficult to see and study with the methods that we have used, not because of a lack of sensitivity but because weak spots are covered by nearby strong spots.

Of the 1,200 proteins seen, we have identified 148, with a bias toward the most abundant proteins. Steady application of the methods already used would allow identification of most of the remaining proteins. Gene overexpression will be particularly useful, since it is not affected by the lower abundance of the remaining visible proteins.

Downloaded from mcb.asm.org by on December 5, 2008

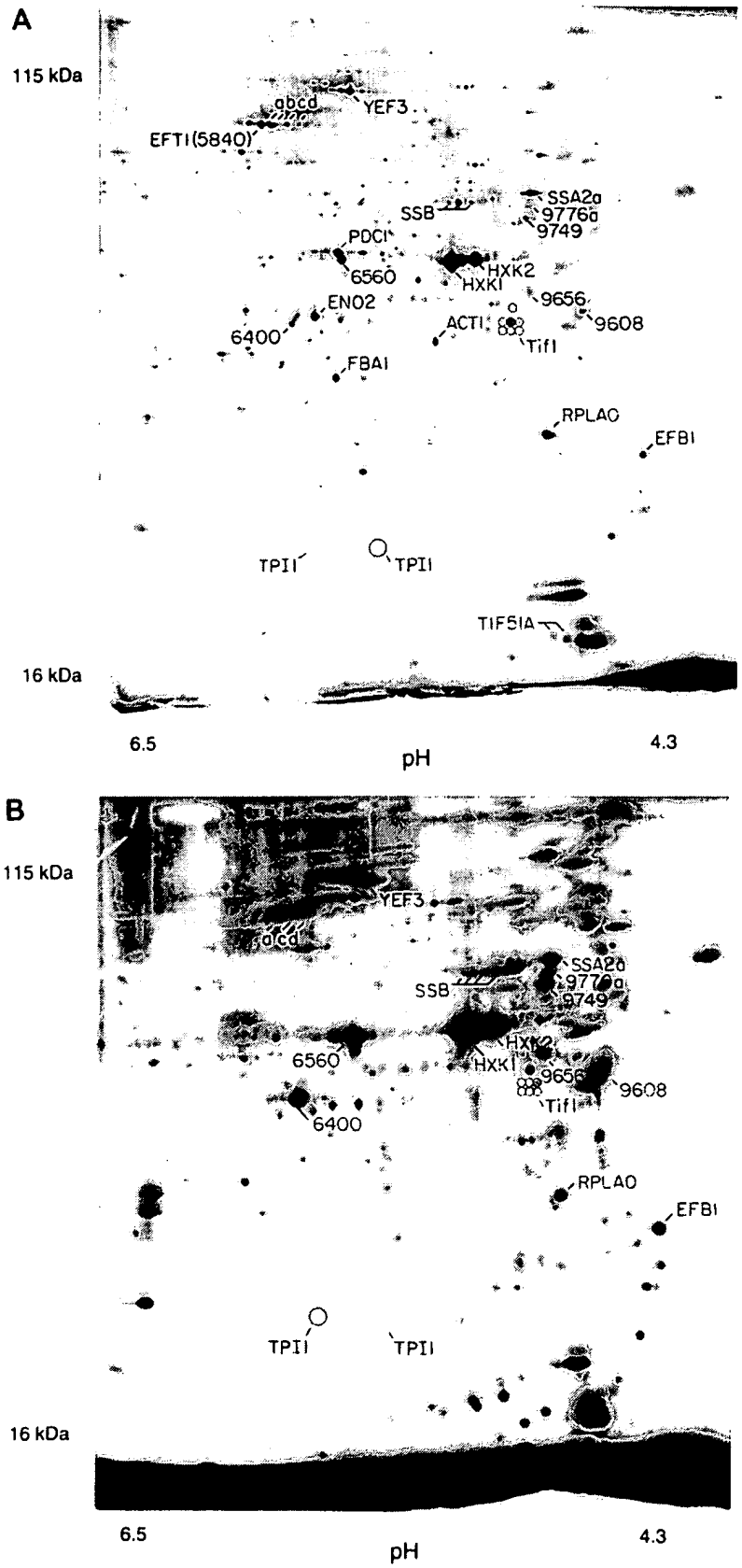

FIG. 5. Phosphorylated proteins. (A) Mixture of ^{32}P-labeled proteins and ^{35}S-labeled proteins. Two separate labeling reactions were done, one with ^{32}P and one with ^{35}S, and extracts were mixed and run on a 2D gel. Spots marked with numbers rather than gene names represent spots noted on ^{35}S gels but unidentified. Spots labeling with ^{32}P were identified by (i) increased labeling compared to the ^{35}S-only gel (not shown); (ii) the characteristic fuzziness of a ^{32}P-labeled spot; and (iii) the decay of signal intensity seen on exposures made 4 weeks later (not shown). A minor form of Tpi1 and at least six minor forms of Tif1 have been noted in overexpression experiments (see also Fig. 6B); positions of the minor forms are indicated by circles. (B) ^{32}P-only labeling. The major form of Tpi1, which is not labeled with ^{32}P, is indicated by a large circle; positions of seven forms of Tif1 are indicated by smaller circles.

Downloaded from mcb.asm.org by on December 5, 2008

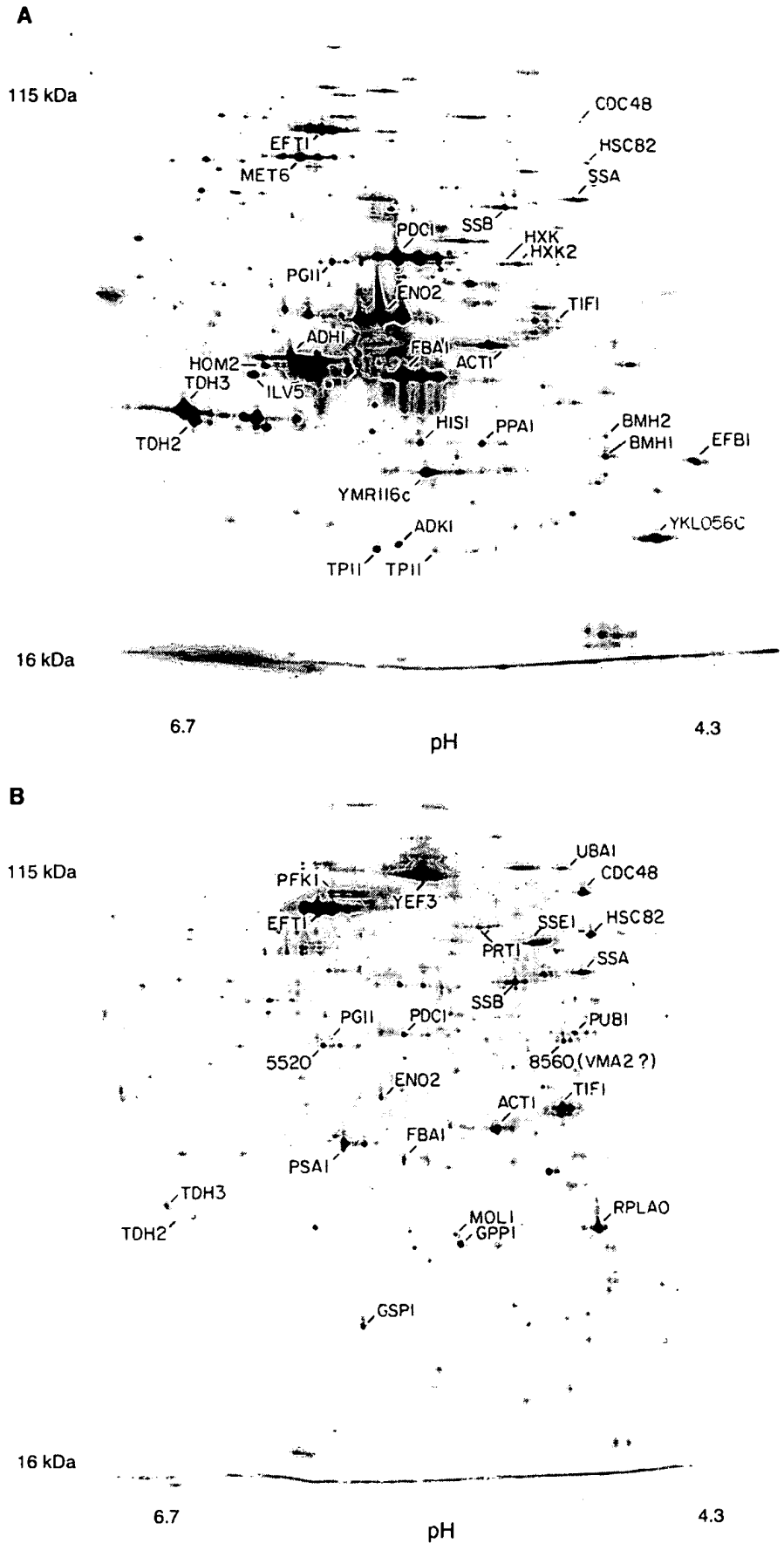

FIG. 6. Fractionation by centrifugation. (A) Proteins in the supernatant of a 100,000 × *g*, 30-min spin; proteins in the pellet of a 16,000 × *g*, 10-min spin. Supernatant fractions examined in multiple experiments done over a wide range of *g* forces looked similar to each other, as did the pellet fractions.

Downloaded from mcb.asm.org by on December 5, 2008

2D gels of the kind that we have used are not suitable for visualization of rare proteins. However it will be possible to study on a global basis metabolic processes involving relatively abundant proteins, such as protein synthesis, glycolysis, gluconeogenesis, amino acid synthesis, cell wall synthesis, nucleotide synthesis, lipid metabolism, and the heat shock response.

Gygi et al. (10) have recently completed a study similar to ours. Despite generating broadly similar data, Gygi et al. reached markedly different conclusions. We believe that both mRNA abundance and codon bias are useful predictors of protein abundance. However, Gygi et al. feel that mRNA abundance is a poor predictor of protein abundance and that "codon bias is not a predictor of either protein or mRNA levels" (10). These different conclusions are partly a matter of viewpoint. Gygi et al. focus on the fact that the correlations of mRNA and codon bias with protein abundance are far from perfect, while we focus on the fact that, considering the wide range of mRNA and protein abundance and the undoubted presence of other mechanisms affecting protein abundance, the correlations are quite good.

However, the different conclusions are also partly due to different methods of statistical analysis and to real differences in data. With respect to statistics, Gygi et al. used the Pearson product-moment correlation coefficient (r_p) to measure the covariance of mRNA and protein abundance. Depending on the subset of data included, their r_p values ranged from 0.1 to 0.94. Because of the low r_p values with some subsets of the data, Gygi et al. concluded that the correlation of mRNA to protein was poor. However, the r_p correlation is a parametric statistic and so requires variates following a bivariate normal distribution; that is, it would be valid only if both mRNA and protein abundances were normally distributed. In fact, both distributions are very far from normal (data not shown), and so a calculation of r_p is inappropriate. There was no statistical backing for the assertion that codon bias fails to predict protein abundance.

We have taken two statistical approaches. First, we have used the Spearman rank correlation coefficient (r_s). Since this statistic is nonparametric, there is no requirement for the data to be normally distributed. Using the r_s, we find that mRNA abundance is well correlated with protein abundance (r_s = 0.74), and the CAI is also well correlated with protein abundance (r_s = 0.80) (and also with mRNA abundance [data not shown]). For the data of Gygi et al. (10), we obtained similar results, though with their data the correlation is not as good; r_s = 0.59 for the mRNA-to-protein correlation, and r_s = 0.59 for the codon bias-to-protein correlation.

In a second approach, we transformed the mRNA and protein data to forms where they were normally distributed, to allow calculation of an r_p (Materials and Methods). Two transformations, Box-Cox and logarithmic, were used; both gave good correlations with our data [e.g., r_p = 0.76 for log(adjusted RNA) to log(protein)]. We were not able to transform the data of Gygi et al. to a normal distribution.

Finally, there are also some differences in data between the two studies. These may be partly due to the different measurement techniques used: Gygi et al. measured protein abundance by cutting spots out of gels and measuring the radioactivity in each spot by scintillation counting, whereas we used phosphorimaging of intact gels coupled to image analysis. We compared our data to theirs for the proteins common between the studies (but excluding proteins whose mRNAs are known to differ between rich and minimal media, and excluding Tif1, which was anomalous in differing by 100-fold between the two data sets). The r_s between the two protein data sets was 0.88 ($P < 0.0001$). Although this is a strong correlation, the fact that it is less than 1.0 suggests that there may have been errors in measuring protein abundance in one or both studies. After normalizing the two data sets to assume the same amount of protein per cell, we found a systematic tendency for the protein abundance data of Gygi et al. to be slightly higher than ours for the highest-abundance proteins and also for the lowest-abundance proteins but slightly lower than ours for the middle-abundance proteins. These systematic differences suggest some systematic errors in protein measurement. Although we do not know what the errors are, we suggest the following as a reasonable speculation. For the highest-abundance proteins, we may have underestimated the amount of protein because of a slightly nonlinear response of the phosphorimager screens. For the lowest-abundance proteins, Gygi et al. may have overestimated the amount of protein because of difficulties in accurately cutting very small spots out of the gel and because of difficulties in background subtraction for these small, weak spots. The difference in the middle abundance proteins may be a consequence of normalization, given the two errors above.

The low-abundance proteins in the data set of Gygi et al. have a poor correlation with mRNA abundance. We calculate that the r_s is 0.74 for the top 54 proteins of Gygi et al. but only 0.22 for the bottom 53 proteins, a statistically significant difference. However, with our data set, the r_s is 0.62 for the top 33 proteins and 0.56 (not significantly different) for the bottom 33 proteins (which are comparable in abundance to the bottom 53 proteins of Gygi et al.). Thus, our data set maintains a good correlation between mRNA and protein abundance even at low protein abundance. This is consistent with our speculation that protein quantification by phosphorimaging and image analysis may be more accurate for small, weak spots than is cutting out spots followed by scintillation counting. Our relatively good correlations even for nonabundant proteins may also reflect the fact that we used both SAGE data and RNA hybridization data, which is most helpful for the least abundant mRNAs. In summary, we feel that the poor correlation of protein to mRNA for the nonabundant proteins of Gygi et al. may reflect difficulty in accurately measuring these nonabundant proteins and mRNAs, rather than indicating a truly poor correlation in vivo. It is not surprising that observed correlations would be poorer with less-abundant proteins and mRNAs, simply because the accuracy of measurement would be worse.

How well can mRNA abundance predict protein abundance? With r_p = 0.76 for logarithmically transformed mRNA and protein data, the coefficient of determination, $(r_p)^2$, is 0.58. This means that more than half (in log space) of the variation in protein abundance is explained by variation in mRNA abundance. When converted back to arithmetic values, protein abundances vary over about 200-fold (Table 1), and $(r_p)^2$ = 0.58 for the log data means that of this 200-fold variation, about 20-fold is explained by variation in the abundance of mRNA and about 10-fold is unexplained (but could be due partly to measurement errors). For proteins much less abundant than those considered here, we imagine the *in vivo* correlation between mRNA and protein abundance will be worse, and other regulatory mechanisms such as protein turnover will be more important.

Some important conclusions can be drawn from this sampling of the proteome. First, there is an enormous range of protein abundance, from nearly 2,000,000 molecules per cell for some glycolytic enzymes to about 100 per cell for some cell cycle proteins (26a). Second, about half of all cellular protein is found in fewer than 100 different gene products, which are mostly involved in carbohydrate metabolism or protein synthe-

Downloaded from mcb.asm.org by on December 5, 2008

sis. Third, the correlation between protein abundance and CAI is log linear as far as we can see, which is from about 10,000 protein molecules per cell to about 1,000,000. This is somewhat surprising, because it implies that selective forces for codon bias are significant even at moderate expression levels. It also means that codon bias is a useful predictor of protein abundance even for moderately low bias proteins. Fourth, there is a good correlation between protein abundance and mRNA abundance for the proteins that we have studied. This validates the use of mRNA abundance as a rough predictor of protein abundance, at least for relatively abundant proteins. Fifth, for these abundant proteins, there are about 4,000 molecules of protein for each molecule of mRNA. This last conclusion raises questions as to how the levels of nonabundant proteins are regulated and suggests that protein instability, regulated translation, suboptimal rates of translation, and other mechanisms in addition to transcriptional control may be very important for these proteins.

ACKNOWLEDGMENTS

We thank Neena Sareen and Nick Bizios (CSHL 2D gel laboratory) for production of 2D gels, Tom Volpe for help with some experiments, Corine Driessens for help with calculations and statistics, and Herman Wijnen and Nick Edgington for comments on the manuscript. We especially thank Tim Tully for in-depth statistical analysis and for insightful discussions on statistical interpretations.

This work was supported by grant P41-RR02188 from the NIH Biomedical Research Technology Program, Division of Research Resources, to J.I.G., by Small Business Innovation Research grant R44 GM54110 to Proteome, Inc., by grant DAMD17-94-J4050 from the Army Breast Cancer Program to B.F., and by NIH grant RO1 GM45410 to B.F.

REFERENCES

1. **Baroni, M. D., E. Martegani, P. Monti, and L. Alberghina.** 1989. Cell size modulation by *CDC25* and *RAS2* genes in *Saccharomyces cerevisiae*. Mol. Cell. Biol. **9**:2715–2723.
2. **Boucherie, H., F. Sagliocco, R. Joubert, I. Maillet, J. Labarre, and M. Perrot.** 1996. Two-dimensional gel protein database of Saccharomyces cerevisiae. Electrophoresis **17**:1683–1699.
3. **Elliott, B., and B. Futcher.** 1993. Stress resistance of yeast cells is largely independent of cell cycle phase. Yeast **9**:33–42.
4. **Entian, K. D., B. Meurer, H. Kohler, K. H. Mann, and D. Mecke.** 1987. Studies on the regulation of enolases and compartmentation of cytosolic enzymes in Saccharomyces cerevisiae. Biochim. Biophys. Acta **923**:214–221.
5. **Ganzhorn, A. J., D. W. Green, A. D. Hershey, R. M. Gould, and B. V. Plapp.** 1987. Kinetic characterization of yeast alcohol dehydrogenases. Amino acid residue 294 and substrate specificity. J. Biol. Chem. **262**:3754–3761.
6. **Garrels, J. I.** 1989. The Quest system for quantitative analysis of two-dimensional gels. J. Biol. Chem. **264**:5269–5282.
7. **Garrels, J. I., B. Futcher, R. Kobayashi, G. I. Latter, B. Schwender, T. Volpe, J. R. Warner, and C. S. McLaughlin.** 1994. Protein identifications for a Saccharomyces cerevisiae protein database. Electrophoresis **15**:1466–1486.
8. **Garrels, J. I., C. S. McLaughlin, J. R. Warner, B. Futcher, G. I. Latter, R. Kobayashi, B. Schwender, T. Volpe, D. S. Anderson, R. Mesquita-Fuentes, and W. E. Payne.** 1997. Proteome studies of S. cerevisiae: identification and characterization of abundant proteins. Electrophoresis **18**:1347–1360.
9. **Goffeau, A., B. G. Barrell, H. Bussey, R. W. Davis, B. Dujon, H. Feldmann, F. Galibert, J. D. Hoheisel, C. Jacq, M. Johnston, E. J. Louis, H. W. Mewes, Y. Murakami, P. Philippsen, H. Tettelin, and S. G. Oliver.** 1996. Life with 6000 genes. Science **274**:563–567.
10. **Gygi, S. P., Y. Rochon, B. R. Franza, and R. Aebersold.** 1999. Correlation between protein and mRNA abundance in yeast. Mol. Cell. Biol. **19**:1720–1730.
11. **Hereford, L. M., and M. Rosbash.** 1977. Number and distribution of polyadenylated RNA sequences in yeast. Cell **10**:453–462.
12. **Herrick, D., R. Parker, and A. Jacobson.** 1990. Identification and comparison of stable and unstable mRNAs in *Saccharomyces cerevisiae*. Mol. Cell. Biol. **10**:2269–2284.
13. **Hodges, P. E., A. H. McKee, B. P. Davis, W. E. Payne, and J. I. Garrels.** 1999. The Yeast Proteome Database (YPD): a model for the organization of genome-wide functional data. Nucleic Acids Res. **27**:69–73.
14. **Ikemura, T.** 1985. Codon usage and tRNA content in unicellular and multicellular organisms. Mol. Biol. Evol. **2**:13–34.
15. **Johnston, G. C., F. R. Pringle, and L. H. Hartwell.** 1977. Coordination of growth with cell division in the yeast S. cerevisiae. Exp. Cell Res. **105**:79–98.
16. **Johnston, M., and M. Carlson.** 1992. Regulation of carbon and phosphate utilization, p. 193–281. *In* E. Jones, J. Pringle, and J. Broach (ed.), The molecular and cellular biology of the yeast Saccharomyces. Cold Spring Harbor Laboratory Press, Cold Spring Harbor, N.Y.
17. **Kornblatt, M. J., and A. Klugerman.** 1989. Characterization of the enolase isozymes of rabbit brain: kinetic differences between mammalian and yeast enolases. Biochem. Cell. Biol. **67**:103–107.

17a. **Latter, G., and B. Futcher.** Unpublished data.

18. **Mathews, B., N. Sonenberg, and J. W. B. Hershey.** 1996. Origins and targets of translational control, p. 1–29. *In* J. W. B. Hershey, M. B. Mathews, and N. Sonenberg (ed.), Translational control. Cold Spring Harbor Laboratory Press, Cold Spring Harbor, N.Y.
19. **McAlister, L., and M. J. Holland.** 1982. Targeted deletion of a yeast enolase structural gene. Identification and isolation of yeast enolase isozymes. J. Biol. Chem. **257**:7181–7188.
20. **Monardo, P. J., T. Boutell, J. I. Garrels, and G. I. Latter.** 1994. A distributed system for two-dimensional gel analysis. Comput. Appl. Biosci. **10**:137–143.
21. **O'Farrell, P. H.** 1975. High resolution two-dimensional electrophoresis of proteins. J. Biol. Chem. **250**:4007–4021.
22. **Patterson, S. D., and G. I. Latter.** 1993. Evaluation of storage phosphor imaging for quantitative analysis of 2-D gels using the Quest II system. BioTechniques **15**:1076–1083.
23. **Sagliocco, F., J. C. Guillemot, C. Monribot, J. Capdevielle, M. Perrot, E. Ferran, P. Ferrara, and H. Boucherie.** 1996. Identification of proteins of the yeast protein map using genetically manipulated strains and peptide-mass fingerprinting. Yeast **12**:1519–1533.
24. **Sharp, P. M., and W. H. Li.** 1987. The Codon Adaptation Index—a measure of directional synonymous codon usage bias, and its potential applications. Nucleic Acids Res. **15**:281–1295.
25. **Shevchenko, A., O. N. Jensen, A. V. Podtelejnikov, F. Sagliocco, M. Wilm, O. Vorm, P. Mortensen, A. Shevchenko, H. Boucherie, and M. Mann.** 1996. Linking genome and proteome by mass spectrometry: large-scale identification of yeast proteins from two dimensional gels. Proc. Natl. Acad. Sci. USA **93**:14440–14445.
26. **Thomas, B. J., and R. Rothstein.** 1989. Elevated recombination rates in transcriptionally active DNA. Cell **56**:619–630.

26a. **Tyers, M., and B. Futcher.** Unpublished data.

27. **Velculescu, V. E., L. Zhang, W. Zhou, J. Vogelstein, M. A. Basrai, D. E. Bassett, Jr., P. Hieter, B. Vogelstein, and K. W. Kinzler.** 1997. Characterization of the yeast transcriptome. Cell **88**:243–251.
28. **Warner, J.** 1991. Labeling of RNA and phosphoproteins in S. cerevisiae. Methods Enzymol. **194**:423–428.
29. **Wills, C.** 1976. Production of yeast alcohol dehydrogenase isoenzymes by selection. Nature **261**:26–29.

29a. **Wodicka, L.** Personal communication.

29b. **Wodicka, L.** Unpublished data.

30. **Wodicka, L., H. Dong, M. Mittmann, M.-H. Ho, and D. J. Lockhart.** 1997. Genome-wide expression monitoring in Saccharomyces cerevisiae. Nat. Biotechnol. **15**:1359–1367.

Downloaded from mcb.asm.org by on December 5, 2008